

AD-A245 983



NAVAL POSTGRADUATE SCHOOL

Monterey, California

2



DTIC
ELECTE
FEB 18 1992
S B D

THESIS

ANALYSIS AND EVALUATION
OF
PROJECT EVERGREEN DATA

by

Antonio Gala

September, 1991

Thesis Advisor:

Xavier Maruyuma

Approved for public release; distribution is unlimited.

92 2 12 024

~~92 2 12 023~~

92-03555



UNCLASSIFIED

SECURITY CLASSIFICATION OF THIS PAGE

REPORT DOCUMENTATION PAGE				Form Approved OMB No. 0704-0188	
1a REPORT SECURITY CLASSIFICATION UNCLASSIFIED			1b RESTRICTIVE MARKINGS		
2a SECURITY CLASSIFICATION AUTHORITY Multiple Sources			3 DISTRIBUTION/AVAILABILITY OF REPORT Approved for public release; Distribution is unlimited		
2b DECLASSIFICATION/DOWNGRADING SCHEDULE					
4 PERFORMING ORGANIZATION REPORT NUMBER(S)			5 MONITORING ORGANIZATION REPORT NUMBER(S)		
6a NAME OF PERFORMING ORGANIZATION Naval Postgraduate School		6b OFFICE SYMBOL (If applicable) 595 / 3A	7a NAME OF MONITORING ORGANIZATION Naval Postgraduate School		
6c ADDRESS (City, State, and ZIP Code) Monterey, California 93943-5000			7b ADDRESS (City, State, and ZIP Code) Monterey, California 93943-5000		
8a NAME OF FUNDING/SPONSORING ORGANIZATION		8b OFFICE SYMBOL (If applicable)	9 PROCUREMENT INSTRUMENT IDENTIFICATION NUMBER		
8c ADDRESS (City, State, and ZIP Code)			10 SOURCE OF FUNDING NUMBERS		
			PROGRAM ELEMENT NO	PROJECT NO	TASK NO
					WORK UNIT ACCESSION NO.
11 TITLE (Include Security Classification) ANALYSIS AND EVALUATION OF PROJECT EVERGREEN DATA (U)					
12 PERSONAL AUTHOR(S) Gala, Antonio					
13a TYPE OF REPORT Master's Thesis		13b TIME COVERED FROM Sept 89 TO Sept 91		14 DATE OF REPORT (Year, Month, Day) September 1991	
15 PAGE COUNT 193					
16 SUPPLEMENTARY NOTATION The views expressed in this thesis are those of the author and do not reflect the official policy or position of the Department of Defense or the US Govt.					
17 COSATI CODES			18 SUBJECT TERMS (Continue on reverse if necessary and identify by block number)		
FIELD	GROUP	SUB-GROUP	Nanosecond pulse		
19 ABSTRACT (Continue on reverse if necessary and identify by block number) Project EVERGREEN tested the response of a modified log periodic antenna and a TEM horn antenna when excited by nanosecond pulses. Analysis of Project EVERGREEN data collected by Naval Postgraduate School test site personnel indicated the following: 1. The antenna output response characteristic is different for the log periodic antenna and the TEM horn antenna. 2. The received polarization is a function of the transmitted polarization and orientation of the receiving site relative to the transmitting site. 3. Signal strength and capture are a function of the polarization alignment between the transmitting and receiving antenna. 4. Pulses on the order of 1 to 10 nanoseconds require bandwidths exceeding 1 Giga-hertz (GHz) in the transmitting and receiving equipment. 5. Broadband equipment with minimum bandwidths of 1 GHz are required to adequately capture and process extremely short time duration signals.					
20 DISTRIBUTION/AVAILABILITY OF ABSTRACT <input checked="" type="checkbox"/> UNCLASSIFIED/UNLIMITED <input type="checkbox"/> SAME AS RPT <input type="checkbox"/> DTIC USERS			21 ABSTRACT SECURITY CLASSIFICATION UNCLASSIFIED		
22a NAME OF RESPONSIBLE INDIVIDUAL Xavier Maruyama			22b TELEPHONE (Include Area Code) 646-2431		22c OFFICE SYMBOL PH/XM

DD Form 1473, JUN 86

Previous editions are obsolete

SECURITY CLASSIFICATION OF THIS PAGE

S/N 0102-LF-014-6603

UNCLASSIFIED

Approved for public release; distribution is unlimited.

ANALYSIS AND EVALUATION
OF
PROJECT EVERGREEN DATA

by

Antonio Gala
Captain, United States Army
B.S., Florida Institute of Technology, 1981

Submitted in partial fulfillment
of the requirements for the degree of

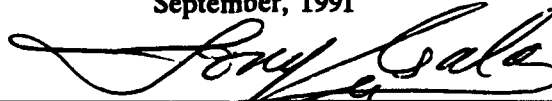
MASTER OF SCIENCE IN SYSTEMS ENGINEERING
(ELECTRONIC WARFARE)

from the

NAVAL POSTGRADUATE SCHOOL

September, 1991

Author:



Antonio Gala

Approved by:



Xavier Maruyama, Thesis Advisor



Stephen Jauregui, Second Reader



Joseph Sternberg, Chairman

Electronic Warfare Academic Group

ABSTRACT

Project Evergreen was an experiment conducted to evaluate antenna responses to nanosecond pulses and the capability of broadband equipment to capture them. The two antennas tested were a log periodic antenna modified by Lawrence Livermore National Laboratories and a TEM horn antenna.

Analysis of the data collected by the Naval Postgraduate School test site personnel indicated the following:

1. The antenna output response characteristic is different for the log periodic antenna and the TEM horn antenna.
2. The received polarization is a function of the transmitted polarization and the orientation of the receiving site relative to the transmitting site.
3. Signal strength and capture are a function of the polarization alignment of the transmitting and receiving antenna.
4. Pulses on the order of 1 to 10 nanoseconds require bandwidths exceeding 1 Gigahertz (GHz) in the transmitting and receiving equipment.
5. Broadband equipment with minimum bandwidths of 1 GHz are required to adequately capture and process extremely short time duration signals.



Accession For	
NTIS GRA&I	<input checked="checked" type="checkbox"/>
DTIC TAB	<input type="checkbox"/>
Unannounced	<input type="checkbox"/>
Justification	
By	
Distribution/	
Availability Codes	
Dist	Avail and/or Special
A-1	

TABLE OF CONTENTS

I.	INTRODUCTION	1
II.	SUMMARY OF RESULTS	7
III.	EXPERIMENT SETUP AND TEST PROCEDURES	15
IV.	DATA ANALYSIS	35
	A. ANALYSIS METHODOLOGY	35
	B. BACKGROUND THEORY	49
	C. ANALYSIS OF INDIVIDUAL WAVEFORMS	52
	1. Directory 5-1-90	58
	a. Waveform NTS04B01.WFM	58
	b. Waveform NTS04E01.WFM	58
	c. Waveform NTS04J01.WFM	59
	d. Waveform NTS04K01.WFM	60
	e. Waveform NTS04L01.WFM	61
	2. Directory 5-2-90	61
	a. Waveform NTS06O01.WFM	61
	b. Waveform NTS07A01.WFM	62
	c. Waveform NTS07B01.WFM	63
	3. Directory 5-3-90	63
	a. Waveform NTS09J01.WFM	63

b.	Waveform NTS09K01.WFM	64
4.	Directory 5-4-90	65
a.	Waveform NTS12J01.WFM	65
b.	Waveform NTS12K01.WFM	65
5.	Directory 5-7-90	66
a.	Waveform NTS13A01.WFM	66
b.	Waveform NTS13B01.WFM	67
c.	Waveform NTS13C01.WFM	67
d.	Waveform NTS13D01.WFM	68
e.	Waveform NTS13E01.WFM	68
f.	Waveform NTS13F01.WFM	69
g.	Waveform NTS13G01.WFM	69
h.	Waveform NTS13H01.WFM	70
i.	Waveform NTS13I01.WFM	71
j.	Waveform NTS13J01.WFM	71
k.	Waveform NTS13K01.WFM	72
l.	Waveform NTS13L01.WFM	72
m.	Waveform NTS13M01.WFM	73
n.	Waveform NTS13N01.WFM	73
o.	Waveform NTS13O01.WFM	74
p.	Waveform NTS13P01.WFM	75
q.	Waveform NTS13Q01.WFM	75
r.	Waveform NTS13R01.WFM	76
s.	Waveform NTS13S01.WFM	77
t.	Waveform NTS13T01.WFM	77
u.	Waveform NTS13U01.WFM	78

v.	Waveform NTS13V01.WFM	78
w.	Waveform NTS13W01.WFM	79
x.	Waveform NTS13X01.WFM	80
y.	Waveform NTS13Y01.WFM	80
z.	Waveform NTS13Z01.WFM	81
aa.	Waveform NTS14A01.WFM	81
ab.	Waveform NTS14B01.WFM	82
ac.	Waveform NTS14C01.WFM	83
ad.	Waveform NTS14D01.WFM	83
6.	Directory 5-8-90	84
a.	Waveform NTS15A01.WFM	84
b.	Waveform NTS15B01.WFM	85
c.	Waveform NTS15C01.WFM	85
d.	Waveform NTS15D01.WFM	86
e.	Waveform NTS15E01.WFM	87
f.	Waveform NTS15F01.WFM	87
g.	Waveform NTS15G01.WFM	88
h.	Waveform NTS15H01.WFM	88
i.	Waveform NTS15I01.WFM	89
j.	Waveform NTS15J01.WFM	89
k.	Waveform NTS15K01.WFM	90
l.	Waveform NTS15L01.WFM	91
m.	Waveform NTS15M01.WFM	91
n.	Waveform NTS15N01.WFM	92
o.	Waveform NTS15O01.WFM	92
p.	Waveform NTS15P01.WFM	93

q.	Waveform NTS15Q01.WFM	94
r.	Waveform NTS15R01.WFM	94
s.	Waveform NTS15S01.WFM	95
t.	Waveform NTS15T01.WFM	95
u.	Waveform NTS15U01.WFM	96
v.	Waveform NTS15V01.WFM	97
w.	Waveform NTS15W01.WFM	97
x.	Waveform NTS15X01.WFM	98
y.	Waveform NTS16A01.WFM	99
z.	Waveform NTS16B01.WFM	99
aa.	Waveform NTS16C01.WFM	100
ab.	Waveform NTS16D01.WFM	101
ac.	Waveform NTS16E01.WFM	101
ad.	Waveform NTS16F01.WFM	102
ae.	Waveform NTS16G01.WFM	102
af.	Waveform NTS16H01.WFM	103
D.	ANALYSIS OF PAIRED WAVEFORMS	104
1.	Directory 5-4-90	104
a.	Waveforms NTS12J01.WFM and NTS12K01.WFM	104
2.	Directory 5-7-90	104
a.	Waveforms NTS13A01.WFM and NTS13C01.WFM	104
b.	Waveforms NTS13F01.WFM and NTS13H01.WFM	105
c.	Waveforms NTS13I01.WFM and NTS13J01.WFM	105
d.	Waveforms NTS13L01.WFM and NTS13O01.WFM	106
e.	Waveforms NTS13M01.WFM and NTS13N01.WFM	106
f.	Waveforms NTS13P01.WFM and NTS13Q01.WFM	106

g.	Waveforms NTS13R01.WFM and NTS13S01.WFM	107
h.	Waveforms NTS13V01.WFM and NTS13W01.WFM	107
i.	Waveforms NTS13X01.WFM and NTS13Z01.WFM	107
3.	Directory 5-8-90	108
a.	Waveforms NTS15A01.WFM and NTS15D01.WFM	108
b.	Waveforms NTS15B01.WFM and NTS15C01.WFM	108
c.	Waveforms NTS15E01.WFM and NTS15H01.WFM	108
d.	Waveforms NTS15I01.WFM and NTS15L01.WFM	109
e.	Waveforms NTS15M01.WFM and NTS15O01.WFM	109
f.	Waveforms NTS15N01.WFM and NTS15P01.WFM	109
g.	Waveforms NTS15S01.WFM and NTS15T01.WFM	110
h.	Waveforms NTS15U01.WFM and NTS15X01.WFM	110
i.	Waveforms NTS15V01.WFM and NTS15W01.WFM	111
j.	Waveforms NTS16A01.WFM and NTS16B01.WFM	111
k.	Waveforms NTS16C01.WFM and NTS16D01.WFM	112
l.	Waveforms NTS16G01.WFM and NTS16H01.WFM	112
V.	CONCLUSION	113
A.	ANALYSIS OF DATA	113
B.	ELECTROMAGNETIC CONSIDERATIONS	153
C.	RECOMMENDATIONS	155
APPENDIX A. MATLAB PROGRAM - POWER SPECTRAL DENSITY		
	GRAPH	157

APPENDIX B.	MATLAB PROGRAM - AMPLITUDE vs. TIME	
WAVEFORM	159
APPENDIX C.	MATLAB PROGRAM - POWER vs. TIME WAVEFORM .	160
APPENDIX D.	MATLAB PROGRAM - ENERGY vs. TIME WAVEFORM	161
APPENDIX E.	MATLAB PROGRAM - ENERGY vs. TIME	
(NORMALIZED)	163
APPENDIX F.	MATLAB PROGRAM - PHASE VELOCITY	166
LIST OF REFERENCES	167
BIBLIOGRAPHY	168
INITIAL DISTRIBUTION LIST	170

LIST OF TABLES

Table I	CASE 2 - RELATIVE ORIENTATION OF NPS RECEIVING SITE # 2 TO LLNL MODIFIED LOG PERIODIC ANTENNA	16
Table II	CASE 2 - RELATIVE ORIENTATION OF NPS RECEIVING SITE #2 TO TEM HORN TRANSMITTING ANTENNA	17
Table III	SURVEYING CORRECTIONS FOR RECEIVER SITES . .	30
Table IV	DIRECTORIES 5-1-90, 5-2-90, 5-3-90 AND 5-4-90	53
Table V	DIRECTORY 5-7-90	54
Table VI	DIRECTORY 5-7-90	55
Table VII	DIRECTORY 5-8-90	56
Table VIII	DIRECTORY 5-8-90	57

LIST OF FIGURES

Figure 1	LLNL Technical Note 2-1-90, fig 7, p 7. [Ref. 2]	
	Test response from modified 7 element Log Periodic Antenna.	
	Shown are power gain, transient response, radiated field	
	magnitude (-----) and phase (- - - -) to a gaussian pulse	
	with 1 nanosecond FWHM.	6
Figure 2	Waveform NTS15A01.WFM - Directory 5-8-90	
	Transmitting Antenna - LLNL Log Periodic	11
Figure 3	Waveform NTS15H01.WFM - Directory 5-8-90	
	Transmitting Antenna - LLNL Log Periodic	11
Figure 4	Waveform NTS13A01.WFM - Directory 5-7-90	
	Transmitting Antenna - TEM Horn	12
Figure 5	Waveform NTS13V01.WFM - Directory 5-7-90	
	Transmitting Antenna - TEM Horn	12
Figure 6	NBS Technical Note 1008, fig. 9, p. 14. [Ref. 3]	
	Test Response from TEM Horn Antenna.	13
Figure 7	LLNL Technical Note 2-1-90, fig 7, p 7. [Ref. 2]	
	Test Response from modified Log Periodic Antenna. . . .	13
Figure 8	Febetron Output Pulse into Dummy Load	
	Risetime = 1.0 nanosecond (ns)	
	Full Width at Half Maximum (FWHM) = 2.5 ns	14
Figure 9	Project Evergreen - Nevada Test Site . . .	20

Figure 10	Project Evergreen - Nevada Test	
Area 25 [former MX Race Track]	21
Figure 11	Project Evergreen - Nevada Test Site	
Location of Transmitting and Receiving Sites	22
Figure 12	Project Evergreen - Source Antenna Map	23
Figure 13	Project Evergreen -	
Receiver Locations Relative to Source Antennas	24
Figure 14	Project Evergreen - Surveyed Positional Data	
for Naval Postgraduate School Receiver Site Location	25
Figure 15	Project Evergreen -	
Surveyed Site Location of Near Objects	26
Figure 16	Project Evergreen -	
Surveyed Site Location of Near Objects	27
Figure 17	Project Evergreen -	
Surveyed Site Location of Far Objects	28
Figure 18	Project Evergreen -	
Surveyed Site Location of Far Objects	29
Figure 19	Project Evergreen - CASE 1 and CASE 2	
Relative Orientation of NPS Site to Source Antennas		
Surveying Corrections for Receiver Sites	30
Figure 20	Project Evergreen - CASE 2	
Surveying Site Correction for NPS Receiving Site 2	31
Figure 21	Project Evergreen - CASE 2	
Relative Orientation of NPS Site 2 to TEM Horn Antenna		32
Figure 22	Project Evergreen - CASE 2	
Relative Orientation of NPS Site 2 to LLNL LP Antenna	33

Figure 23	Project EVERGREEN	
Naval Postgraduate School Test Site Experimental Setup		34
Figure 24	Waveform NTS15A01.WFM - Directory 5-8-90	
LLNL Log Periodic Antenna	- DC Level = +6.48 mV . . .	37
Figure 25	Waveform NTS15A01.WFM - LLNL Log Periodic	
Power versus Time Graph	- DC Level = + 6.48 mV . . .	38
Figure 26	Waveform NTS15A01.WFM - LLNL Log Periodic	
Energy versus Time Graph	- DC Level = + 6.48 mV . . .	38
Figure 27	Waveform NTS15A01.WFM - Power Spectral Density	
Frequency Range	= 0 Hz to Fs (Sampling Frequency)	
Spectra at 5 GHz	is mirror image of spectra at 0 Hz which	
is artifact induced by the periodicity of Fs	at 5 GHz .	39
Figure 28	Waveform NTS15A01.WFM - LLNL Log Periodic	
Power Spectral Density	- DC Level = + 6.48 mV	
Frequency Range	= 0 Hz to Fs/2	39
Figure 29	Waveform NTS15A01.WFM - LLNL Log Periodic	
Power Spectral Density	- DC Level = + 6.48 mV	
Frequency Range	= 0 Hz to Fs/4	40
Figure 30	Waveform NTS15A01.WFM - LLNL Log Periodic	
Power Spectral Density	- DC Level = + 6.48 mV	
Frequency Range	= 0 Hz to Fs/8	40
Figure 31	Waveform NTS15A01.WFM - LLNL Log Periodic	
Power Spectral Density	- DC Level = + 6.48 mV	
Semilog (Y-axis), Log (X-axis) plot	41

Figure 32	Waveform NTS15A01.WFM - LLNL Log Periodic	
Power Spectral Density - DC Level = + 6.48 mV		
Semilog (Y-axis), Log (X-axis) plot		41
Figure 33	Waveform NTS15A01.WFM - LLNL Log Periodic	
Power Spectral Density - DC Level = + 6.48 mV		
Semilog (Y-axis), Log (X-axis) plot		42
Figure 34	Waveform NTS15A01.WFM - LLNL Log Periodic	
Power Spectral Density - DC Level = + 6.48 mV		
Semilog (Y-axis), Log (X-axis) plot		42
Figure 35	Waveform NTS15A01.WFM - Directory 5-8-90	
LLNL Log Periodic Antenna - DC Offset = - 6.48 mV . .		43
Figure 36	Waveform NTS15A01.WFM - LLNL Log Periodic	
Power versus Time Graph - DC Offset = - 6.48 mV . . .		44
Figure 37	Waveform NTS15A01.WFM - LLNL Log Periodic	
Energy versus Time Graph - DC Offset = - 6.48 mV . .		44
Figure 38	Waveform NTS15A01.WFM - LLNL Log Periodic	
Frequency Range = 0 Hz to F_s (Sampling Frequency)		
Spectra at 5 GHz is mirror image of spectra at 0 Hz which		
is artifact induced by the periodicity of F_s at 5 GHz .		45
Figure 39	Waveform NTS15A01.WFM - LLNL Log Periodic	
Power Spectral Density - DC Offset = - 6.48 mV		
Frequency Range = 0 Hz to $F_s/2$		45
Figure 40	Waveform NTS15A01.WFM - LLNL Log Periodic	
Power Spectral Density - DC Offset = - 6.48 mV		
Frequency Range = 0 Hz to $F_s/4$		46

Figure 41	Waveform NTS15A01.WFM - LLNL Log Periodic	
	Power Spectral Density - DC Offset = - 6.48 mV	
	Frequency Range = 0 Hz to $F_s/8$	46
Figure 42	Waveform NTS15A01.WFM - LLNL Log Periodic	
	Power Spectral Density - DC Offset = - 6.48 mV	
	Semilog (Y-axis), Log (X-axis) plot	47
Figure 43	Waveform NTS15A01.WFM - LLNL Log Periodic	
	Power Spectral Density - DC Offset = - 6.48 mV	
	Semilog (Y-axis), Log (X-axis) plot	47
Figure 44	Waveform NTS15A01.WFM - LLNL Log Periodic	
	Power Spectral Density - DC Offset = - 6.48 mV	
	Semilog (Y-axis), Log (X-axis) plot	48
Figure 45	Waveform NTS15A01.WFM - LLNL Log Periodic	
	Power Spectral Density - DC Offset = - 6.48 mV	
	Semilog (Y-axis), Log (X-axis) plot	48
Figure 46	Waveform NTS15A01.WFM - Directory 5-8-90	
	Transmitting Antenna - LLNL Log Periodic	118
Figure 47	Waveform NTS15H01.WFM - Directory 5-8-90	
	Transmitting Antenna - LLNL Log Periodic	118
Figure 48	Waveform NTS13A01.WFM - Directory 5-7-90	
	Transmitting Antenna - Big TEM Horn	119
Figure 49	Waveform NTS13V01.WFM - Directory 5-7-90	
	Transmitting Antenna - Big TEM Horn	119
Figure 50	NBS Technical Note 1008, figure 9, p. 14	
	Test Response from TEM Horn	120

Figure 51	LLNL Technical Note 2-1-90, figure 7, p. 7	
Test Response from modified Log Periodic Antenna	. . .	120
Figure 52	Waveform NTS13M01.WFM - Directory 5-7-90	
Horizontal Polarization [Paired with NTS13N01.WFM]	. . .	121
Figure 53	Waveform NTS13N01.WFM - Directory 5-7-90	
Vertical Polarization [Paired with NTS13M01.WFM]	. . .	121
Figure 54	Waveform NTS13R01.WFM - Directory 5-7-90	
Horizontal Polarization [Paired with NTS13S01.WFM]	. . .	122
Figure 55	Waveform NTS13S01.WFM - Directory 5-7-90	
Vertical Polarization [Paired with NTS13R01.WFM]	. . .	122
Figure 56	Waveform NTS15A01.WFM - Directory 5-8-90	
LLNL Log Periodic Antenna \ Horizontal Polarization	. . .	123
Figure 57	Waveform NTS15H01.WFM - Directory 5-8-90	
LLNL Log Periodic Antenna \ Horizontal Polarization	. . .	123
Figure 58	Waveform NTS13V01.WFM - Directory 5-7-90	
Big TEM Horn Antenna \ Horizontal Polarization	124
Figure 59	Waveform NTS13A01.WFM - Directory 5-7-90	
Big TEM Horn Antenna \ Horizontal Polarization	124
Figure 60	Waveform NTS15E01.WFM - Directory 5-8-90	
LLNL Log Periodic Antenna \ Vertical Polarization	. . .	125
Figure 61	Waveform NTS15D01.WFM - Directory 5-8-90	
LLNL Log Periodic Antenna \ Vertical Polarization	. . .	125
Figure 62	Waveform NTS13C01.WFM - Directory 5-7-90	
Big TEM Horn Antenna \ Vertical Polarization	126
Figure 63	Waveform NTS13W01.WFM - Directory 5-7-90	
Big TEM Horn Antenna \ Vertical Polarization	126

Figure 64 Waveform NTS15H01.WFM [Paired with NTS15E01.WFM]	
LLNL Log Periodic Antenna \ Horizontal Polarization . . .	127
Figure 65 Waveform NTS15E01.WFM [Paired with NTS15H01.WFM]	
LLNL Log Periodic Antenna \ Vertical Polarization . . .	127
Figure 66 Waveform NTS15A01.WFM [Paired with NTS15D01.WFM]	
LLNL Log Periodic Antenna \ Horizontal Polarization . . .	128
Figure 67 Waveform NTS15D01.WFM [Paired with NTS15A01.WFM]	
LLNL Log Periodic Antenna \ Vertical Polarization . . .	128
Figure 68 Waveform NTS13A01.WFM [Paired with NTS13C01.WFM]	
Big TEM Horn Antenna \ Horizontal Polarization	129
Figure 69 Waveform NTS13C01.WFM [Paired with NTS13A01.WFM]	
Big TEM Horn Antenna \ Vertical Polarization	129
Figure 70 Waveform NTS13V01.WFM [Paired with NTS13W01.WFM]	
Big TEM Horn Antenna \ Horizontal Polarization	130
Figure 71 Waveform NTS13W01.WFM [Paired with NTS13V01.WFM]	
Big TEM Horn Antenna \ Vertical Polarization	130
Figure 72 Reference Frame - Coordinate Axes	131
Figure 73 Reference Frame - Elevation Angle = 45 degrees	
Relative to the Horizontal Plane	131
Figure 74 Waveform NTS15W01.WFM [Paired with NTS15V01.WFM]	
Horizontal Component \ Elevation Angle = 45 degrees	
LLNL modified LP Antenna	132
Figure 75 Waveform NTS15V01.WFM [Paired with NTS15W01.WFM]	
Vertical Component \ Elevation Angle = 45 degrees	
LLNL modified LP Antenna	132

Figure 76 Waveform NTS12J01.WFM [Paired with NTS12K01.WFM]	
Horizontal Component \ Elevation Angle = 45 degrees	
Big TEM Horn Antenna	133
Figure 77 Waveform NTS12K01.WFM [Paired with NTS12J01.WFM]	
Vertical Component \ Elevation Angle = 45 degrees	
Big TEM Horn Antenna	133
Figure 78 Waveform NTS15A01.WFM [Paired with NTS15D01.WFM]	
Horizontal Component \ LLNL Log Periodic Antenna	
Energy versus Time Graph	134
Figure 79 Waveform NTS15D01.WFM [Paired with NTS15A01.WFM]	
Vertical Component \ LLNL Log Periodic Antenna	
Energy versus Time Graph	134
Figure 80 Energy versus Time Graph - "NORMALIZED"	
Waveforms NTS15A01.WFM and NTS15D01.WFM	135
Figure 81 Waveform NTS13A01.WFM [Paired with NTS13C01.WFM]	
Horizontal Component \ Big TEM Horn Antenna	
Energy versus Time Graph	136
Figure 82 Waveform NTS13C01.WFM [Paired with NTS13A01.WFM]	
Vertical Component \ Big TEM Horn Antenna	
Energy versus Time Graph	136
Figure 83 Energy versus Time Graph - "NORMALIZED"	
Waveforms NTS13A01.WFM and NTS13C01.WFM	137
Figure 84 Waveform NTS15W01.WFM [Paired with NTS15V01.WFM]	
Horizontal Component \ Elevation Angle = 45 degrees	
Energy versus Time Graph - LLNL Log Periodic Antenna	138

Figure 85 Waveform NTS15V01.WFM [Paired with NTS15W01.WFM]	
Vertical Component \ Elevation Angle = 45 degrees	
Energy versus Time Graph - LLNL Log Periodic Antenna	138
Figure 86 Energy versus Time Graph - "NORMALIZED"	
Waveforms NTS15V01.WFM and NTS15W01.WFM	139
Figure 87 Waveform NTS12J01.WFM [Paired with NTS12K01.WFM]	
Horizontal Component \ Elevation Angle = 45 degrees	
Energy versus Time Graph - Big TEM Horn Antenna . . .	140
Figure 88 Waveform NTS12K01.WFM [Paired with NTS12J01.WFM]	
Vertical Component \ Elevation Angle = 45 degrees	
Energy versus Time Graph - Big TEM Horn Antenna . . .	140
Figure 89 Energy versus Time Graph - "NORMALIZED"	
Waveforms NTS12J01.WFM and NTS12K01.WFM	141
Figure 90 Waveform NTS15P01.WFM [Paired with NTS15N01.WFM]	
LLNL Log Periodic Antenna - Horizontal Component . .	142
Figure 91 Waveform NTS15P01.WFM [Paired with NTS15N01.WFM]	
Power Spectral Density Graph - Horizontal Component .	142
Figure 92 Waveform NTS15N01.WFM [Paired with NTS15P01.WFM]	
LLNL Log Periodic Antenna - Vertical Component . . .	143
Figure 93 Waveform NTS15N01.WFM [Paired with NTS15P01.WFM]	
Power Spectral Density Graph - Vertical Component . .	143
Figure 94 Waveform NTS16D01.WFM [Paired with NTS16C01.WFM]	
Big TEM Horn Antenna - Horizontal Component	144
Figure 95 Waveform NTS16D01.WFM [Paired with NTS16C01.WFM]	
Power Spectral Density Graph - Horizontal Component .	144

Figure 96 Waveform NTS16C01.WFM [Paired with NTS16D01.WFM]	
Big TEM Horn Antenna - Vertical Component	145
Figure 97 Waveform NTS16C01.WFM [Paired with NTS16D01.WFM]	
Power Spectral Density Graph - Vertical Component . .	145
Figure 98 Waveform NTS15A01.WFM [Paired with NTS15D01.WFM]	
LLNL Log Periodic Antenna - Horizontal Component . .	146
Figure 99 Waveform NTS15A01.WFM [Paired with NTS15D01.WFM]	
Power Spectral Density Graph - Horizontal Component .	146
Figure 100 Waveform NTS15D01.WFM [Paired w/ NTS15A01.WFM]	
LLNL Log Periodic Antenna - Vertical Component . . .	147
Figure 101 Waveform NTS15D01.WFM [Paired w/ NTS15A01.WFM]	
Power Spectral Density Graph - Vertical Component . .	147
Figure 102 Waveform NTS13V01.WFM [Paired w/ NTS13W01.WFM]	
Big Tem Horn Antenna - Horizontal Component	148
Figure 103 Waveform NTS13V01.WFM [Paired w/ NTS13W01.WFM]	
Power Spectral Density Graph - Horizontal Component .	148
Figure 104 Waveform NTS13W01.WFM [Paired w/ NTS13V01.WFM]	
Big TEM Horn Antenna - Vertical Component	149
Figure 105 Waveform NTS13W01.WFM [Paired w/ NTS13V01.WFM]	
Power Spectral Density Graph - Vertical Component . .	149
Figure 106 Waveform NTS06O01.WFM - Directory 5-1-90	
LLNL Log Periodic Antenna	150
Figure 107 Waveform NTS06O01.WFM - Directory 5-1-90	
Power Spectral Density Graph	150
Figure 108 Waveform NTS04K01.WFM - Directory 5-1-90	
Big TEM Horn Antenna	151

Figure 109	waveform NTS04K01.WFM - Directory 5-1-90	
Power Spectral Density Graph	151
Figure 110	Project Evergreen - LLNL modified LP Antenna	
Signal Strength as a Function of Azimuthal Direction	.	152
Figure 111	Project Evergreen - Big TEM Horn Antenna	
Signal Strength as a Function of Azimuthal Direction	.	152

ACKNOWLEDGEMENTS

I would like to extend my deepest appreciation to Professor S. Gnanalingham. As my instructor in the Advanced Electromagnetic Theory courses offered by the Physics Department, his insight and advice proved invaluable to my understanding and evaluation of the EVERGREEN data. In addition, I strongly recommend taking the three quarter sequence in Classical Electromagnetic Theory offered by the Physics Department to any student who desires a greater understanding into the nature and propagation of electromagnetic waves.

I would also like to thank Dr. Edna Didwell and her staff for assisting me in the initial evaluation and understanding of Project EVERGREEN.

To Professors John Neighbours, Dale Galarowicz and Xavier Maruyama, I commend you for the attention to detail shown during the collection and recording of the EVERGREEN data.

To Professor Stephen Jauregui, your advice provided me with a much greater understanding of equipment bandwidth and how it relates to signal detection and processing.

Lastly, I extend my appreciation and gratitude to all the individuals who helped me throughout my analysis. Without their assistance and advice, I would never have finished.

I. INTRODUCTION

Project Evergreen was conducted at the Nevada Test Site during the period 30 April to 8 May 1990. The purpose of the experiment was to evaluate antenna output responses to various pulsed inputs. Additionally, the capability of broadband equipment to adequately capture short time duration signals was evaluated.

To test antenna responses and the ability of broadband equipment to adequately capture these pulses, a Febetron and a UK pulser were used to generate pulses on the order of 1 - 10 nanoseconds in duration. The Febetron and UK pulser are spark gap discharge devices, consisting of several capacitors each.

To evaluate the received signal characteristics as a function of azimuthal angle, the transmitting antenna was rotated while the receiving sites remained stationary. This simulated a receiver physically moving around the periphery of a transmitting antenna and evaluating the antenna radiation pattern.

The Naval Postgraduate School test site personnel used two different L-band horn antennas, a Tektronix 7104 oscilloscope and the Digitizing Camera System (DCS) software for reception and digital capture of the transmitted pulses. One horn

antenna was used as a trigger to detect the incoming pulses. The second horn antenna with well established and understood frequency response characteristics [see Ref. 3] was used as the receiving antenna.

Two antenna configurations, a modified log-periodic and a transverse electric-magnetic (TEM) horn antenna were tested. The modified log-periodic antenna was designed by Lawrence Livermore National Laboratories to specifically take into account the inherent frequency delays experienced by the antenna. The output characteristic of the modified log-periodic (LP) antenna maintained a relatively flat response over the frequency range from 0 Hertz (Hz) to 1 Gigahertz (GHz) with minimal distortion in the pulse shape resulting from induced phase delay shifts. Figure 1 illustrates the output characteristics of the modified LP antenna designed by Lawrence Livermore National Laboratories.

Three signal waveforms were generated for testing and measuring the output frequency responses of each antenna. The three waveforms used for the test were:

1. A pulsed continuous wave (CW) signal that was transmitted using on-off keying.
2. Short time duration (impulse) signal using a spark-gap discharge device (Febetron).
3. Short time duration (impulse) signal using a spark-gap discharge device (UK pulser).

The transmission characteristics of the pulsed CW signal were:[Ref. 1]

1. Pulse width: less than 10 milliseconds.
2. Repetition rate: time between pulses at least nine (9) times the pulse width (i.e. 10 % maximum duty cycle) for bursts of 1 to 100 pulses.
3. Time between bursts: at least 4 minutes.
4. CW frequencies:
Band(s) between: 100 Megahertz (MHz) and 400 MHz.
Bandwidth: 10 MHz sweep.
5. Power to antenna: 5 Watt (W) maximum, averaged over any single burst. 100 W maximum peak power.

The transmission characteristics of the pulsed signals were:[Ref. 1:pp. 6-7]

1. Input pulse width: will vary from a few hundred picoseconds (ps) up to a few nanoseconds (ns).
2. Pulse repetition rate: between 10 Hz and 1 kilohertz (KHz). Burst lengths for the higher frequency repetition rates will be limited to 1 or 2 seconds, but burst lengths at frequencies near 10 Hz may be as long as 10 seconds.
3. Time between bursts: at least four (4) minutes.
4. Frequency: the radiated frequency spectrum from the antennas is primarily contained between 100 MHz and 1.2 GHz with considerably lower output up to 2 GHz, confined to a window of less than 100 nanoseconds (typically about 20 ns).
5. Field strength: the maximum peak field strengths expected were well below 100 volts/meter at 1 kilometer (probably less than 30 V/m at 1 km).
6. Power to antenna: average power was less than 10 W during any transmission and was limited to less than 1 W when necessary.

The continuous wave (CW) on-off keyed signal was used during the first few days during set-up to test the equipment, allow for calibration and to allow the different groups participating in the test to test and calibrate their equipment properly.

The transmitting and receiving frequency response characteristics of antennas will vary depending on the antenna type and signal. A log-periodic antenna and a TEM horn antenna were chosen for the test since they have well known and established frequency response characteristics.

The log-periodic antenna will maintain a relatively flat output frequency response within the bandwidth for which it was designed. Signals containing frequencies outside this "designed bandwidth" will experience distortion due to induced phase delays that have not been compensated for. The induced phase delays are frequency dependent, with the phased delay increasing for progressively greater frequencies. For signals of extremely short time duration with correspondingly large bandwidths (on the order of 1 GHz or greater), the aggregate phase delays can be significant and result in a severely distorted output pulse compared to the input pulse. To minimize this effect and achieve a relatively flat response over a wide frequency range, a log-periodic antenna can be modified and designed to transmit very short time duration signals. The modified log-periodic antenna tested during Project Evergreen was developed by Lawrence Livermore National

Laboratory, Applied Technology Section for just this purpose.[Ref. 2]

The second antenna type tested was a TEM horn antenna. Measurements and tests were conducted by the Electromagnetic Technology Division at the National Bureau of Standards on TEM horn antennas to determine their operating characteristics when excited by impulsive fields. Impulsive fields on the order of 1 nanosecond were used to test the characteristics of the TEM horn antenna when used in both the transmitting and receiving mode. Test results indicated that the TEM horn antenna maintained a relatively flat frequency response (± 3 dB) from 200 Mhz to 4 GHz.[Ref. 3]

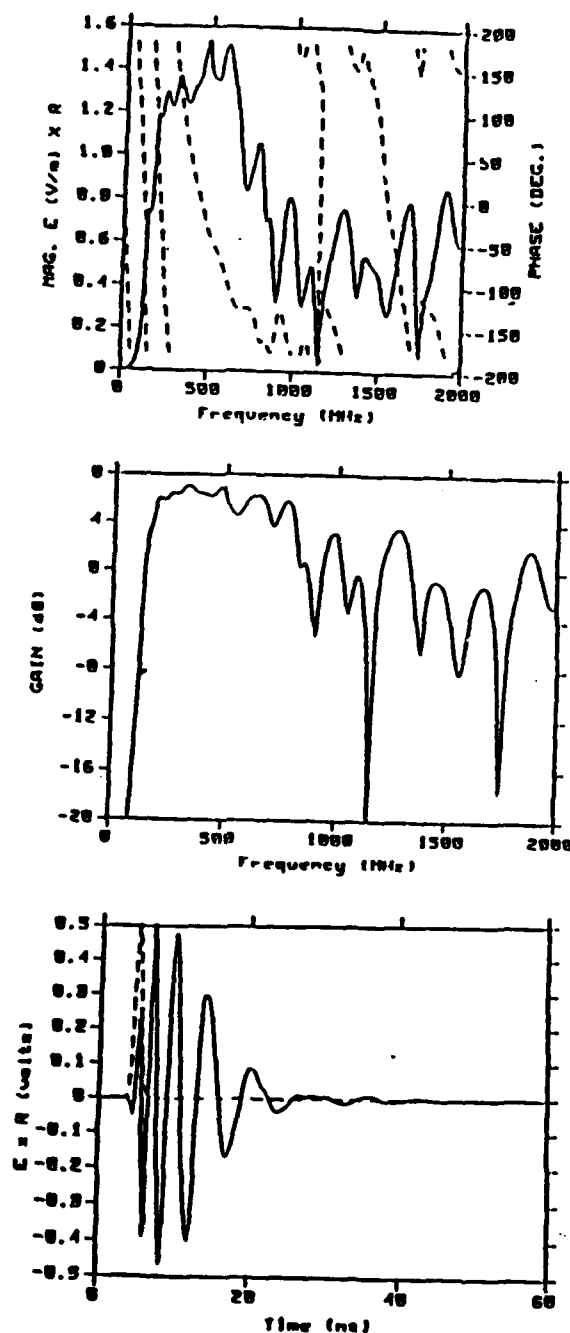


Figure 1 LLNL Technical Note 2-1-90, fig. 7, p. 7. [Ref. 2] Test response from modified 7 element Log Periodic Antenna. Shown are power gain, transient response, radiated field magnitude (-----) and phase (- - - -) to a gaussian pulse with 1 nanosecond FWHM.

II. SUMMARY OF RESULTS

In analyzing the data, the power spectral density (PSD) of the digitized waveforms was computed. In this process, the straight PSD was computed, without windowing or smoothing in time or frequency. Additionally, no averaging of sample points was done to minimize the effects of noise as this would distort the actual data. In this analysis, extracting the true shape of the pulsed signal from the effects of noise was not an objective.

For the data that was analyzed, the 20 dB bandwidth of the signals was less than the oscilloscope bandwidth. The digitized signals were therefore, accurate representations of the true analog signal as determined by the Nyquist sampling theorem. The one caution that must be noted, however, is that if a signal pulse contained individual frequencies exceeding the 1 Ghz bandwidth of the oscilloscope filter or the maximum Nyquist bandwidth (determined by looking at the photograph to determine the time duration of a single cycle), then signal information would be lost, specifically the higher frequencies.

The following is a summary of the trends and patterns observed in analyzing the Evergreen data:

1. The shape of the received pulse was noticeably different when the transmitting antenna used was a TEM horn versus

the LLNL modified LP antenna. Figure 2 and Figure 3 illustrate the received waveform shape when the LLNL LP antenna was used for transmission. Figure 4 and Figure 5 illustrate the received waveform shape when the TEM horn antenna was used for transmission. These differences, reflect the different transmitting characteristics of a TEM horn [see Figure 6] versus the LLNL modified LP antenna [see Figure 7]. Figure 6 is the response of the receiving horn antenna used by the Naval Postgraduate School test site personnel, although it is characteristic of other horn antennas of similar configuration and construction. Figures 1 through 4, furthermore, are for the case in which the receiving antenna was oriented to match the transmitting antenna's polarization (i.e. horizontal).

2. The TEM horn when used as the transmitting antenna appeared to produce symmetric looking waveforms in both the horizontal and vertical direction. The amplitude of the pulse for the vertically received polarization, however, was still less than the corresponding amplitude for the horizontally received polarization.
3. When the receiving antenna was oriented in the horizontal direction to pick up the horizontally polarized, transmitted wave, the main pulse was distinctly observed. When the transmitting antenna used was the LLNL modified LP antenna, the main pulse was discernible and resembled the waveform shape depicted in Figure 7. The TEM horn antenna when used for transmission, generated a main pulse that was similarly discernible, though the pulse shape was different, resembling the output from the Febetron [see Figure 8].
4. When the receiving antenna was oriented in the vertical direction with the transmitting antenna remaining oriented in the horizontal direction, the main pulse was not distinctly discernible. Instead, what appears to be a highly distorted main pulse is observed. This result is most probably indicative of the effects of multipath, reflections, refraction and the fact that due to the actual physical geometry, a strict horizontal versus vertical alignment could not be achieved between the transmitting and the receiving antenna, resulting in some "leakage" of the main pulse in the vertical direction. When the LLNL modified LP antenna was used for transmission, the distortion was quite noticeable. When the TEM horn antenna was used for transmission, the distortion of the main pulse was not as pronounced.

5. The correlation between polarization and the discernment and shape of the main pulse captured is clearly seen when a comparison is made of those series of shots where both the vertical and horizontal component of the horizontally transmitted wave was recorded.
6. When the elevation angle of the transmitting antenna was oriented at 45 degrees relative to the horizontal, what appears to be a distorted main pulse appears initially and both the horizontally and vertically received components of the transmitted wave were nearly identical in appearance. This observation was noted when both the modified LP antenna and the TEM horn antenna were used.
7. Analysis of the energy versus time graphs show a pattern that is indicative of whether the main pulse is present or not. For the horizontally received component of the horizontally polarized wave, a distinct rise in energy is initially observed. For the vertically received component of the horizontally polarized wave, a gradual rise in the energy curve is observed. This is illustrative of the fact that instead of a main pulse being captured, the effects of multipath and reflections are observed. For the case when the transmitting antenna is elevated by 45 degrees relative to the horizontal, the energy versus time graph shows a pattern that is a mixture of both the horizontal and the vertical case.
8. Analysis of the power spectral density graphs for the various collect times (i.e. record lengths) resulted in the following observations:
 - a. 500 ns collect time - virtually all the energy is contained in the frequency range from 0 MHz to 100 MHz.
 - b. 100 ns collect time - virtually all the energy is contained in the frequency range from 0 MHz to 600 MHz.
 - c. 50 ns collect time - virtually all the energy is contained in the frequency range from 0 MHz to 1.1 GHz.
9. The observations noted in sub-paragraph 8 above is perhaps due to the fact that for the longer collect times, more of the energy is proportionately contained in the lower frequencies. As a result, the high frequency energy content is low in proportion to the more abundant low frequency energy content. It is important to stress, however, that for all three collect times, the main pulse is present. Energy at frequencies up to 1 GHz and beyond are present in the main pulse. Therefore, to adequately

capture the signal, hardware bandwidths of at least 1 GHz are required.

10. Correlation of received signal strength to the azimuthal direction of the receiving site relative to the transmitting antenna resulted in the following observations:

- a. The received signal strength dropped off as the receiving site moved off center relative to the transmitting antenna location. This was observed in both cases in which the TEM Horn antenna and the LLNL modified Log Periodic antenna was used.

- b. A comparison of waveforms NTS15M01.WFM, NTS15H01.WFM and NTS15A01.WFM shows that the signal strength dropped off as the receiving site moved off center relative to the transmitting antenna location. These waveforms were collected for the case in which the LLNL Log Periodic antenna was used. It is interesting to note that the received signal strengths of waveform NTS15M01.WFM and NTS15H01.WFM indicate good symmetry in the radiation pattern of the LP antenna. Waveform NTS15M01.WFM was captured at a bearing of 24 degrees left of center and waveform NTS15H01.WFM was captured at a bearing of 25 degrees right of center.

- c. A comparison of waveforms NTS13L01.WFM, NTS16G01.WFM, NTS13V01.WFM, NTS13Z01.WFM and NTS13A01.WFM shows that the signal strength drops off as the receiving site moved off center relative to the transmitting antenna location. The waveforms were collected for the case in which the TEM horn antenna was used for transmission.

- d. In the above noted observations, caution must be used, however, in the evaluation of the data. The attenuation settings were varied throughout the entire experiment. The settings and subsequent changes were not well documented. As a result, the amplitude of the received signal could also be a function of the attenuation setting in use at that particular moment.

11. The "ringing effect" observed after the main pulse is most probably due to transients induced in the circuitry of the transmitting system due to the high energy pulse. The excitation of the transmitting system by the high energy pulse generated low frequency transient currents. These "low frequency components" are subsequently observed trailing the main pulse.

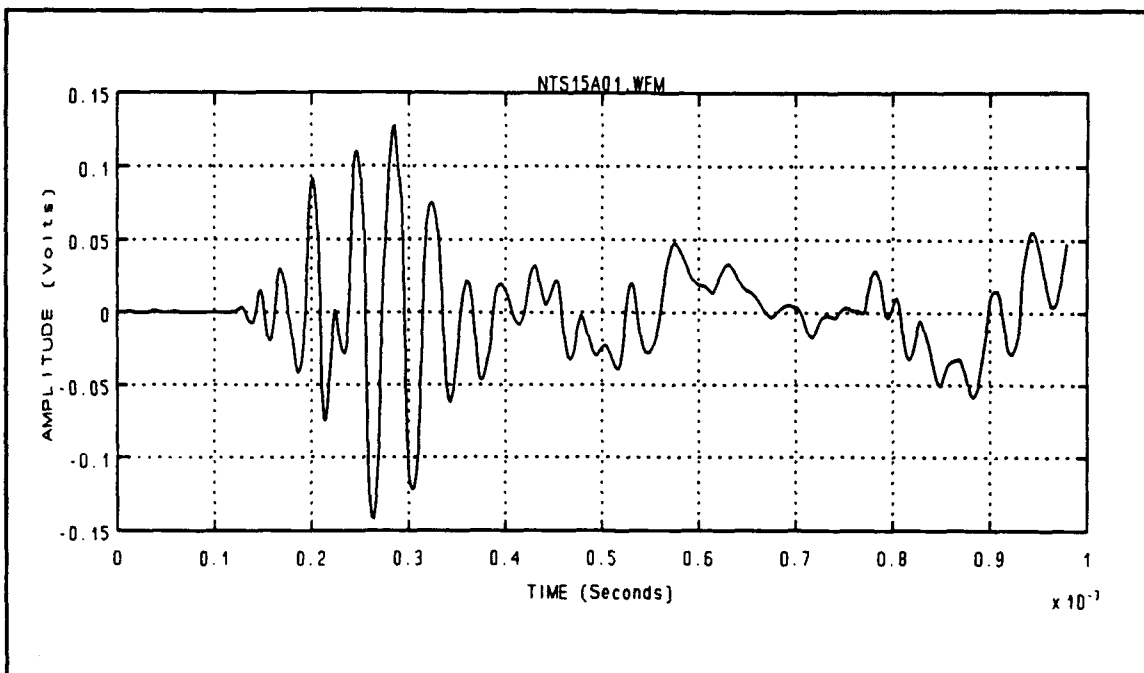


Figure 2 Waveform NTS15A01.WFM - Directory 5-8-90
Transmitting Antenna - LLNL Log Periodic

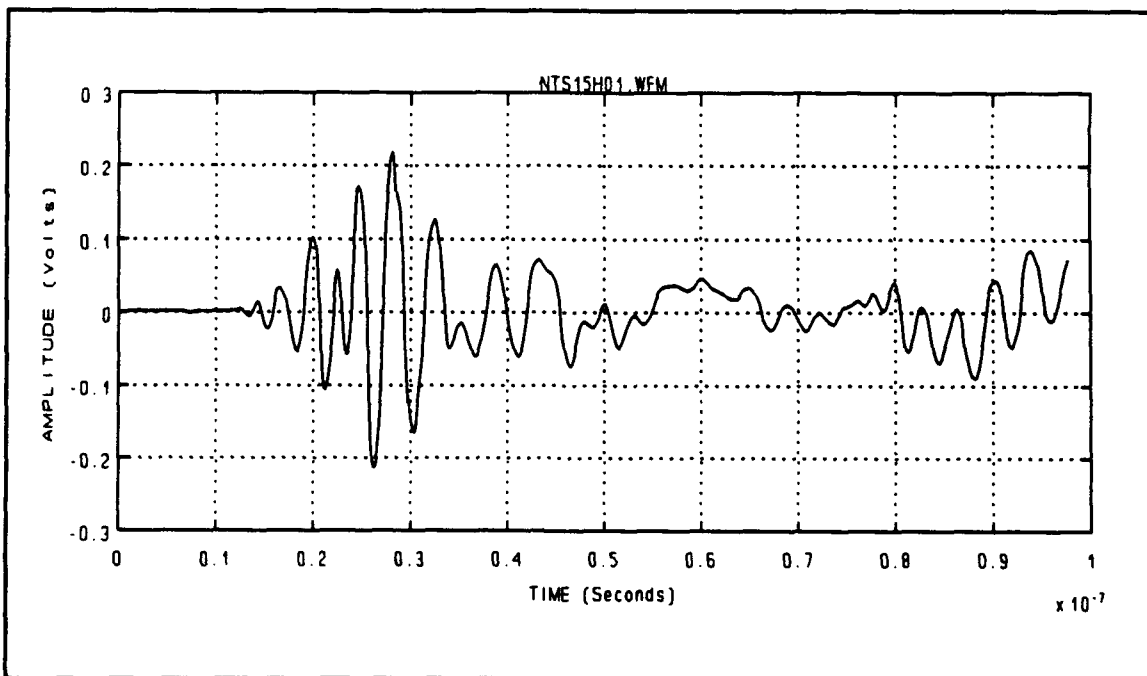


Figure 3 Waveform NTS15H01.WFM - Directory 5-8-90
Transmitting Antenna - LLNL Log Periodic

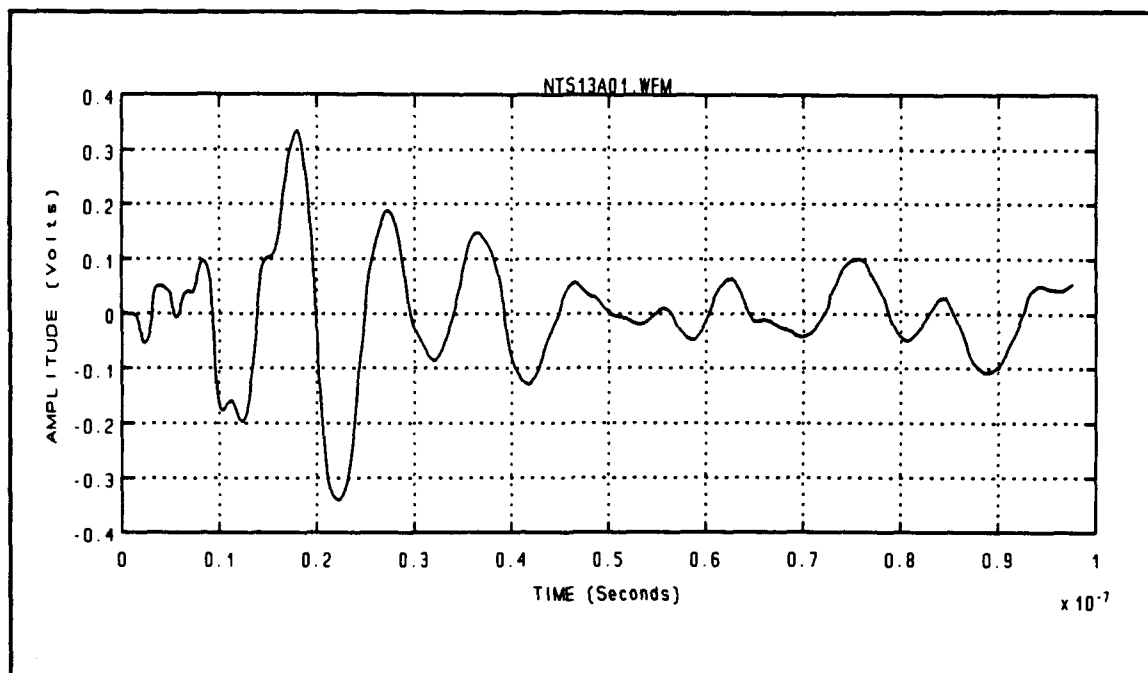


Figure 4 Waveform NTS13A01.WFM - Directory 5-7-90
Transmitting Antenna - TEM Horn

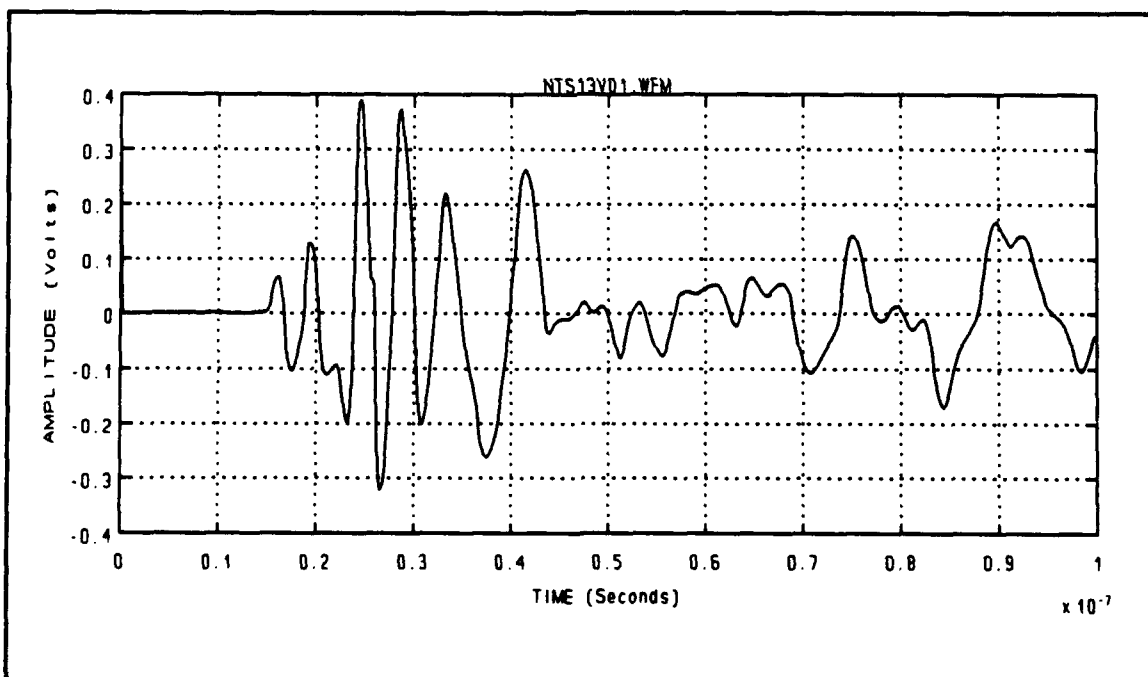


Figure 5 Waveform NTS13V01.WFM - Directory 5-7-90
Transmitting Antenna - TEM Horn

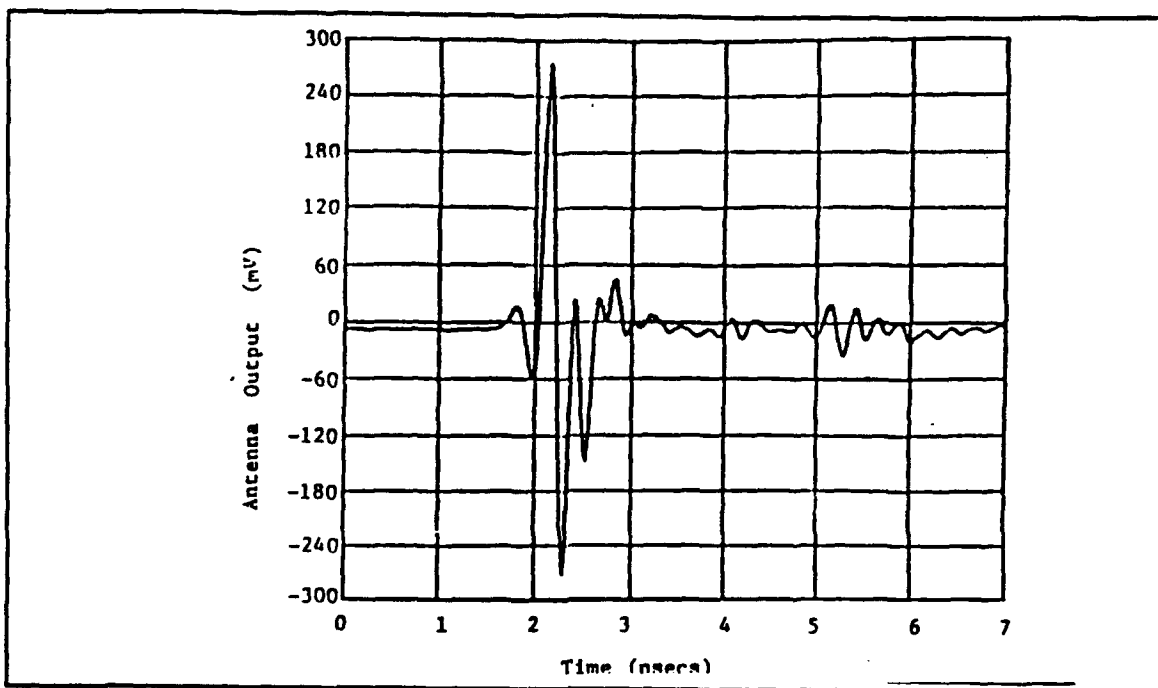


Figure 6 NBS Technical Note 1008, fig. 9, p. 14. [Ref. 3]
Test Response from TEM Horn Antenna.

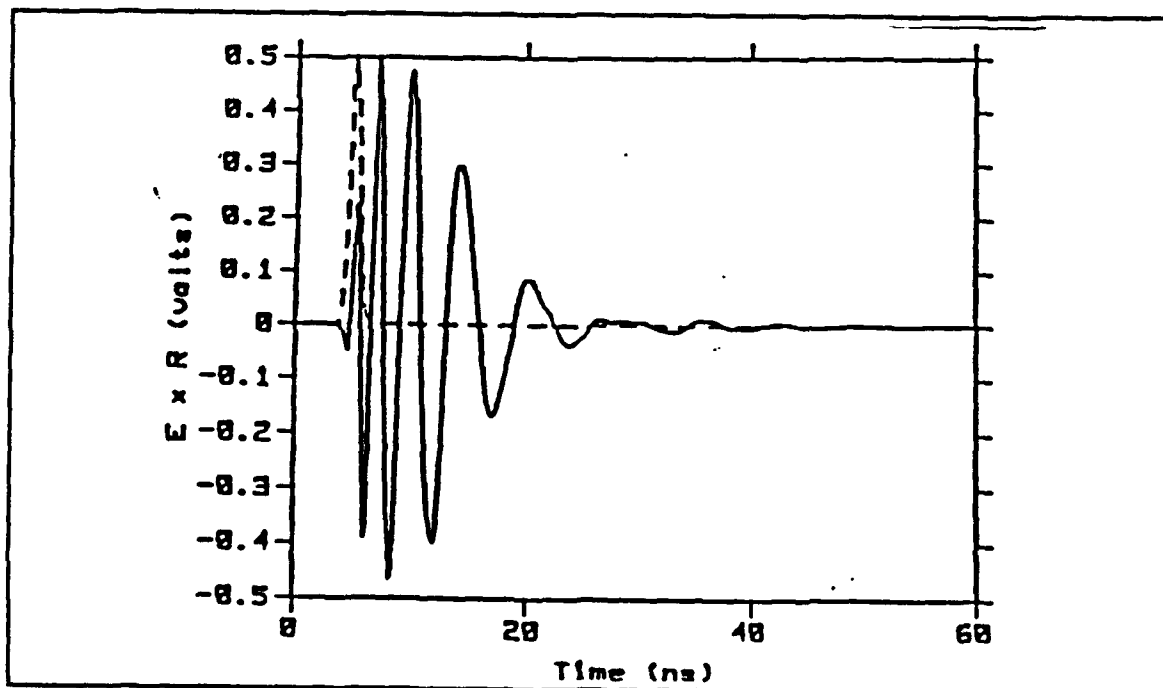


Figure 7 LLNL Technical Note 2-1-90, fig. 7, p. 7. [Ref. 2]
Test Response from modified Log Periodic Antenna.

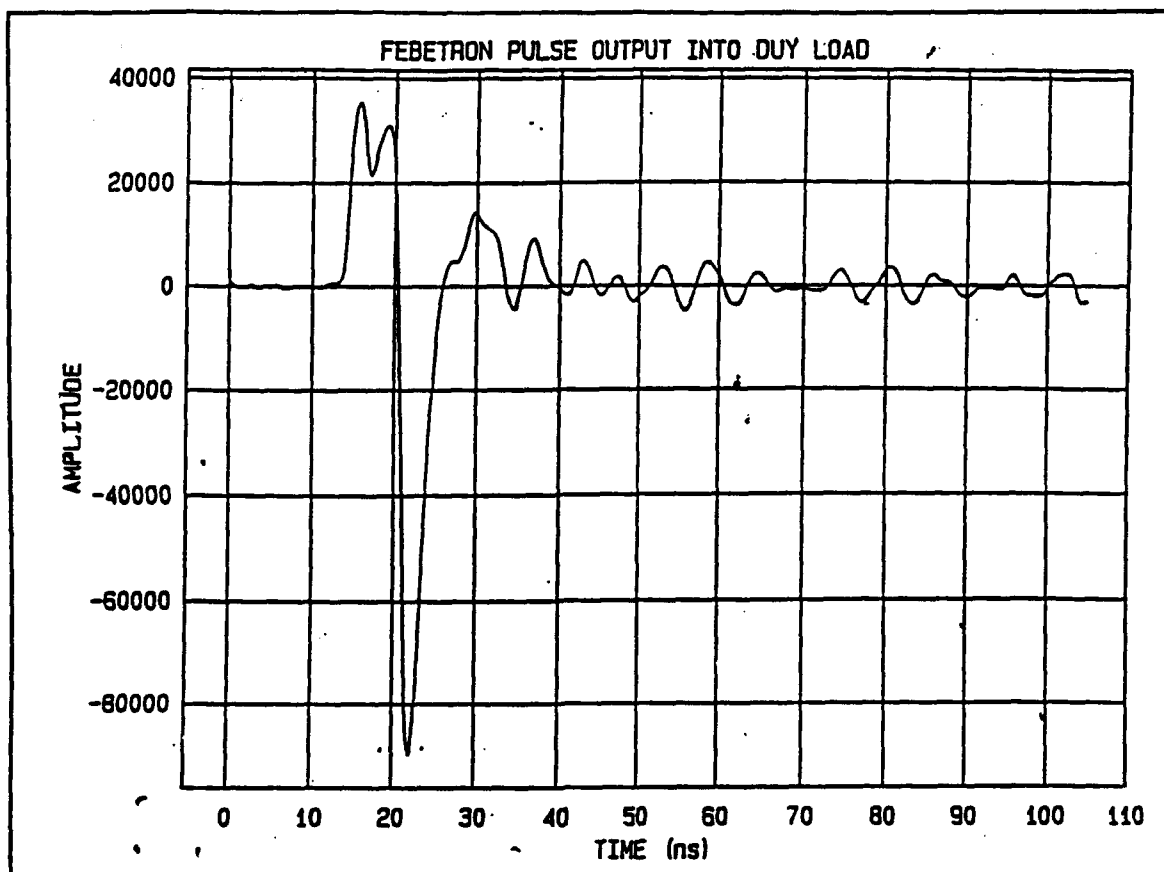


Figure 8 Febetron Output Pulse into Dummy Load
Risetime = 1.0 nanosecond (ns)
Full Width at Half Maximum (FWHM) = 2.5 ns

III. EXPERIMENT SETUP AND TEST PROCEDURES

The site chosen for the experiment was the former MX Race Track located in Area 25 at the Nevada Test Site (see Figure 9, Figure 10 and Figure 11). The radio frequency (rf) transmitter site was located near the southwest tip of the racetrack. Ground-based receiving equipment was positioned at several locations in a quadrant north and east of the transmitter site, generally within two (2) kilometers of the transmitter site (see Figure 11).[Ref. 1:p. 1]

The source antennas used for transmission were situated as shown in Figure 12. To determine the relative orientation of each receiver to the source antenna, a correction factor had to be applied. The geometry used for those calculations is shown in Figure 13. The site locations of each organization participating in the data collection was surveyed and adjusted relative to Figure 13. The corresponding data for both NPS sites are shown in Figure 14. Additionally, the locations of near and far objects in the general area were also surveyed.[Ref. 4]

Ideally, measurements would need to be taken at various locations around the source antenna covering a full 360 degrees. This would allow for data collection and signal measurement information in all directions to determine propagation characteristics along the mainlobe, sidelobes and

backlobe. As the location of the receiver sites remained stationary and were not allowed to move, the source antennas were rotated in place to simulate the receivers being moved around the periphery of the source antennas. This resulted in an absolute bearing with respect to the surveying reference point (shown in Figure 13) and the location of the receiver. To obtain a relative orientation, a correction factor had to be applied based on the specific geometry of the source antenna with the receiver site. For the two NPS sites, the geometry is shown in Figure 19 - Figure 22. The resulting calculations showing the absolute (true bearing) and the relative bearings are shown below in Table I and Table II.

Table I CASE 2 - RELATIVE ORIENTATION OF NPS RECEIVING SITE # 2 TO LLNL MODIFIED LOG PERIODIC ANTENNA

TRUE BEARING ϕ	RELATIVE BEARING θ
0 degrees	336.2 degrees
32 degrees	304.2 degrees
153 degrees	183.2 degrees
293 degrees	43.2 degrees
311 degrees	25.2 degrees
324 degrees	12.2 degrees

The measurement set-up used by the Naval Postgraduate School is shown in Figure 23. The procedure used to capture

Table II CASE 2 - RELATIVE ORIENTATION OF NPS RECEIVING SITE #2 TO TEM HORN TRANSMITTING ANTENNA

TRUE BEARING ϕ	RELATIVE BEARING θ
0 degrees	325.5 degrees
32 degrees	293.5 degrees
153 degrees	172.5 degrees
293 degrees	32.5 degrees
311 degrees	14.5 degrees
324 degrees	1.5 degrees
326 degrees	-0.48 degrees

the transmitted pulses was as follows:

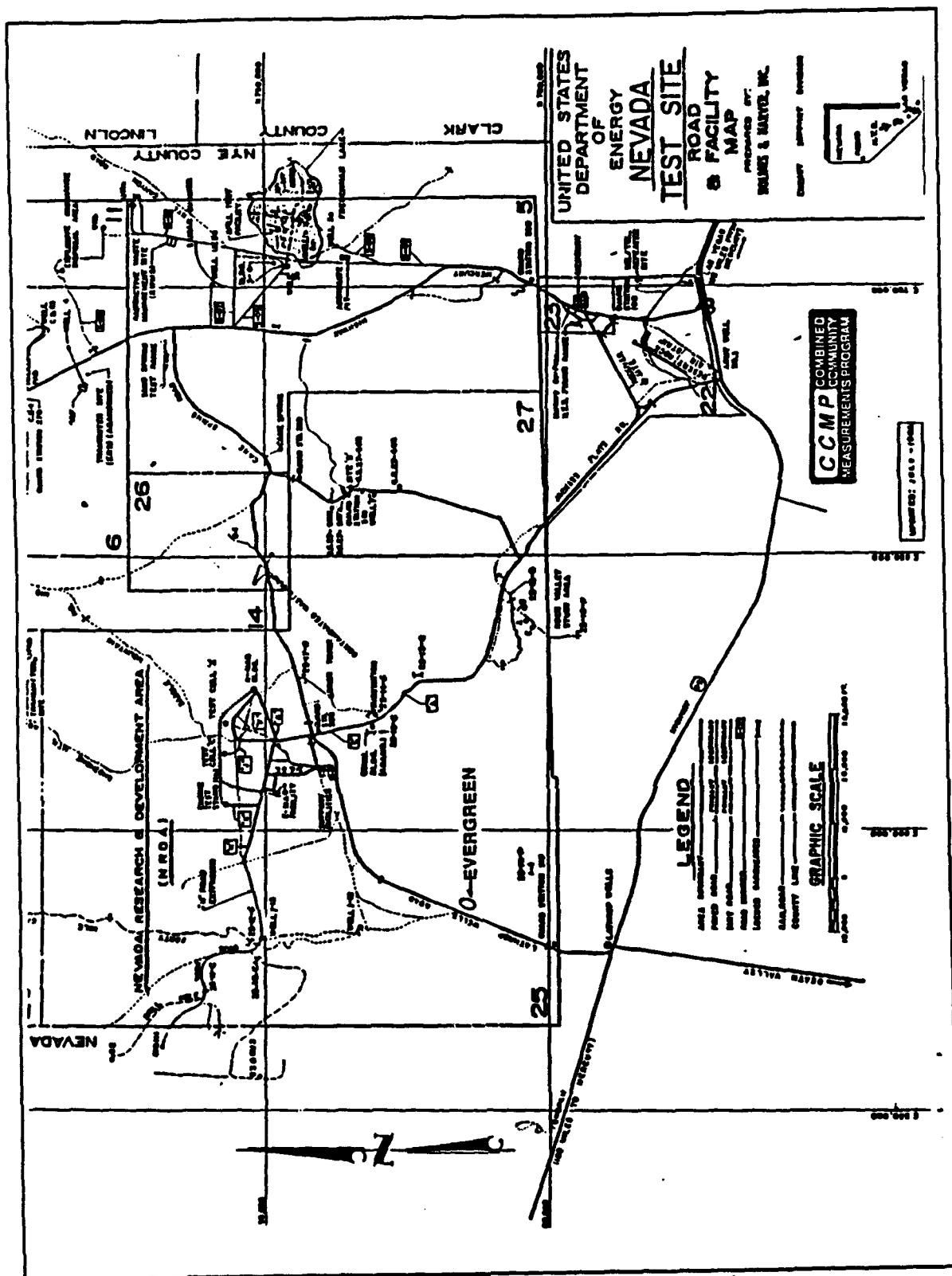
1. An L-band TEM horn antenna was used as a "trigger". This horn antenna was used to detect when the pulsed transmissions arrived. Upon receiving the first pulse, the horn triggered the oscilloscope to begin receiving the signal from the second TEM horn antenna.
2. The second horn antenna was used in the reception and collection of the transmitted pulsed signal. This antenna was oriented to collect either the vertically polarized or the horizontally polarized component of the transmitted pulsed signal.
3. The TEK 7104 Oscilloscope displayed the received signal pulse and was adjusted/calibrated to allow the TEK digital camera system to obtain a good digitized sample of the analog waveform appearing on the oscilloscope.
4. The TEK Digital Camera System (DCS) digitized the analog waveform displayed on the oscilloscope. It is important to point out that the DCS system digitized strictly what it "saw" displayed on the oscilloscope. There was no sampling done on the received pulse since the output from the TEM horn antenna was fed directly into the TEK 7104 oscilloscope. Furthermore, there was no storage of the received analog signal other than the digitized sample

taken. In other words, once the snapshot in time had occurred, there was no way to redigitize the signal by "calling it up again".

5. A hard copy photo was simultaneously taken at the same time the digitized sample of the analog waveform was taken.

To account for the time delay occurring between the time the L-band antenna triggered the oscilloscope and the time the analog signal was digitally captured, a shorter cable was used to connect the TEM horn antenna oriented to capture a specific polarization to the oscilloscope so the signal would arrive at the oscilloscope in time to be completely captured. Furthermore, the time base on the oscilloscope was adjusted when a close-up of the transmitted signal was to be seen. Specifically, if the front part of the transmitted signal seen on the oscilloscope was to be captured and digitized, the time base was changed from 50 ns to 10 ns. This had the effect of displaying a time duration of the first 100 ns of the signal versus 500 ns on the oscilloscope (i.e $10 \text{ ns/div} * 10 \text{ div} = 100 \text{ ns}$. Similarly, $50 \text{ ns/div} * 10 \text{ div} = 500 \text{ ns window}$). As a result, in the series of shots taken and analyzed in chapter 4, it is important to point out that whether the time duration was 50 ns, 100 ns or 500 ns, the signal was the same. What changed was how much of the signal was displayed. When the objective was to capture the actual pulse minus the reflections and multipath effects, the short time duration collect times were used (i.e. 50 ns and 100 ns windows). The

different time scales do not imply pulses that were either 100 ns long or 500 ns long. All pulses generated maintained consistent waveform characteristics. The Febetron had good repeatability, producing short time duration signals with constant pulse widths and pulse shapes.



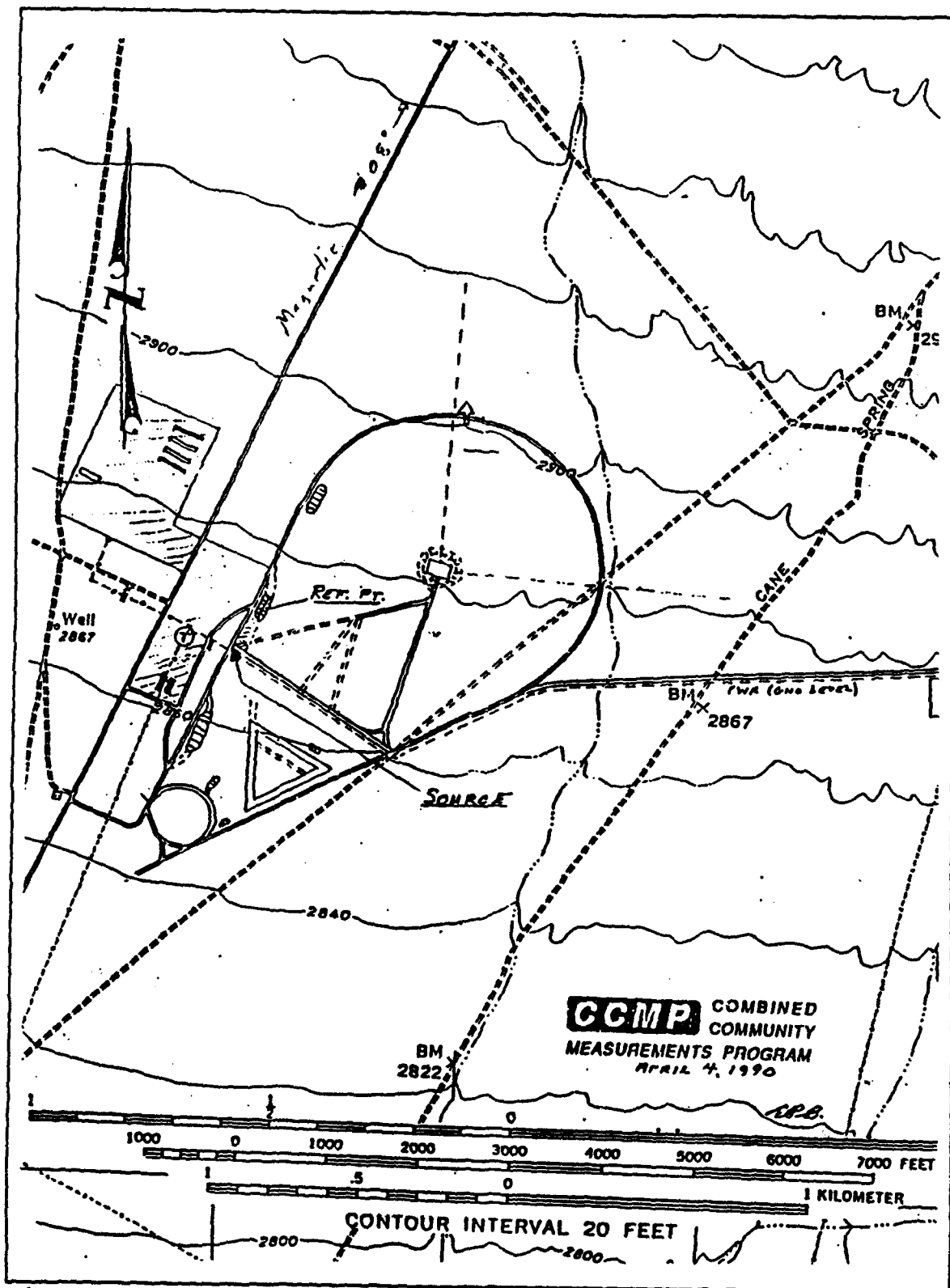


Figure 10 Project Evergreen - Nevada Test
Area 25 [former MX Race Track]

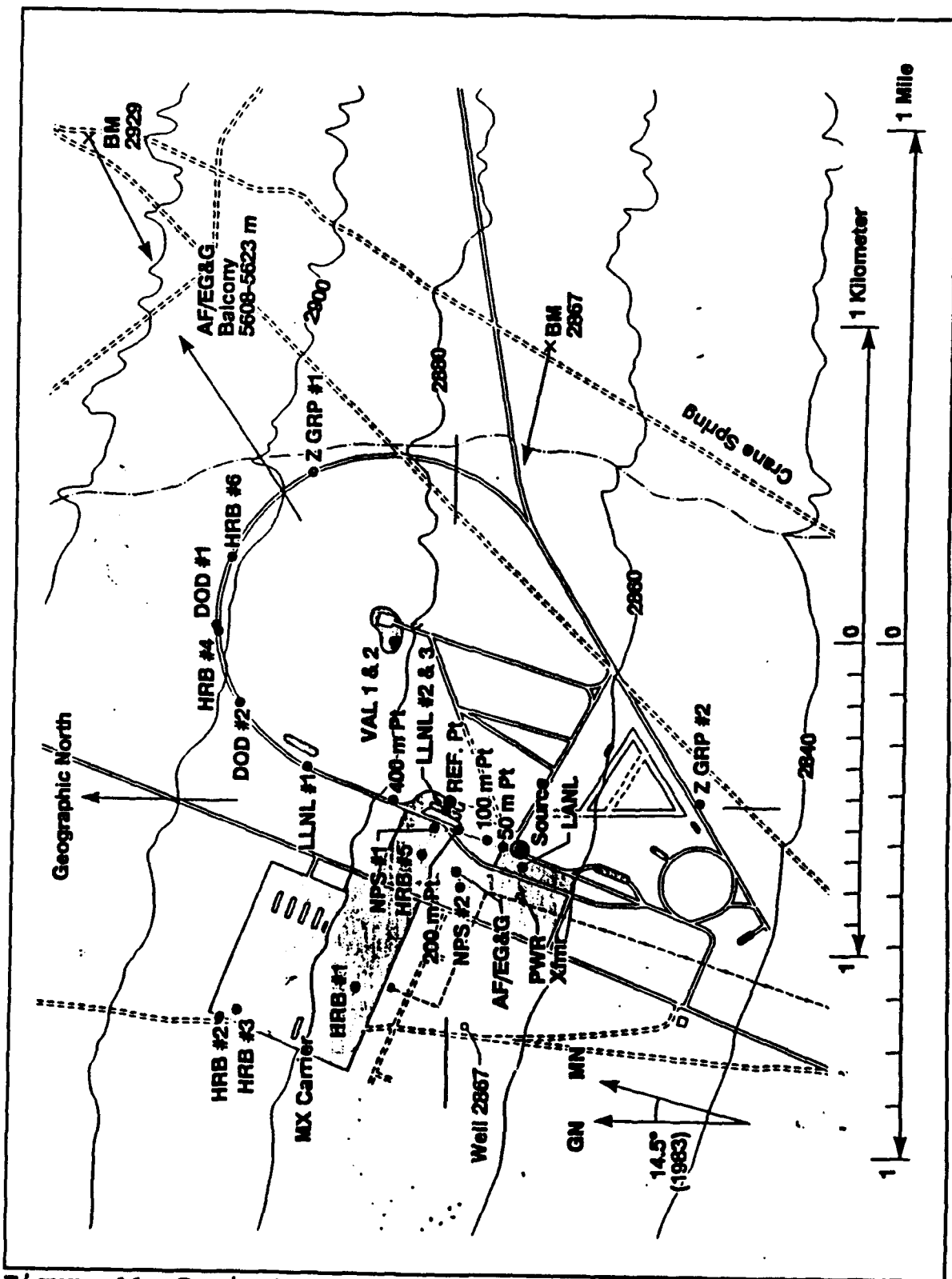
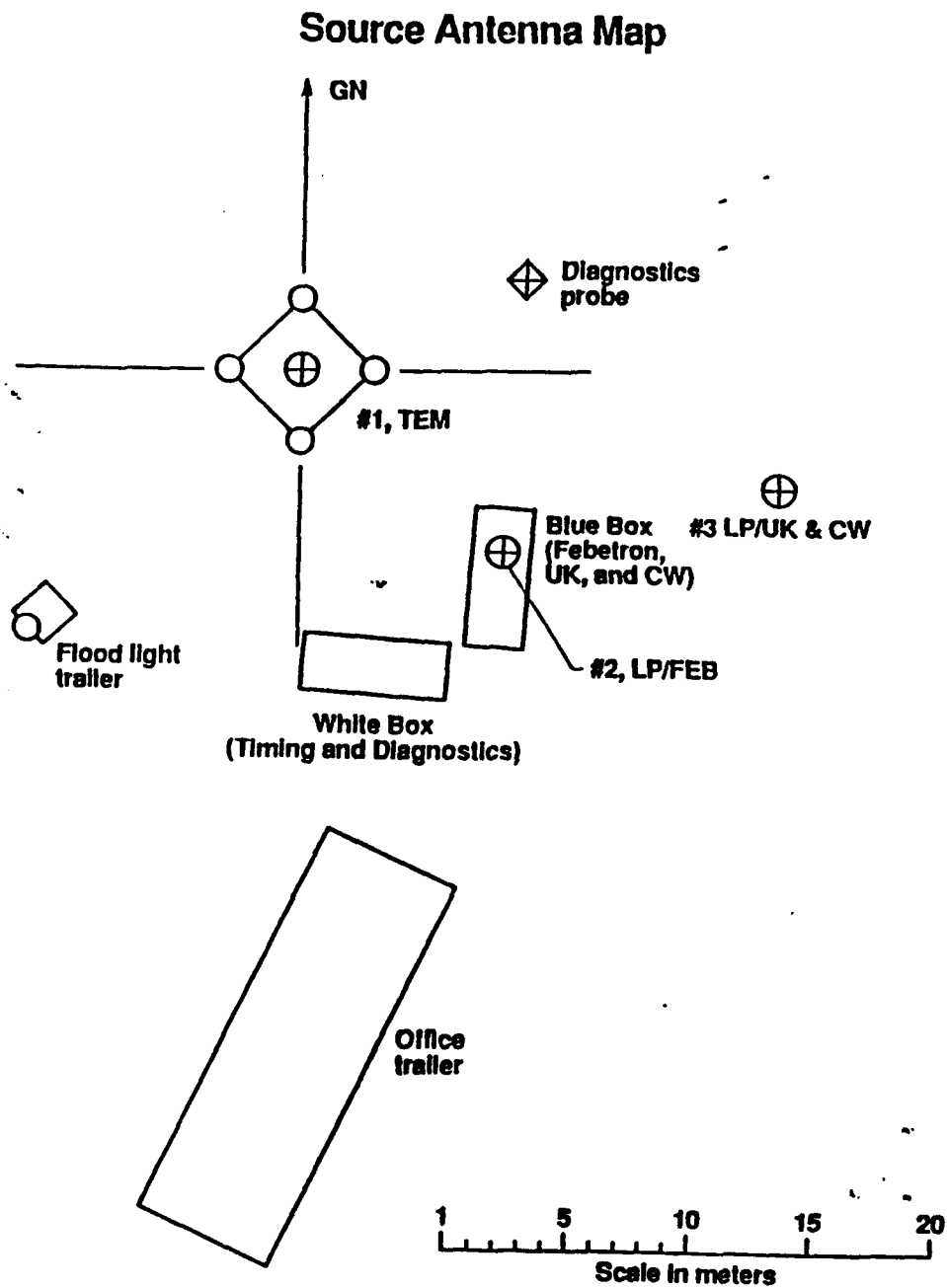


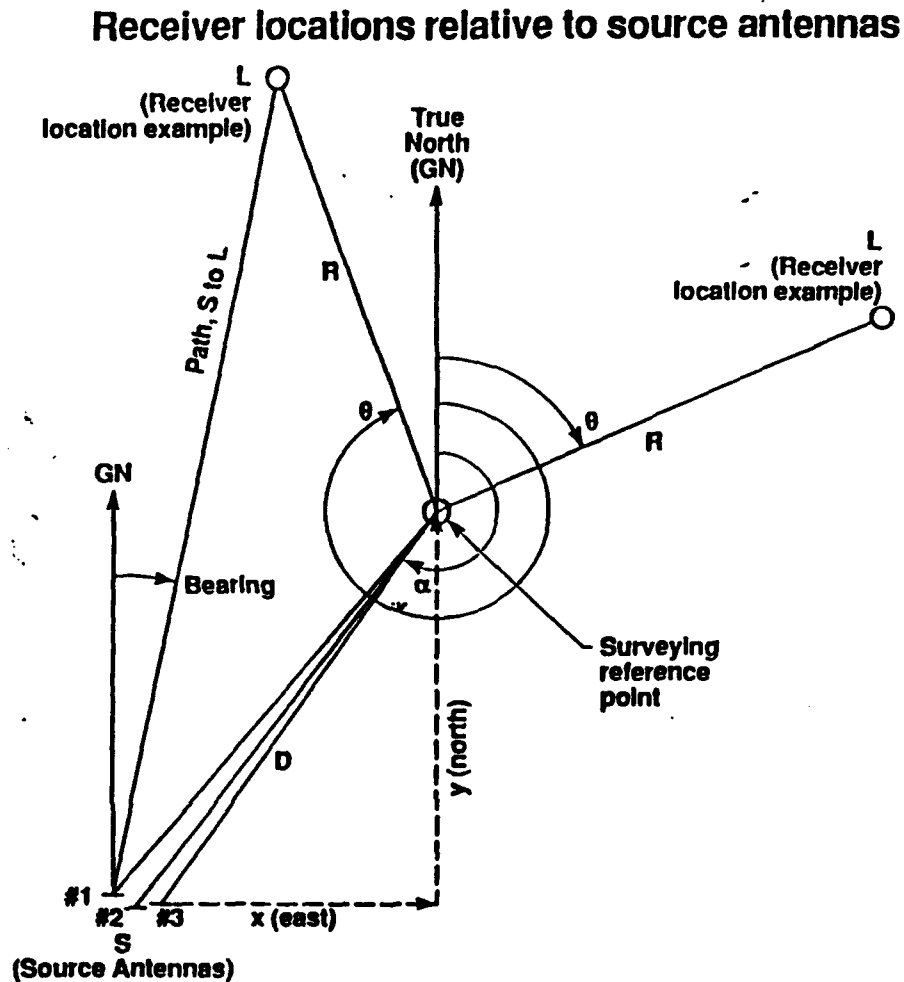
Figure 11 Project Evergreen - Nevada Test Site
Location of Transmitting and Receiving Sites



FD01-12383-000

EP 920/00

Figure 12 Project Evergreen - Source Antenna Map



Source Antenna	D (m)	α , CW from GN	x (m)	y (m)
#1, TEM	253.459	218° 23' 22" (218.3894°)	157.399	198.663
#2, LP/Feb	254.453	215° 47' 36" (215.7933°)	148.820	206.395
#3, LP/UK & CW	245.603	214° 04' 51" (214.0808°)	137.627	203.420

EPB 8/28/90

10-F 001-4-12203-002

**Figure 13 Project Evergreen -
Receiver Locations Relative to Source Antennas**

Naval Postgraduate School

Location, L	R, horiz (meters)	θ, CW from True North			Z, height above Ref (m)	Source, S	Path, horiz S to L (m)	Bearing, S to L, CW from N			Height diff L above S (m)
		deg	min	sec				deg	min	sec	
NPS, Pt #1	90.180	306°	50'	03"	-2.447	#1, TEM #2, LP/Feb. #3, LP/UK & CW	266.709 271.501 265.672	18° 16° 14°	38' 23' 15'	04" 49" 42"	2.908 0.121 2.795
NPS, Pt #2	278.151	264°	58'	10"	-3.799	#1, TEM #2, LP/Feb. #3, LP/UK & CW	211.411 222.657 226.934	325° 324° 322°	31' 49' 05'	15" 39" 01"	1.556 -1.231 1.443

DOD Locations

Location, L	R, horiz (meters)	θ, CW from True North			Z, height above Ref (m)	Source, S	Path, horiz S to L (m)	Bearing, S to L, CW from N			Height diff L above S (m)
		deg	min	sec				deg	min	sec	
DOD, Pt #1	915.508	37°	27'	12"	4.750	#1, TEM #2, LP/Feb. #3, LP/UK & CW	1168.941 1169.877 1160.776	37° 37° 36°	39' 05' 44'	22" 32" 24"	10.105 7.318 9.992
DOD, Pt #2	723.720	26°	29'	39"	4.363	#1, TEM #2, LP/Feb. #3, LP/UK & CW	973.140 975.696 967.716	29° 28° 28°	34' 54' 24'	17" 33" 51"	9.718 6.931 9.605

Figure 14 Project Evergreen - Surveyed Positional Data for Naval Postgraduate School Receiver Site Location

General Area - Near Objects, p1

Location, L	R, horiz (meters)	θ, CW from True North		Z, height above Ref (m)	Source, S	Path, horiz S to L(m)	Bearing, S to L, CW from N		Height diff L above S (m)	
		deg	min sec				deg	min sec		
A-1 Corner Pwr Pole	309.946	250°	02' 19"	-4.698	#1, TEM #2, LP/Febr. #3, LP/UK & CW	162.965 174.427 182.074	304° 305° 302°	44' 01" 12' 55" 25' 05"	304.733709° 305.215342° 302.418195°	0.657 -2.130 0.544
A-2 Xfmr Pole, North	373.706	238°	57' 56"	-5.843	#1, TEM #2, LP/Febr. #3, LP/UK & CW	162.924 171.942 182.903	272° 274° 273°	06' 35" 34' 47" 22' 15"	272.109731° 274.579959° 273.370974°	-0.488 -3.275 -0.601
A-3 Pwr Dist Pad, N-E	367.342	237°	37' 02"	-5.786	#1, TEM #2, LP/Febr. #3, LP/UK & CW	152.829 161.685 172.719	270° 273° 272°	43' 17" 25' 26" 13' 01"	270.721594° 273.423983° 272.217064°	-0.431 -3.218 -0.544
A-4 Tower Frame, on ground, N-E corner	331.836	235°	00' 43"	-5.594	#1, TEM #2, LP/Febr. #3, LP/UK & CW	114.772 124.095 134.879	274° 277° 275°	11' 25" 27' 47" 35' 31"	274.190413° 277.463061° 275.592153°	-0.239 -3.026 -0.352
B-1 Blue Box, N-E	252.260	215°	48' 10"	-5.229	#1, TEM #2, LP/Febr. #3, LP/UK & CW	11.477 2.193 10.014	121° 34° 263°	06' 04" 42' 25" 16' 50"	121.101210° 34.707074° 263.280618°	0.126 -2.661 0.013
B-2 Blue Box, S-E	257.513	215°	06' 16"	-5.337	#1, TEM #2, LP/Febr. #3, LP/UK & CW	15.196 4.340 12.729	142° 170° 235°	12' 46" 16' 57" 16' 00"	142.212889° 170.282563° 235.266896°	0.018 -2.769 -0.095
B-3 White Box, N-W	262.188	216°	46' 17"	-5.289	#1, TEM #2, LP/Febr. #3, LP/UK & CW	11.366 8.903 20.421	177° 245° 251°	44' 46" 58' 11" 08' 34"	177.746365° 245.969766° 251.142858°	0.066 -2.721 -0.047
B-4 TEM, W-corner	255.053	218°	54' 57"	-5.065	#1, TEM #2, LP/Febr. #3, LP/UK & CW	2.828 13.895 23.133	274° 304° 282°	20' 36" 52' 50" 24' 34"	274.343567° 304.880597° 282.409601°	0.290 -2.497 0.177
B-5 TEM, N-corner	251.287	218°	47' 12"	-5.127	#1, TEM #2, LP/Febr. #3, LP/UK & CW	2.789 13.583 21.175	359° 320° 290°	44' 04" 45' 50" 52' 36"	359.734667° 320.763928° 290.876669°	0.228 -2.559 0.115

Figure 15 Project Evergreen -
Surveyed Site Location of Near Objects

General Area - Near Objects, p2

Location, L	R, horiz (meters)	θ, CW from True North		Z, height above Ref (m)	Source, S	Path, horiz S to L(m)	Bearing, S to L, CW from N		Height diff L above S (m)	
		deg	min sec				deg	dec deg		
B-6 Office Trl, N-E	267.346	214°	20' 11"	214.336389°	#1, TEM #2, LP/feb. #3, LP/UK & CW	23.061 14.499 21.773	163° 187° 217°	21' 48" 50' 05" 13' 13"	163.363411° 187.834873° 217.220303°	-0.138 -2.925 -0.251
B-7 Office Trl, S-E	285.515	213°	43' 31"	213.725278°	#1, TEM #2, LP/feb. #3, LP/UK & CW	38.819 32.550 39.946	181° 197° 211°	39' 24" 20' 22" 32' 19"	181.656718° 197.339619° 211.538662°	-0.298 -3.085 -0.411
B-8 Max-Lite Trl	269.344	218°	44' 47"	218.746389°	#1, TEM #2, LP/feb. #3, LP/UK & CW	15.968 20.094 31.655	224° 259° 257°	25' 16" 28' 04" 52' 38"	224.421318° 259.467845° 257.877336°	0.220 -2.567 0.107
B-9 Xfmr Wagon, N-E corner	276.541	220°	22' 38"	220.377222°	#1, TEM #2, LP/feb. #3, LP/UK & CW	24.842 30.627 42.149	241° 261° 260°	06' 10" 58' 49" 05' 55"	241.103034° 261.980414° 260.098658°	0.052 -2.735 -0.061
B-10 Motor-Gen, N-E	280.608	220°	01' 19"	220.021944°	#1, TEM #2, LP/feb. #3, LP/UK & CW	28.192 32.754 44.336	234° 254° 255°	51' 43" 58' 10" 00' 29"	234.862122° 254.969575° 255.008157°	0.073 -2.714 -0.040
B-11 Silo Pad, N-E	300.360	226°	54' 51"	226.914167°	#1, TEM #2, LP/feb. #3, LP/UK & CW	62.304 70.553 81.755	264° 270° 268°	00' 06" 59' 30" 46' 15"	264.001734° 270.991673° 268.770847°	-0.047 -2.834 -0.160
B-12 Silo Pad, S-E	346.335	223°	28' 26"	223.473889°	#1, TEM #2, LP/feb. #3, LP/UK & CW	96.523 100.118 111.481	236° 243° 244°	55' 51" 19' 51" 32' 49"	236.930904° 243.331071° 244.547061°	-0.061 -2.848 -0.174
B-13 Silo, Center	327.597	225°	53' 35"	225.893056°	#1, TEM #2, LP/feb. #3, LP/UK & CW	83.178 89.070 100.651	249° 255° 255°	20' 30" 57' 25" 51' 38"	249.341895° 255.957219° 255.860567°	-0.045 -2.832 -0.158
B-14 Vertical Pipe	322.192	215°	24' 09"	215.402500°	#1, TEM #2, LP/feb. #3, LP/UK & CW	70.329 67.767 76.863	204° 213° 219°	34' 42" 56' 05" 37' 44"	204.578383° 213.934845° 219.629104°	-0.973 -3.760 -1.086

Figure 16 Project Evergreen -
Surveyed Site Location of Near Objects

General Area - Far Objects, p1

Location, L	R, horiz (meters)	θ, CW from True North		Z, height above Ref (m)	Source, S	Path, horiz S to L (m)	Bearing, S to L, CW from N			Height diff L above S (m)
		deg	min sec				deg	min	sec	
S-1 Horiz. Silo #1, South Most Long Pipe, S-E Corner	517.650	317°	45' 31"	0.520	#1, TEM #2, LP/Feb. #3, LP/UK & CW	612.308 622.353 623.224	341°	51'	50"	341.864118° 341.335133° 340.272589°
S-2 Horiz. Silo #1, South Most Long Pipe, N-E Corner	520.302	318°	19' 50"	0.639	#1, TEM #2, LP/Feb. #3, LP/UK & CW	616.837 626.848 627.650	342°	12'	17"	342.204853° 341.674225° 340.618780°
S-3 Horiz. Silo #1, South Most Long Pipe, S-W Corner	565.077	315°	25' 19"	0.051	#1, TEM #2, LP/Feb. #3, LP/UK & CW	647.012 657.387 658.951	338°	18'	04"	338.301230° 337.855667° 336.856623°
S-4 Horiz. Silo #2, Long Pipe, S-E Corner	539.544	322°	07' 39"	0.522	#1, TEM #2, LP/Feb. #3, LP/UK & CW	648.307 658.085 658.431	344°	26'	49"	344.446974° 343.907913° 342.900220°
S-6 Horiz. Silo #3, Long Pipe, S-E Corner	563.476	326°	03' 14"	1.035	#1, TEM #2, LP/Feb. #3, LP/UK & CW	684.413 693.940 693.823	346°	43'	00"	346.716822° 346.174134° 345.217798°
S-8 Horiz. Silo #4, North Most Long Pipe, S-E Corner	591.089	329°	47' 13"	1.612	#1, TEM #2, LP/Feb. #3, LP/UK & CW	723.149 732.429 731.879	348°	50'	00"	348.833386° 348.292131° 347.386764°
S-9 Horiz. Silo #4, North Most Long Pipe, S-W Corner	633.154	326°	52' 58"	1.576	#1, TEM #2, LP/Feb. #3, LP/UK & CW	752.948 762.608 762.716	345°	29'	58"	345.499690° 345.021136° 344.151042°
S-10 Horiz. Silo, Short Pipe, S-E Corner	546.753	313°	50' 18"	0.149	#1, TEM #2, LP/Feb. #3, LP/UK & CW	624.098 634.528 636.220	337°	41'	04"	337.684674° 337.233148° 336.199900°

Figure 17 Project Evergreen -
Surveyed Site Location of Far Objects

General Area - Far Objects, p2

Location, L	R, horiz (meters)	θ, CW from True North			Z, height above Ref (m)	Source, S	Path, horiz S to L(m)	Bearing, S to L, CW from N			Height diff L above S (m)	
		deg	min	sec				deg	min	sec		
PP-1 Corner Pwr Pole South of Silo Area	640.990	273°	18'	16"	273.304444°	#1, TEM #2, LP/Feb. #3, LP/UK & CW	536.976 548.086 556.848	296° 296° 295°	01' 21' 34'	32" 30" 22"	296.025646° 296.358462° 295.572815°	1.206 -1.581 1.093
PP-2 Fenced Pwr Pole & Xfour Area South of Silo Area N-E Corner	604.553	287°	31'	22"	287.522778°	#1, TEM #2, LP/Feb. #3, LP/UK & CW	566.186 577.735 584.102	312° 312° 311°	15' 14' 17'	00" 44" 28"	312.250015° 312.245570° 311.291313°	2.866 0.079 2.753
MX-1 MX Carrier Vehicle, S-E Corner	822.731	302°	35'	07"	302.585278°	#1, TEM #2, LP/Feb. #3, LP/UK & CW	836.033 847.468 852.443	320° 320° 319°	08' 01' 19'	23" 46" 28"	320.139870° 320.029691° 319.324634°	5.146 2.359 5.033
MX-2 MX Carrier Vehicle, S-W Corner	872.513	302°	06'	11"	302.103056°	#1, TEM #2, LP/Feb. #3, LP/UK & CW	881.527 892.999 898.225	318° 318° 317°	42' 37' 57'	33" 23" 42"	318.709356° 318.623140° 317.961912°	4.881 2.094 4.768
Misc. Pl. #1 Tail Junk Near MX Carrier Vehicle, N-E Corner	812.097	294°	19'	39"	294.327500°	#1, TEM #2, LP/Feb. #3, LP/UK & CW	789.759 801.308 807.617	312° 312° 311°	27' 27' 46'	57" 34" 04"	312.465979° 312.459662° 311.767856°	3.745 0.958 3.632
Misc. Pl. #2 S-W Corner of Graded Silo & Junk Area	895.406	289°	58'	32"	289.975556°	#1, TEM #2, LP/Feb. #3, LP/UK & CW	850.069 861.563 868.841	306° 306° 305°	24' 29' 53'	31" 02" 14"	306.408731° 306.483929° 305.887280°	2.806 0.019 2.693
Misc. Pl. #3 S-E Corner of Graded Silo & Junk Area Near Road	321.848	287°	07'	08"	287.118889°	#1, TEM #2, LP/Feb. #3, LP/UK & CW	329.607 340.424 343.199	332° 332° 330°	53' 12' 18'	32" 00" 54"	332.892394° 332.200089° 330.315076°	2.997 0.210 2.884

Figure 18 Project Evergreen -
Surveyed Site Location of Far Objects

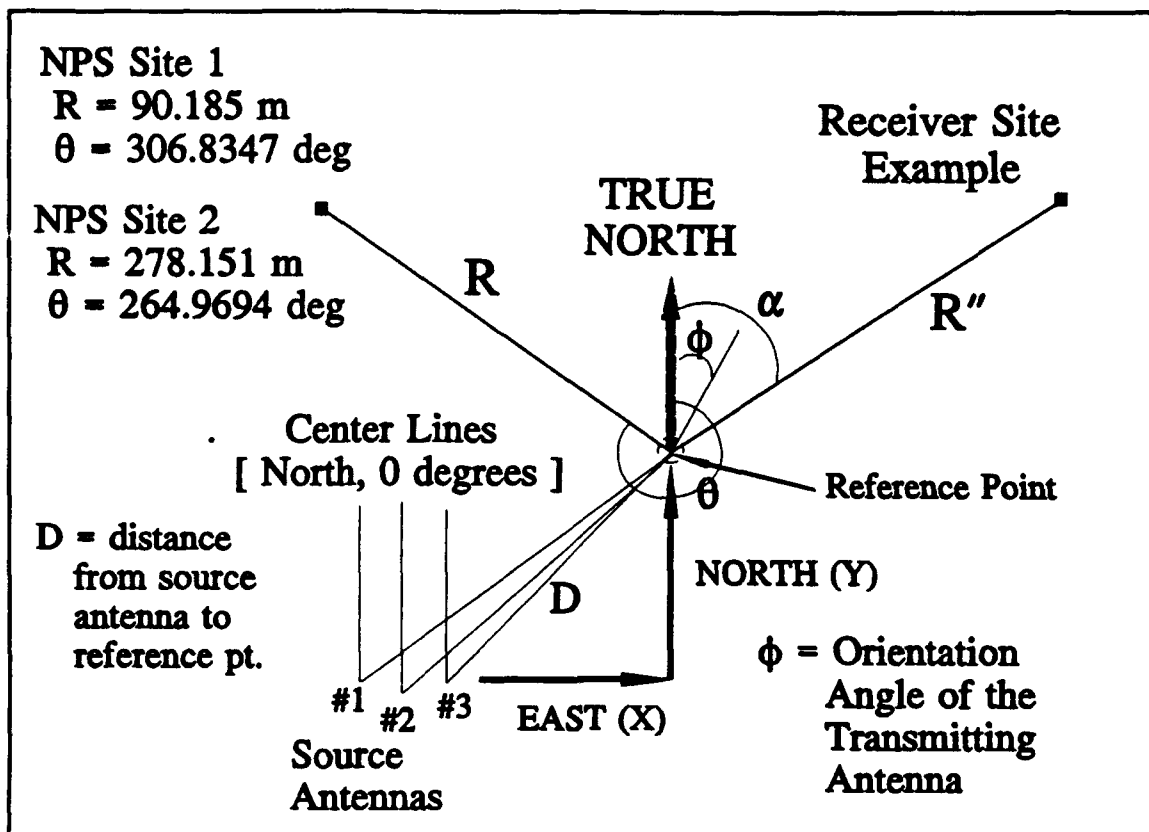


Figure 19 Project Evergreen - CASE 1 and CASE 2
 Relative Orientation of NPS Site to Source Antennas
 Surveying Corrections for Receiver Sites

Table III SURVEYING CORRECTIONS FOR RECEIVER SITES

ANTENNAS	α (degrees)	D (meters)	X (meters)	Y (meters)
#1, TEM	38.3894	253.459	157.399	198.663
#2, LP-PULSED	35.7933	254.453	148.820	206.395
#3, LP-CW	34.0808	245.603	137.627	203.420

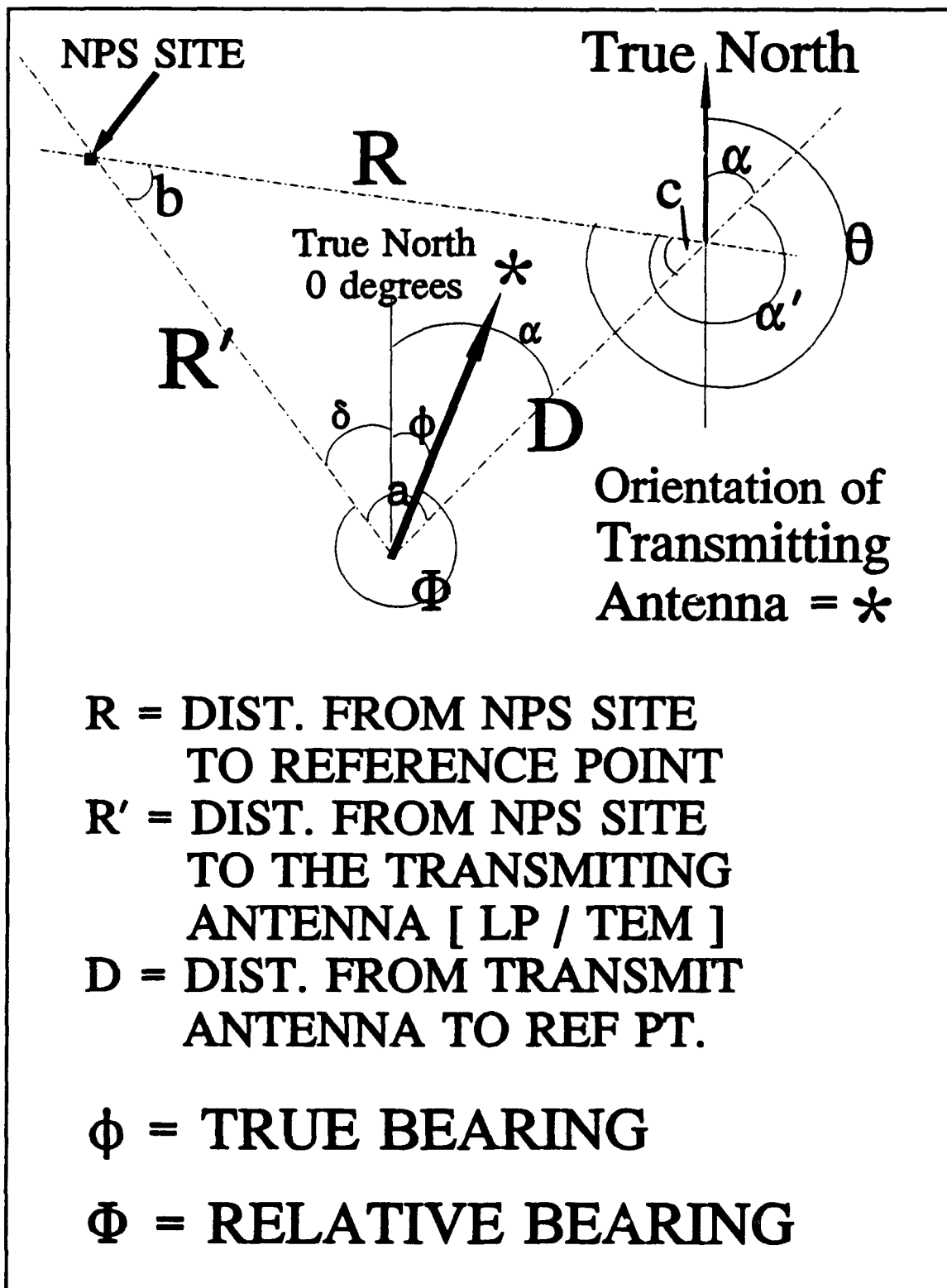


Figure 20 Project Evergreen - CASE 2
Surveying Site Correction for NPS Receiving Site 2

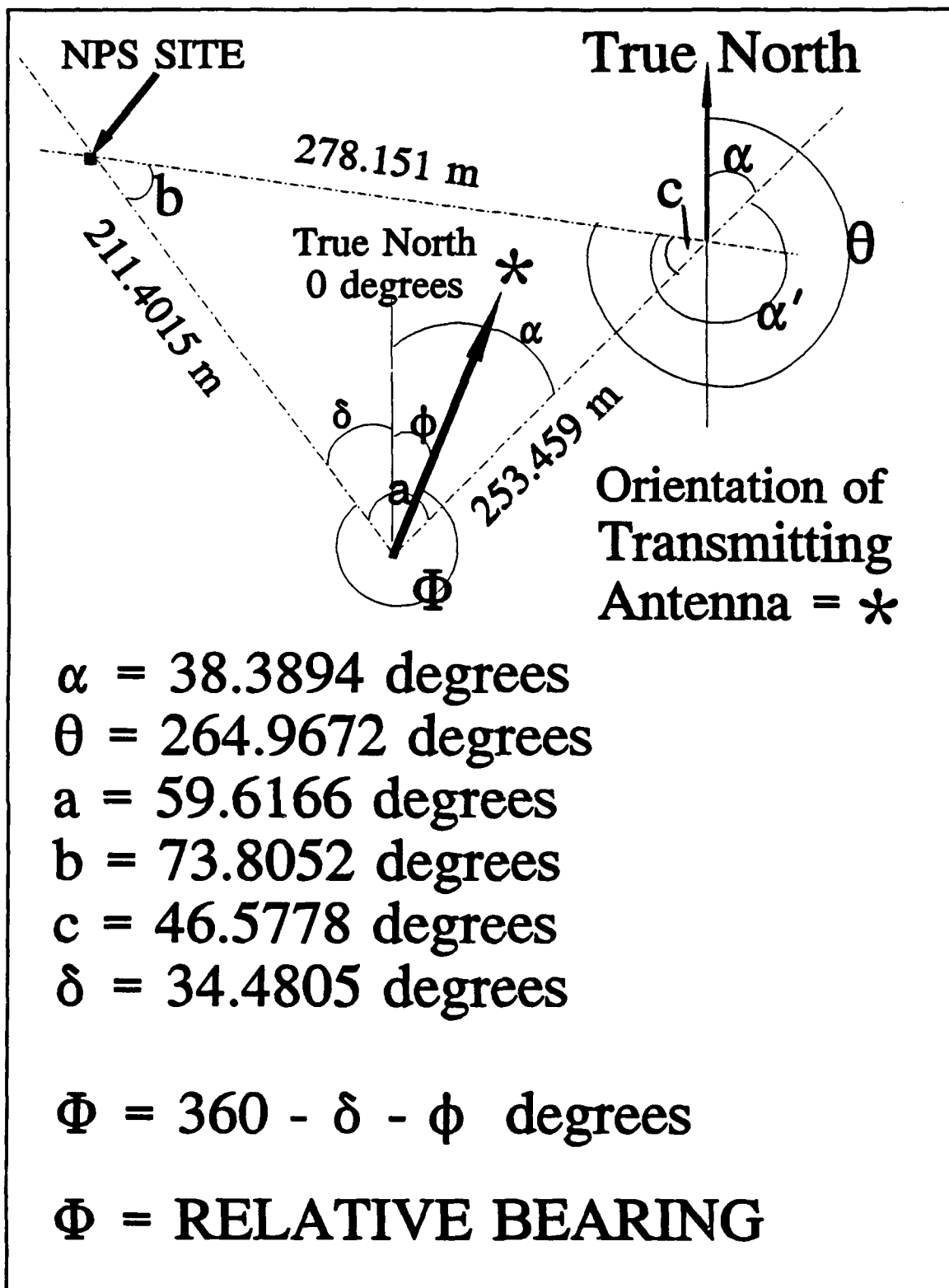


Figure 21 Project Evergreen - CASE 2
Relative Orientation of NPS Site 2 to TEM Horn Antenna

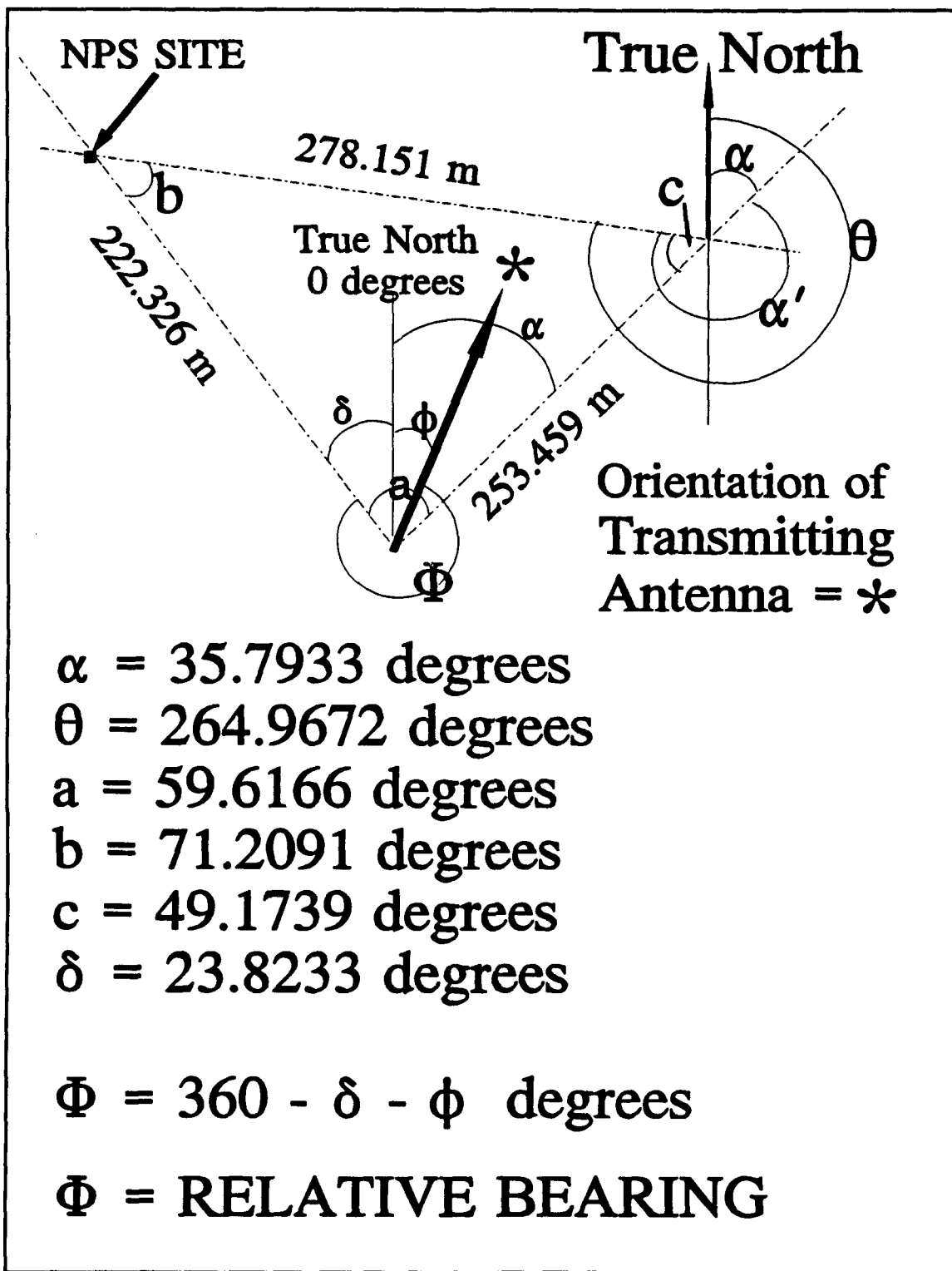


Figure 22 Project Evergreen - CASE 2
Relative Orientation of NPS Site 2 to LLNL LP Antenna

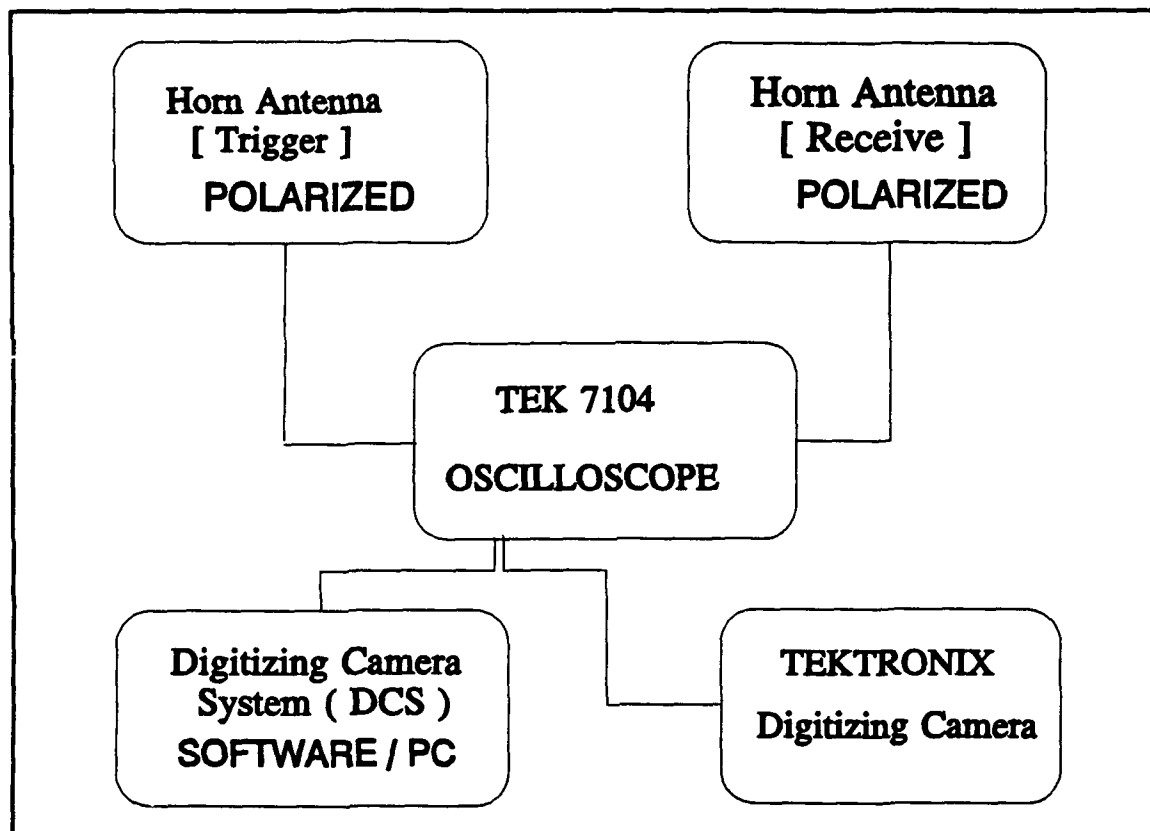


Figure 23 Project EVERGREEN
Naval Postgraduate School Test Site Experimental Setup

IV. DATA ANALYSIS

A. ANALYSIS METHODOLOGY

In analyzing the digitized waveforms, I went through a series of steps to obtain the power spectral density (PSD) of each waveform analyzed. To compute the PSD, I used MATLAB. MATLAB is a computer software program developed by The MathWorks, Inc. MATLAB is based on vector mathematics and is ideally suited for signals analysis. The analysis proceeded in the following manner:

1. Step 1 - The Tektronix Digitizing Camera System (DCS) upon digitizing the analog waveform displayed on the oscilloscope introduced a false DC level. A combination of the oscilloscope calibration setup procedures and the DCS operating system, this induced DC level led to a portion of the energy appearing at zero frequency (i.e. a DC term). A well established fact in electromagnetic theory is that a signal must be time varying in order to propagate and likewise a direct current signal cannot propagate. To correct for this anomaly induced during the digitizing process, I subtracted the DC level from the digitized signal prior to computing the power spectral density and the power and energy waveforms. The associated ASCII data file for the digitized waveform was saved and edited. This ASCII data file contained the text header and the sampled data point values. This file was broken up into two files: one containing only the text header information and the second containing only the sampled data point values. This was necessary since the MATLAB program used to compute the PSD will only accept data files (i.e files containing numbers).
2. Step 2 - I then computed the power waveform in the time domain by squaring the voltage versus time waveform.
3. Step 3 - The next waveform generated was the energy output as a function of time. This waveform was

generated by integrating the power versus time waveform obtained in step 2.

4. Step 4 - Using MATLAB, I then computed the power spectral density of the waveform. This was accomplished by importing the ASCII data file containing the sampled data points for the signal into MATLAB and running the program I wrote to compute the PSD of the signal. A copy of the program is included in Appendices A - F.
5. Step 5 - Upon completing the PSD calculations, I printed the outputs before proceeding to the next digitized waveform and repeating the procedure.
6. Two programs were used in accomplishing the above analysis. The DCS program and the associated directories containing the files of the digitized waveforms were used in printing out the voltage versus time, power versus time and energy versus time waveforms. The MATLAB program was used to compute the energy versus time waveform, power versus time waveform and PSD of the digitized waveforms.

Initially, when I computed the PSD of each waveform, I produced four outputs, each successive output a zoomed in version of the previous graph. This was done to show greater detail when analyzing the PSD to determine at what frequencies the energy resided. Additionally, I produced four additional plots of the same PSD output on a semilog scale. This was done to provide greater detail at the lower power levels. For the sake of brevity and not overburdening the reader with information, I have included all plots and graphical output used in analyzing the Evergreen data in the addendum to this report. For illustrative purposes, however, I have included a complete set of graphical output illustrating the above stated procedures in Figure 24 through Figure 45.

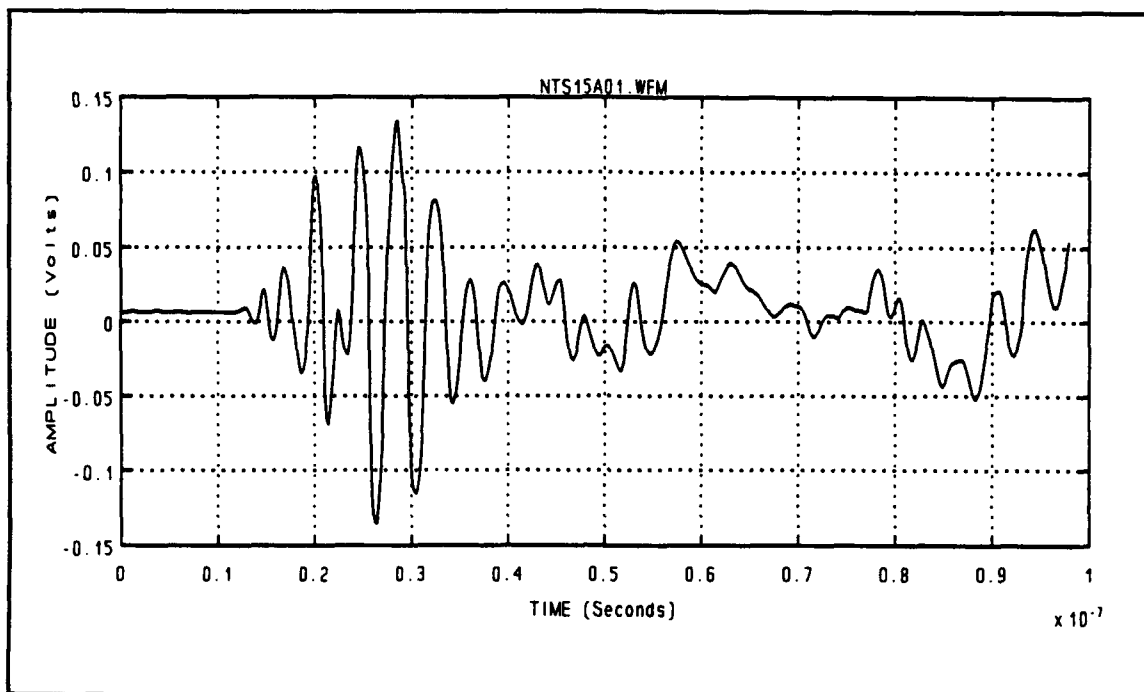


Figure 24 Waveform NTS15A01.WFM - Directory 5-8-90
LLNL Log Periodic Antenna - DC Level = +6.48 mV

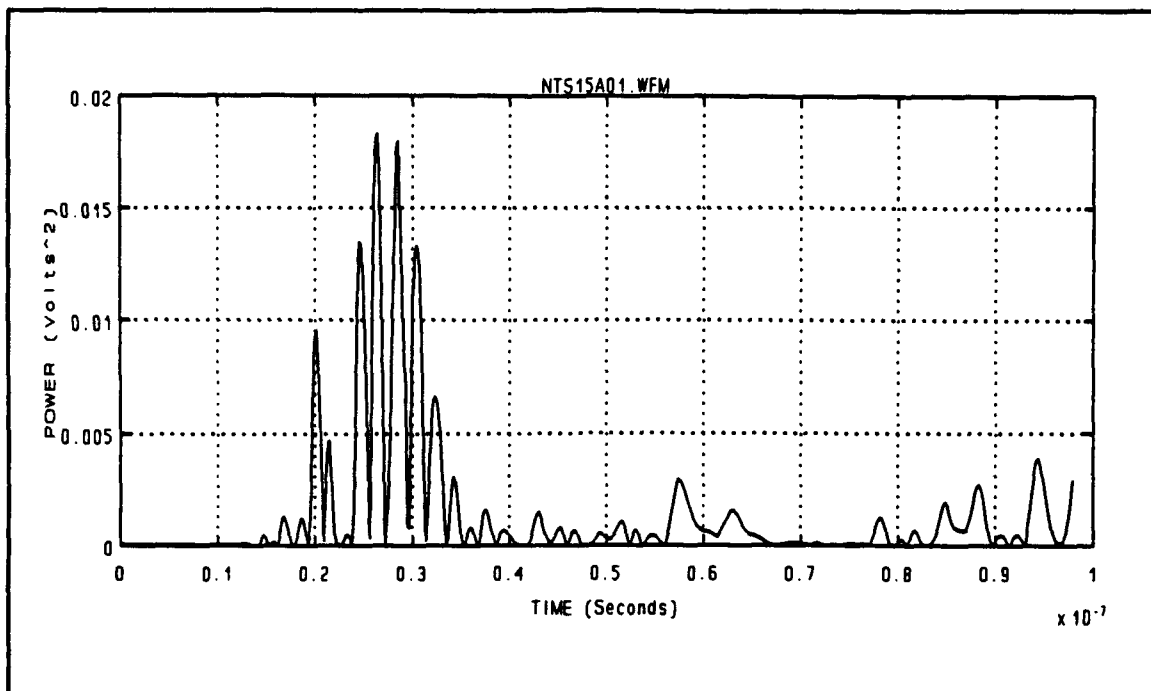


Figure 25 Waveform NTS15A01.WFM - LLNL Log Periodic Power versus Time Graph - DC Level = + 6.48 mV

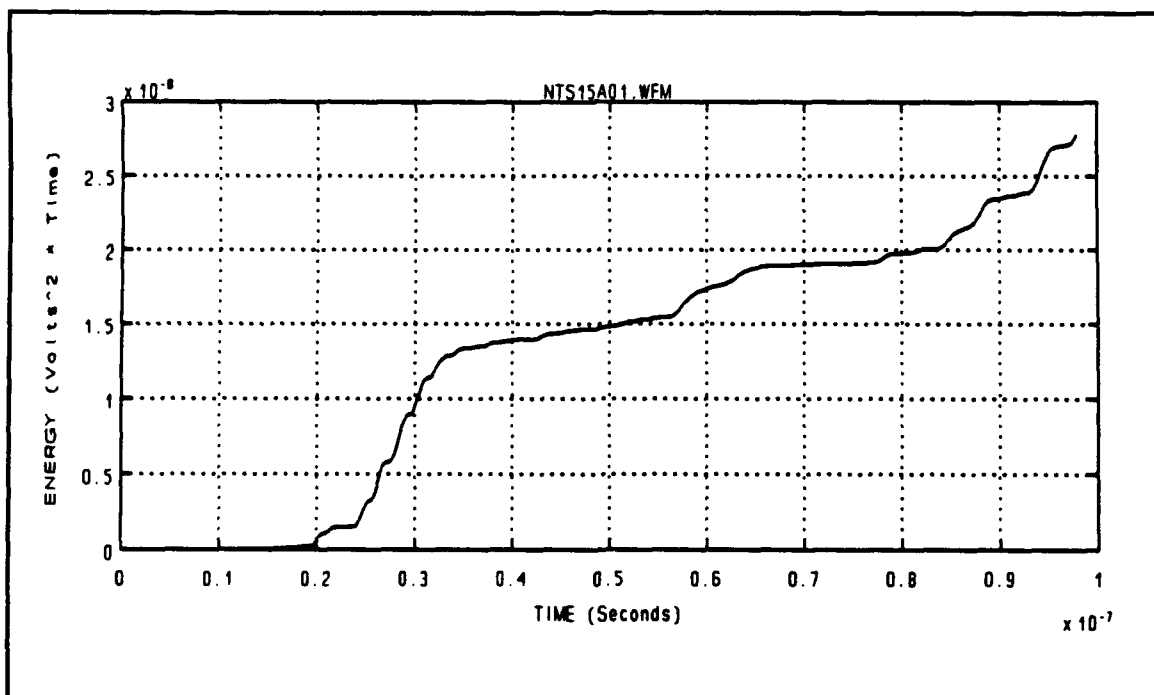


Figure 26 Waveform NTS15A01.WFM - LLNL Log Periodic Energy versus Time Graph - DC Level = + 6.48 mV

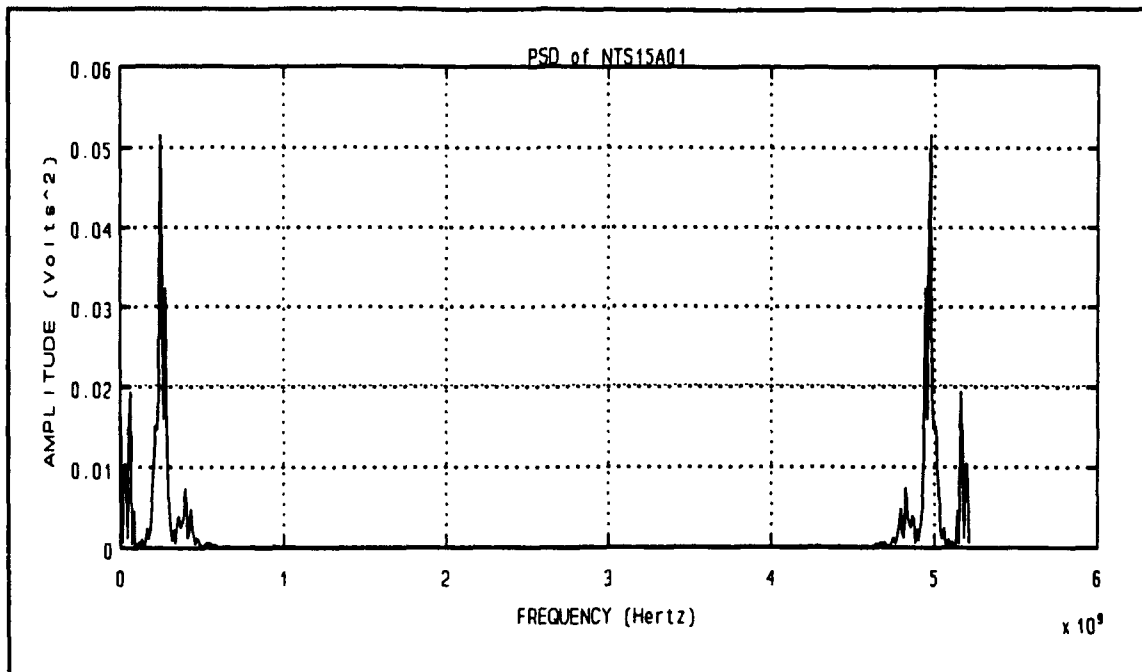


Figure 27 Waveform NTS15A01.WFM - Power Spectral Density
 Frequency Range = 0 Hz to F_s (Sampling Frequency)
 Spectra at 5 GHz is mirror image of spectra at 0 Hz which
 is an artifact induced by the periodicity of F_s at 5 GHz

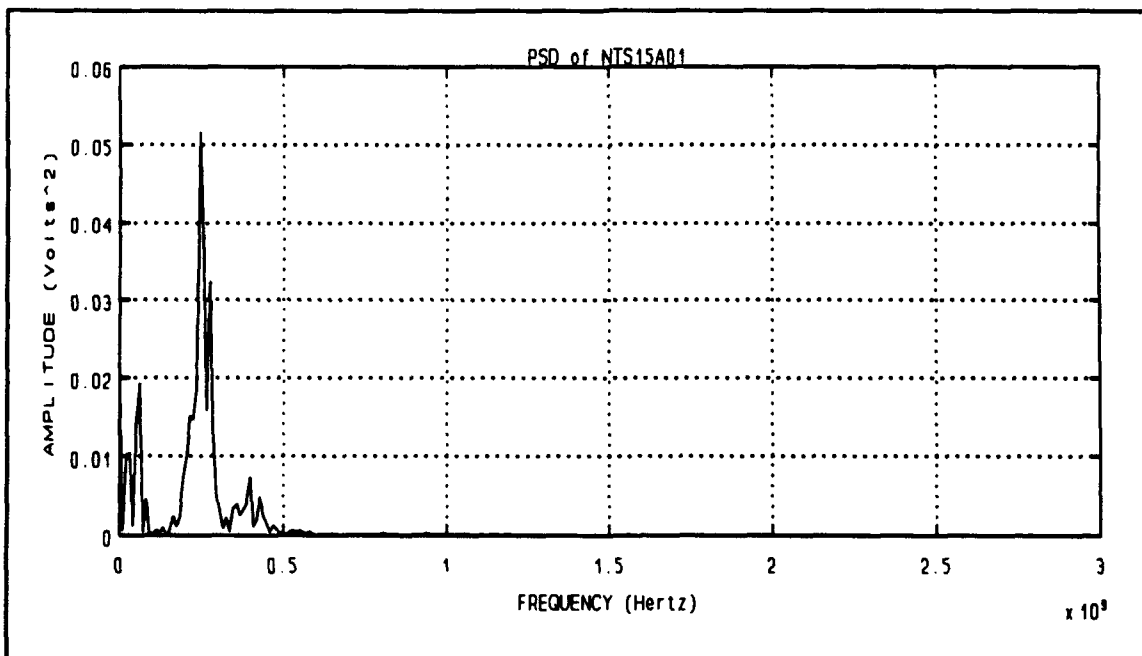


Figure 28 Waveform NTS15A01.WFM - LLNL Log Periodic
 Power Spectral Density - DC Level = + 6.48 mV
 Frequency Range = 0 Hz to $F_s/2$

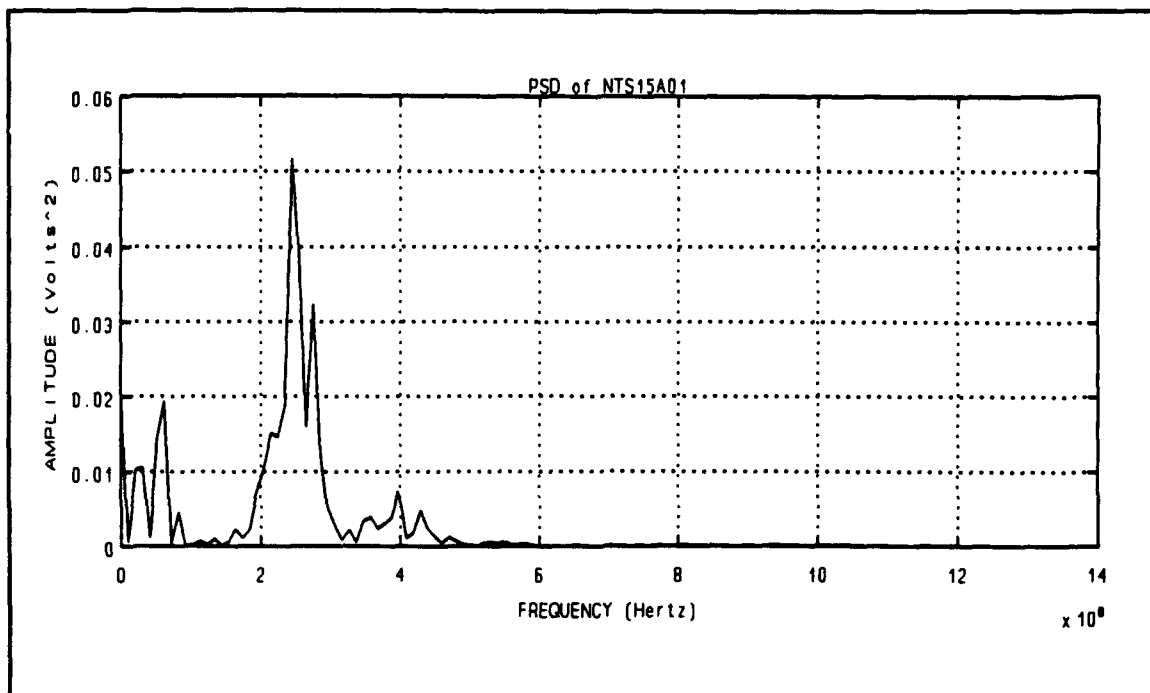


Figure 29 Waveform NTS15A01.WFM - LLNL Log Periodic Power Spectral Density - DC Level = + 6.48 mV
Frequency Range = 0 Hz to $F_s/4$

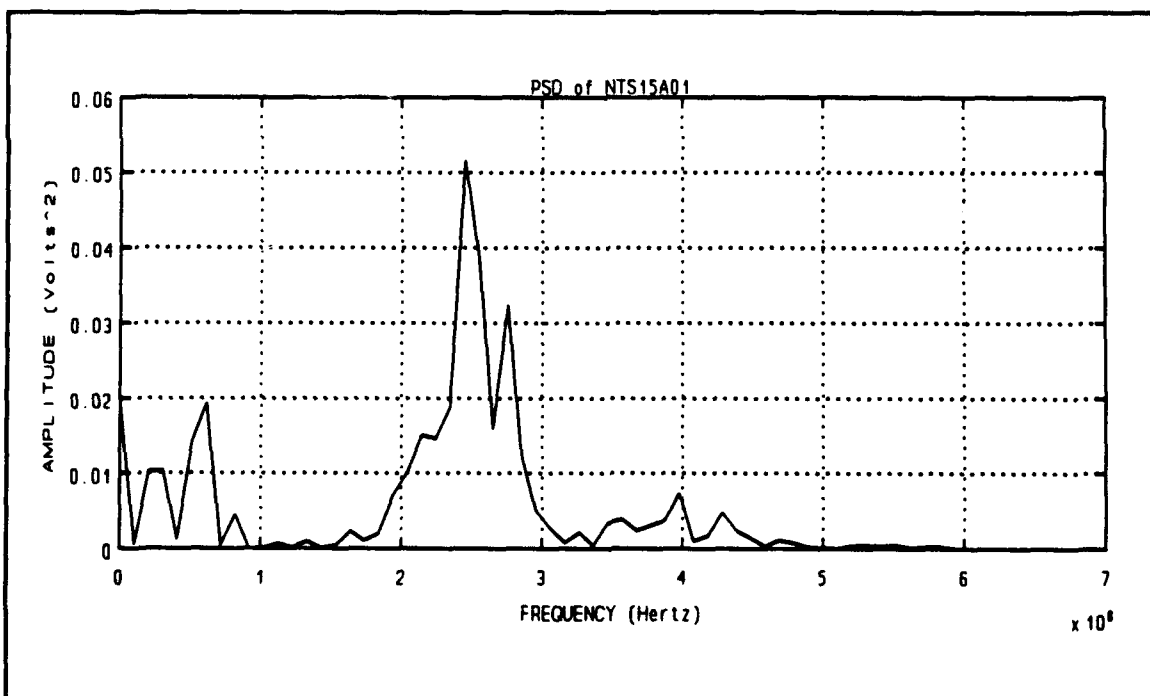


Figure 30 Waveform NTS15A01.WFM - LLNL Log Periodic Power Spectral Density - DC Level = + 6.48 mV
Frequency Range = 0 Hz to $F_s/8$

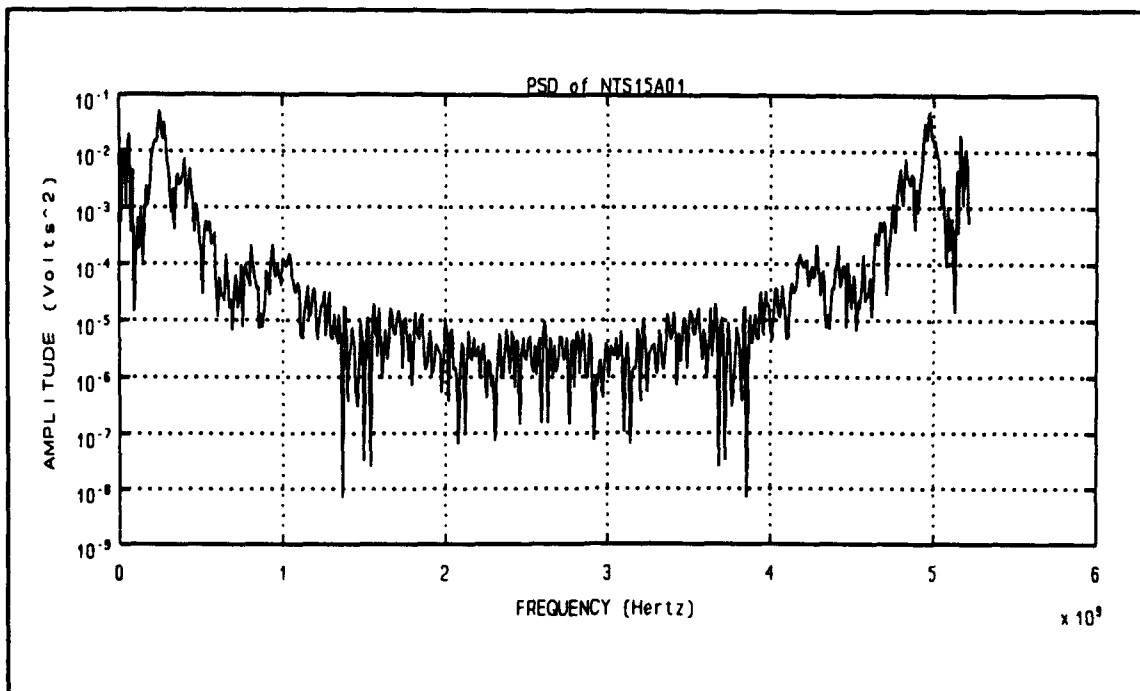


Figure 31 Waveform NTS15A01.WFM - LLNL Log Periodic Power Spectral Density - DC Level = + 6.48 mV Semilog (Y-axis), Log (X-axis) plot

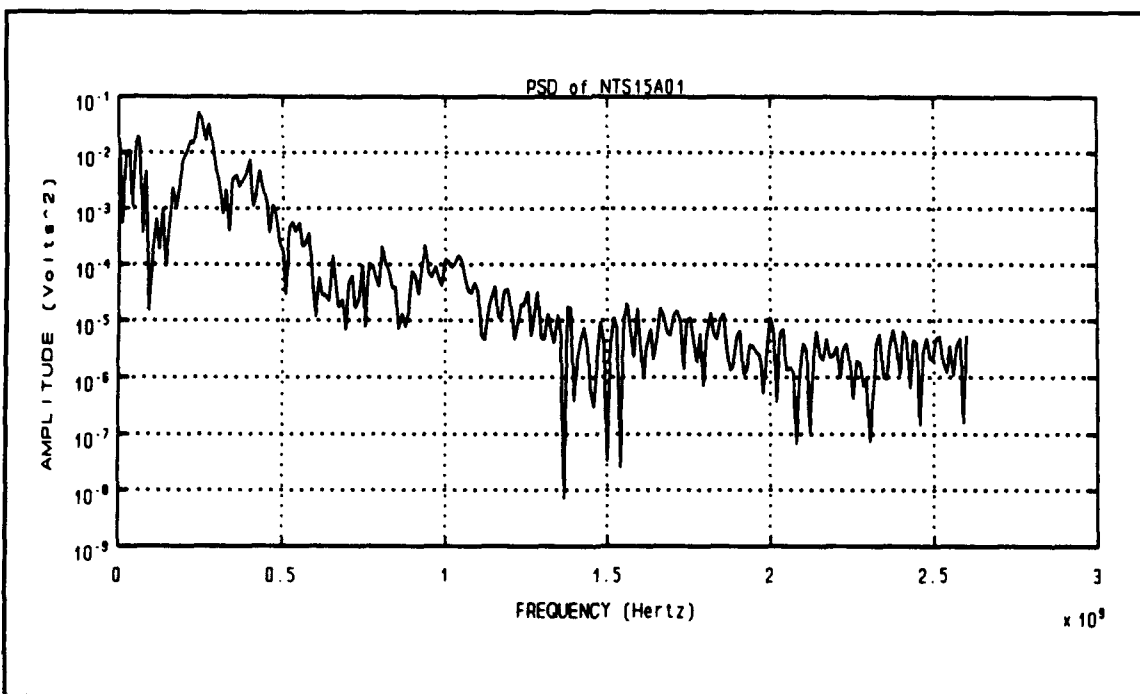


Figure 32 Waveform NTS15A01.WFM - LLNL Log Periodic Power Spectral Density - DC Level = + 6.48 mV Semilog (Y-axis), Log (X-axis) plot

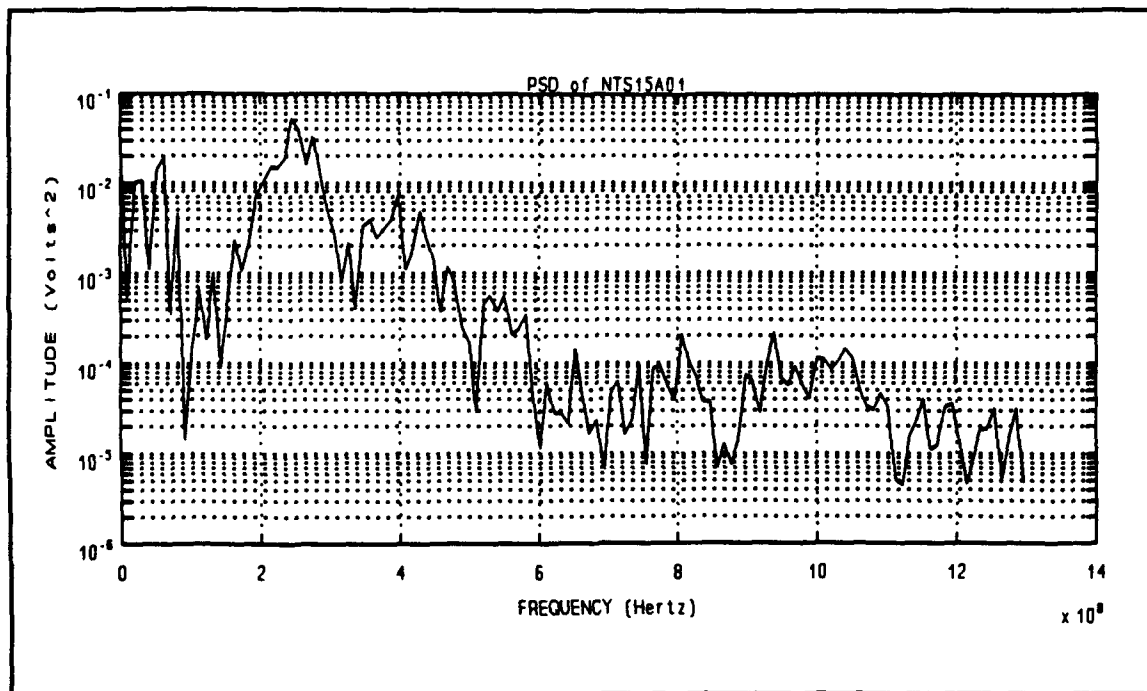


Figure 33 Waveform NTS15A01.WFM - LLNL Log Periodic Power Spectral Density - DC Level = + 6.48 mV Semilog (Y-axis), Log (X-axis) plot

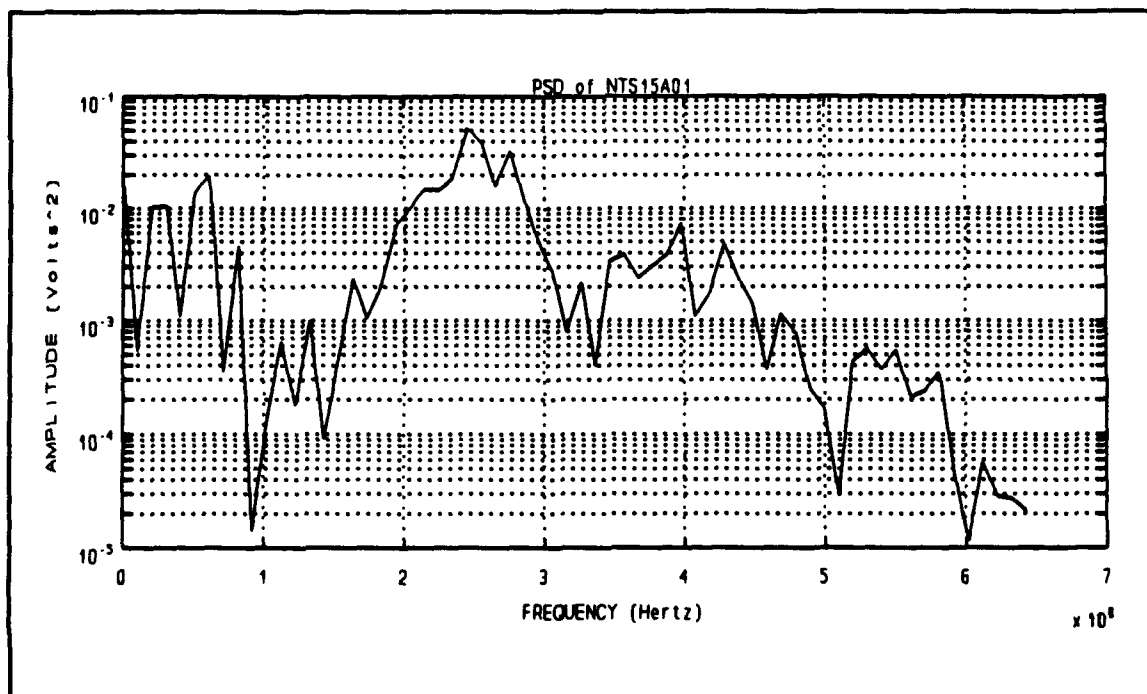


Figure 34 Waveform NTS15A01.WFM - LLNL Log Periodic Power Spectral Density - DC Level = + 6.48 mV Semilog (Y-axis), Log (X-axis) plot

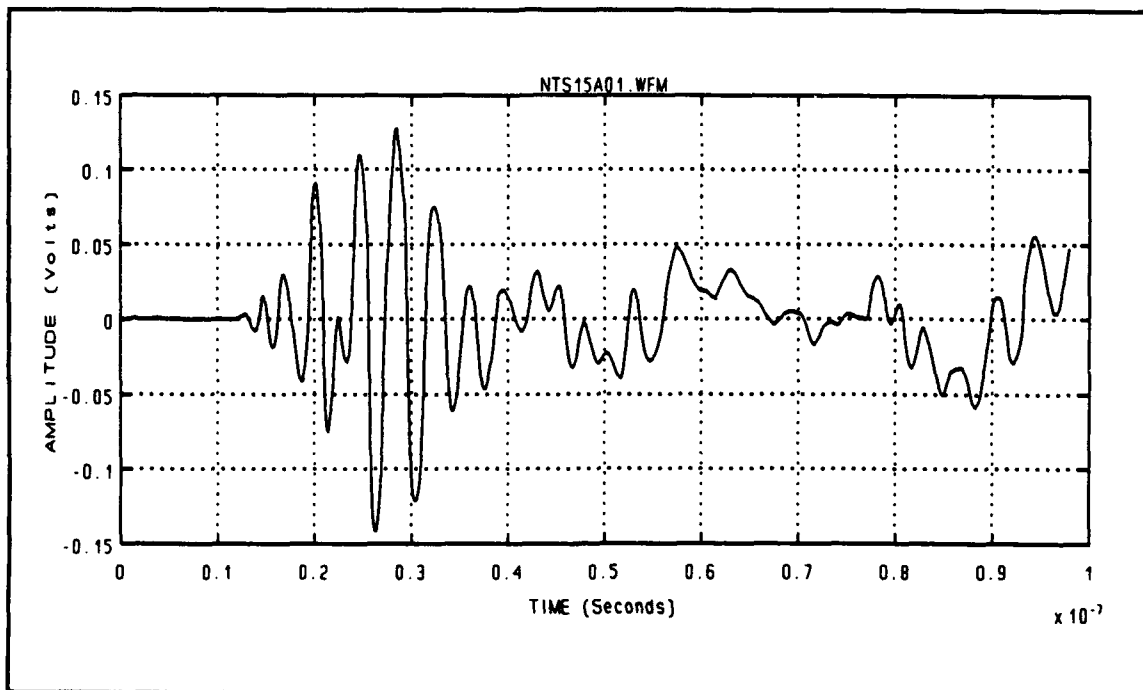


Figure 35 Waveform NTS15A01.WFM - Directory 5-8-90
LLNL Log Periodic Antenna - DC Offset = - 6.48 mV

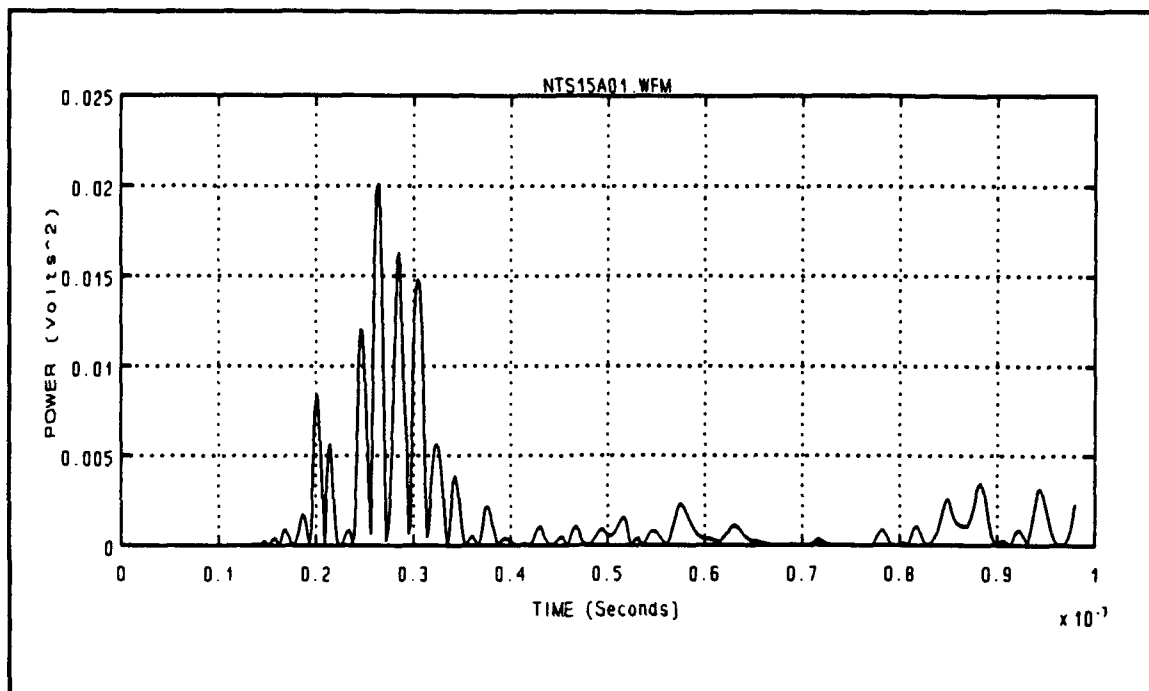


Figure 36 Waveform NTS15A01.WFM - LLNL Log Periodic Power versus Time Graph - DC Offset = - 6.48 mV

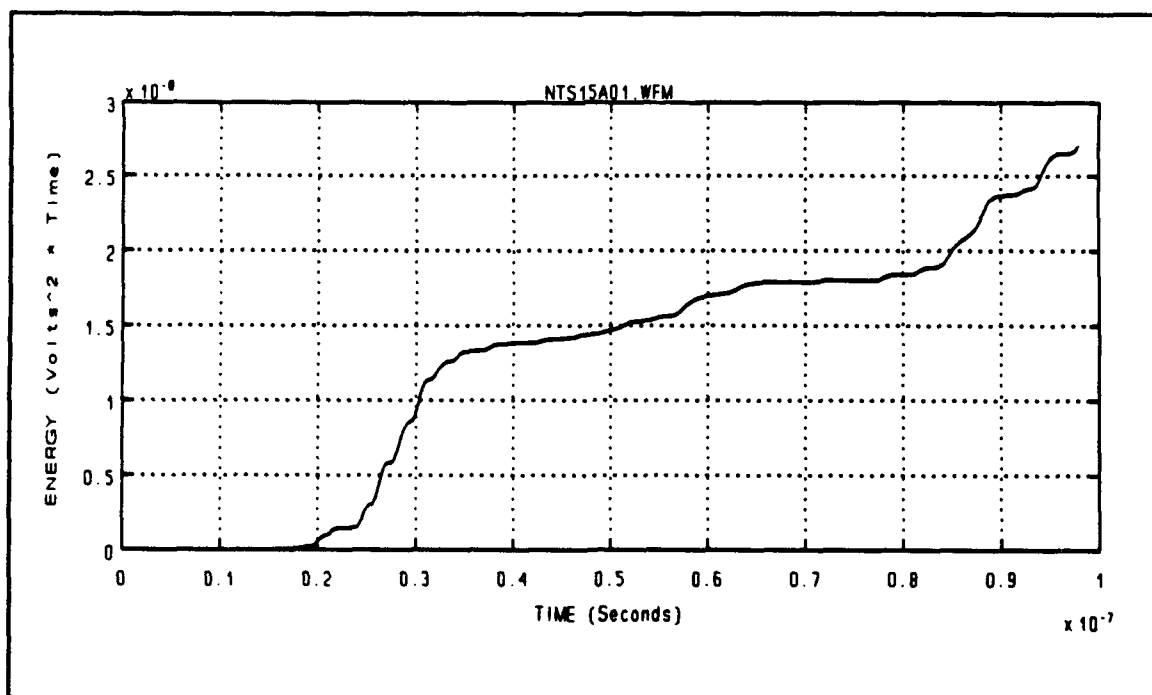


Figure 37 Waveform NTS15A01.WFM - LLNL Log Periodic Energy versus Time Graph - DC Offset = - 6.48 mV

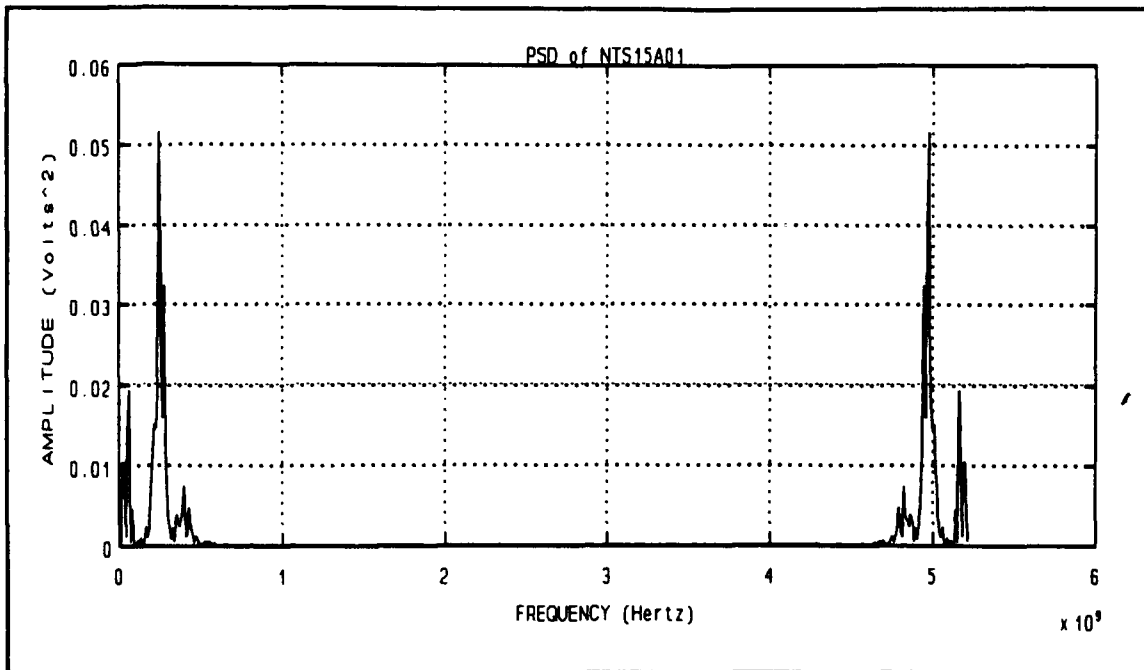


Figure 38 Waveform NTS15A01.WFM - LLNL Log Periodic
 Frequency Range = 0 Hz to F_s (Sampling Frequency)
 Spectra at 5 GHz is mirror image of spectra at 0 Hz which
 is an artifact induced by the periodicity of F_s at 5 GHz

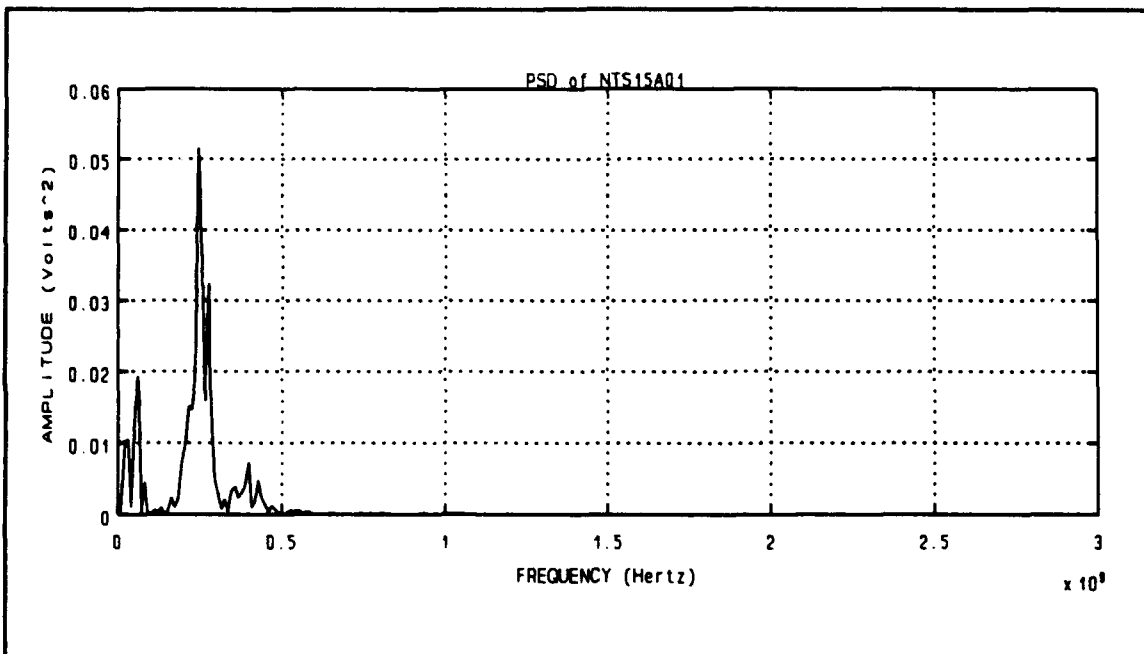


Figure 39 Waveform NTS15A01.WFM - LLNL Log Periodic
 Power Spectral Density - DC Offset = - 6.48 mV
 Frequency Range = 0 Hz to $F_s/2$

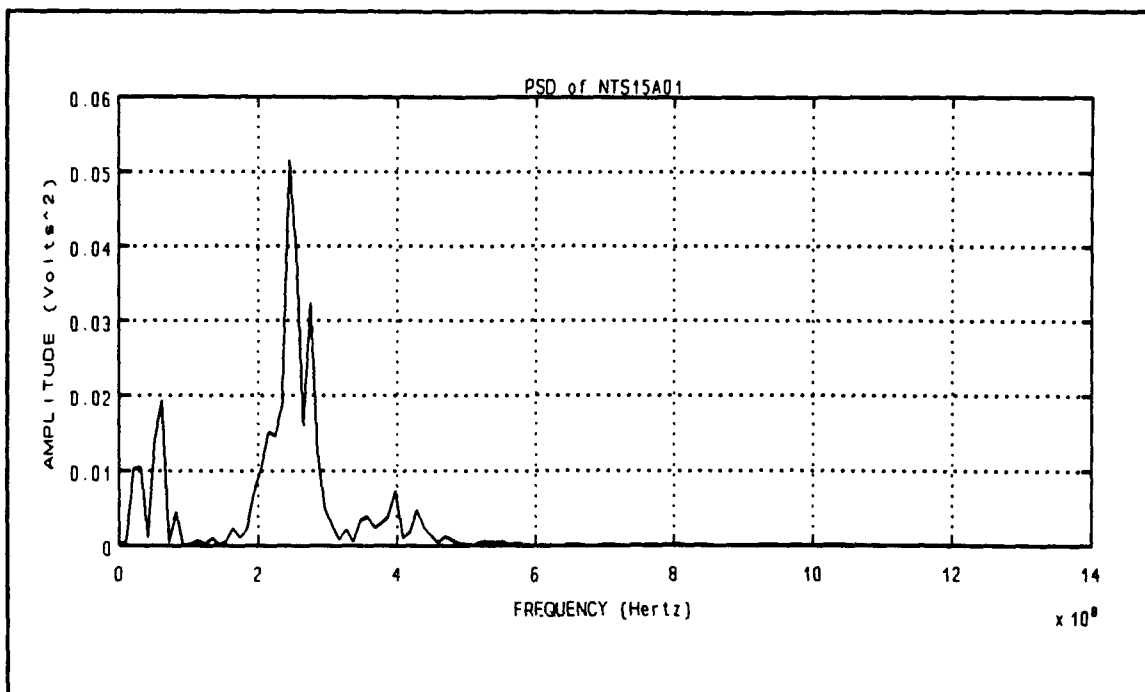


Figure 40 Waveform NTS15A01.WFM - LLNL Log Periodic Power Spectral Density - DC Offset = - 6.48 mV
Frequency Range = 0 Hz to $F_s/4$

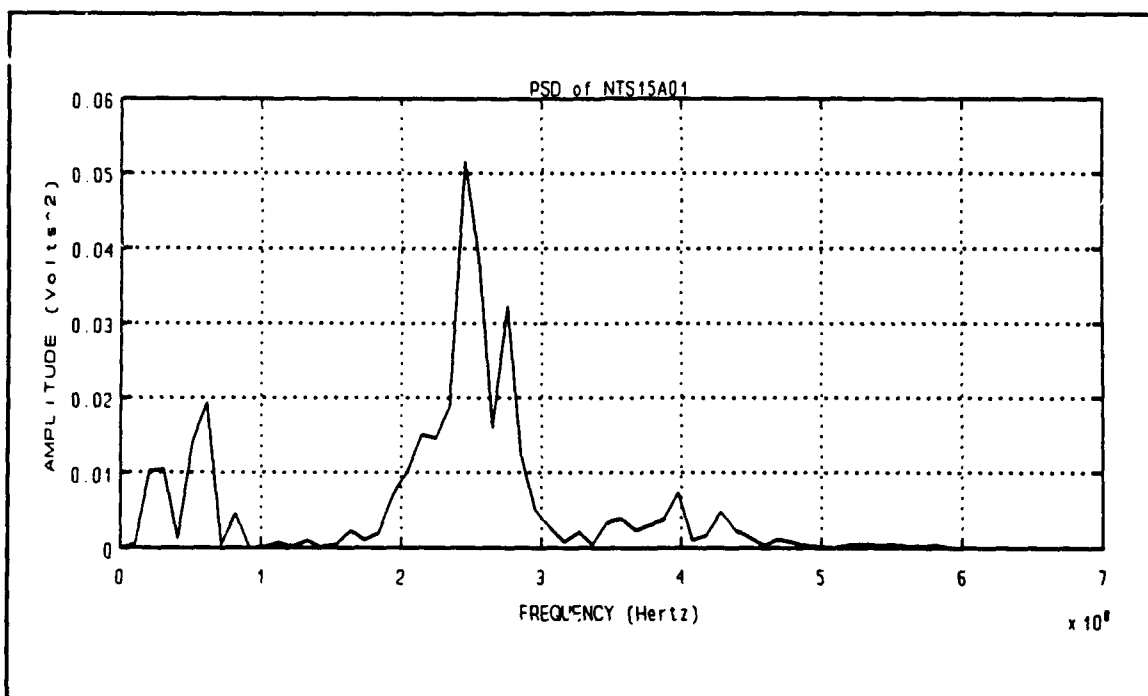


Figure 41 Waveform NTS15A01.WFM - LLNL Log Periodic Power Spectral Density - DC Offset = - 6.48 mV
Frequency Range = 0 Hz to $F_s/8$

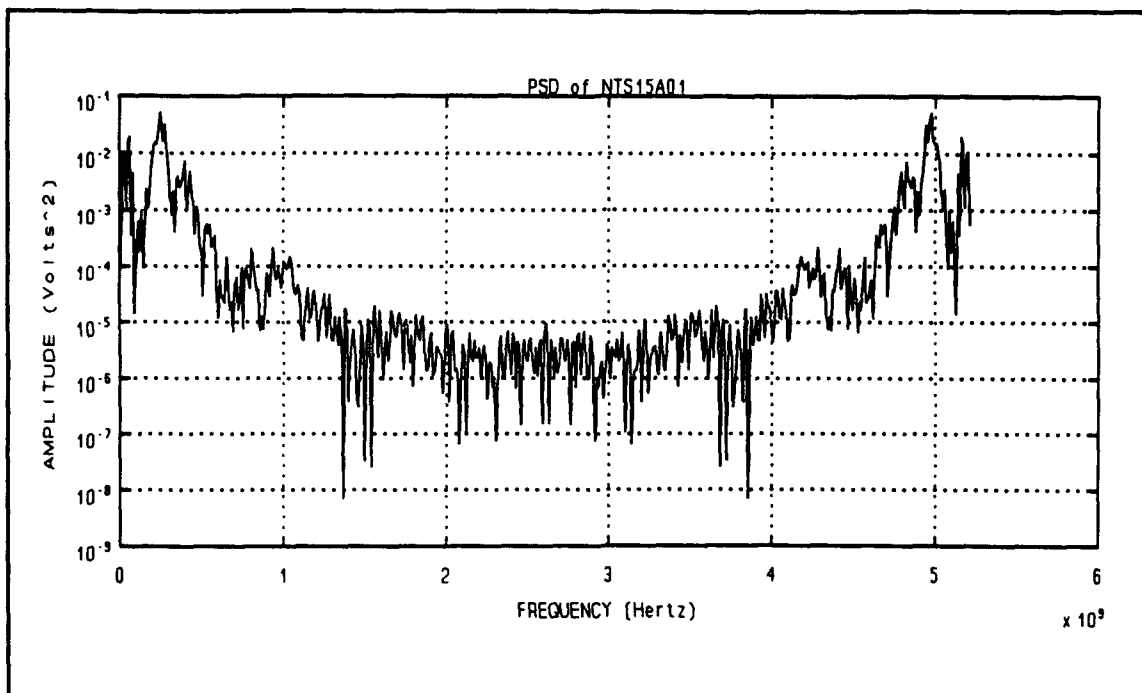


Figure 42 Waveform NTS15A01.WFM - LLNL Log Periodic Power Spectral Density - DC Offset = - 6.48 mV Semilog (Y-axis), Log (X-axis) plot

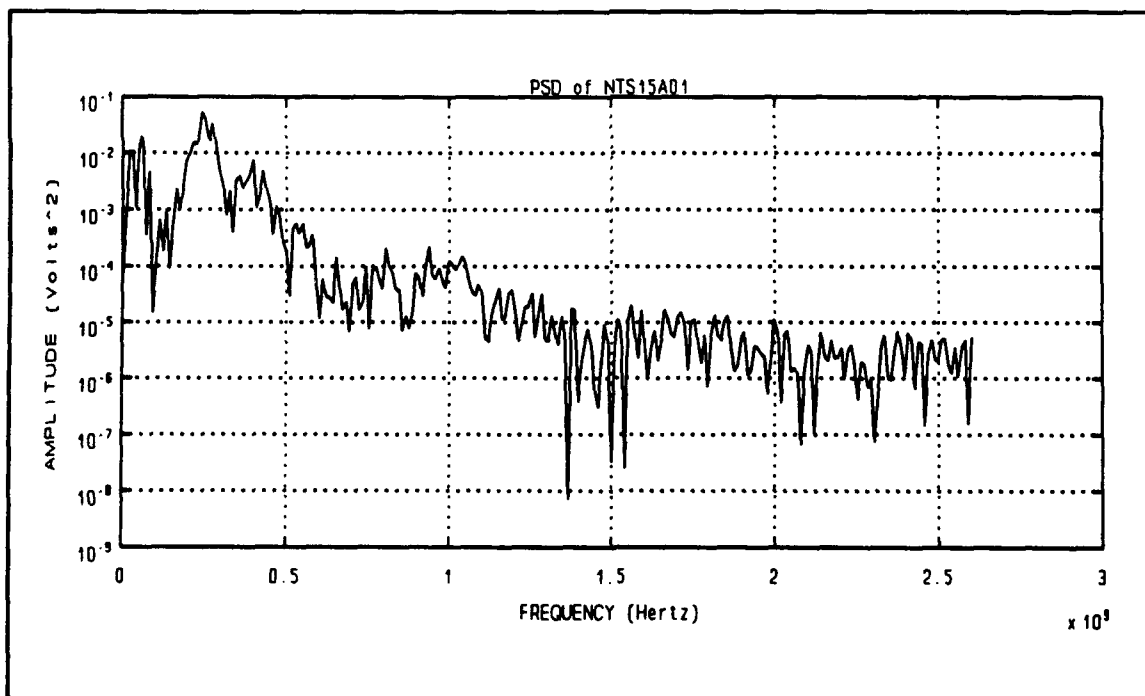


Figure 43 Waveform NTS15A01.WFM - LLNL Log Periodic Power Spectral Density - DC Offset = - 6.48 mV Semilog (Y-axis), Log (X-axis) plot

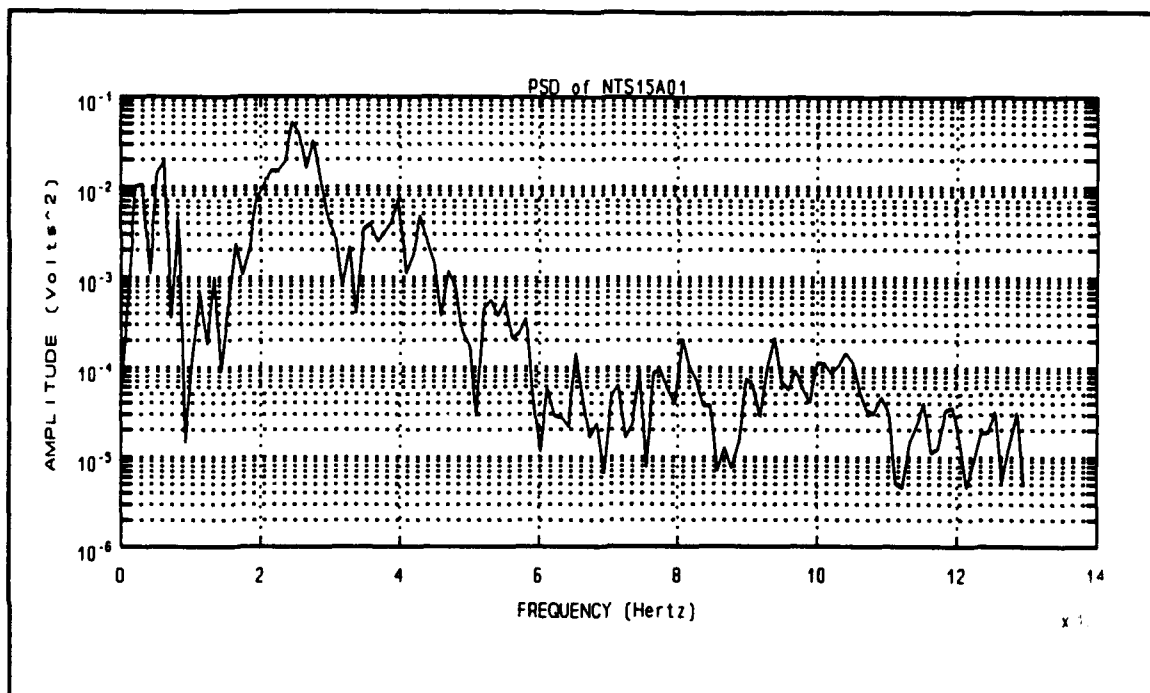


Figure 44 Waveform NTS15A01.WFM - LLNL Log Periodic Power Spectral Density - DC Offset = - 6.48 mV Semilog (Y-axis), Log (X-axis) plot

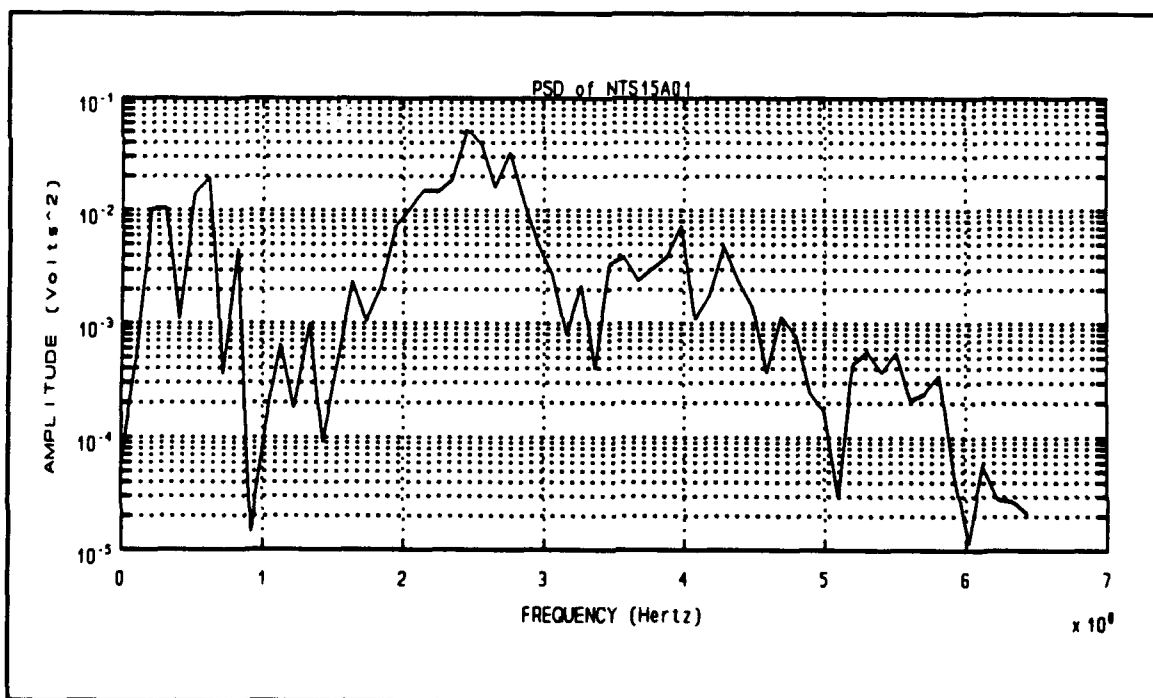


Figure 45 Waveform NTS15A01.WFM - LLNL Log Periodic Power Spectral Density - DC Offset = - 6.48 mV Semilog (Y-axis), Log (X-axis) plot

B. BACKGROUND THEORY

The power spectral density (PSD) of the digitized signals was computed using the following formula:

$$S_N = \frac{1}{N} \times |X(k)|^2 \quad (1)$$

where:

S_N = Power Spectral Density (PSD)

N = Number of sampled data points

$X(k)$ = magnitude of Fast Fourier Transform (FFT) of data point

In computing the power spectral density of each digitized waveform, no sort of "signal processing" was done to "clean up" the signal. Specifically, no averaging of the sampled data points was done to minimize the effects of noise. In addition, no form of windowing, time smoothing or frequency smoothing was performed on the PSD obtained. The reason for not performing these signal processing operations was that "information" was not modulated (i.e. contained) in the signal and therefore, extracting a "clean signal" was not necessarily the objective. Performing any of the above mentioned procedures would distort the parameters being analyzed in the signal actually received and prove counterproductive for the purposes of this analysis.

In the course of the analysis, an objective was to determine the minimum bandwidth (i.e containing 90 - 95 % of the energy) of the various pulsed signals. This was necessary in order to determine the minimum bandwidth requirements of

the collection equipment in order to adequately capture and digitize the signal. To address this issue, three different bandwidths must be considered:

1. Signal bandwidth - different signals and forms of modulation will require different minimum bandwidths. There is no simple formula for determining this minimum. Basic fourier theory, however, states that the shorter the signal duration in time, the wider the required bandwidth in the frequency domain. Given the time duration of the pulsed signals transmitted, it was known beforehand that each individual pulse contained frequency bandwidths on the order of 1 GHz or greater.
2. Tektronix 7104 oscilloscope bandwidth - by design, the TEK 7104 has a relatively flat frequency response from zero to one (1) GHz. Signals with bandwidths up to 1 GHz can be processed and captured with minimal attenuation or distortion. Frequencies beyond 1 GHz are severely attenuated due to the 3 dB roll-off of the oscilloscope filter. Given the frequency bandwidth of the TEK 7104 oscilloscope, the analog waveform of the pulsed signals transmitted was adequately captured and displayed with minimal distortion or loss of high frequency components.
3. Nyquist bandwidth - signal sampling theory dictates the maximum frequency that can be resolved in a digitized waveform is determined by the Nyquist criteria. The Nyquist criteria states the maximum resolvable frequency is equal to half the sampling frequency. This is stated mathematically as:

$$f_s \geq 2f_m \quad (2)$$

where:

f_s = Nyquist sampling frequency

f_m = maximum resolvable frequency. This is equivalent to maximum bandwidth if a baseband signal is considered (i.e one whose frequency spectrum start at zero frequency).

The following terms, used in analyzing the data, are defined [Ref. 5]:

1. Record length (or equivalently, collect time) - this is equivalent to time duration of the digitized signal. It is expressed mathematically as:

$$T_o = NT_s \quad (3)$$

where:

T_o = record length
 N = number of sampled data points
 T_s = sampling time interval

2. Sampling time interval (T_s) - time between successive sampled data points.
3. Sampling frequency - this is equivalent to the Nyquist sampling frequency f_s and is equal to the inverse of the sampling time interval. It is expressed mathematically as:

$$f_s = \frac{1}{T_s} \quad (4)$$

4. Frequency resolution - the frequency resolution determines the closest spacing between adjacent frequencies that can be resolved by the discrete fourier transform (DFT). If a signal contains frequency components spaced closer than the frequency resolution, they will not be represented as separate and distinct frequencies. The frequency resolution is expressed mathematically as:

$$\Delta f = \frac{1}{NT_s} = \frac{1}{T_o} \quad (5)$$

C. ANALYSIS OF INDIVIDUAL WAVEFORMS

The graphs of the digitized waveforms, the power versus time graphs, the energy versus time graphs and the calculated power spectral density graphs are included in the addendum to this report. The associated observations for each waveform analyzed are provided in the following subsections.

A concise list of the digitized waveforms that were analyzed are listed in Table IV through Table VIII.

Table IV DIRECTORIES 5-1-90, 5-2-90, 5-3-90 AND 5-4-90

DIGITIZED WAVEFORM	RECEIVED POLARIZATION	TRUE BEARING / ELEVATION ANGLE	TRANSMITTER / XMIT ANTENNA
NTS04B01.WFM	HORIZONTAL ?	? DEGREES	FEB/TEM ?
NTS04E01.WFM	HORIZONTAL ?	? DEGREES	FEB/LP ?
NTS04J01.WFM	HORIZONTAL ?	? DEGREES	FEB/TEM ?
NTS04K01.WFM	HORIZONTAL ?	? DEGREES	FEB/TEM ?
NTS04L01.WFM	HORIZONTAL ?	? DEGREES	FEB/TEM ?
NTS06O01.WFM	HORIZONTAL	153/45 DEGREES	FEBETRON / LP
NTS07A01.WFM	HORIZONTAL	32/0 DEGREES	FEBETRON / LP
NTS07B01.WFM	HORIZONTAL	32/0 DEGREES	FEBETRON / LP
NTS09J01.WFM	HORIZONTAL	0/0 DEGREES	UK PULSER/ LP
NTS09K01.WFM	HORIZONTAL	0/0 DEGREES	UK PULSER/ LP
NTS12J01.WFM	HORIZONTAL	311/45 DEGREES	FEB / TEM
NTS12K01.WFM	VERTICAL	311/45 DEGREES	FEB / TEM

Table V DIRECTORY 5-7-90

DIGITIZED WAVEFORM	RECEIVED POLARIZATION	TRUE BEARING / ELEVATION ANGLE	TRANSMITTER / XMIT ANTENNA
NTS13A01.WFM	HORIZONTAL	293/0 DEGREES	FEB / TEM
NTS13B01.WFM	HORIZONTAL	293/0 DEGREES	FEB / TEM
NTS13C01.WFM	VERTICAL	293/0 DEGREES	FEB / TEM
NTS13D01.WFM	VERTICAL	293/0 DEGREES	FEB / TEM
NTS13E01.WFM	HORIZONTAL	293/0 DEGREES	FEB / TEM
NTS13F01.WFM	HORIZONTAL	153/45 DEGREES	FEB / TEM
NTS13G01.WFM	HORIZONTAL	153/45 DEGREES	FEB / TEM
NTS13H01.WFM	VERTICAL	153/45 DEGREES	FEB / TEM
NTS13I01.WFM	VERTICAL	153/45 DEGREES	FEB / TEM
NTS13J01.WFM	HORIZONTAL	153/45 DEGREES	FEB / TEM
NTS13K01.WFM	HORIZONTAL	153/45 DEGREES	FEB / TEM
NTS13L01.WFM	HORIZONTAL	32/0 DEGREES	FEB / TEM
NTS13M01.WFM	HORIZONTAL	32/0 DEGREES	FEB / TEM
NTS13N01.WFM	VERTICAL	32/0 DEGREES	FEB / TEM
NTS13O01.WFM	VERTICAL	32/0 DEGREES	FEB / TEM
NTS13P01.WFM	VERTICAL	0/0 DEGREES	FEB / TEM
NTS13Q01.WFM	HORIZONTAL	0/0 DEGREES	FEB / TEM
NTS13R01.WFM	HORIZONTAL	0/0 DEGREES	FEB / TEM
NTS13S01.WFM	VERTICAL	0/0 DEGREES	FEB / TEM
NTS13T01.WFM	VERTICAL	324/0 DEGREES	FEB / TEM
NTS13U01.WFM	HORIZONTAL	324/0 DEGREES	FEB / TEM
NTS13V01.WFM	HORIZONTAL	324/0 DEGREES	FEB / TEM
NTS13W01.WFM	VERTICAL	324/0 DEGREES	FEB / TEM
NTS13X01.WFM	VERTICAL	311/0 DEGREES	FEB / TEM

Table VI DIRECTORY 5-7-90

DIGITIZED WAVEFORM	RECEIVED POLARIZATION	TRUE BEARING / ELEVATION ANGLE	TRANSMITTER / XMIT ANTENNA
NTS13Y01.WFM	VERTICAL	311/0 DEGREES	FEB / TEM
NTS13Z01.WFM	HORIZONTAL	311/0 DEGREES	FEB / TEM
NTS14A01.WFM	HORIZONTAL	311/0 DEGREES	FEB / TEM
NTS14B01.WFM	HORIZONTAL	311/0 DEGREES	FEB / TEM
NTS14C01.WFM	VERTICAL	311/0 DEGREES	FEB / TEM
NTS14D01.WFM	45 DEG ANGLE	311/0 DEGREES	FEB / TEM

Table VII DIRECTORY 5-8-90

DIGITIZED WAVEFORM	RECEIVED POLARIZATION	TRUE BEARING / ELEVATION ANGLE	TRANSMITTER / XMIT ANTENNA
NTS15A01.WFM	HORIZONTAL	293/0 DEGREES	FEBETRON / LP
NTS15B01.WFM	HORIZONTAL	293/0 DEGREES	FEBETRON / LP
NTS15C01.WFM	VERTICAL	293/0 DEGREES	FEBETRON / LP
NTS15D01.WFM	VERTICAL	293/0 DEGREES	FEBETRON / LP
NTS15E01.WFM	VERTICAL	311/0 DEGREES	FEBETRON / LP
NTS15F01.WFM	MISFIRE		
NTS15G01.WFM	HORIZONTAL	311/0 DEGREES	FEBETRON / LP
NTS15H01.WFM	HORIZONTAL	311/0 DEGREES	FEBETRON / LP
NTS15I01.WFM	HORIZONTAL	324/0 DEGREES	FEBETRON / LP
NTS15J01.WFM	HORIZONTAL	324/0 DEGREES	FEBETRON / LP
NTS15K01.WFM	MISFIRE		
NTS15L01.WFM	VERTICAL	324/0 DEGREES	FEBETRON / LP
NTS15M01.WFM	HORIZONTAL	0/0 DEGREES	FEBETRON / LP
NTS15N01.WFM	VERTICAL	0/0 DEGREES	FEBETRON / LP
NTS15O01.WFM	VERTICAL	0/0 DEGREES	FEBETRON / LP
NTS15P01.WFM	HORIZONTAL	0/0 DEGREES	FEBETRON / LP
NTS15Q01.WFM	HORIZONTAL	32/0 DEGREES	FEBETRON / LP
NTS15R01.WFM	HORIZONTAL	32/0 DEGREES	FEBETRON / LP
NTS15S01.WFM	HORIZONTAL	32/0 DEGREES	FEBETRON / LP
NTS15T01.WFM	VERTICAL	32/0 DEGREES	FEBETRON / LP
NTS15U01.WFM	VERTICAL	153/45 DEGREES	FEBETRON / LP
NTS15V01.WFM	VERTICAL	153/45 DEGREES	FEBETRON / LP
NTS15W01.WFM	HORIZONTAL	153/45 DEGREES	FEBETRON / LP
NTS15X01.WFM	HORIZONTAL	153/45 DEGREES	FEBETRON / LP

Table VIII DIRECTORY 5-8-90

DIGITIZED WAVEFORM	RECEIVED POLARIZATION	TRUE BEARING / ELEVATION ANGLE	TRANSMITTER / XMIT ANTENNA
NTS16A01.WFM	HORIZONTAL	153/45 DEGREES	FEB / TEM
NTS16B01.WFM	VERTICAL	153/45 DEGREES	FEB / TEM
NTS16C01.WFM	VERTICAL	153/45 DEGREES	FEB / TEM
NTS16D01.WFM	HORIZONTAL	153/45 DEGREES	FEB / TEM
NTS16E01.WFM	HORIZONTAL	153/45 DEGREES	FEB / TEM
NTS16F01.WFM	HORIZONTAL	153/45 DEGREES	FEB / TEM
NTS16G01.WFM	HORIZONTAL	326/0 DEGREES	FEB / TEM
NTS16H01.WFM	VERTICAL	326/0 DEGREES	FEB / TEM

1. Directory 5-1-90

The following waveforms were captured and digitized on
1 May, 1990.

a. Waveform NTS04B01.WFM

1. Transmitting antenna used - TEM horn (?).
2. Transmitter used - Febetron (?).
3. Elevation angle (Source) = 0 degrees (?).
4. Polarization transmitted - Horizontal (?).
5. Polarization captured - Horizontal (?).
6. NOTE - Parameters 1 - 5 were not annotated in the log book. I am fairly certain that the parameters I listed are correct, however, based on the shape of the pulse and analysis of the waveforms in directories 5-7-90 and 5-8-90.
7. Record length - 50 nanoseconds.
8. Pulse clearly visible.
9. Pulse shape resembles output from Febetron.
10. Pulse duration - approximately 5 nanoseconds.
11. Energy versus time graph shows an immediate, distinct rise in energy indicative of a main pulse.
12. PSD graph shows 98 % of the energy is contained in the frequency range from 0 to 520 MHz.
13. Energy extends out to 710 MHz.

b. Waveform NTS04E01.WFM

1. Transmitting antenna used - LLNL modified log periodic (?).
2. Transmitter used - Febetron (?).
3. Elevation angle (Source) = 0 degrees (?).

4. Polarization transmitted - Horizontal (?).
5. Polarization captured - Horizontal (?).
6. NOTE - Parameters 1 - 5 were not annotated in the log book. I am fairly certain that the parameters I listed are correct, however, based on the shape of the pulse and analysis of the waveforms in directories 5-7-90 and 5-8-90.
7. Record length - 50 nanoseconds.
8. Pulse clearly visible.
9. Pulse shape resembles output from the LLNL modified log periodic antenna.
10. Pulse duration - approximately 9 nanoseconds.
11. Energy versus time graph shows an immediate, distinct rise in energy indicative of a main pulse.
12. PSD graph shows 97 % of the energy is contained in the frequency range from 0 to 1 GHz.
13. Energy extends out to 1.7 GHz.

c. Waveform NTS04J01.WFM

1. Transmitting antenna used - TEM horn (?).
2. Transmitter used - Febetron (?).
3. Elevation angle (Source) = 0 degrees (?).
4. Polarization transmitted - Horizontal (?).
5. Polarization captured - Horizontal (?).
6. NOTE - Parameters 1 - 5 were not annotated in the log book. I am fairly certain that the parameters I listed are correct, however, based on the shape of the pulse and analysis of the waveforms in directories 5-7-90 and 5-8-90.
7. Record length - 50 nanoseconds.
8. Pulse clearly visible.
9. Pulse shape resembles output from Febetron.

10. Pulse duration - approximately 3 nanoseconds.
11. Energy versus time graph shows an immediate, distinct rise in energy indicative of a main pulse.
12. PSD graph shows 98 % of the energy is contained in the frequency range from 0 to 1 GHz.
13. Energy extends out to 1.3 GHz.

d. Waveform NTS04K01.WFM

1. Transmitting antenna used - TEM horn (?).
2. Transmitter used - Febetron (?).
3. Elevation angle (Source) = 0 degrees (?).
4. Polarization transmitted - Horizontal (?).
5. Polarization captured - Horizontal (?).
6. NOTE - Parameters 1 - 5 were not annotated in the log book. I am fairly certain that the parameters I listed are correct, however, based on the shape of the pulse and analysis of the waveforms in directories 5-7-90 and 5-8-90.
7. Record length - 50 nanoseconds.
8. Pulse clearly visible.
9. Pulse shape resembles output from Febetron.
10. Pulse duration - approximately 7 nanoseconds.
11. Energy versus time graph shows an immediate, distinct rise in energy indicative of a main pulse.
12. PSD graph shows 98 % of the energy is contained in the frequency range from 0 to 1 GHz.
13. Energy extends out to 1.8 GHz.

e. Waveform NTS04L01.WFM

1. Transmitting antenna used - TEM horn (?).
2. Transmitter used - Febetron (?).
3. Elevation angle (Source) = 0 degrees (?).
4. Polarization transmitted - Horizontal (?).
5. Polarization captured - Horizontal (?).
6. NOTE - Parameters 1 - 5 were not annotated in the log book. I am fairly certain that the parameters I listed are correct, however, based on the shape of the pulse and analysis of the waveforms in directories 5-7-90 and 5-8-90.
7. Record length - 50 nanoseconds.
8. Pulse clearly visible.
9. Pulse shape resembles output from Febetron.
10. Pulse duration - approximately 8 nanoseconds.
11. Energy versus time graph shows an immediate, distinct rise in energy indicative of a main pulse.
12. PSD graph shows 98 % of the energy is contained in the frequency range from 0 to 1 GHz.
13. Energy extends out to 1.3 GHz.

2. Directory 5-2-90

The following waveforms were captured and digitized on
2 May, 1990.

a. Waveform NTS06O01.WFM

1. Transmitting antenna used - LLNL modified log periodic.
2. Transmitter used - Febetron.
3. Elevation angle (Source) = 45 degrees.

4. Polarization transmitted - Horizontal.
5. Polarization captured - Horizontal.
6. Record length - 50 nanoseconds.
7. Pulse clearly visible.
8. Pulse shape resembles output from the LLNL modified log periodic antenna.
9. Pulse duration - approximately 12 nanoseconds.
10. Energy versus time graph shows an immediate, distinct rise in energy indicative of a main pulse.
11. PSD graph shows 95 % of the energy is contained in the frequency range from 0 to 500 MHz.
12. Energy extends out to 1.5 GHz.

b. Waveform NTS07A01.WFM

1. Transmitting antenna used - LLNL modified log periodic.
2. Transmitter used - Febetron.
3. Elevation angle (Source) = 0 degrees.
4. Polarization transmitted - Horizontal.
5. Polarization captured - Horizontal.
6. Record length - 50 nanoseconds.
7. Pulse clearly visible.
8. Pulse shape resembles output from the LLNL modified log periodic antenna.
9. Pulse duration - approximately 12 nanoseconds.
10. Energy versus time graph shows an immediate, distinct rise in energy indicative of a main pulse.
11. PSD graph shows 99 % of the energy is contained in the frequency range from 0 to 500 MHz.

12. Energy extends out to 700 MHz.

c. Waveform NTS07B01.WFM

1. Transmitting antenna used - LLNL modified log periodic.
2. Transmitter used - Febetron.
3. Elevation angle (Source) = 0 degrees.
4. Polarization transmitted - Horizontal.
5. Polarization captured - Horizontal.
6. Record length - 50 nanoseconds.
7. Pulse clearly visible.
8. Pulse shape resembles output from the LLNL modified log periodic antenna.
9. Pulse duration - approximately 12 nanoseconds.
10. Energy versus time graph shows an immediate, distinct rise in energy indicative of a main pulse.
11. PSD graph shows over 99 % of the energy is contained in the frequency range from 0 to 600 MHz.

3. Directory 5-3-90

The following waveforms were captured and digitized on 3 May, 1990.

a. Waveform NTS09J01.WFM

1. Transmitting antenna used - LLNL modified log periodic.
2. Transmitter used - UK pulser.
3. Elevation angle (Source) = 0 degrees.
4. Polarization transmitted - Horizontal.

5. Polarization captured - Horizontal.
6. Record length - 50 nanoseconds.
7. Pulse clearly visible.
8. Pulse shape resembles output from the LLNL modified log periodic antenna.
9. Pulse duration - approximately 15 nanoseconds.
10. Energy versus time graph shows an immediate, distinct rise in energy indicative of a main pulse.
11. PSD graph shows 98 % of the energy is contained in the frequency range from 0 to 600 MHz.
12. Energy visibly extends out to 800 MHz. Residual energy extends out to 1.3 GHz.

b. Waveform NTS09K01.WFM

1. Transmitting antenna used - LLNL modified log periodic.
2. Transmitter used - UK pulser.
3. Elevation angle (Source) = 0 degrees.
4. Polarization transmitted - Horizontal.
5. Polarization captured - Horizontal.
6. Record length - 50 nanoseconds.
7. Pulse clearly visible.
8. Pulse shape resembles output from the LLNL modified log periodic antenna.
9. Pulse duration - approximately 15 nanoseconds.
10. Energy versus time graph shows an immediate, distinct rise in energy indicative of a main pulse.
11. PSD graph shows 92 % of the energy is contained in the frequency range from 0 to 500 MHz.

12. Energy visibly extends out to 2.5 GHz.

4. Directory 5-4-90

The following waveforms was captured and digitized on
4 May, 1990.

a. Waveform NTS12J01.WFM

1. Transmitting antenna used was a TEM horn.
2. Transmitter used was a Febetron.
3. Elevation angle (Source) = 45 degrees.
4. Polarization transmitted - Horizontal.
5. Polarization captured - Horizontal.
6. Record length - 100 nanoseconds.
7. A "distorted" main pulse is visible.
8. Pulse duration - approx. 20 nanoseconds.
9. Pulse shape resembles output from Febetron.
10. Energy versus time graph shows a gradual rise in energy. No distinct, immediate rise in energy indicative of a main pulse is visible.
11. PSD graph shows that over 99 % of energy contained within the first 200 MHz.
12. Residual energy extends out to 250 MHz.

b. Waveform NTS12K01.WFM

1. Transmitting antenna used was a TEM horn.
2. Transmitter used was a Febetron.
3. Elevation angle (Source) = 45 degrees.
4. Polarization transmitted - Horizontal.

5. Polarization captured - Vertical.
6. Record length - 100 nanoseconds.
7. A "distorted" main pulse is visible.
8. Pulse duration - approx. 20 nanoseconds.
9. Pulse shape resembles output from Febetron.
10. Energy versus time graph shows a gradual rise in energy. No distinct, immediate rise in energy indicative of a main pulse is visible.
11. PSD graph shows that over 98 % of energy contained within the first 200 MHz.
12. Energy extends out to 350 MHz.

5. Directory 5-7-90

The following waveforms were captured and digitized on 7 May, 1990.

a. Waveform NTS13A01.WFM

1. Transmitting antenna used was a TEM horn.
2. Transmitter used was a Febetron.
3. Elevation angle (Source) = 0 degrees.
4. Polarization transmitted - Horizontal.
5. Polarization captured - Horizontal.
6. Record length - 100 nanoseconds.
7. Pulse visible.
8. Pulse duration - approx. 49 nanoseconds.
9. Pulse shape resembles output from Febetron.
10. Energy versus time graph shows immediate rise of energy within first 47 - 48 nanoseconds.

11. PSD graph shows that over 90 % of energy contained within first 150 MHz.

12. Energy extends noticeably to 230 MHz. Residual energy out to 380 MHz.

b. Waveform NTS13B01.WFM

1. Transmitting antenna used was a TEM horn.
2. Transmitter used was a Febetron.
3. Polarization captured - Horizontal.
4. Record length - 100 nanoseconds.
5. Pulse apparently appears visible within first 20 - 30 nanoseconds.
6. Subsequent analysis was not performed on this waveform. Captured waveform was a "bad shot".

c. Waveform NTS13C01.WFM

1. Transmitting antenna used was a TEM Horn.
2. Transmitter used was a Febetron.
3. Elevation angle (Source) = 0 degrees.
4. Polarization transmitted - Horizontal.
5. Polarization captured - Vertical.
6. Record length - 100 nanoseconds.
7. Slightly distorted pulse visible.
8. Pulse shape resembles output from Febetron.
9. Pulse duration - approximately 51 nanoseconds.
10. Energy versus time graph shows immediate build-up of energy within first 52 nanoseconds.

11. PSD graph shows that approximately 90 % of energy contained within first 150 MHz. Approximately 8 % of energy contained within the band 150 MHz to 250 MHz.

d. Waveform NTS13D01.WFM

1. Transmitting antenna used was a TEM horn.
2. Transmitter used was a Febetron.
3. Polarization captured - Vertical.
4. Record length - 100 nanoseconds.
5. No analysis was performed on this waveform. "Bad shot".

e. Waveform NTS13E01.WFM

1. Transmitting antenna used was a TEM horn.
2. Transmitter used was a Febetron.
3. Elevation angle (Source) = 0 degrees.
4. Polarization transmitted - Horizontal.
5. Polarization captured - Horizontal.
6. Record length - 100 nanoseconds.
7. Pulse visible.
8. Pulse duration - approximately 10 nanoseconds.
9. Pulse shape resembles output from Febetron.
10. A second pulse appears 1 nanosecond after first pulse. This could be a reflection due to impedance mismatching between the transmitter cable and the antenna.
10. Energy versus time graph shows two distinct steps in energy build-up. Time wise, these two steps coincide with the two initial pulses mentioned in above.

11. PSD graph shows over 90 % of energy contained within the frequency range 200 MHz to 600 MHz.

12. The fact that majority of energy shows up at frequencies greater than 150 MHz even though collect time is 100 nanoseconds is most probably due to the very short pulse (ie. 10 nanoseconds) that was digitally captured.

f. Waveform NTS13F01.WFM

1. Transmitting antenna used was a TEM Horn.
2. Transmitter used was a Febetron.
3. Elevation angle (Source) = 45 degrees.
4. Polarization transmitted - Linear "Horizontal".
5. Polarization captured - Horizontal.
6. Record length - 100 nanoseconds.
7. Highly distorted pulse shape visible followed by what appears to be returns from multipath effects and reflections.
8. Energy versus time graph shows a gradual build-up of energy over the entire collect time. There is no distinct sudden rise of energy indicative of a main pulse followed by smaller returns due to multipath and/or reflections as illustrated in NTS13A01 and NTS13C01.
9. PSD graph shows that approximately 95 % of energy contained within first 100 MHz.

g. Waveform NTS13G01.WFM

1. Transmitting antenna used was a TEM horn.
2. Transmitter used was a Febetron.
3. Elevation angle (Source) = 45 degrees.
4. Polarization transmitted - Linear "Horizontal".
5. Polarization captured - Horizontal.

6. Record length - 100 nanoseconds.
7. Two pulses visible.
8. First pulse appears followed by second larger time duration pulse about 1 nanosecond later. This is probably indicative of the elevation angle used by the transmitting antenna. The geometry at the receiving antenna would be such that horizontal component would be received. Second pulse probably due to multipath and/or reflections.
9. Energy versus time graph shows a gradual build-up of energy. No immediate rise indicative of a main pulse followed by multipath and reflections.
10. PSD graph shows approximately 95 % of energy contained within 100 MHz to 400 MHz range.

h. Waveform NTS13H01.WFM

1. Transmitting antenna used was a TEM horn.
2. Transmitter used was a Febetron.
3. Elevation angle (Source) = 45 degrees.
4. Polarization transmitted - Linear "Horizontal".
5. Polarization captured - Vertical
6. Record length - 100 nanoseconds.
7. No pulse shape clearly visible.
8. The outline of what appears to be a highly distorted pulse appears at first. This is probably indicative of the elevation angle used by the transmitting antenna resulting in the receiving antenna receiving the vertical component followed by reflections and multipath.
9. Energy versus time graph shows a gradual build-up of the energy. No distinct, immediate rise in energy indicative of a main pulse.
10. PSD graphs shows that approximately 95 % of energy contained within first 100 MHz.
11. Energy extends out to 225 MHz.

i. Waveform NTS13I01.WFM

1. Transmitting antenna used was a TEM horn.
2. Transmitter used was a Febetron.
3. Elevation angle (Source) = 45 degrees.
4. Polarization transmitted - Linear "Horizontal".
5. Polarization captured - Vertical.
6. Record length - 100 nanoseconds.
7. Pulse - what appears to be a highly distorted pulse shape is visible. Three (3) highly distorted pulse shapes appear to follow the main "pulse" at equal spacings of about 3 nanoseconds. This could be indicative of multipath effects and/or reflections due to impedance mismatching.
8. Energy versus time graph shows a gradual buildup of the energy. Shape of energy curve appears to be a mixture of a steep rise indicative of a main pulse and a gradual rise indicative of multipath effects.
9. PSD graph shows that approximately 90 % of the energy is contained in the first 200 MHz. The frequency range from 200 MHz to 550 MHz contains approximately 10 % of the energy.

j. Waveform NTS13J01.WFM

1. Transmitting antenna used was a TEM Horn.
2. Transmitter used was a Febetron.
3. Elevation angle (Source) = 45 degrees.
4. Polarization transmitted - Linear "Horizontal".
5. Polarization captured - Horizontal.
6. Record length - 100 nanoseconds.
7. No main pulse clearly discernible.

8. Two highly distorted pulses appear in the first 40 nanoseconds. The second "pulse" follows the first by about 2 nanoseconds. This could be indicative of the 45 degree elevation angle which would result in two components, one in the horizontal and one in the vertical direction.

9. Energy versus time graph shows a distinct rise in energy. There is an intermediate rise in energy occurring at 31 nanoseconds. This coincides with the second observed "pulse".

10. PSD graph shows that 99 % of energy contained in the frequency range from 100 MHz to 580 MHz.

k. Waveform NTS13K01.WFM

1. Transmitting antenna used was a TEM horn.
2. Transmitter used was a Febetron.
3. Elevation angle (Source) = 45 degrees.
4. Polarization transmitted - Linear "Horizontal".
5. Polarization captured - Horizontal.
6. No analysis done on this waveform. Bad shot.

l. Waveform NTS13L01.WFM

1. Transmitting antenna used was a TEM horn.
2. Transmitter used was a Febetron.
3. Elevation angle (Source) = 0 degrees.
4. Polarization transmitted - Horizontal.
5. Polarization captured - Horizontal.
6. Record length - 100 nanoseconds.
7. No main pulse clearly discernible.
8. What appears to be highly distorted main pulse visible in the first 15 nanoseconds.

9. Energy versus time graph shows a distinct rise in energy. An intermediate rise occurs at 15 nanoseconds. This appears to indicate the presence of two distinct pulses.

10. PSD graph shows approximately 21 % of energy within first 160 MHz. Approximately 8 % of energy contained from 160 MHz to 400 MHz.

m. Waveform NTS13M01.WFM

1. Transmitting antenna used was a TEM horn.
2. Transmitter used was a Febetron.
3. Elevation angle (Source) = 0 degrees.
4. Polarization transmitted - Horizontal.
5. Polarization captured - Horizontal.
6. Record length - 500 nanoseconds.
7. Pulse visible.
8. Pulse duration - approximately 30 nanoseconds.

9. Energy versus time graph shows a distinct rise in energy. A second gradual rise starts at about 160 nanoseconds. This is most probably due to the large numbers of what appear to be multipath effects visible after the main pulse.

10. PSD graph shows about 1 % of energy contained within first 20 MHz. Approximately 98 % of energy contained in the frequency range from 20 MHz to 160 MHz.

n. Waveform NTS13N01.WFM

1. Transmitting antenna used was a TEM horn.
2. Transmitter used was a Febetron.
3. Elevation angle (Source) = 0 degrees.
4. Polarization transmitted - Horizontal.

5. Polarization captured - Vertical.
6. Record length - 500 nanoseconds.
7. Pulse visible.
8. Pulse duration - approximately 30 nanoseconds.
9. Energy versus time graph shows two distinct rises in energy followed by a gradual rise. This is indicative of two distinct pulses followed by reflections and/or multipath effects.
10. NOTE - the anomaly of observing a main pulse when capturing the vertical component is probably due to the actual geometry of transmitting antenna and the receiving antenna and possibly diffractive effects due to objects in the path. Under ideal conditions, a perfectly horizontally polarized wave would have no component in the vertical direction that could be received and detected.
11. PSD graph shows about 1 % of energy contained within first 20 MHz. Approximately 99 % of energy contained in the frequency range from 20 MHz to 140 MHz.

o. Waveform NTS13001.WFM

1. Transmitting antenna used was a TEM horn.
2. Transmitter used was a Febetron.
3. Elevation angle (Source) = 0 degrees.
4. Polarization transmitted - Horizontal.
5. Polarization captured - Vertical.
6. Record length - 100 nanoseconds.
7. Pulse visible.
8. The pulse appears to be highly "stretched" out. This would seem to indicate the effects of multipath and reflections. Moreover, it could also indicate that the geometry was such that to the receiving antenna, a small component of the horizontally transmitted wave was captured.

9. Energy versus time graph shows a somewhat gradual but distinct rise in energy within first 45 nanoseconds. This coincides with the pulse visible in the digitally captured signal.

10. PSD graph shows approximately 9 % of energy contained within first 40 MHz. Approximately 89 % of energy contained in the frequency range from 40 MHz to 140 MHz. About 2 % of energy contained in the frequency range from 140 MHz to 200 MHz.

p. Waveform NTS13P01.WFM

1. Transmitting antenna used was a Febetron.

2. Transmitter used was a Febetron.

3. Elevation angle = 0 degrees.

4. Polarization transmitted - Horizontal.

5. Polarization captured - Vertical.

6. Record length - 100 nanoseconds.

7. No main pulse visible.

8. What appears to be a highly distorted main pulse is visible within first 25 nanoseconds. This is probably indicated of multipath effects and reflections.

9. Unable to generate energy versus time graph.

10. PSD graph shows approximately 98 % of energy contained within first 140 MHz. Energy extends out to about 260 MHz.

q. Waveform NTS13Q01.WFM

1. Transmitting antenna used was a TEM horn.

2. Transmitter used was a Febetron.

3. Elevation angle (Source) = 0 degrees.

4. Polarization transmitted - Horizontal.

5. Polarization captured - Horizontal.
6. Record length - 100 nanoseconds.
7. Pulse not visible.
8. No distinct main pulse visible. What may be a highly distorted main pulse is visible within first 45 nanoseconds.
9. Unable to generate energy versus time graph.
10. PSD graph shows approximately 7 % of energy within first 50 MHz. Approximately 92 % of energy contained in the frequency range from 50 MHz to 300 MHz.

r. Waveform NTS13R01.WFM

1. Transmitting antenna used was a TEM horn.
2. Transmitter used was a Febetron.
3. Elevation angle (Source) = 0 degrees.
4. Polarization transmitted - Horizontal.
5. Polarization captured - Horizontal.
6. Record length - 500 nanoseconds.
7. Pulse visible.
8. A main pulse is visible followed some 10 nanoseconds later by what appears to a second pulse. This could be indicative of an internal reflection due to impedance mismatching (i.e. similar to what was observed by aircraft - see notes in brown notebook).
9. Energy versus time graph shows two distinct rises in energy followed by a slow gradual increase. The curve of the energy graph is indicative of two pulses followed by multipath effects and/or reflections.
10. PSD graph shows that approximately 96 % of energy is contained in the frequency range from 20 MHz to 100 MHz. Energy extends out to about 150 MHz.

s. Waveform NTS13S01.WFM

1. Transmitting antenna used was a TEM horn.
2. Transmitter used was a Febetron.
3. Elevation angle (Source) = 0 degrees.
4. Polarization transmitted - Horizontal.
5. Polarization captured - Vertical.
6. Record length - 500 nanoseconds.
7. No main pulse is visible.
8. What appears to be a distorted "stretched out" main pulse is visible within the first 130 nanoseconds. This is followed by what appears to be a second more distorted, highly elongated pulse. This could be indicative of multipath effects and reflections.
9. Energy versus time graph shows a gradual increase in the energy. Two distinct rises are visible, however, indicative of two distinct pulses.
10. PSD graph shows 100 % of energy contained within first 125 MHz.

t. Waveform NTS13T01.WFM

1. Transmitting antenna used was a TEM horn.
2. Transmitter used was a Febetron.
3. Elevation angle (Source) = 0 degrees.
4. Polarization transmitted - Horizontal.
5. Polarization captured - Vertical.
6. Record length - 500 nanoseconds.
7. Pulse visible.
8. Pulse duration - approx. 25 nanoseconds.

9. A main pulse is visible followed by a second, distorted pulse about 10 nanoseconds later. This is probably indicative of internal reflections due to impedance mismatching.

10. This anomaly in observing a clean, distinct pulse in the vertically polarized plane is probably a result of an imperfect geometric set-up between the transmitting antenna and the receiving antenna.

11. The energy versus time graph shows two distinct rises in energy followed by a gradual increase. This is indicative of two pulses followed by multipath and/or reflections.

12. PSD graph shows approximately 99 % of energy contained in the frequency range from 20 MHz to 140 MHz.

u. Waveform NTS13U01.WFM

1. Transmitting antenna used was a TEM horn.
2. Transmitter used was a Febetron.
3. Elevation angle (Source) = 0 degrees.
4. Polarization transmitted - Horizontal.
5. Polarization captured - Horizontal.
6. Record length - 500 nanoseconds.
7. Pulse visible.
8. Pulse duration - approx. 45 nanoseconds.
9. Energy versus time graph shows a distinct rise in energy indicative of a main pulse.
10. PSD graph shows approximately 99 % of energy contained within first 150 MHz.

v. Waveform NTS13V01.WFM

1. Transmitting antenna used was a TEM horn.

2. Transmitter used was a Febetron.
3. Elevation angle (Source) = 0 degrees.
4. Polarization transmitted - Horizontal.
5. Polarization captured - Horizontal.
6. Record length - 100 nanoseconds.
7. Pulse visible.
8. Pulse duration - approx. 21 nanoseconds.
9. Pulse shape resembles output from Febetron.
10. Unable to generate energy versus time graph.
11. PSD graph shows that over 90% of energy of contained within first 300 MHz.
12. Energy extends noticeably to 400 MHz. Residual energy out to 800 MHz.

w. Waveform NTS13W01.WFM

1. Transmitting antenna used was a TEM horn.
2. Transmitter used was a Febetron.
3. Elevation angle (Source) = 0 degrees.
4. Polarization transmitted - Horizontal.
5. Polarization captured - Vertical.
6. Record length - 100 nanoseconds.
7. Highly distorted main pulse visible.
8. Highly distorted "main" pulse resembles output from Febetron.
9. Unable to generate energy versus time graph.
10. PSD graph shows that over 95% of energy contained within first 300 MHz.
11. Residual energy extends out to 1.2 GHz.

x. Waveform NTS13X01.WFM

1. Transmitting antenna used was a TEM horn.
2. Transmitter used was a Febetron.
3. Elevation angle (Source) = 0 degrees.
4. Polarization transmitted - Horizontal.
5. Polarization captured - Vertical.
6. Record length - 100 nanoseconds.
7. Highly distorted main pulse visible.
8. Distorted "main" pulse resembles output from Febetron.
9. Unable to generate energy versus time graph.
10. PSD graph shows 99% of energy contained within the frequency range from 0 MHz to 300 MHz.

y. Waveform NTS13Y01.WFM

1. Transmitting antenna used was a TEM horn.
2. Transmitter used was a Febetron.
3. Elevation angle (Source) = 0 degrees.
4. Polarization transmitted - Horizontal.
5. Polarization captured - Vertical.
6. Record length - 500 nanoseconds.
7. What appears as two distinct pulses shows up in the first 200 nanoseconds. The "first" pulse appears to be 25 nanoseconds wide followed by the second pulse 15 nanoseconds later. The "second" pulse is approximately 50 nanoseconds wide.
8. Energy versus time graph shows two distinct rises in energy indicative of two main pulses. ~~The two distinct~~

energy rises coincide in time with the appearance of the "two pulses".

9. PSD graph shows 98% of energy contained within the frequency range from 0 MHz to 135 MHz.

10. Residual energy extends out to 250 MHz.

z. Waveform NTS13Z01.WFM

1. Transmitting antenna used was a TEM horn.

2. Transmitter used was a Febetron.

3. Elevation angle (Source) = 0 degrees.

4. Polarization transmitted - Horizontal.

5. Polarization captured - Horizontal.

6. Record length - 100 nanoseconds.

7. A distorted main pulse is visible.

8. Pulse duration - approximately 20 nanoseconds.

9. Distorted pulse resembles output from Febetron.

10. Unable to generate energy versus time graph.

11. PSD graph shows that 98 % of energy contained in the frequency range from 0 MHz to 590 MHz.

12. Energy extends noticeably out to 820 MHz. Residual energy extends out to 1 GHz.

aa. Waveform NTS14A01.WFM

1. Transmitting antenna used was a TEM horn.

2. Transmitter used was a Febetron.

3. Elevation angle (Source) = 0 degrees.

4. Polarization transmitted - Horizontal.

5. Polarization captured - Horizontal.
6. Record length - 500 nanoseconds.
7. What appears to be a highly distorted main pulse is visible initially. A "second" pulse is visible approximately 200 nanoseconds after the first.
8. Pulse shape of distorted "main" pulse resembles output from Febetron.
9. Energy versus time graph shows an immediate, distinct rise in energy indicative of a main pulse. A second distinct rise in energy is visible and coincides in time with the appearance of the "second" pulse.
10. PSD graph shows that over 98 % of the energy is contained within the frequency range from 0 to 150 MHz.
11. Residual energy extends out to 180 MHz.

ab. *Waveform NTS14B01.WFM*

1. Transmitting antenna used was a TEM horn.
2. Transmitter used was a Febetron.
3. Elevation angle (Source) = 0 degrees.
4. Polarization transmitted - Horizontal.
5. Polarization captured - Horizontal.
6. Record length - 2000 nanoseconds.
7. No distinct, discernible, "main" pulse is visible. This is probably due to the long collect time (i.e. 2000 nanoseconds) resulting in a loss of detail. The digitized waveform shows that what appears to be the main signal appears within the first 300 nanoseconds.
8. Energy versus time graph shows an immediate, distinct rise energy. This coincides in time and is indicative what appears to be the main signal.
9. PSD graph shows that 98 % of energy contained within the frequency range from 0 MHz to 25 MHz.

10. Energy extends noticeably out to 33 MHz.
Residual energy extends out to 45 MHz.

ac. Waveform NTS14C01.WFM

1. Transmitting antenna used was a TEM horn.
2. Transmitter used was a Febetron.
3. Elevation angle (Source) = 0 degrees.
4. Polarization transmitted - Horizontal.
5. Polarization captured - Vertical.
6. Record length - 2000 nanoseconds.
7. No discernible, distinct, main pulse is visible.
This is probably due to the long collect time resulting in a loss of detail.
8. The digitized waveform shows that the "main" signal occurs within the first 300 nanoseconds.
9. Energy versus time graph shows an immediate, distinct rise in energy. This coincides in time and is indicative of the "main" signal.
10. PSD graph shows that 99 % of energy contained in the frequency range from 0 MHz to 60 MHz.
11. Residual energy extends out to 80 MHz.

ad. Waveform NTS14D01.WFM

1. Transmitting antenna used was a TEM horn.
2. Transmitter used was a Febetron.
3. Elevation angle (Source) = 0 degrees.
4. Polarization transmitted - Horizontal.
5. Polarization captured - Receiving antenna was elevated 45 degrees relative to the horizontal.

6. Record length - 2000 nanoseconds.

7. No distinct, discernible, main pulse is visible. This is probably due in part to the long collect time resulting in a loss of detail. Additionally, the relative orientation of the receiving antenna (i.e. elevated by 45 degrees) further contributed to the lack of capturing the main pulse.

8. Energy versus time graph shows an immediate, distinct rise in energy. This is indicative that the "main" part of the signal occurs within the first 300 nanoseconds.

9. PSD graph shows that 99 % of energy contained within the frequency range from 0 MHz 60 MHz.

10. Residual energy extends out to 80 MHz.

6. Directory 5-8-90

The following waveforms were captured and digitized on 8 May, 1990.

a. Waveform NTS15A01.WFM

1. Transmitting antenna used was the Lawrence Livermore National Laboratories (LLNL) modified log periodic.

2. Transmitter used was a Febetron.

3. Elevation angle (Source) = 0 degrees.

4. Polarization transmitted - Horizontal.

5. Polarization captured - Horizontal.

6. Record length - 100 nanoseconds.

7. Pulse visible.

8. Pulse duration - approximately 30 nanoseconds.

9. Pulse shape resembles output from LLNL modified log periodic antenna versus output from Febetron.

10. Energy versus time graph shows immediate rise in energy.

11. PSD graph shows approximately 10 % of the energy is contained within the first 100 MHz. The frequency range from 100 MHz to 500 MHz contains approximately 89 % of the energy.

12. Residual energy extends out to 600 MHz.

b. Waveform NTS15B01.WFM

1. Transmitting antenna used was the LLNL modified log periodic.

2. Transmitter used was the Febetron.

3. Elevation angle (Source) = 0 degrees.

4. Polarization transmitted - Horizontal.

5. Polarization captured - Horizontal.

6. Record length - 500 nanoseconds.

7. Highly distorted main pulse visible.

8. Distorted pulse resembles output from the LLNL modified log periodic antenna.

9. Energy versus time graph does not show an immediate, distinct rise in energy. Instead, the energy curve exhibits a 45 degree "rise" slope. This is indicative that a "clean" main pulse was not visible, but rather a highly distorted main pulse.

10. PSD graph shows that virtually all the energy is contained in the frequency range from 0 MHz to 110 MHz.

c. Waveform NTS15C01.WFM

1. Transmitting antenna used was the LLNL modified log periodic.

2. Transmitter used was a Febetron.

3. Elevation angle (Source) = 0 degrees.

4. Polarization transmitted - Horizontal.
5. Polarization captured - Vertical.
6. Record length - 500 nanoseconds.
7. No distinct main pulse is visible.
8. What appears to be a highly dispersed, distorted pulse is initially visible. This is most probably indicative of multipath effects and reflections.
9. Energy versus time graph shows a gradual rise in the energy curve. The absence of a distinct, immediate rise in energy is indicative of no "main" pulse being captured.
10. PSD graph shows 99 % of the energy is contained within the frequency range from 0 to 60 MHz.
11. Residual energy extends out to 70 MHz.

d. Waveform NTS15D01.WFM

1. Transmitting antenna used was the LLNL modified log periodic.
2. Transmitter used was a Febetron.
3. Elevation angle (Source) = 0 degrees.
4. Polarization transmitted - Horizontal.
5. Polarization captured - Vertical.
6. Record length - 100 nanoseconds.
7. No pulse is clearly visible.
8. What appears to be a highly distorted main pulse appears initially. This is possibly indicative of multipath effects and/or reflections from the horizontally polarized transmitted wave.
9. Energy versus time graph shows a gradual build-up of energy. There is no immediate, distinct rise in energy indicative of a main pulse.

10. PSD graph shows approximately 85 % of the energy is contained within the frequency range from 0 to 100 MHz. The frequency range from 100 MHz to 400 MHz contains approximately 14 % of the energy. Residual energy extends out to 500 MHz.

e. Waveform NTS15E01.WFM

1. Transmitting antenna used was the LLNL modified log periodic.

2. Transmitter used was a Febetron.

3. Elevation angle (Source) = 0 degrees.

4. Polarization transmitted - Horizontal.

5. Polarization captured - Vertical.

6. Record length - 100 nanoseconds.

7. No distinct main pulse is visible.

8. What appears to be a highly distorted "main" pulse is visible initially. This is probably indicative of multipath effects and reflections.

9. Energy versus time graph shows a gradual build-up of energy. No distinct, rise in energy is visible indicative of a main pulse.

10. PSD graph shows approximately 98 % of the energy is contained within the frequency range from 0 to 400 MHz.

11. Residual energy extends out to 500 MHz.

f. Waveform NTS15F01.WFM

1. Transmitting antenna used was the LLNL modified log periodic.

2. Transmitter used was a Febetron.

3. No further analysis was performed on this waveform. The digitized sample was a "misfire".

g. Waveform NTS15G01.WFM

1. Transmitting antenna used was the LLNL modified log periodic.
2. Transmitter used was a Febetron.
3. Elevation angle (Source) = 0 degrees.
4. Polarization transmitted - Horizontal.
5. Polarization captured - Horizontal.
6. Record length - 500 nanoseconds.
7. No distinct main pulse is visible.
8. What appears to be a highly distorted, dispersed pulse is visible initially. The absence of a clearly discernible main pulse is probably due to the long collect time resulting in a loss of fine detail.
9. Energy versus time graph shows a gradual build-up of energy. No distinct, immediate rise in energy is visible indicative of a main pulse.
10. PSD graph shows 99 % of the energy is contained in the frequency range from 0 to 60 MHz.
11. Residual energy extends out to 90 MHz.

h. Waveform NTS15H01.WFM

1. Transmitting antenna used was the LLNL modified log periodic.
2. Transmitter used was a Febetron.
3. Elevation angle (Source) = 0 degrees.
4. Polarization transmitted - Horizontal.
5. Polarization captured - Horizontal.
6. Record length - 100 nanoseconds.
7. Pulse visible.

8. Pulse duration - approx. 20 nanoseconds.
9. Pulse shape resembles output from LLNL modified log periodic antenna.
10. Energy versus time graph shows an immediate, distinct rise in energy indicative of a main pulse.
11. PSD graph shows over 99 % of the energy is contained within the frequency range from 0 to 500 MHz.
12. Residual energy extends out to 800 MHz.

i. Waveform NTS15I01.WFM

1. Transmitting antenna used was the LLNL modified log periodic.
2. Transmitter used was a Febetron.
3. Elevation angle (Source) = 0 degrees.
4. Polarization transmitted - Horizontal.
5. Polarization captured - Horizontal.
6. Record length - 100 nanoseconds.
7. Highly distorted main pulse visible.
8. Distorted pulse shape resembles output from the LLNL modified log periodic antenna.
9. Energy versus time graph shows a gradual build-up of energy. No distinct, immediate rise in energy indicative of a main pulse is visible.
10. PSD graph shows that 99 % of the energy is contained in the frequency range from 0 to 400 MHz.
11. Residual energy extends out to 500 MHz.

j. Waveform NTS15J01.WFM

1. Transmitting antenna used was the LLNL modified log periodic.

2. Transmitter used was a Febetron.
3. Elevation angle (Source) = 0 degrees.
4. Polarization transmitted - Horizontal.
5. Polarization captured - Horizontal.
6. Record length - 100 nanoseconds.
7. What appears to be a distorted main pulse is visible.
8. Energy versus time graph shows a gradual build-up of energy. No distinct, immediate rise in energy indicative of a main pulse is visible.
9. PSD graph shows over 98 % of the energy is contained in the frequency range from 0 to 300 MHz.
10. Residual energy extends out to 500 MHz.

k. Waveform NTS15K01.WFM

1. Transmitting antenna used was the LLNL modified log periodic.
2. Transmitter used was a Febetron.
3. Elevation angle (Source) = 0 degrees.
4. Polarization transmitted - Horizontal.
5. Polarization captured - Not Annotated in Notes.
6. Record length - 100 nanoseconds.
7. No clearly discernible pulse is visible.
8. Energy versus time graph shows a gradual build-up of energy. No distinct rise in the energy curve indicative of a main pulse is visible.
9. PSD graph shows 98 % of energy contained within the frequency range from 0 to 450 MHz.
10. Energy extends noticeably out to 850 MHz.

1. Waveform NTS15L01.WFM

1. Transmitting antenna used was the LLNL modified log periodic.

2. Transmitter used was a Febetron.

3. Elevation angle (Source) = 0 degrees.

4. Polarization transmitted - Horizontal.

5. Polarization captured - Vertical.

6. Record length - 100 nanoseconds.

7. No pulse is visible. What appears to be an extremely distorted main pulse appears initially.

8. Unable to generate energy versus time graph.

9. PSD graph shows that 98 % of the energy is contained in the frequency range from 0 to 400 MHz.

10. Energy extends noticeably out to 600 MHz. Residual energy extends out to 1.3 GHz.

m. Waveform NTS15M01.WFM

1. Transmitting antenna used was the LLNL modified log periodic.

2. Transmitter used was a Febetron.

3. Elevation angle (Source) = 0 degrees.

4. Polarization transmitted - Horizontal.

5. Polarization captured - Horizontal.

6. Record length - 100 nanoseconds.

7. Pulse visible.

8. Pulse duration - approx. 20 nanoseconds.

9. Pulse shape resembles output from the LLNL modified log periodic antenna.

10. Energy versus time graph shows a distinct rise in energy indicative of a main pulse.

11. PSD graph shows that 98 % of the energy is contained in the frequency range from 0 to 430 MHz.

12. Energy extends out to 600 MHz.

n. Waveform NTS15N01.WFM

1. Transmitting antenna used was the LLNL modified log periodic.

2. Transmitter uses was a Febetron.

3. Elevation angle (Source) = 0 degrees.

4. Polarization transmitted - Horizontal.

5. Polarization captured - Vertical.

6. Record length - 500 nanoseconds.

7. No clearly discernible pulse is visible.

8. What appears to be a highly distorted pulse is visible initially.

9. Energy versus time graph shows a gradual build-up of energy. No distinct rise in energy indicative of a main pulse is visible.

10. PSD graph shows that 99 % of the energy is contained in the frequency range from 0 to 100 MHz.

11. Residual energy extends out to 150 MHz.

o. Waveform NTS15O01.WFM

1. Transmitting antenna used was the LLNL modified log periodic.

2. Transmitter used was a Febetron.

3. Elevation angle (Source) = 0 degrees.

4. Polarization transmitted - Horizontal.
5. Polarization captured - Vertical.
6. Record length - 100 nanoseconds.
7. No clearly discernible pulse is visible.
8. What appears to be a highly distorted pulse is visible initially. This is probably due to the effects of multipath and reflections of the horizontally polarized main pulse.
9. Energy versus time graph shows a gradual build-up of energy. No distinct rise in energy indicative of a main pulse is visible.
10. PSD graph shows that 99 % of the energy is contained in the frequency range from 0 to 400 MHz.
11. Residual energy extends out to 420 MHz.

p. Waveform NTS15P01.WFM

1. Transmitting antenna used was the LLNL modified log periodic.
2. Transmitter used was a Febetron.
3. Elevation angle (Source) = 0 degrees.
4. Polarization transmitted - Horizontal.
5. Polarization captured - Horizontal.
6. Record length - 500 nanoseconds.
7. No clearly discernible main pulse is visible.
8. What appears to be a highly distorted pulse is visible initially.
9. Energy versus time graph shows a gradual build-up of energy. No distinct rise in energy indicative of a main pulse is visible.
10. PSD graph shows that 99 % of the energy is contained in the frequency range from 0 to 90 MHz.

11. Residual energy extends out to 200 MHz.

q. Waveform NTS15Q01.WFM

1. Transmitting antenna used was the LLNL modified log periodic.

2. Transmitter used was a Febetron.

3. Elevation angle (Source) = 0 degrees.

4. Polarization transmitted - Horizontal.

5. Polarization captured - Horizontal.

6. Record length - 500 nanoseconds.

7. No clearly discernible pulse is visible.

8. Energy versus time graph shows a gradual rise in energy. No immediate, distinct rise in energy indicative of a main pulse is visible.

9. PSD graph shows that 98 % of the energy is contained in the frequency range from 0 to 70 MHz.

10. Energy extends out to 90 MHz.

r. Waveform NTS15R01.WFM

1. Transmitting antenna used was the LLNL modified log periodic.

2. Transmitter used was a Febetron.

3. Elevation angle (Source) = 0 degrees.

4. Polarization transmitted - Horizontal.

5. Polarization captured - Horizontal.

6. Record length - 100 nanoseconds.

7. Highly distorted main pulse is visible.

8. Distorted main pulse resembles output from the LLNL modified log periodic antenna.

9. Energy versus time graph shows a gradual build-up of energy. No immediate, distinct rise in energy indicative of a main pulse is visible.

10. PSD graph shows that 98 % of the energy is contained in the frequency range from 0 to 300 MHz.

11. Energy extends out to 500 MHz.

s. Waveform NTS15S01.WFM

1. Transmitting antenna used was the LLNL modified log periodic.

2. Transmitter used was a Febetron.

3. Elevation angle (Source) = 0 degrees.

4. Polarization transmitted - Horizontal.

5. Polarization captured - Horizontal.

6. Record length - 100 nanoseconds.

7. No clearly discernible main pulse is visible.

8. What appears to be an extremely distorted pulse is visible initially.

9. Unable to generate energy versus time graph.

10. PSD graph shows that 99 % of the energy is contained in the frequency range from 0 to 400 MHz.

11. Residual energy extends out to 520 MHz.

t. Waveform NTS15T01.WFM

1. Transmitting antenna used was the LLNL modified log periodic.

2. Transmitter used was a Febetron.

3. Elevation angle (Source) = 0 degrees.
4. Polarization transmitted - Horizontal.
5. Polarization captured - Vertical.
6. Record length - 100 nanoseconds.
7. No pulse is visible.
8. Multipath effects and reflections of the horizontally polarized main pulse is most probably what was captured and digitized.
9. Energy versus time graph shows a gradual build-up of energy. No immediate, distinct rise in energy indicative of a main pulse is visible.
10. PSD graph shows that 99 % of the energy is contained in the frequency range from 0 to 220 MHz.
11. Residual energy extends out to 300 MHz.

u. Waveform NTS15U01.WFM

1. Transmitting antenna used was the LLNL modified log periodic.
2. Transmitter used was a Febetron.
3. Elevation angle (Source) = 45 degrees.
4. Polarization transmitted - Horizontal.
5. Polarization captured - Vertical.
6. Record length - 100 nanoseconds.
7. No pulse is visible.
8. Multipath effects and reflections of the main pulse is what is most probably visible in the digitized waveform.
9. Energy versus time graph shows a very gradual rise in the energy curve. No immediate, distinct build-up of energy indicative of a main pulse is visible.

10. PSD graph shows that 98 % of energy is contained in the frequency range from 0 to 100 MHz.

11. Energy extends out to 230 MHz.

v. Waveform NTS15V01.WFM

1. Transmitting antenna used was the LLNL modified log periodic.

2. Transmitter used was a Febetron.

3. Elevation angle (Source) = 45 degrees.

4. Polarization transmitted - Horizontal.

5. Polarization captured - Vertical.

6. Record length - 500 nanoseconds.

7. No clearly discernible main pulse is visible.

8. What appears to be a highly distorted pulse is visible initially. The shape of this "pulse" appears to exhibit dispersion in time of the waveshape. This could be due to multipath effects and reflections. Furthermore, due to the 45 degree elevation of the transmitting antenna, the antenna radiation pattern could be such that in both the horizontal and vertical plane, the receiving antenna may not be receiving either the main lobe or side radiation lobe.

9. Energy versus time graph shows a combination between the distinct, immediate rise in energy evident when a main pulse is present and the gradual build-up of energy evident when no main pulse is visible.

10. PSD graph shows that over 99 % of energy is contained in the frequency range from 0 to 90 MHz.

w. Waveform NTS15W01.WFM

1. Transmitting antenna used was the LLNL modified log periodic.

2. Transmitter used was a Febetron.

3. Elevation angle (Source) = 45 degrees.
4. Polarization transmitted - Horizontal.
5. Polarization captured - Horizontal.
6. Record length - 500 nanoseconds.
7. No clearly discernible main pulse is visible.
8. What appears to be a highly distorted pulse is visible initially. The shape of this "pulse" appears to exhibit dispersion in time of the waveshape. This could be due to multipath effects and reflections. Furthermore, due to the 45 degree elevation of the transmitting antenna, the antenna radiation pattern could be such that in both the horizontal and vertical plane, the receiving antenna may not be receiving either the main lobe or side lobe radiation.
9. Energy versus time graph shows a combination between the distinct, immediate rise in energy evident when a main pulse is present and the gradual build-up of energy evident when no main pulse is visible.
10. PSD graph shows that over 99 % of energy is contained in the frequency range from 0 to 90 MHz.
11. Residual energy extends out 120 MHz.

x. Waveform NTS15X01.WFM

1. Transmitting antenna used was the LLNL modified log periodic.
2. Transmitter used was a Febetron.
3. Elevation angle (Source) = 45 degrees.
4. Polarization transmitted - Horizontal.
5. Polarization captured - Horizontal.
6. Record length - 100 nanoseconds.
7. No pulse is visible.

8. Multipath effects and reflections of the main pulse is what is most probably visible in the digitized waveform.

9. Energy versus time graph shows a very gradual rise in the energy curve. No immediate, distinct build-up of energy indicative of a main pulse is visible.

10. PSD graph shows that 98 % of energy is contained in the frequency range from 0 to 110 MHz.

11. Energy noticeably extends out to 400 MHz. Residual energy extends out to 520 MHz.

y. Waveform NTS16A01.WFM

1. Transmitting antenna used was a TEM horn.

2. Transmitter used was a Febetron.

3. Elevation angle (Source) = 45 degrees.

4. Polarization transmitted - Horizontal.

5. Polarization captured - Horizontal.

6. Record length - 100 nanoseconds.

7. No pulse is visible.

8. What appears to be an extremely distorted main pulse is visible initially.

9. Energy versus time graph shows a gradual build-up of energy. No distinct, immediate rise in energy indicative of a main pulse is visible.

10. PSD graph shows that 95 % of energy is contained in the frequency range from 0 to 150 MHz.

11. Energy extends out to 300 MHz.

z. Waveform NTS16B01.WFM

1. Transmitting antenna used was a TEM horn.

2. Transmitter used was a Febetron.
3. Elevation angle (Source) = 45 degrees.
4. Polarization transmitted - Horizontal.
5. Polarization captured - Vertical.
6. Record length - 100 nanoseconds.
7. No pulse is visible.
8. What appears to be an extremely distorted main pulse is visible initially.
9. Energy versus time graph shows a gradual build-up of energy. No distinct, immediate rise in energy indicative of a main pulse is visible.
10. PSD graph shows that 99 % of energy is contained in the frequency range from 0 to 200 MHz.
11. Residual energy extends out to 250 MHz.

aa. *Waveform NTS16C01.WFM*

1. Transmitting antenna used was a TEM horn.
2. Transmitter used was a Febetron.
3. Elevation angle (Source) = 45 degrees.
4. Polarization transmitted - Horizontal.
5. Polarization captured - Vertical.
6. Record length - 500 nanoseconds.
7. Two pulses are visible. The second pulse occurs about 5 nanoseconds after the first pulse.
8. Pulse duration for the first pulse is approx. 30 nanoseconds. Pulse duration for the second pulse is approx. 50 nanoseconds.
9. Pulse shape for both pulses resembles output from Febetron.

10. Energy versus time graph shows two (2) distinct rises in energy indicative of two main pulses.

11. PSD graph shows that 98 % of energy is contained in the frequency range from 0 to 100 MHz.

12. Energy extends out to 120 MHz.

ab. Waveform NTS16D01.WFM

1. Transmitting antenna used was a TEM horn.

2. Transmitter used was a Febetron.

3. Elevation angle (Source) = 45 degrees.

4. Polarization transmitted - Horizontal.

5. Polarization captured - Horizontal.

6. Record length - 500 nanoseconds.

7. Two pulses are visible. The second pulse occurs about 15 nanoseconds after the first pulse.

8. Pulse duration for the first pulse is approx. 50 nanoseconds. Pulse duration for the second pulse is approx. 50 nanoseconds.

9. Pulse shape for both pulses resembles output from Febetron.

10. Energy versus time graph shows two (2) distinct rises in energy indicative of two main pulses.

11. PSD graph shows that 98 % of energy is contained in the frequency range from 0 to 100 MHz.

12. Energy extends out to 150 MHz.

ac. Waveform NTS16E01.WFM

1. Transmitting antenna used was a TEM horn.

2. Transmitter used was a Febetron.

3. Elevation angle (Source) = 45 degrees.
4. Polarization transmitted - Horizontal.
5. Polarization captured - Horizontal.
6. Record length - 2000 nanoseconds.
7. No further analysis performed. This digitized signal was a "misfire" resulting in a bad shot.

ad. Waveform NTS16F01.WFM

1. Transmitting antenna used was a TEM horn.
2. Transmitter used was a Febetron.
3. Elevation angle (Source) = 45 degrees.
4. Polarization transmitted - Horizontal.
5. Polarization captured - Horizontal.
6. Record length - 100 nanoseconds.
7. No pulse is visible.
8. What appears to be an extremely distorted main pulse is visible initially.
9. Energy versus time graph shows a gradual build-up of energy. No distinct, immediate rise in energy indicative of a main pulse is visible. The shape of the curve, however, shows distinct minor rises in energy indicating that a pulse or a distorted pulse may be present in the signal.
10. PSD graph shows that 95 % of energy is contained in the frequency range from 0 to 150 MHz.
11. Energy extends out to 300 MHz.

ae. Waveform NTS16G01.WFM

1. Transmitting antenna used was a TEM horn.
2. Transmitter used was a Febetron.
3. Elevation angle (Source) = 0 degrees.
4. Polarization transmitted - Horizontal.
5. Polarization captured - Horizontal.
6. Record length - 100 nanoseconds.
7. No clearly discernible pulse is visible.
8. A distorted main pulse is visible initially.
9. Pulse shape of distorted "pulse" resembles output from Febetron.
10. Unable to generate energy versus time graph.
11. PSD graph shows that 98 % of energy is contained in the frequency range from 0 to 400 MHz.
12. Energy extends out to 1 GHz.

af. Waveform NTS16H01.WFM

1. Transmitting antenna used was a TEM horn.
2. Transmitter used was a Febetron.
3. Elevation angle (Source) = 0 degrees.
4. Polarization transmitted - Horizontal.
5. Polarization captured - Vertical.
6. Record length - 100 nanoseconds.
7. No clearly discernible pulse is visible.
8. What appears to be a highly distorted pulse is visible initially.

9. Pulse shape of distorted "pulse" resembles output from Febetron.

10. Energy versus time graph shows a distinct, immediate rise in energy indicative of a main pulse.

11. PSD graph shows that 99 % of energy is contained in the frequency range from 0 to 250 MHz.

12. Energy extends out to 300 MHz.

D. ANALYSIS OF PAIRED WAVEFORMS

The following analysis is for those digitized waveforms in which both the horizontal and vertical components were obtained using the same time base.

1. Directory 5-4-90

The following observations were noted:

a. Waveforms NTS12J01.WFM and NTS12K01.WFM

1. Transmitting antenna used was a TEM horn antenna.
2. Elevation angle (Source) = 45 degrees.
3. Horizontally polarized component (NTS12J01) clearly shows the main pulse.
4. Vertically polarized component (NTS12K01) shows a signal trace that is very similar to the horizontal component. Amplitude of pulse is less than corresponding amplitude for horizontal component.

2. Directory 5-7-90

The following observations were noted:

a. Waveforms NTS13A01.WFM and NTS13C01.WFM

1. Transmitting antenna used was a TEM horn antenna.

2. Horizontally polarized component (NTS13A01) clearly shows the main pulse.

3. Vertically polarized component (NTS13C01) shows a signal trace that is very similar to the horizontal component. Amplitude of pulse is less than corresponding amplitude for horizontal component.

b. Waveforms NTS13F01.WFM and NTS13H01.WFM

1. Transmitting antenna used was a TEM horn antenna.

2. Elevation angle (Source) = 45 degrees.

3. Horizontally polarized component (NTS13F01) shows an extremely distorted main pulse.

4. Vertically polarized component (NTS13H01) shows a slight trace of the remnants of a highly distorted pulse.

5. The waveform shape for both the horizontal and vertical components are nearly identical in appearance. This apparent depolarization of the transmitted wave is an anomaly since there is no readily available effect that would account for this. Reflections off conducting surfaces in the test site area could induce some depolarizing effects. This contributory factor, however, is considered negligible since no depolarization was noted when the transmitting antenna was not elevated by 45 degrees relative to the horizontal.

c. Waveforms NTS13I01.WFM and NTS13J01.WFM

1. Transmitting antenna used was a TEM horn antenna.

2. Elevation angle (Source) = 45 degrees.

3. Horizontally polarized component (NTS13J01) clearly shows a main pulse. A second pulse follows the main pulse by approximately 2 nanoseconds.

4. Vertically polarized component (NTS13I01) shows what appears to be a highly distorted main pulse. A second distorted pulse appears to follow the first by approximately 5 nanoseconds.

5. The horizontally and vertically polarized components show some similarity in appearance. The similarity, however, is not as pronounced as in the other paired shots where the transmitting antenna was elevated by 45 degrees relative to the horizontal.

d. Waveforms NTS13L01.WFM and NTS13O01.WFM

1. Transmitting antenna used was the TEM horn antenna.

2. Horizontally polarized component (NTS13O01) shows a slightly distorted main pulse.

3. Vertically polarized component (NTS13O01) shows a distorted main pulse. The amplitude of the "distorted" pulse is significantly less than the horizontally polarized component of the transmitted pulse.

e. Waveforms NTS13M01.WFM and NTS13N01.WFM

1. Transmitting antenna used was the TEM horn antenna.

2. Horizontally polarized component clearly shows a main pulse.

3. Vertically polarized component clearly shows a main pulse.

4. An excellent example illustrating the apparent circularly polarized nature of the TEM horn antenna used for transmitting the signal pulse.

f. Waveforms NTS13P01.WFM and NTS13Q01.WFM

1. Transmitting antenna used was the TEM horn antenna.

2. Horizontally polarized component (NTS13Q01) clearly shows a main pulse.

3. Vertically polarized component (NTS13P01) shows what appears to be a pulse. The amplitude of this "pulse" is less than the horizontally polarized component.

g. Waveforms NTS13R01.WFM and NTS13S01.WFM

1. Transmitting antenna used was the TEM horn antenna.

2. Horizontally polarized component (NTS13R01) clearly shows a main pulse. A second "pulse" follows the first pulse by approximately 20 nanoseconds.

3. Vertically polarized component (NTS13S01) clearly shows a main pulse. A second "pulse" follows the first pulse by approximately 20 nanoseconds.

4. An excellent example illustrating the apparent circularly polarized nature of the TEM horn antenna used for transmitting the signal pulse.

h. Waveforms NTS13V01.WFM and NTS13W01.WFM

1. Transmitting antenna used was the TEM horn antenna.

2. Horizontally polarized component clearly shows a main pulse.

3. Vertically polarized component shows a distorted pulse. The amplitude of the pulse is less than the corresponding horizontally polarized component.

i. Waveforms NTS13X01.WFM and NTS13Z01.WFM

1. Transmitting antenna used was the TEM horn antenna.

2. Horizontally polarized component (NTS13Z01) shows a slightly distorted main pulse.

3. Vertically polarized component (NTS13X01) shows a distorted pulse. The amplitude of the pulse is less than the corresponding horizontally polarized component.

3. Directory 5-8-90

The following observations were noted:

a. Waveforms NTS15A01.WFM and NTS15D01.WFM

1. Transmitting antenna used was the LLNL modified log periodic antenna.
2. Horizontally polarized component (NTS15A01) clearly shows the main pulse.
3. Vertically polarized component (NTS15D01) does not show the main pulse. Instead, what appears to multipath effects and reflections are seen initially.

b. Waveforms NTS15B01.WFM and NTS15C01.WFM

1. Transmitting antenna used was the LLNL modified log periodic antenna.
2. Horizontally polarized component (NTS15B01) shows a highly distorted main pulse.
3. Vertically polarized component (NTS15C01) shows a distorted "main" pulse. A second, smaller "pulse" follows the main pulse by approximately 10 nanoseconds.
4. The shape of the waveform for the horizontally polarized versus the vertically polarized signal would suggest that a mistake was made when annotating the polarization of the received signal. Assuming that the annotation is correct as to the polarization, this observed feature would suggest a curious anomaly.

c. Waveforms NTS15E01.WFM and NTS15H01.WFM

1. Transmitting antenna used was the LLNL modified log periodic antenna.
2. Horizontally polarized component (NTS15H01) clearly shows a main pulse.

3. Vertically polarized component (NTS15E01) does not show a main pulse. What appears to be the remnants of a "highly distorted pulse" arising from multipath effects and reflections appears initially.

d. Waveforms NTS15I01.WFM and NTS15L01.WFM

1. Transmitting antenna used was the LLNL modified log periodic antenna.

2. Horizontally polarized component (NTS15I01) shows a distorted main pulse.

3. Vertically polarized component (NTS15L01) does not show a main pulse. What appears to be the remnants of a "highly distorted pulse" arising from multipath effects and reflections appears initially.

e. Waveforms NTS15M01.WFM and NTS15O01.WFM

1. Transmitting antenna used was the LLNL modified log periodic antenna.

2. Horizontally polarized component (NTS15M01) clearly shows a main pulse.

3. Vertically polarized component (NTS15O01) does not show a main pulse. What appears to be the remnants of a "highly distorted pulse" resulting from multipath effects and reflections appears initially.

f. Waveforms NTS15N01.WFM and NTS15P01.WFM

1. Transmitting antenna used was the LLNL modified log periodic antenna.

2. Horizontally polarized component (NTS15P01) does not show a main pulse. What appears to be a "distorted" main pulse is visible initially.

3. Vertically polarized component (NTS15N01) does not show a main pulse. What appears to be a "distorted" main pulse is visible initially.

4. The waveform shape of the received signal looks very similar for both the horizontally and vertically polarized directions. This observed feature would suggest that the transmitting antenna was elevated by 45 degrees and that an error was made when cataloging the parameters. Assuming that the information was correctly recorded, this observed feature would indicate a curious anomaly.

g. Waveforms NTS15S01.WFM and NTS15T01.WFM

1. Transmitting antenna used was the LLNL modified log periodic antenna.

2. Horizontally polarized component (NTS15S01) shows a highly distorted main pulse. The waveform shape suggests a significant destructive interference may have taken place due to multipath effects and reflections.

3. Vertically polarized component (NTS15T01) does not show a main pulse. What appears to be the remnants of an extremely distorted pulse due to multipath effects and reflections is visible initially.

h. Waveforms NTS15U01.WFM and NTS15X01.WFM

1. Transmitting antenna used was the LLNL modified log periodic antenna.

2. Elevation angle (Source) = 45 degrees.

3. Horizontally polarized component (NTS15X01) does not show a clearly discernible main pulse. What appears to be the remnants of an extremely distorted pulse is visible initially.

4. Vertically polarized component (NTS15U01) does not show a main pulse. What could be a trace of the remnants of an extremely distorted pulse is visible initially.

5. The waveform shape for both the horizontal and vertical components are nearly identical in appearance. This apparent depolarization of the transmitted wave is an anomaly since there is no readily available effect that would account for this. Reflections off conducting surfaces in the test site area could induce some depolarizing

effects. This contributory factor, however, is considered negligible since no depolarization was noted when the transmitting antenna was not elevated by 45 degrees relative to the horizontal.

i. Waveforms NTS15V01.WFM and NTS15W01.WFM

1. Transmitting antenna used was the LLNL modified log periodic antenna.

2. Elevation angle (Source) = 45 degrees.

3. Horizontally polarized component (NTS15W01) shows a distorted main pulse.

4. Vertically polarized component (NTS15V01) shows a distorted main pulse.

5. The waveform shape for both the horizontal and vertical components are nearly identical in appearance. This apparent depolarization of the transmitted wave is an anomaly since there is no readily available effect that would account for this. Reflections off conducting surfaces in the test site area could induce some depolarizing effects. This contributory factor, however, is considered negligible since no depolarization was noted when the transmitting antenna was not elevated by 45 degrees relative to the horizontal.

j. Waveforms NTS16A01.WFM and NTS16B01.WFM

1. Transmitting antenna used was the TEM horn antenna.

2. Elevation angle (Source) = 45 degrees.

3. Horizontally polarized component (NTS16A01) shows a distorted main pulse.

4. Vertically polarized component (NTS16B01) shows a highly distorted main pulse.

5. The waveform shape for both the horizontal and vertical components are very similar in appearance. This apparent depolarization of the transmitted wave is an anomaly since there is no readily available effect that

would account for this. Reflections off conducting surfaces in the test site area could induce some depolarizing effects. This contributory factor, however, is considered negligible since no depolarization was noted when the transmitting antenna was not elevated by 45 degrees relative to the horizontal.

k. Waveforms NTS16C01.WFM and NTS16D01.WFM

1. Transmitting antenna used was the TEM horn antenna.
2. Elevation angle (Source) = 45 degrees.
3. Horizontally polarized component (NTS16D01) clearly shows a main pulse. A second pulse is visible approximately 20 nanoseconds after the first pulse.
4. Vertically polarized component (NTS16C01) clearly shows a main pulse. A second pulse is visible approximately 10 nanoseconds after the first pulse.
5. The waveform shape for both the horizontal and vertical components are very similar in appearance. This apparent depolarization of the transmitted wave is an anomaly since there is no readily available effect that would account for this. Reflections off conducting surfaces in the test site area could induce some depolarizing effects. This contributory factor, however, is considered negligible since no depolarization was noted when the transmitting antenna was not elevated by 45 degrees relative to the horizontal.

l. Waveforms NTS16G01.WFM and NTS16H01.WFM

1. Transmitting antenna used was the TEM horn antenna.
2. Horizontally polarized component (NTS16G01) shows a main pulse.
3. Vertically polarized component (NTS16H01) shows a distorted pulse.

V. CONCLUSION

A. ANALYSIS OF DATA

A summary of the trends and patterns observed in analyzing the Evergreen data follows. The horn antenna used for reception remained the same regardless of whether the LLNL modified log periodic or the TEM horn antenna was used for transmission. The waveforms chosen were the "cleanest" signals that best illustrated each of the following features:

1. The shape of the received pulse was noticeably different when the transmitting antenna used was a TEM horn versus the LLNL modified LP antenna. Figure 46 and Figure 47 illustrate the received waveform shape when the LLNL LP antenna was used for transmission. Figure 48 and Figure 49 illustrate the received waveform shape when the TEM horn antenna was used for transmission. These differences, reflect the different transmitting characteristics of the TEM horn [See Figure 50] versus the LLNL modified LP antenna [see Figure 51]. Figure 46 through Figure 49, furthermore, are for the case in which the receiving antenna was oriented to match the transmitting antenna's polarization (i.e. horizontal).
2. The TEM horn when used as the transmitting antenna appeared to produce symmetric looking waveforms in both the horizontal and vertical direction. The pulse amplitude of the vertically received component of the transmitted signal, however, was less than the pulse amplitude of the horizontally polarized component. Figure 52 through Figure 55 illustrate this observed feature in the NTS data obtained during the Evergreen test. This "observed feature" would tend to suggest that the transmitting characteristics of the TEM horn antenna produces a somewhat circularly polarized versus a strictly linearly polarized wave.
3. When the receiving antenna was oriented in the horizontal direction to pick up the horizontally polarized,

transmitted wave, the main pulse was distinctly observed. When the transmitting antenna used was the LLNL modified LP antenna, the main pulse was discernible and resembled the waveform shape depicted in Figure 51. Figure 56 and Figure 57 illustrate the pulse shapes obtained when the LLNL log periodic antenna was used. The TEM horn antenna when used for transmission, generated a main pulse that was similarly discernible, though the pulse shape was different, resembling the output from the Febetron (see Figure 8). Figure 58 and Figure 59 illustrate the pulse shapes obtained when the TEM horn antenna was used for transmission.

4. When the receiving antenna was oriented in the vertical direction with the transmitting antenna remaining oriented in the horizontal direction, the main pulse was not distinctly discernible. Instead, what appears to be a highly distorted main pulse is observed. This result is most probably indicative of the effects of multipath, reflection and the fact that due to the actual physical geometry, a strict horizontal versus vertical alignment cannot be achieved between the transmitting and the receiving antenna, resulting in some "leakage" of the main pulse in the vertical direction. When the LLNL modified LP antenna was used for transmission, the distortion was quite noticeable. Figure 60 and Figure 61 illustrate this case. When the TEM horn antenna was used for transmission, the distortion of the main pulse was not as pronounced. Figure 62 and Figure 63 illustrate this condition and support the observation noted in paragraph 2, above.
5. The correlation between polarization and the discernment and shape of the main pulse captured is clearly seen when a comparison is made of those series of shots where both the vertical and horizontal component of the horizontally transmitted wave was recorded. Figure 64 through Figure 67 illustrate this observation for the case when the LLNL modified LP antenna was used for transmission. Figure 68 through Figure 71 illustrate the case when the TEM horn antenna was used for transmission.
6. **ANOMALY** - When the elevation angle of the transmitting antenna was oriented at 45 degrees relative to the horizontal, [see Figure 72 and Figure 73], both the horizontally and vertically received components of the transmitted wave were nearly identical in appearance. Figure 74 and Figure 75 illustrate this when the LLNL modified LP antenna was used for transmission. Figure 76 and Figure 77 illustrate this for the case when the TEM horn was used for transmission. In both these cases,

what appears to be a distorted main pulse appears initially. No effect that I am aware of will cause this "depolarization" of the transmitted signal. A possible contributing factor are any reflections from conducting surfaces that would tend to change the orientation of the horizontally polarized wave. This factor, however, is unlikely since no depolarization was observed for the case when the transmitting antenna was orientated in the horizontal direction. Furthermore, the geometry is such that with a 45 degree up angle of transmission, the linearly polarized nature of the transmitted wave will not contain equal components in both the vertical and horizontal direction. The transmitting antenna would have to be tilted 45 degrees either left or right for this effect to be observed.

7. Analysis of the energy versus time graphs show a pattern that is indicative of whether the main pulse is present or not. For the horizontally received component of the horizontally polarized wave, a distinct rise in energy is initially observed. Figure 78 illustrates this for the LP antenna case and Figure 81 illustrates this for the TEM horn case. For the vertically received component of the horizontally polarized wave, a gradual rise in the energy curve is observed. This is illustrative of the fact that instead of a main pulse being captured, the effects of multipath and reflections are observed. Figure 79 illustrates this for the LP antenna case and Figure 82 illustrates this for the TEM case. For the case when the transmitting antenna is elevated by 45 degrees relative to the horizontal, the energy versus time graph shows a pattern that is a mixture of both the horizontal and the vertical case. Figure 84 and Figure 85 illustrate this for the LP antenna case. Figure 87 and Figure 88 illustrate this for the TEM horn case.
8. Analysis of the power spectral density graphs for the various collect times (i.e. record lengths) led to the following observations:
 - a. 500 ns collect time - virtually all the energy is contained in the frequency range from 0 MHz to 100 MHz. Figure 91 and Figure 93 illustrate this for the LP antenna case. Figure 95 and Figure 97 illustrate this for the TEM horn antenna case.
 - b. 100 ns collect time - virtually all the energy is contained in the frequency range from 0 MHz to 600 MHz. Figure 99 and Figure 101 illustrate this for the LP antenna

case. Figure 103 and Figure 105 illustrate this for the TEM horn antenna case.

c. 50 ns collect time - virtually all the energy is contained in the frequency range from 0 MHz to 1.1 GHz. Figure 107 illustrates this for the LP antenna case and Figure 109 illustrates this for the TEM horn antenna case.

9. The observations noted in sub-paragraph 8 are probably a function of the record length. As the collect time increases, more of the energy is proportionately contained in the lower frequencies. As a result, the high frequency energy content is low in proportion to the more abundant low frequency energy content. It is important to stress, however, that for all three collect times, the main pulse is present. Energy at frequencies up to 1 GHz and beyond are present in the main pulse. Therefore, to adequately capture the signal, hardware bandwidths of at least 1 GHz are required.

10. Correlation of received signal strength to the azimuthal direction of the receiving site relative to the transmitting antenna led to the following observations:

a. The received signal strength dropped off as the receiving site moved off center relative to the transmitting antenna location. This was observed in both cases in which the TEM Horn antenna and the LLNL modified Log Periodic antenna was used.

b. A comparison of waveforms NTS15M01.WFM, NTS15H01.WFM and NTS15A01.WFM [see Figure 110] shows that the signal strength dropped off as the receiving site moved off center relative to the transmitting antenna location. These waveforms were digitally captured for the case in which the LLNL Log Periodic antenna was used. It is interesting to note that the received signal strengths of waveform NTS15M01.WFM and NTS15H01.WFM indicate good symmetry in the radiation pattern of the LP antenna. Waveform NTS15M01.WFM was captured at a bearing of 24 degrees left of center and waveform NTS15H01.WFM was captured at a bearing of 25 degrees right of center.

c. A comparison of waveforms NTS13L01.WFM, NTS16G01.WFM, NTS13V01.WFM, NTS13Z01.WFM and NTS13A01.WFM [see Figure 111] shows that the signal strength dropped off as the receiving site moved off center relative to the transmitting antenna location. The waveforms were digitally captured for the case in which the TEM horn antenna was used as the transmitting antenna.

d. In the above noted observations, caution must be used, however, in the evaluation of the data. The attenuation settings were varied throughout the entire experiment. The settings and when the changes occurred were not well documented. As a result, the received signals strengths could also be a function of the attenuation setting in place at that particular moment.

11. The ringing effect observed after the main pulse is most probably due to transients induced in the circuitry of the transmitting system due to the high energy pulse. As a result, low frequency components are generated and observed trailing the main pulse. [see Figure 46 through Figure 49].

In summary, the observations noted above strongly indicate that the polarization of the received signal will be a function of the polarization of the transmitted signal and the orientation of the receiving site relative to the transmitting site. Furthermore, the effects of multipath and reflections will affect the fidelity with which the transmitted signal is received and copied. The final important point is concerned with bandwidth. Analysis of the waveforms for the short record lengths (i.e from 50 nanoseconds to 100 nanoseconds) indicated that the nanosecond pulses generated had significant frequencies extending up to 1 GHz and beyond. Therefore, to adequately capture these pulse, the hardware (i.e. antenna, receivers, oscilloscopes, etc.) will require a minimum bandwidth of 1 GHz. For faithful reproduction during the digitizing process, the Nyquist sampling rate f_s must be sufficiently great so that as a minimum, the highest frequency that can be digitized is equal to 1 GHz.

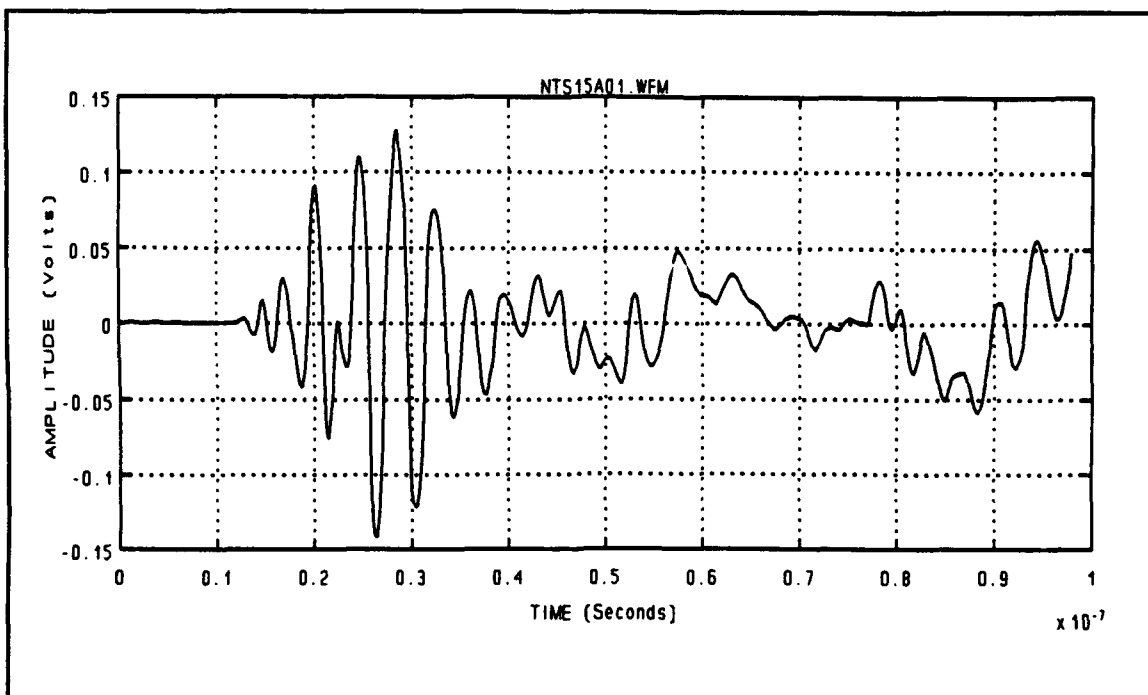


Figure 46 Waveform NTS15A01.WFM - Directory 5-8-90
Transmitting Antenna - LLNL Log Periodic

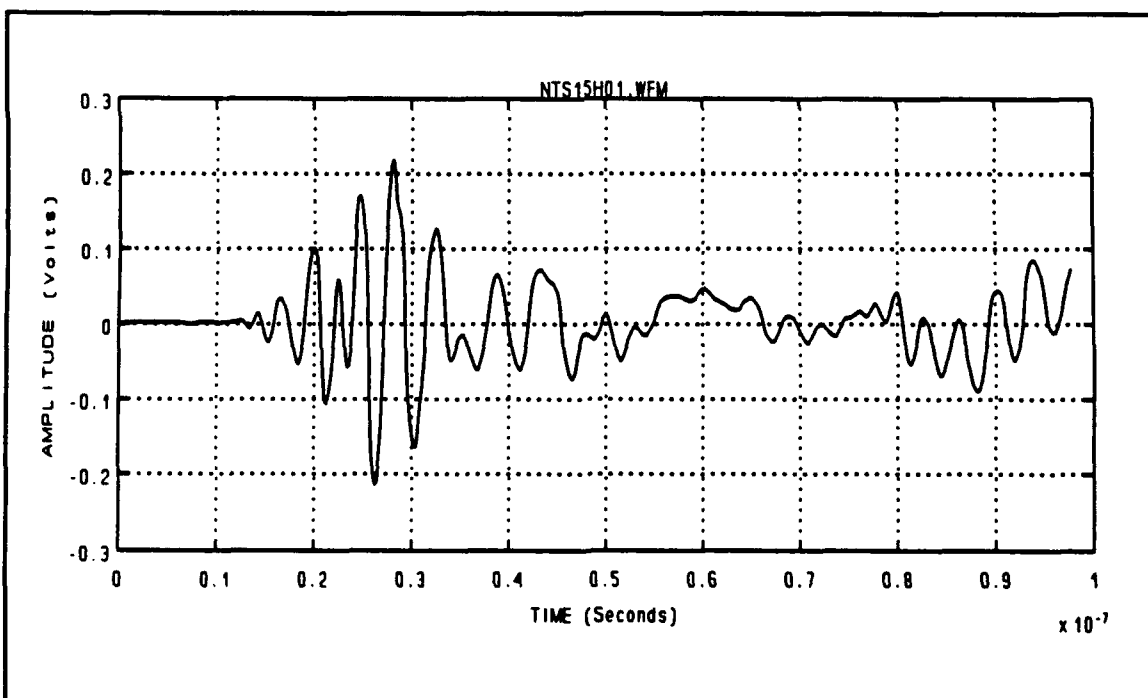


Figure 47 Waveform NTS15H01.WFM - Directory 5-8-90
Transmitting Antenna - LLNL Log Periodic

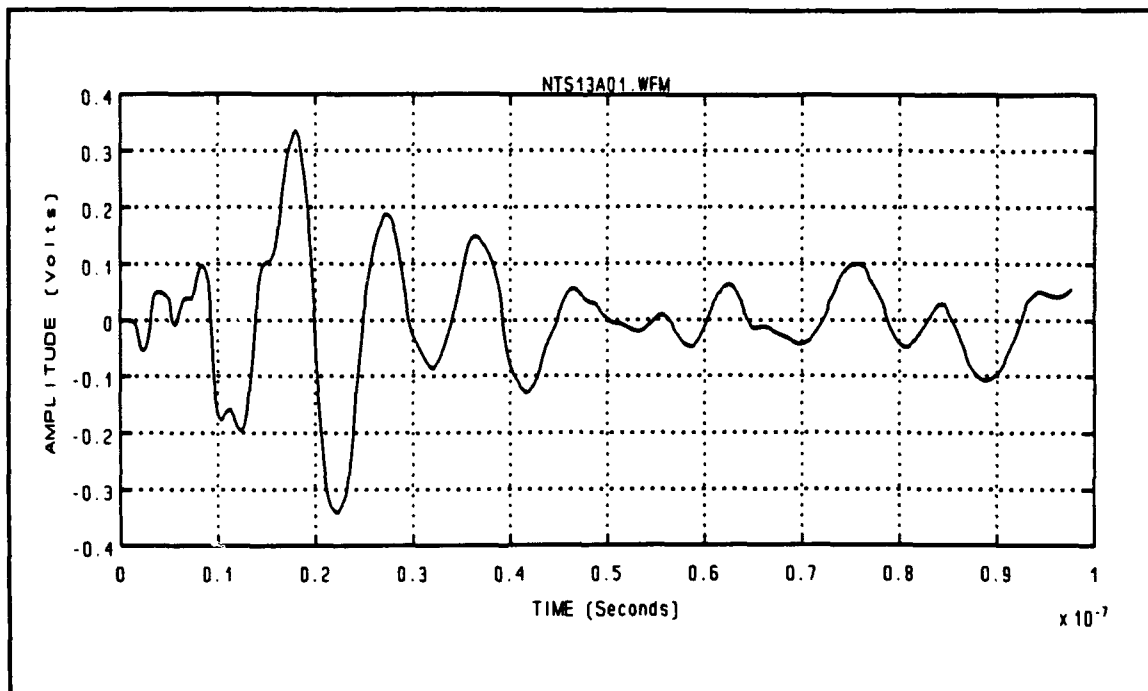


Figure 48 Waveform NTS13A01.WFM - Directory 5-7-90
Transmitting Antenna - Big TEM Horn

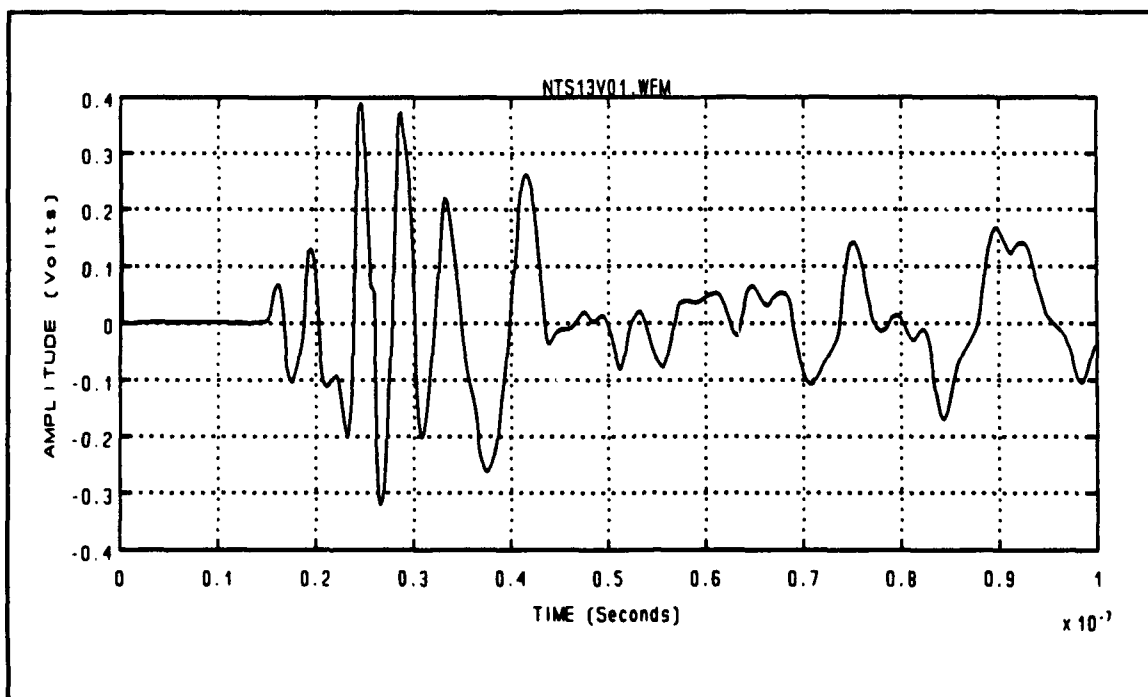


Figure 49 Waveform NTS13V01.WFM - Directory 5-7-90
Transmitting Antenna - Big TEM Horn

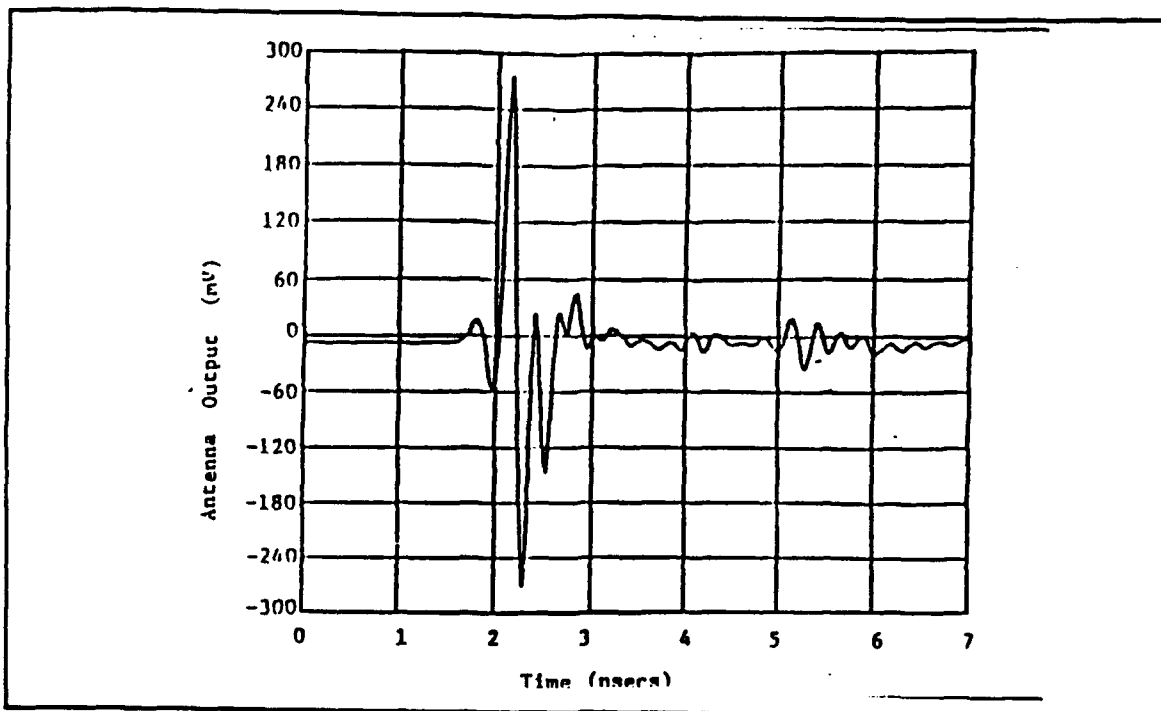


Figure 50 NBS Technical Note 1008, figure 9, p. 14
Test Response from TEM Horn

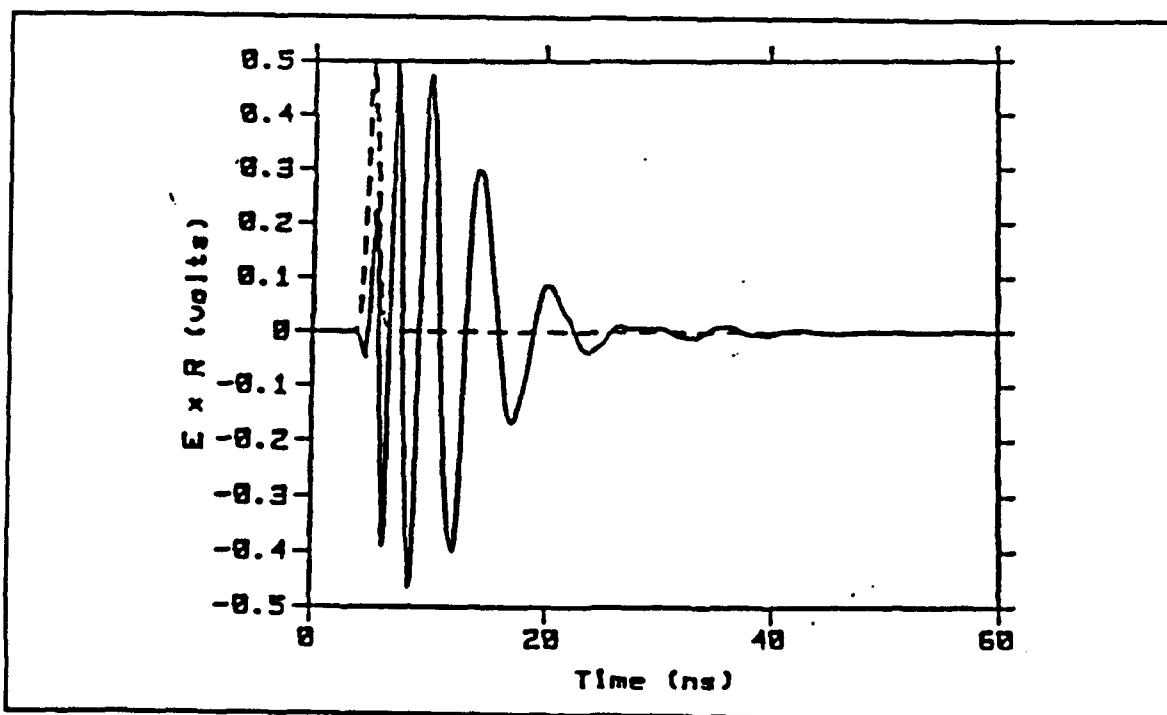


Figure 51 LLNL Technical Note 2-1-90, figure 7, p. 7
Test Response from modified Log Periodic Antenna

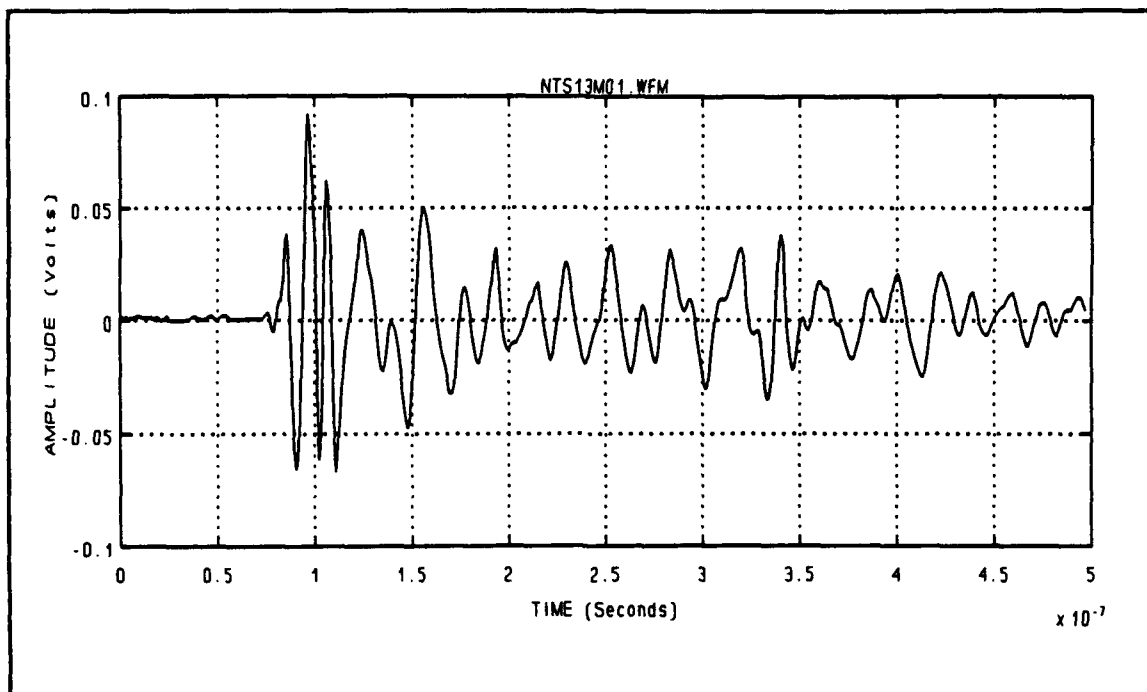


Figure 52 Waveform NTS13M01.WFM - Directory 5-7-90
Horizontal Polarization [Paired with NTS13N01.WFM]

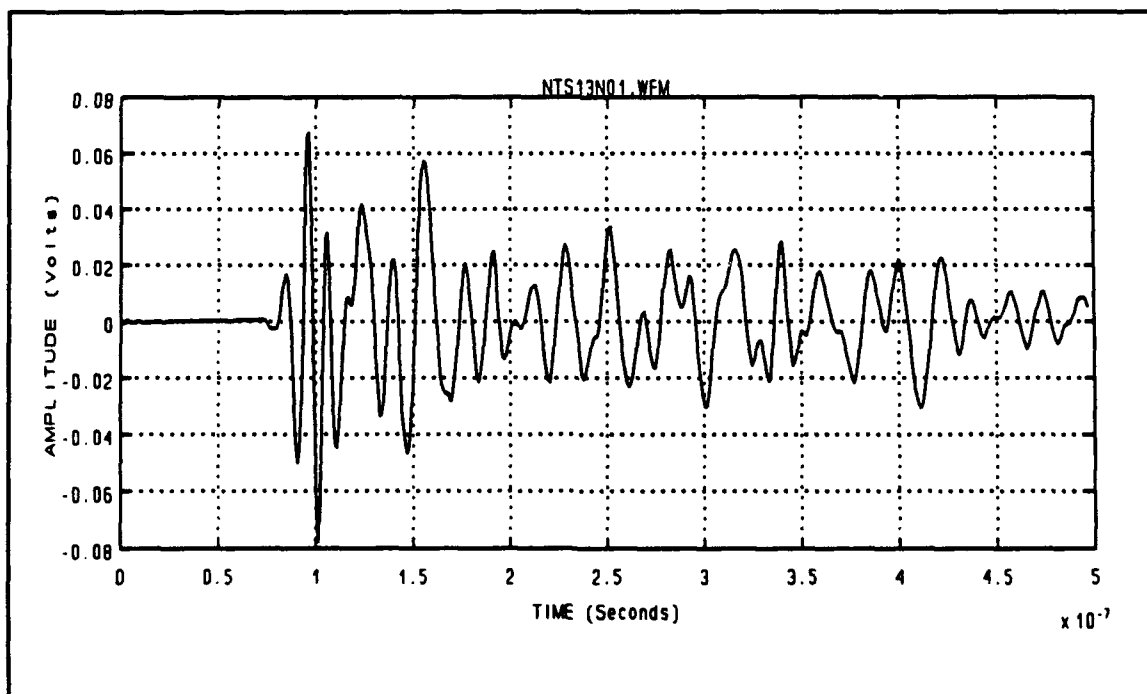


Figure 53 Waveform NTS13N01.WFM - Directory 5-7-90
Vertical Polarization [Paired with NTS13M01.WFM]

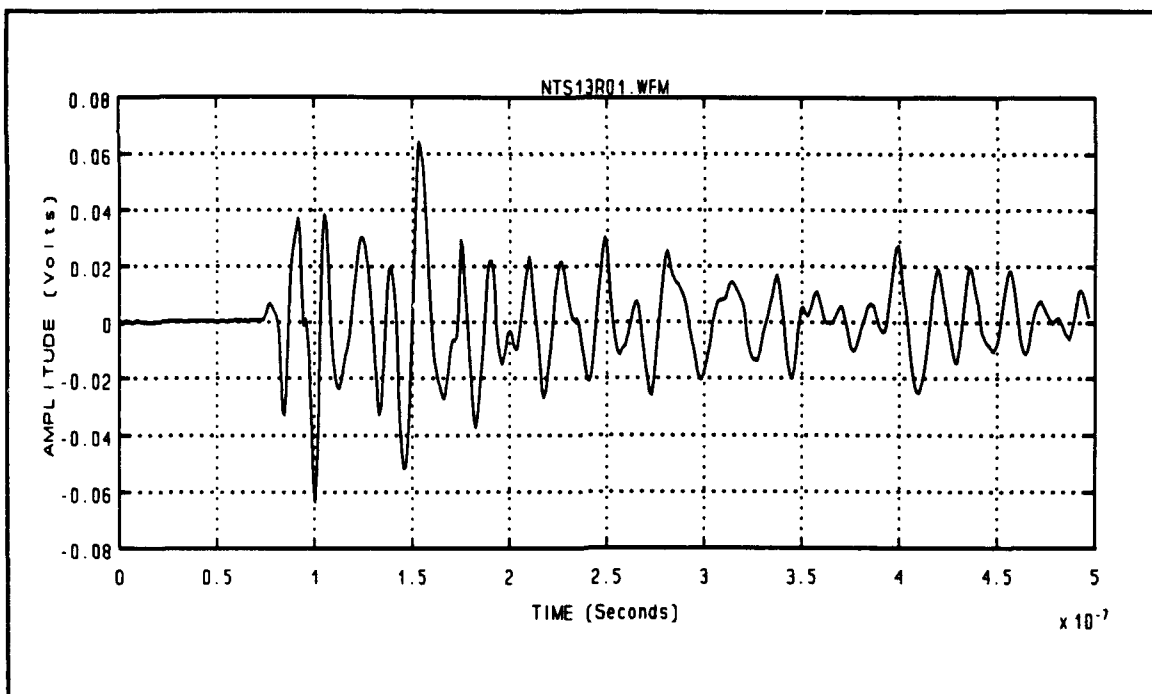


Figure 54 Waveform NTS13R01.WFM - Directory 5-7-90
Horizontal Polarization [Paired with NTS13S01.WFM]

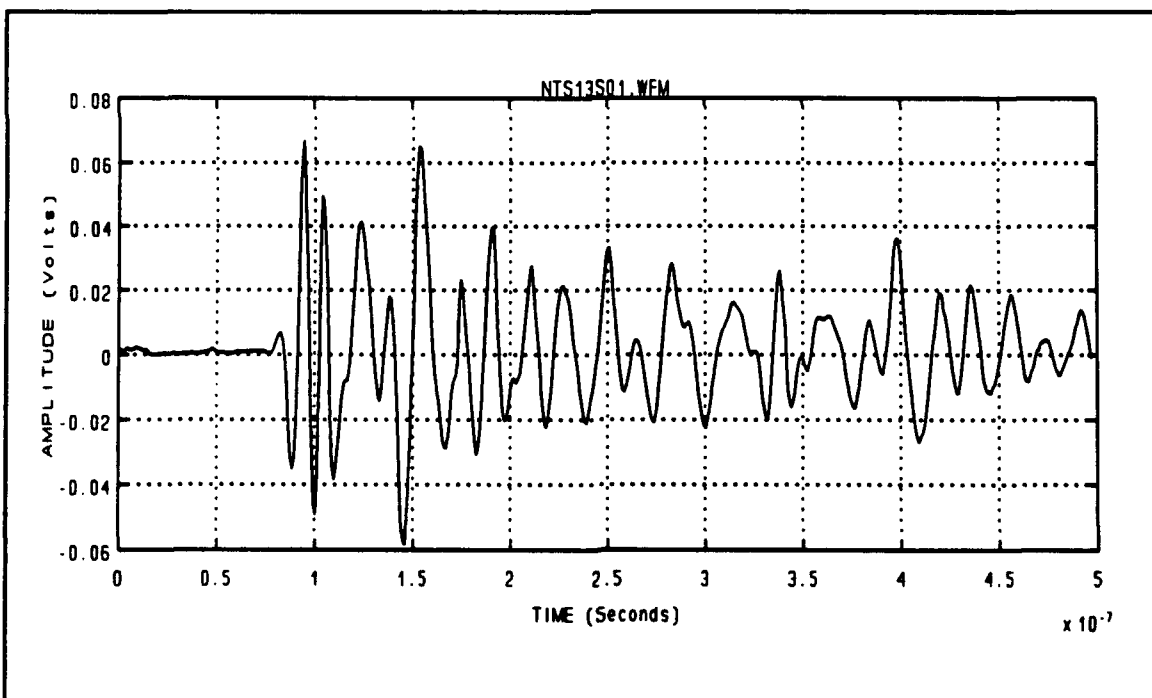


Figure 55 Waveform NTS13S01.WFM - Directory 5-7-90
Vertical Polarization [Paired with NTS13R01.WFM]

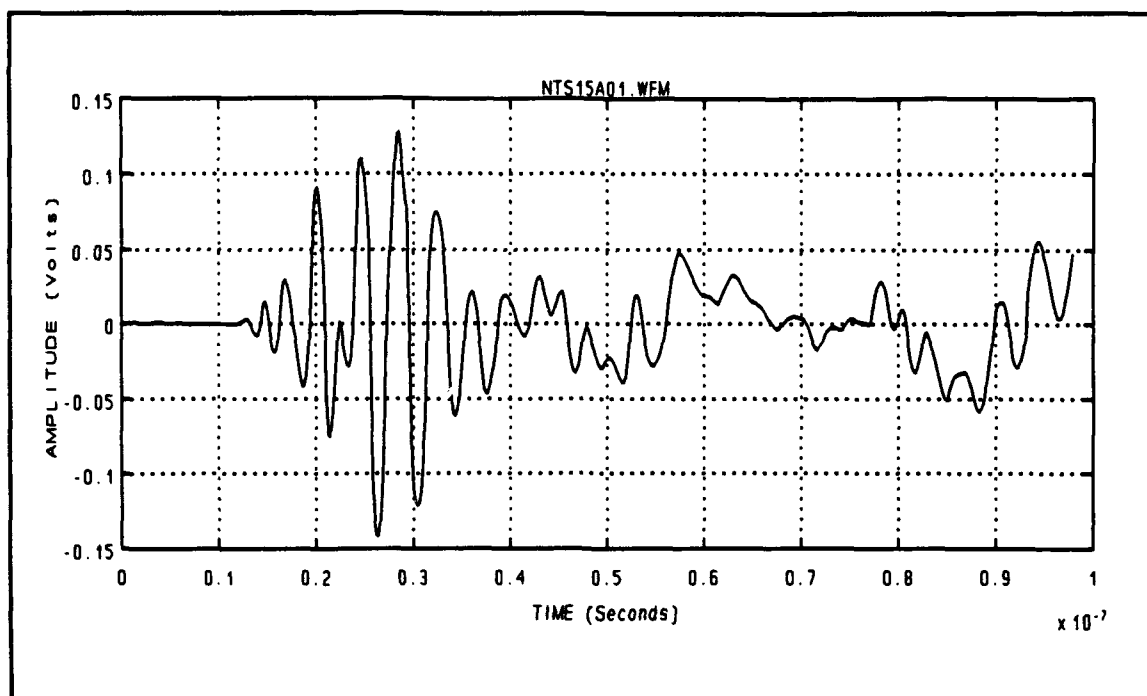


Figure 56 Waveform NTS15A01.WFM - Directory 5-8-90
LLNL Log Periodic Antenna \ Horizontal Polarization

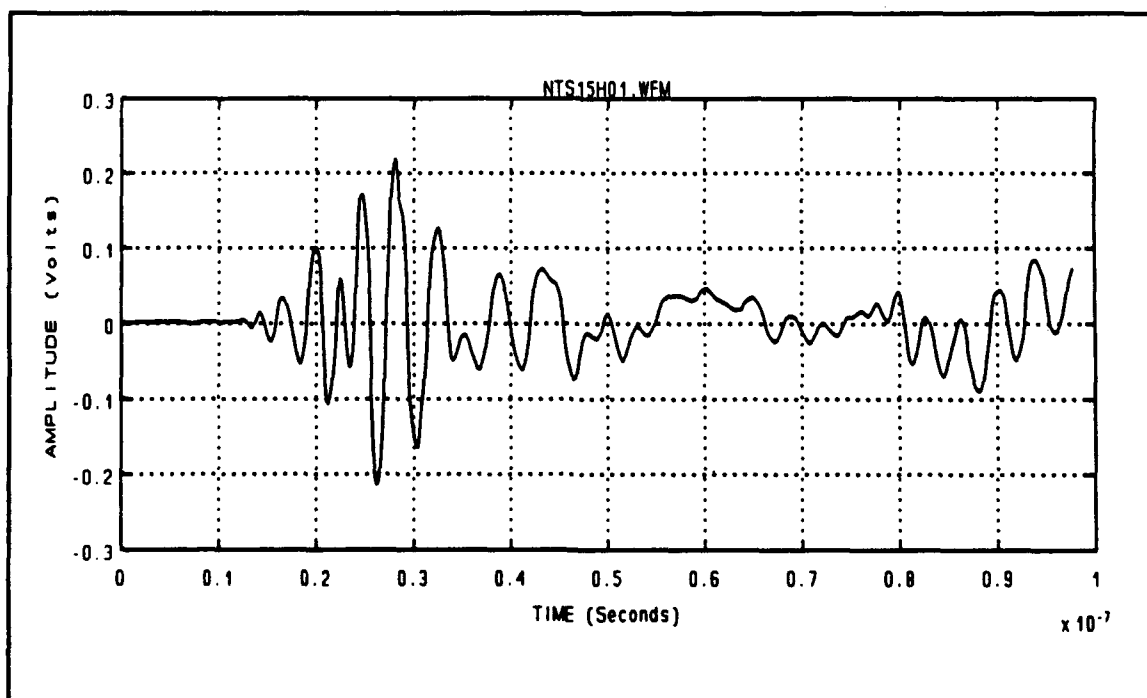


Figure 57 Waveform NTS15H01.WFM - Directory 5-8-90
LLNL Log Periodic Antenna \ Horizontal Polarization

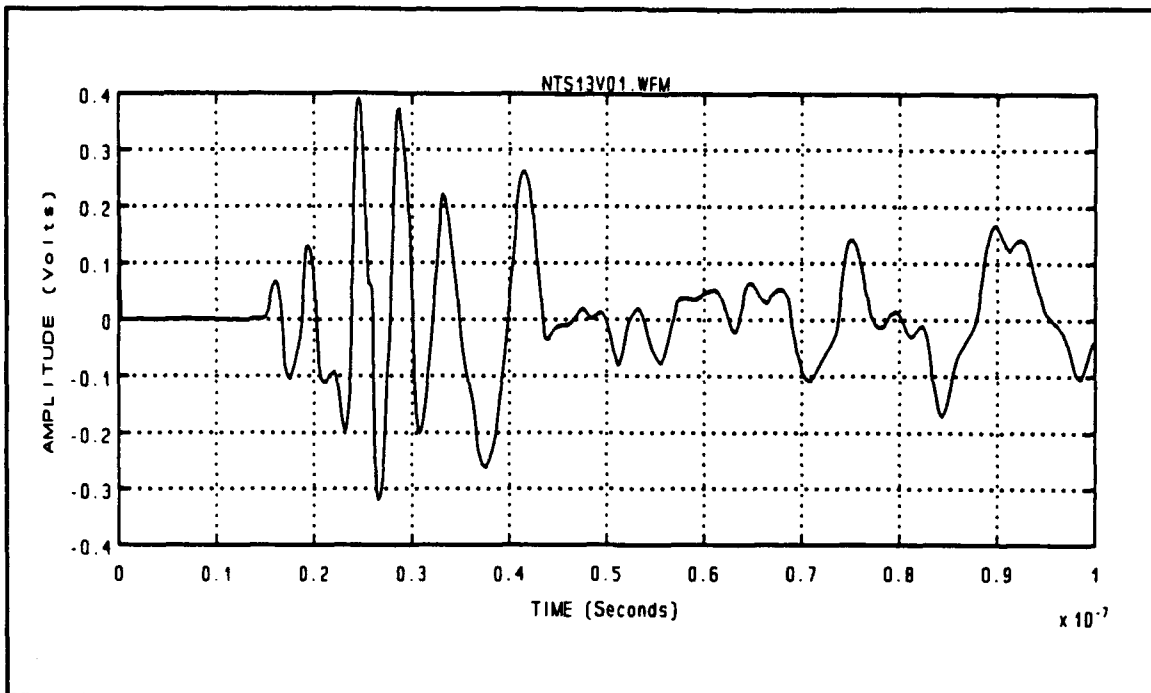


Figure 58 Waveform NTS13V01.WFM - Directory 5-7-90
Big TEM Horn Antenna \ Horizontal Polarization

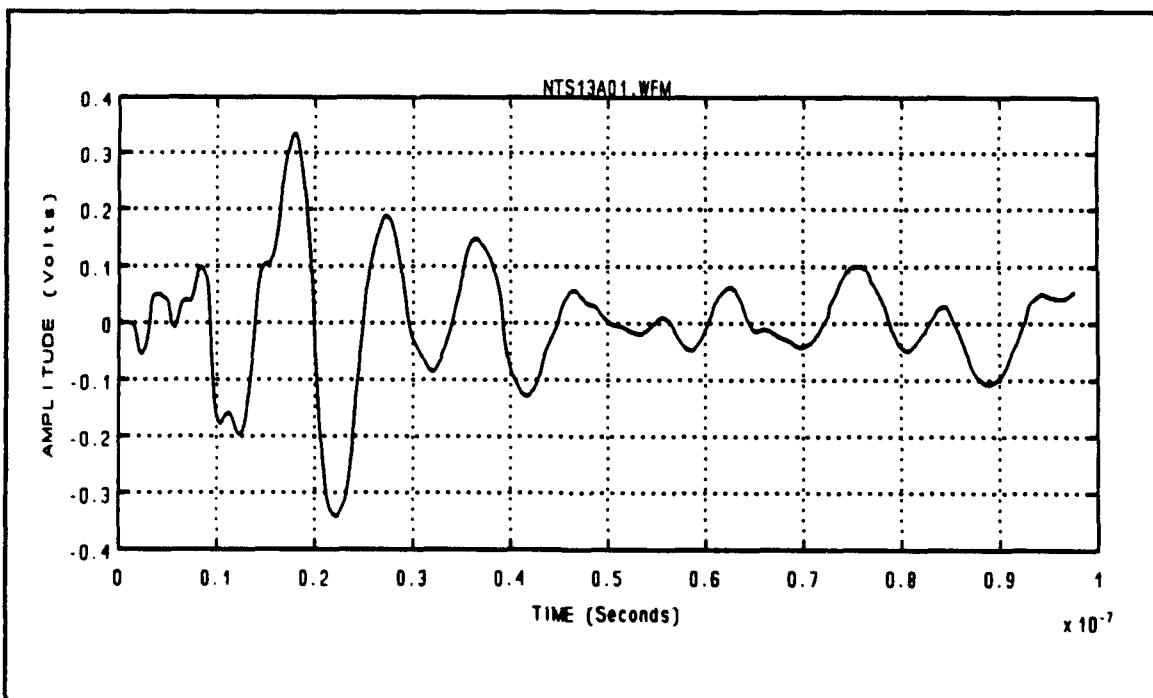


Figure 59 Waveform NTS13A01.WFM - Directory 5-7-90
Big TEM Horn Antenna \ Horizontal Polarization

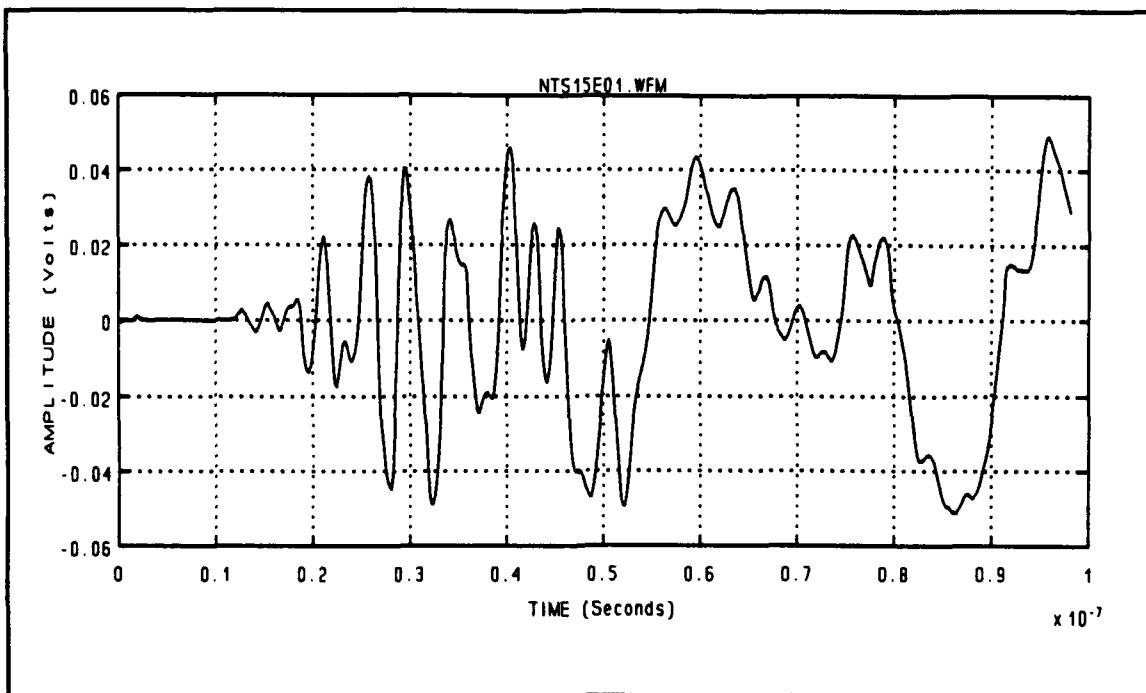


Figure 60 Waveform NTS15E01.WFM - Directory 5-8-90
LLNL Log Periodic Antenna \ Vertical Polarization

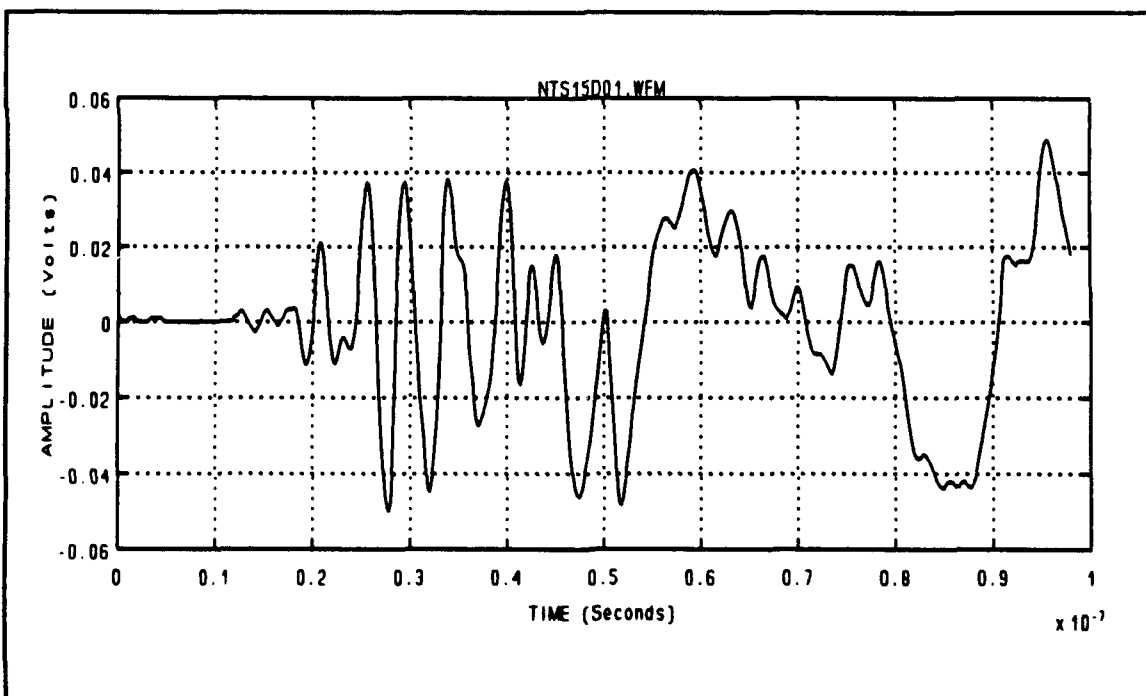


Figure 61 Waveform NTS15D01.WFM - Directory 5-8-90
LLNL Log Periodic Antenna \ Vertical Polarization

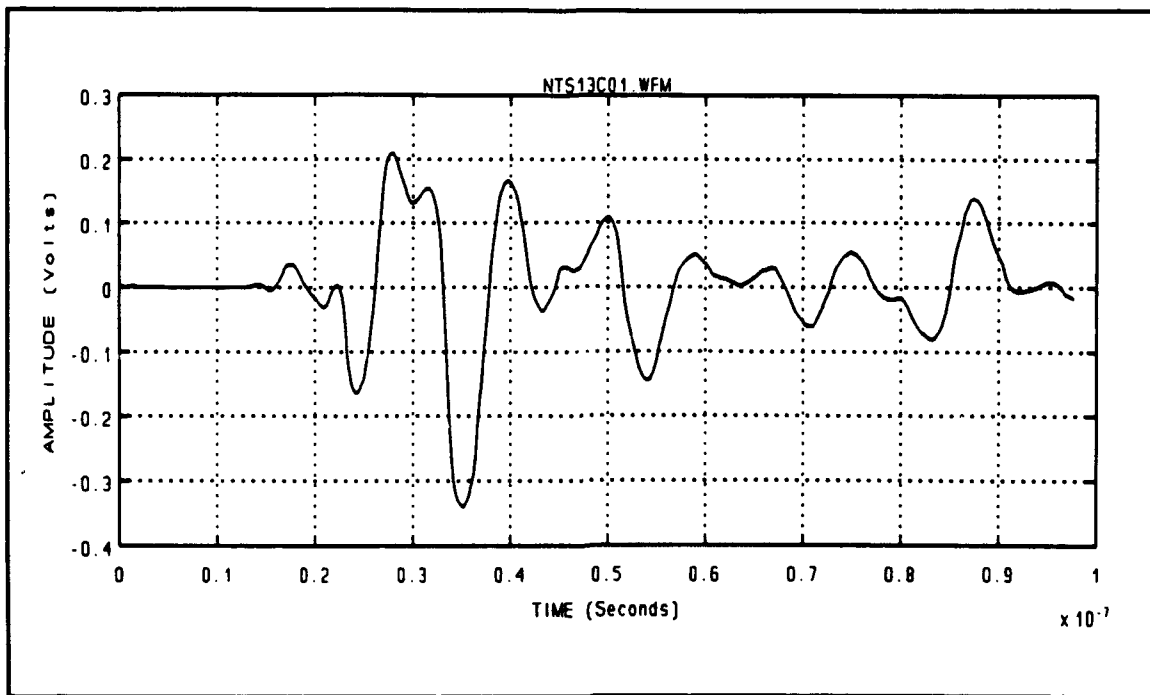


Figure 62 Waveform NTS13C01.WFM - Directory 5-7-90
Big TEM Horn Antenna \ Vertical Polarization

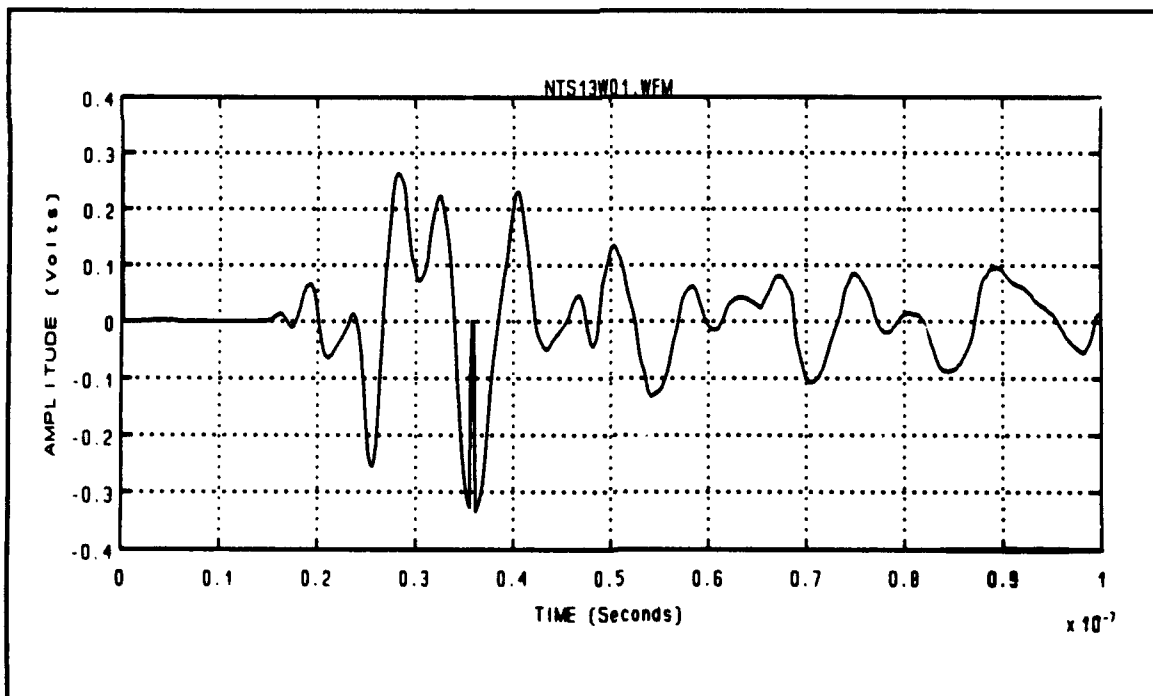


Figure 63 Waveform NTS13W01.WFM - Directory 5-7-90
Big TEM Horn Antenna \ Vertical Polarization

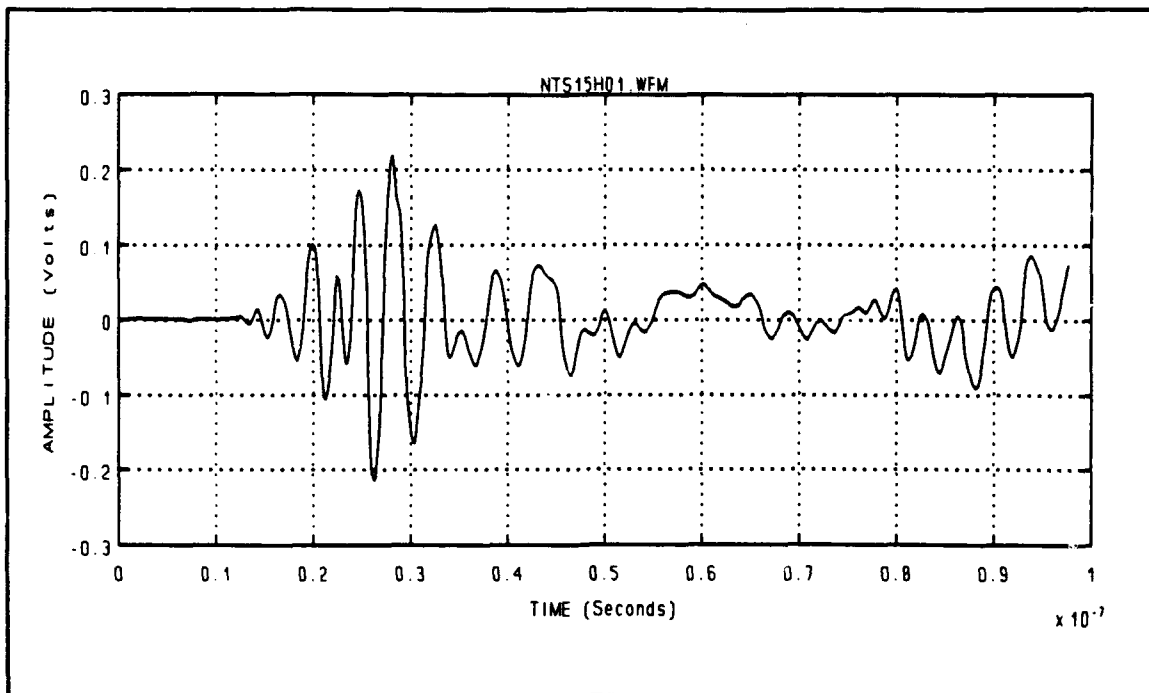


Figure 64 Waveform NTS15H01.WFM [Paired with NTS15E01.WFM]
LLNL Log Periodic Antenna \ Horizontal Polarization

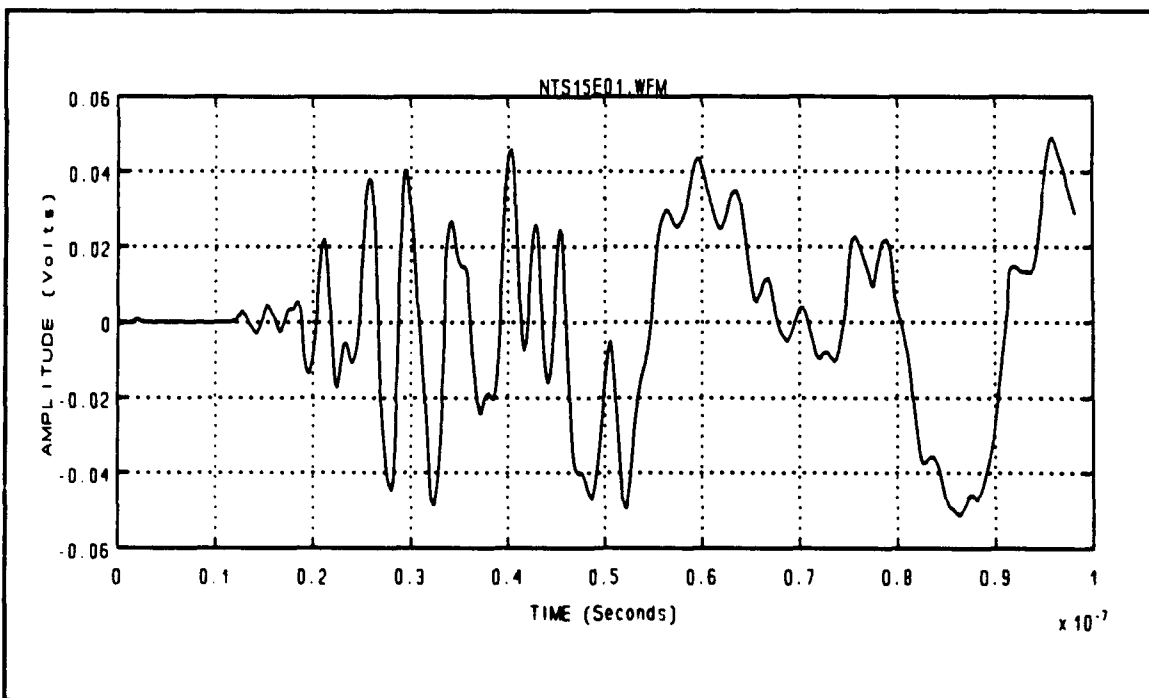


Figure 65 Waveform NTS15E01.WFM [Paired with NTS15H01.WFM]
LLNL Log Periodic Antenna \ Vertical Polarization

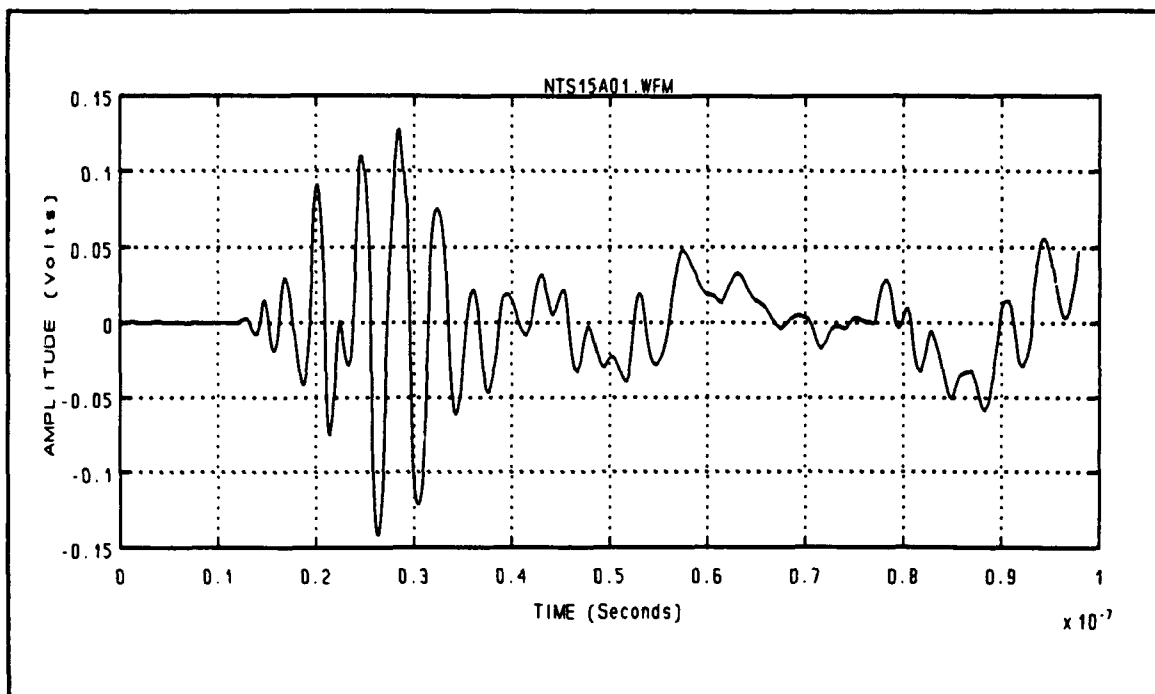


Figure 66 Waveform NTS15A01.WFM [Paired with NTS15D01.WFM]
LLNL Log Periodic Antenna \ Horizontal Polarization

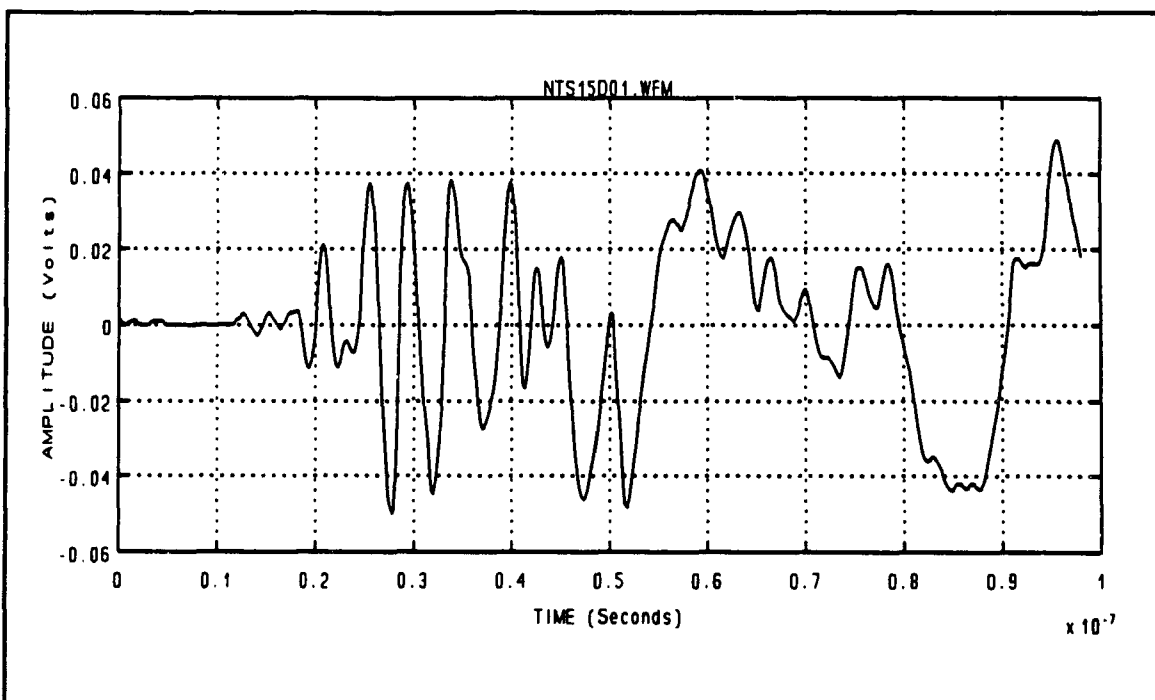


Figure 67 Waveform NTS15D01.WFM [Paired with NTS15A01.WFM]
LLNL Log Periodic Antenna \ Vertical Polarization

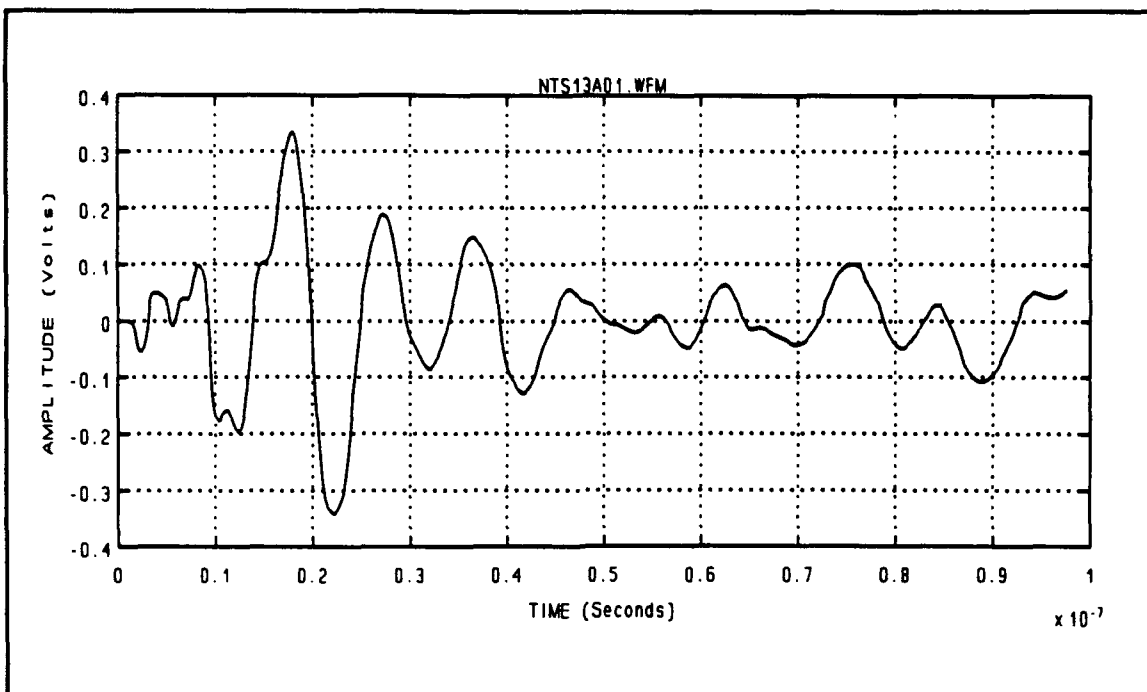


Figure 68 Waveform NTS13A01.WFM [Paired with NTS13C01.WFM]
Big TEM Horn Antenna \ Horizontal Polarization

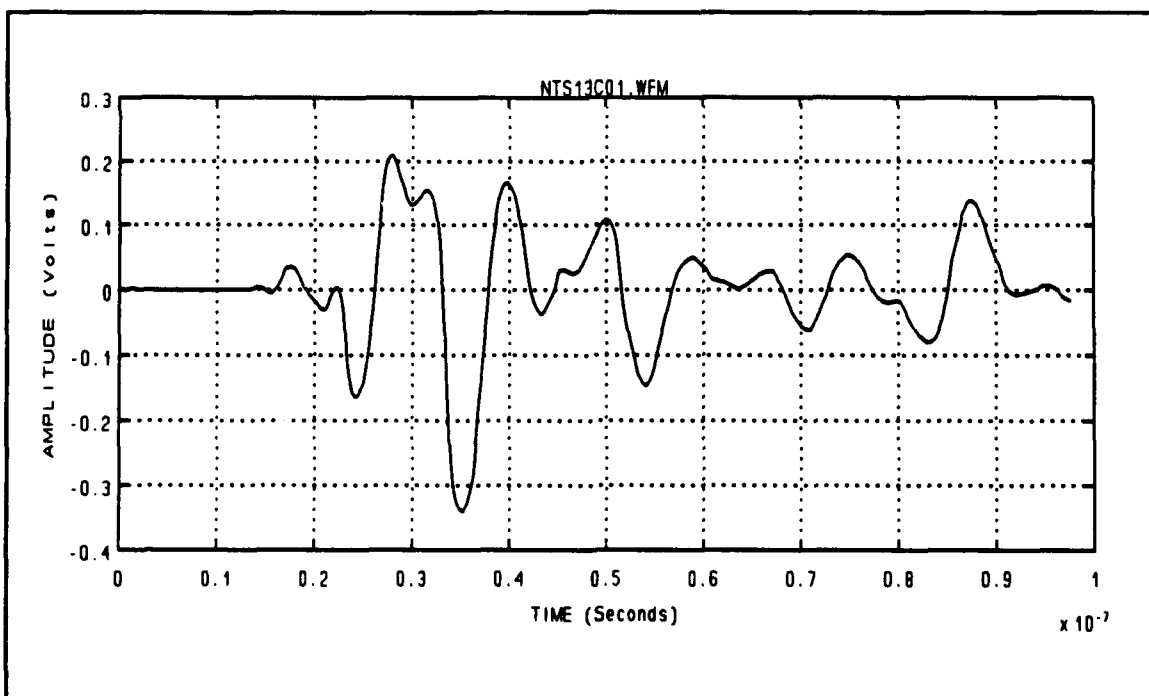


Figure 69 Waveform NTS13C01.WFM [Paired with NTS13A01.WFM]
Big TEM Horn Antenna \ Vertical Polarization

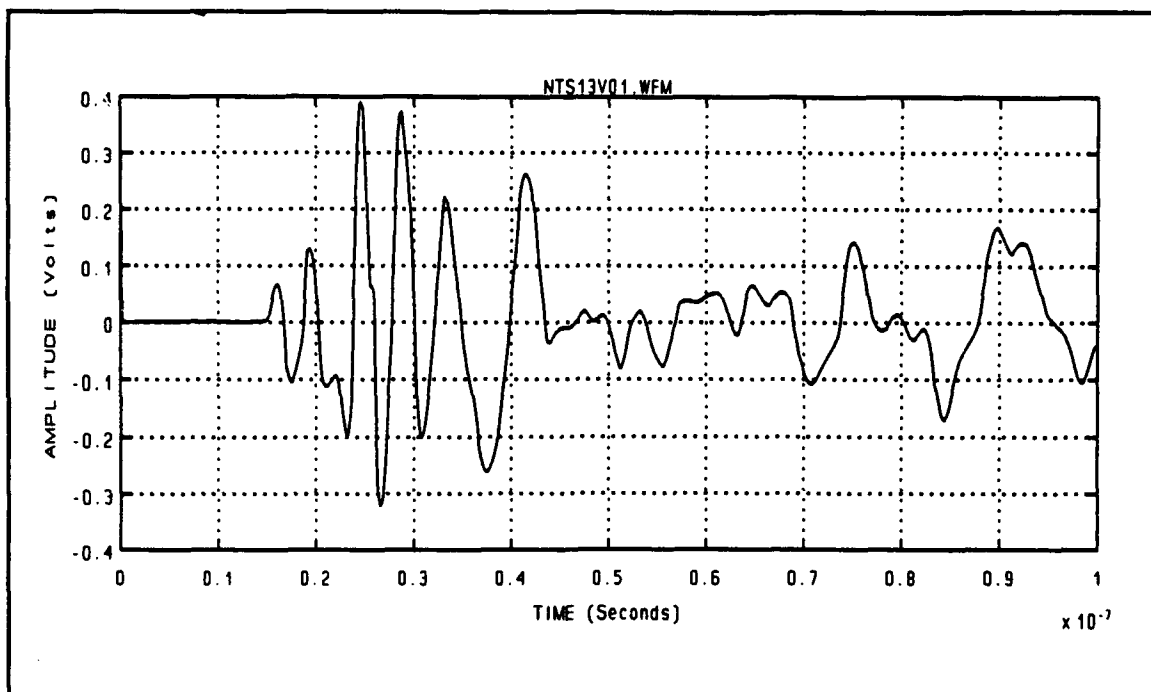


Figure 70 Waveform NTS13V01.WFM [Paired with NTS13W01.WFM]
Big TEM Horn Antenna \ Horizontal Polarization

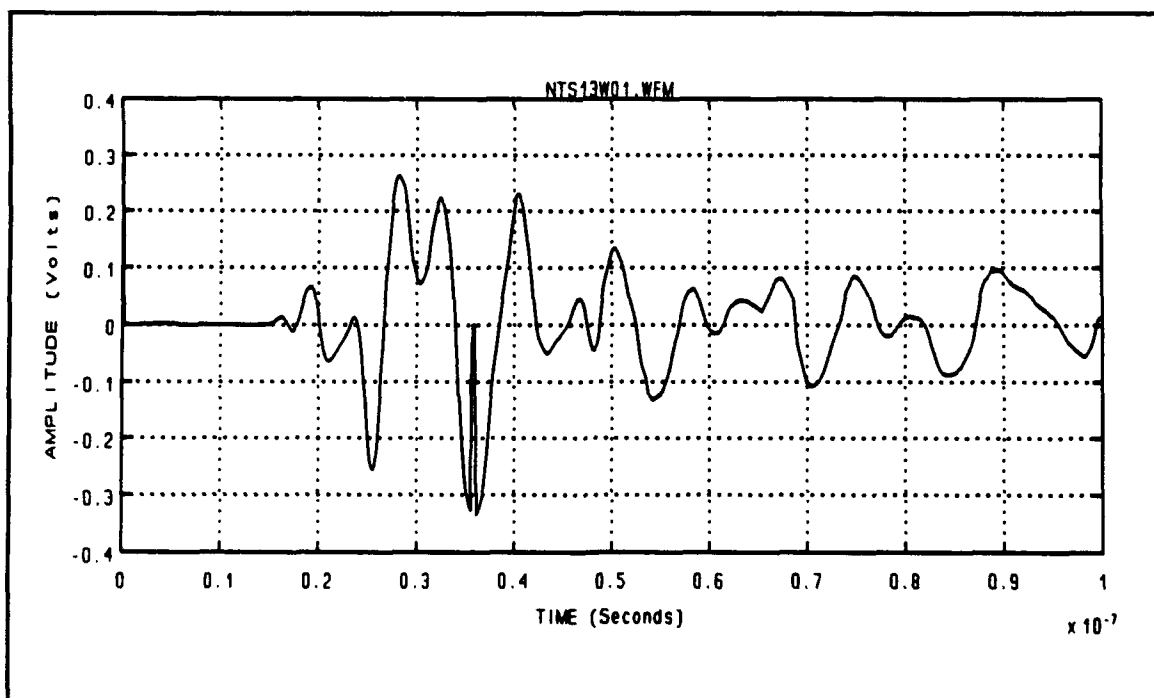


Figure 71 Waveform NTS13W01.WFM [Paired with NTS13V01.WFM]
Big TEM Horn Antenna \ Vertical Polarization

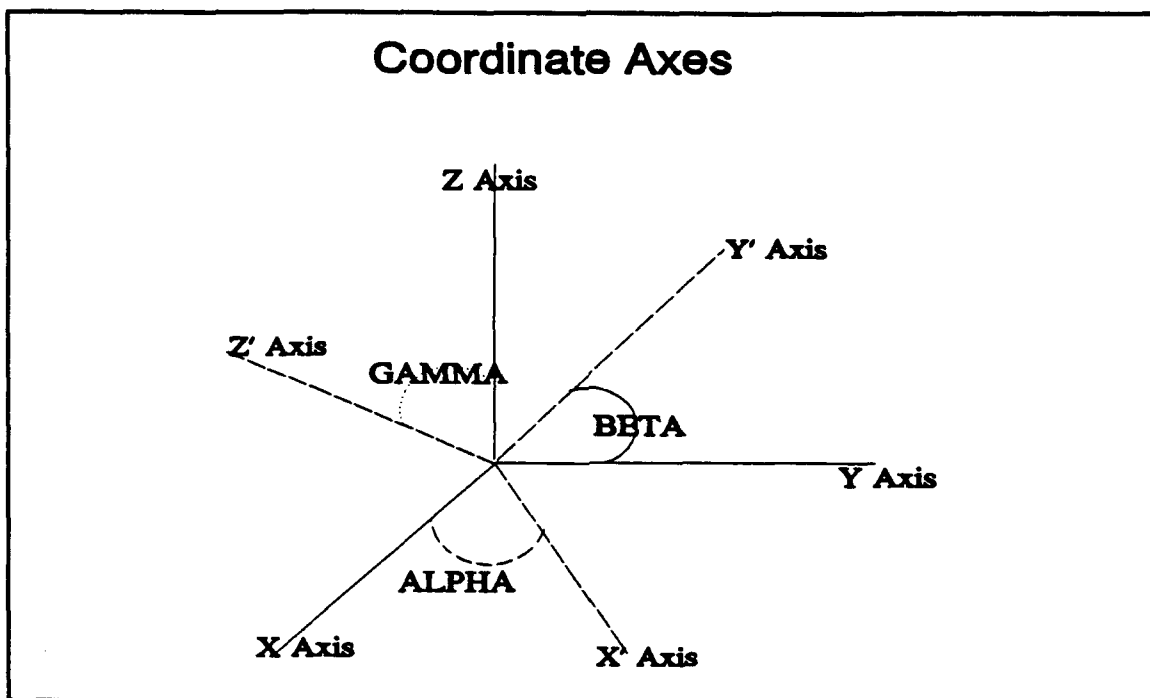


Figure 72 Reference Frame - Coordinate Axes

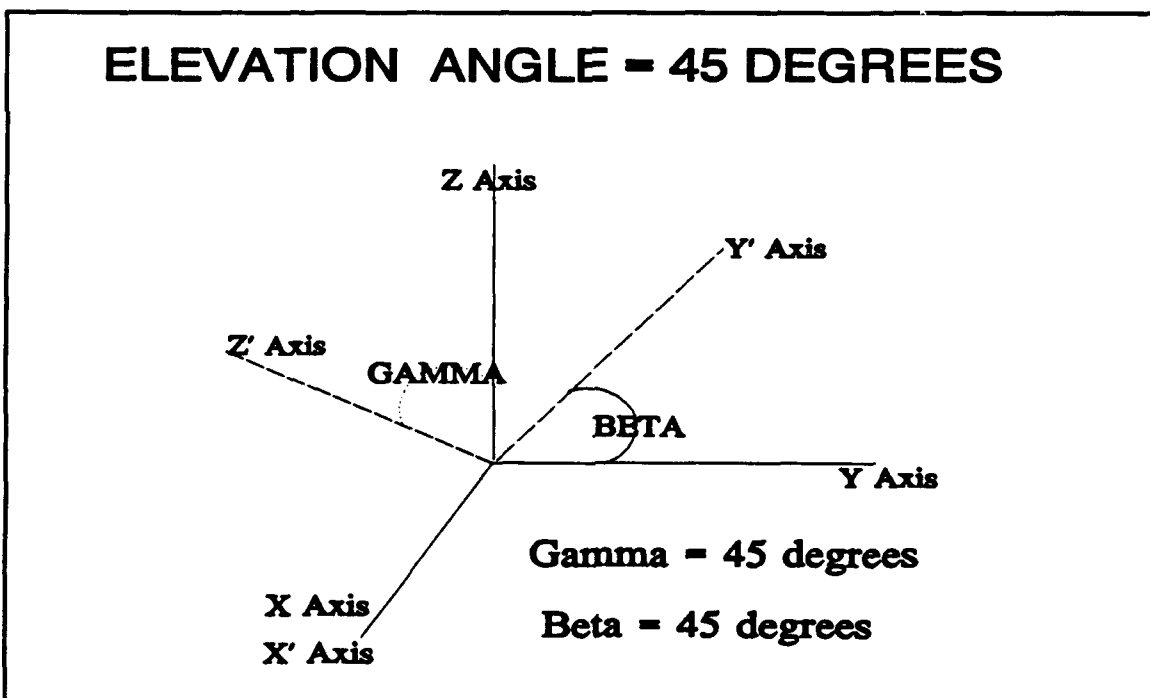


Figure 73 Reference Frame - Elevation Angle = 45 degrees Relative to the Horizontal Plane

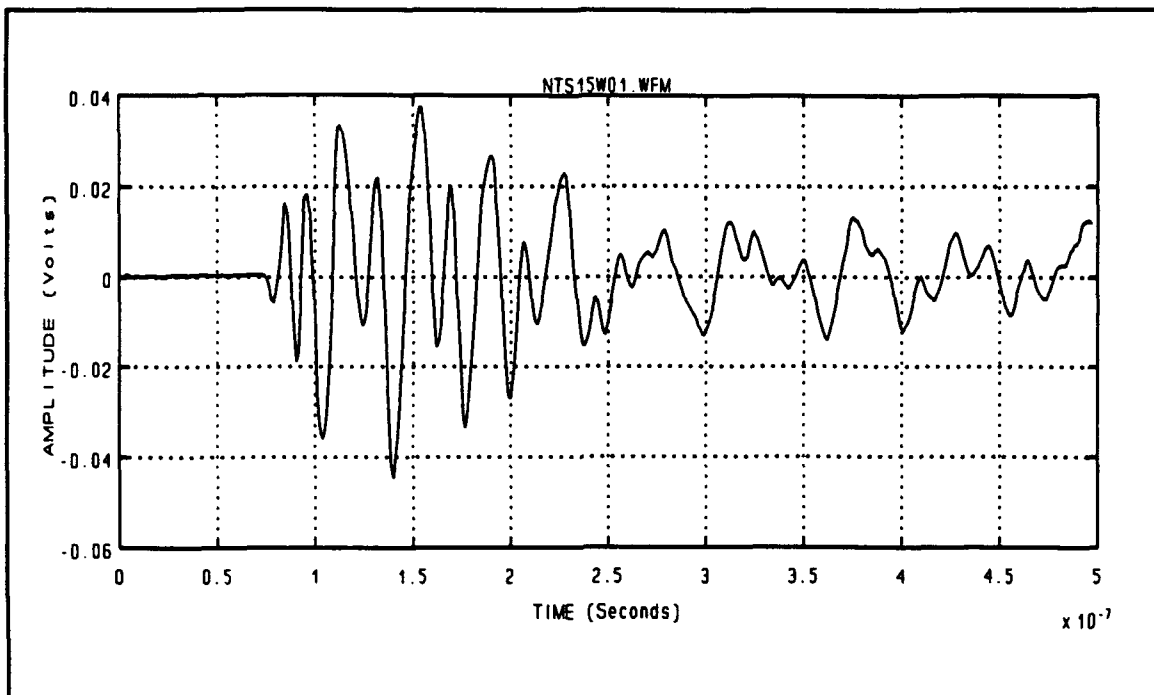


Figure 74 Waveform NTS15W01.WFM [Paired with NTS15V01.WFM]
Horizontal Component \ Elevation Angle = 45 degrees
LLNL modified LP Antenna

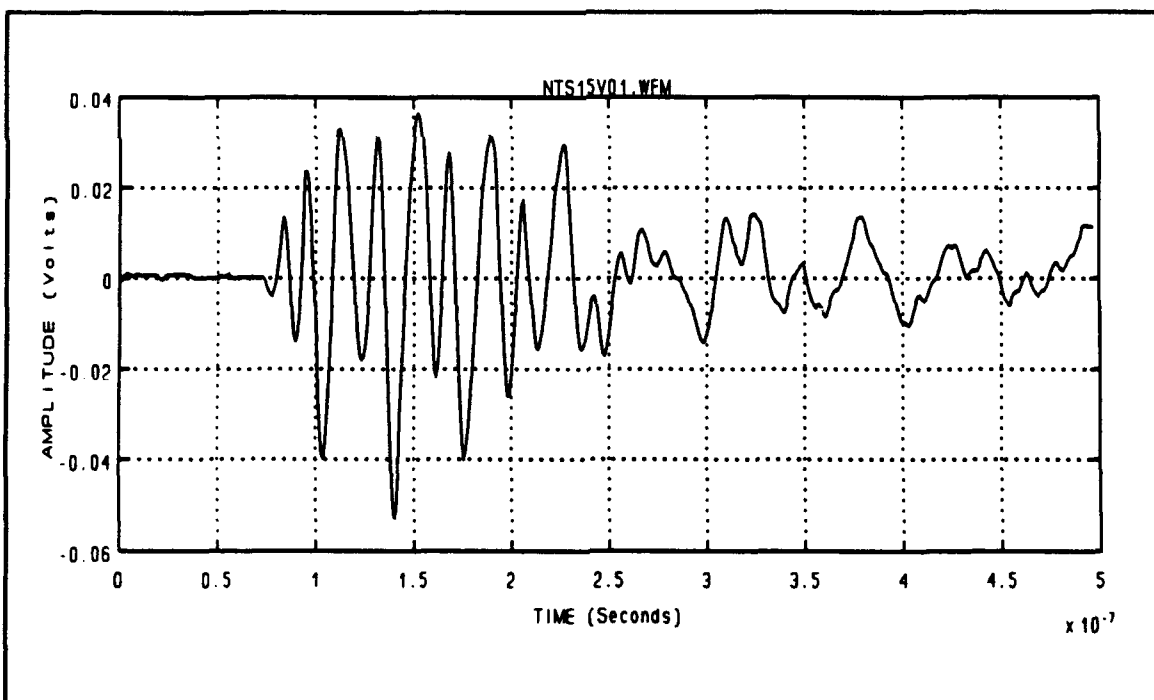


Figure 75 Waveform NTS15V01.WFM [Paired with NTS15W01.WFM]
Vertical Component \ Elevation Angle = 45 degrees
LLNL modified LP Antenna

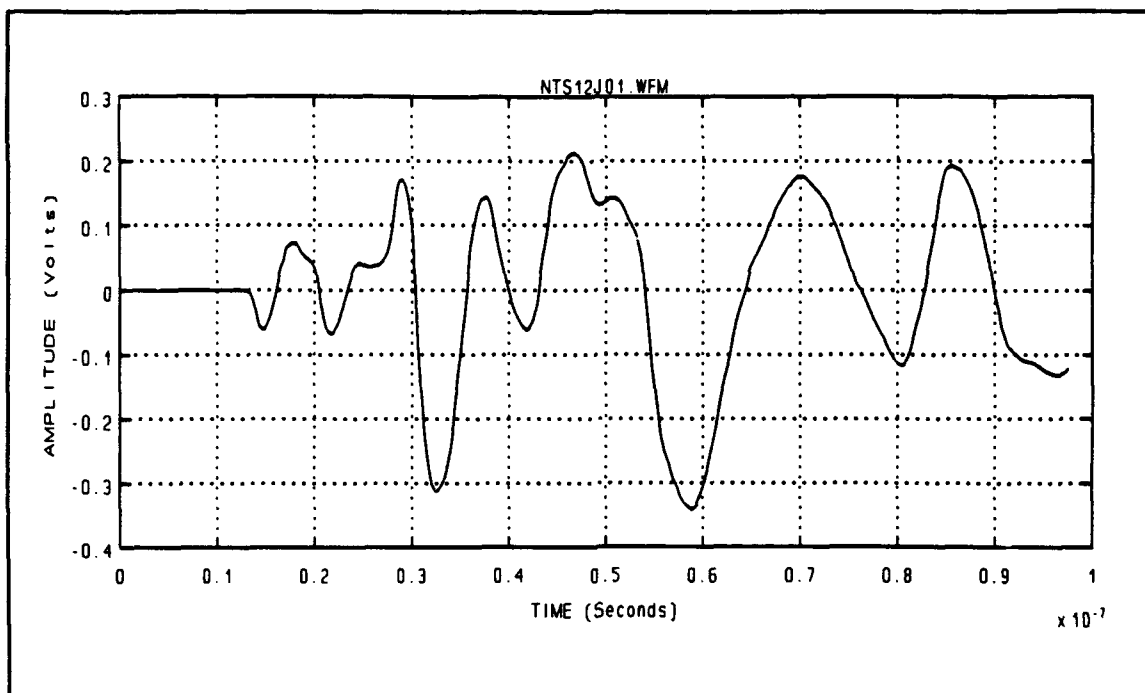


Figure 76 Waveform NTS12J01.WFM [Paired with NTS12K01.WFM]
Horizontal Component \ Elevation Angle = 45 degrees
Big TEM Horn Antenna

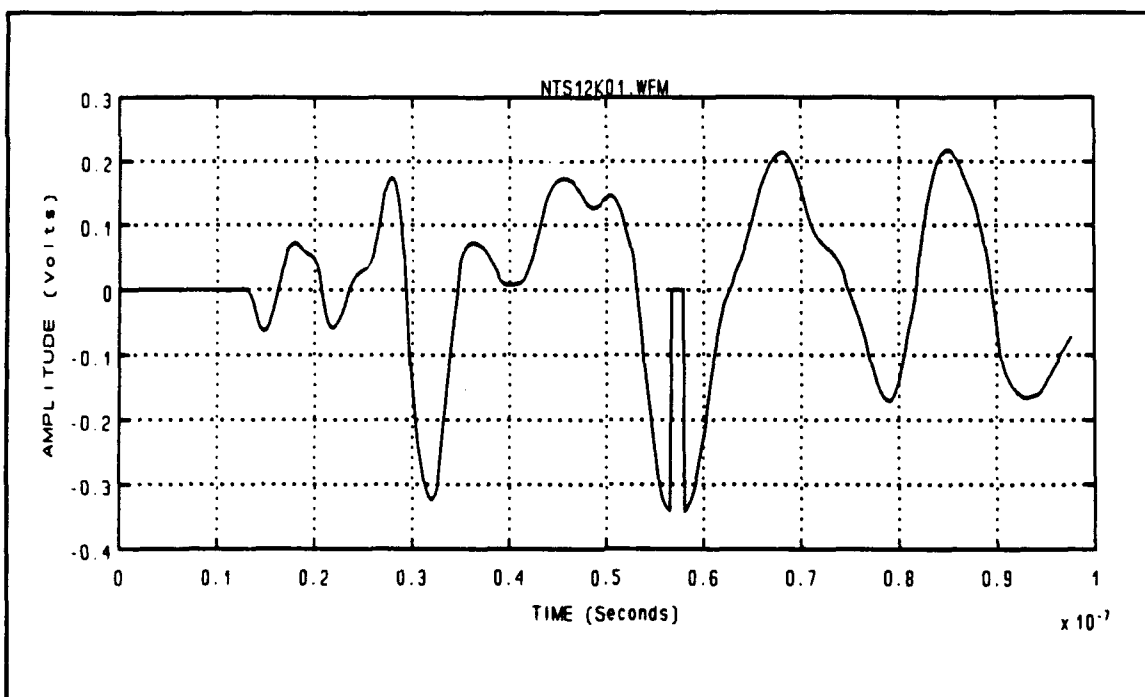


Figure 77 Waveform NTS12K01.WFM [Paired with NTS12J01.WFM]
Vertical Component \ Elevation Angle = 45 degrees
Big TEM Horn Antenna

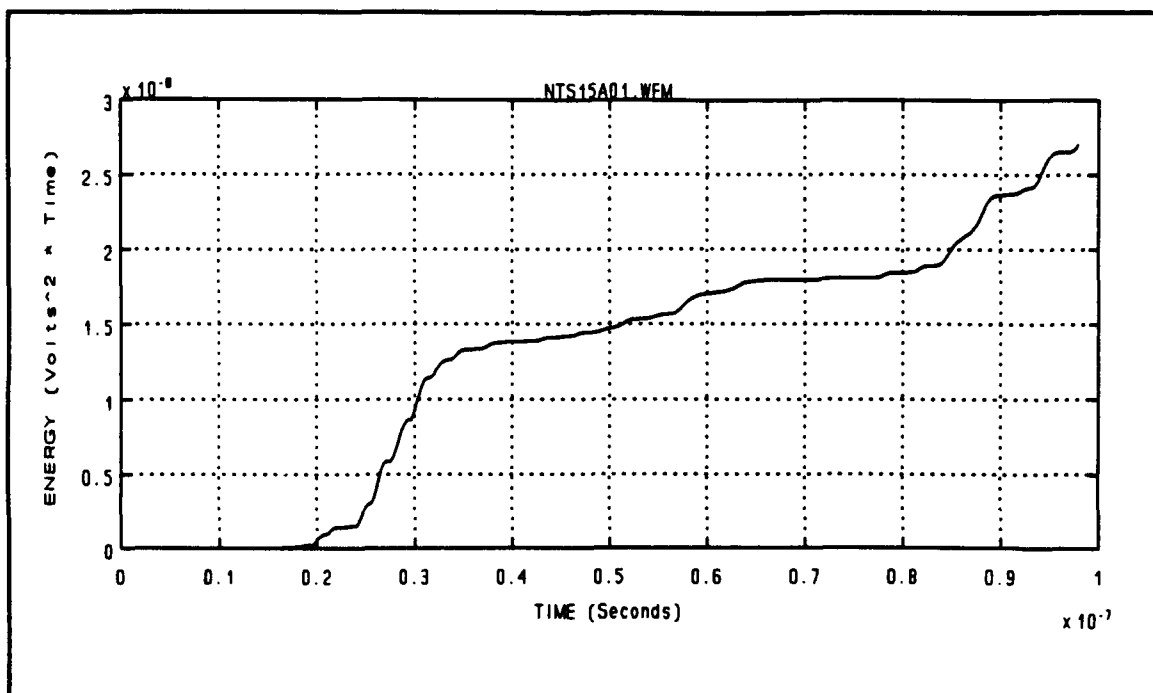


Figure 78 Waveform NTS15A01.WFM [Paired with NTS15D01.WFM]
Horizontal Component \ LLNL Log Periodic Antenna
Energy versus Time Graph

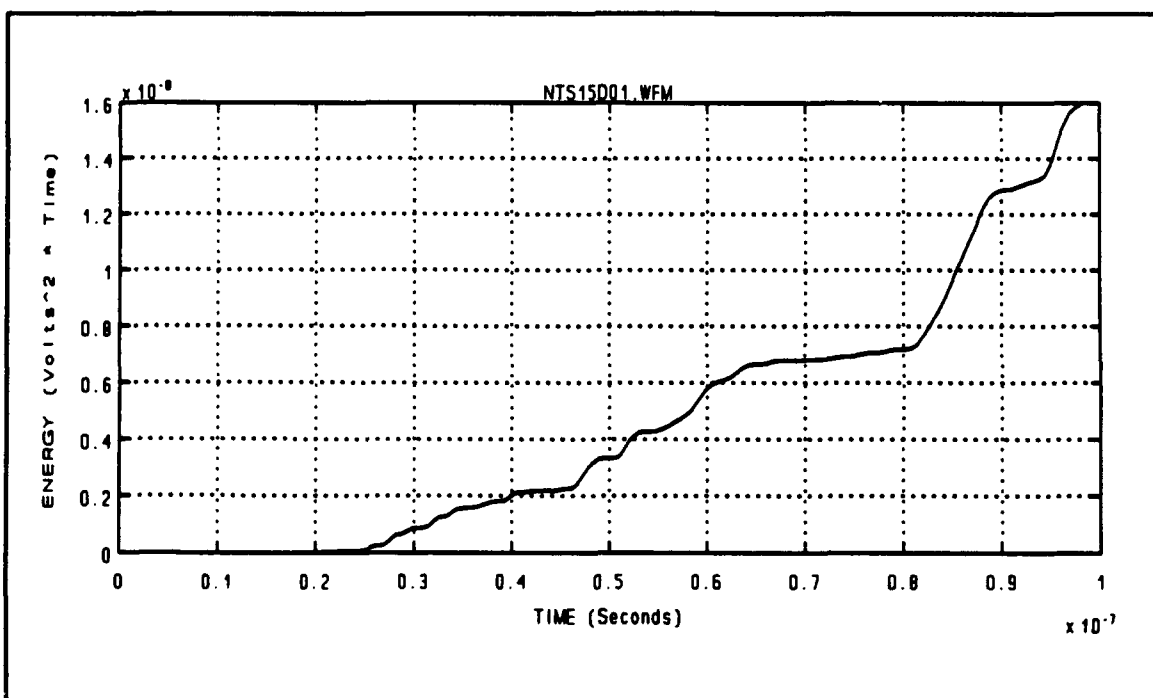


Figure 79 Waveform NTS15D01.WFM [Paired with NTS15A01.WFM]
Vertical Component \ LLNL Log Periodic Antenna
Energy versus Time Graph

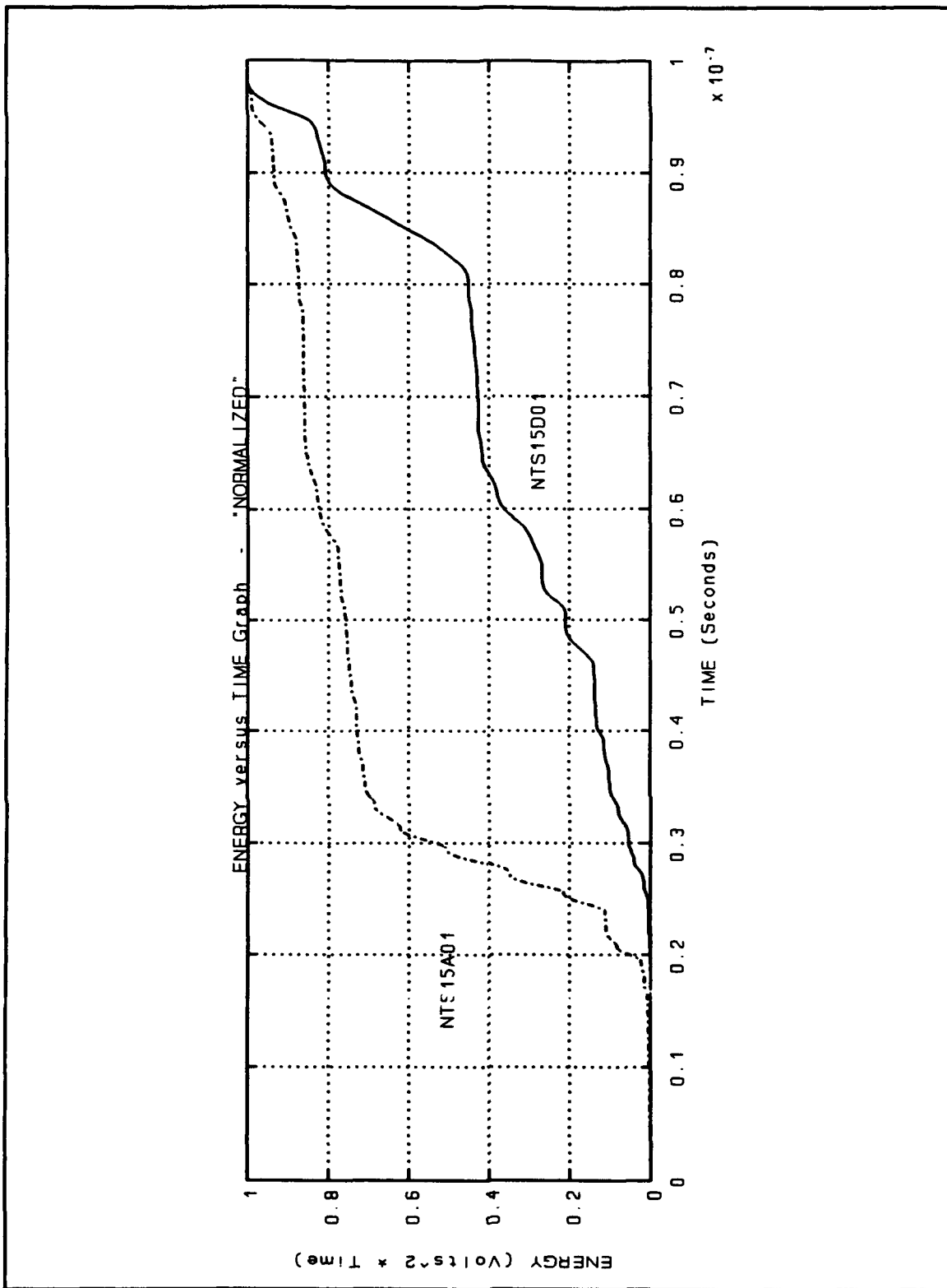


Figure 80 Energy versus Time Graph - "NORMALIZED"
Waveforms NTS15A01.WFM and NTS15D01.WFM

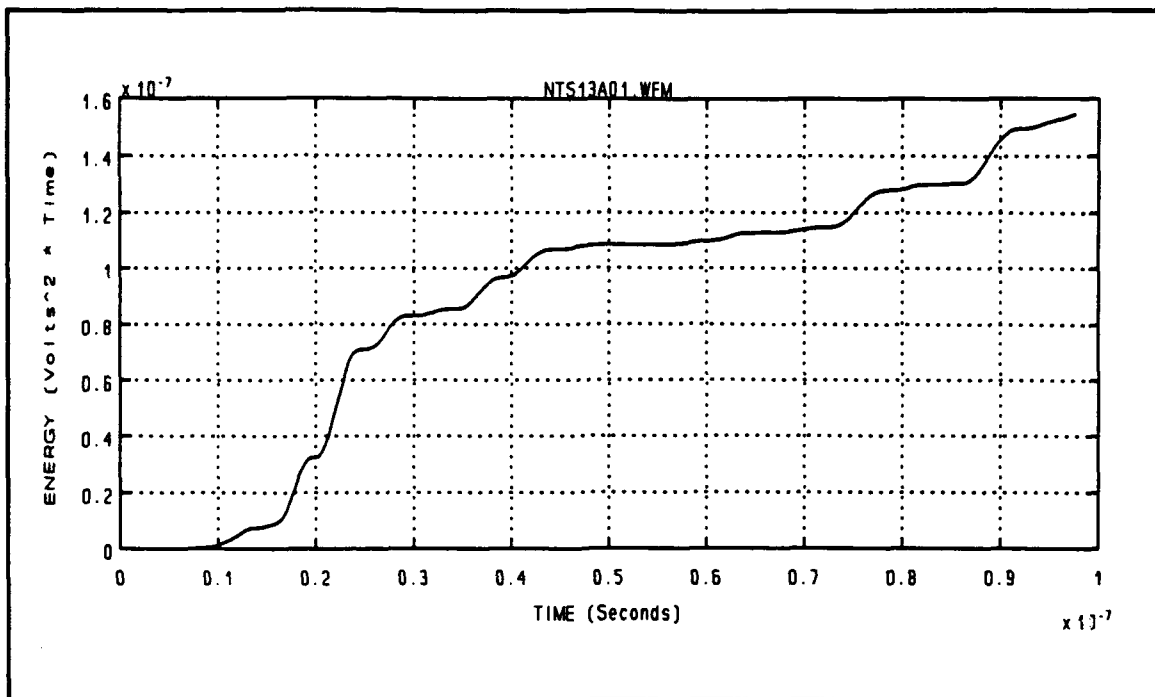


Figure 81 Waveform NTS13A01.WFM [Paired with NTS13C01.WFM]
Horizontal Component \ Big TEM Horn Antenna
Energy versus Time Graph

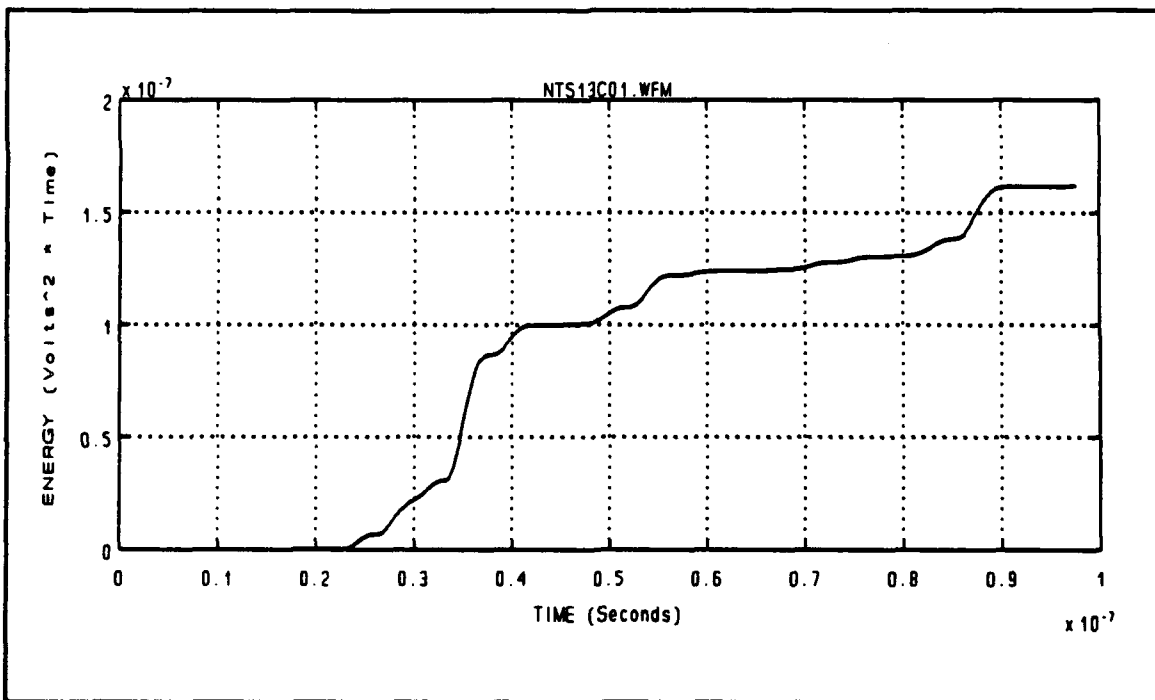


Figure 82 Waveform NTS13C01.WFM [Paired with NTS13A01.WFM]
Vertical Component \ Big TEM Horn Antenna
Energy versus Time Graph

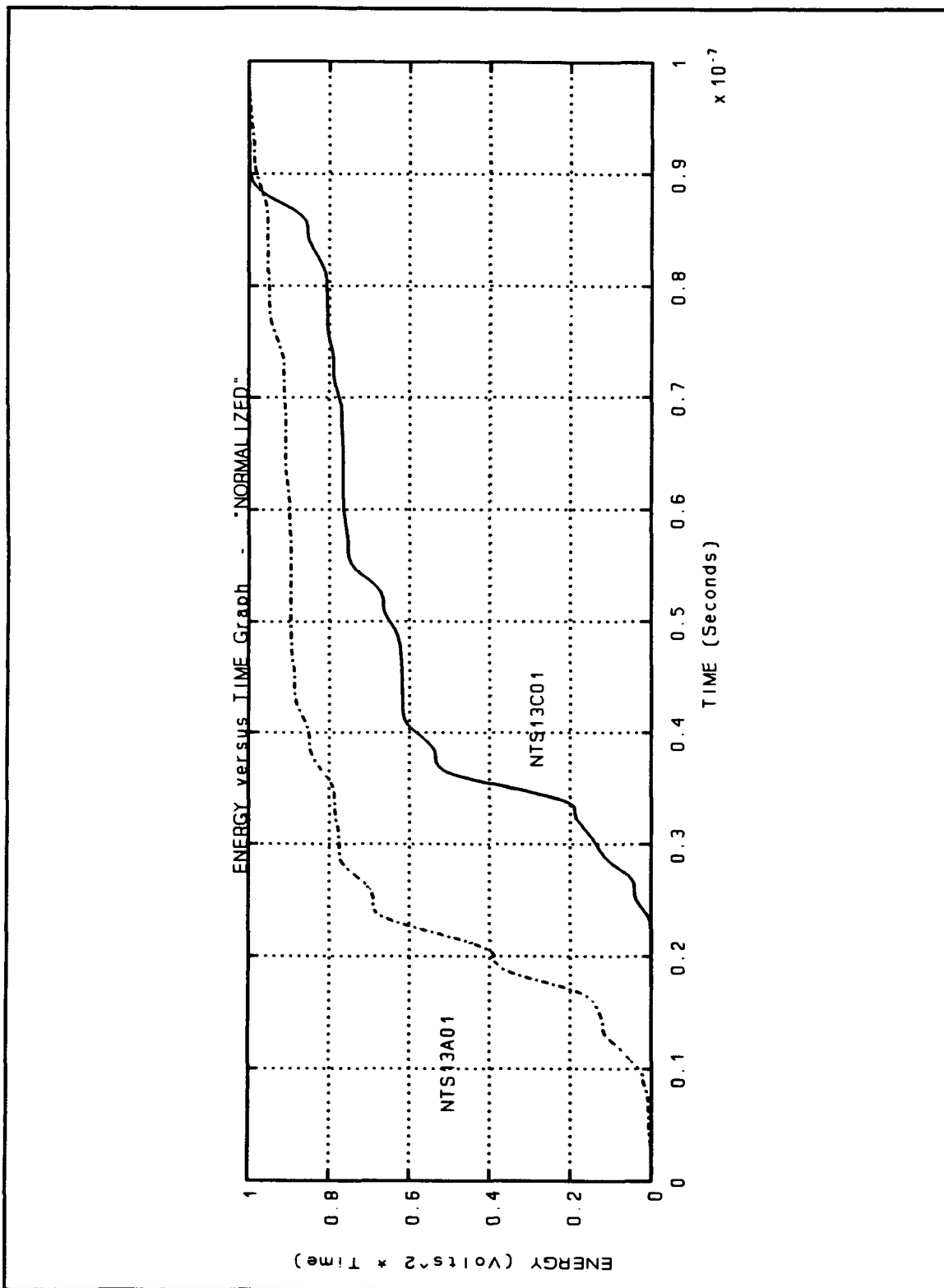


Figure 83 Energy versus Time Graph - "NORMALIZED"
Waveforms NTS13A01.WFM and NTS13C01.WFM

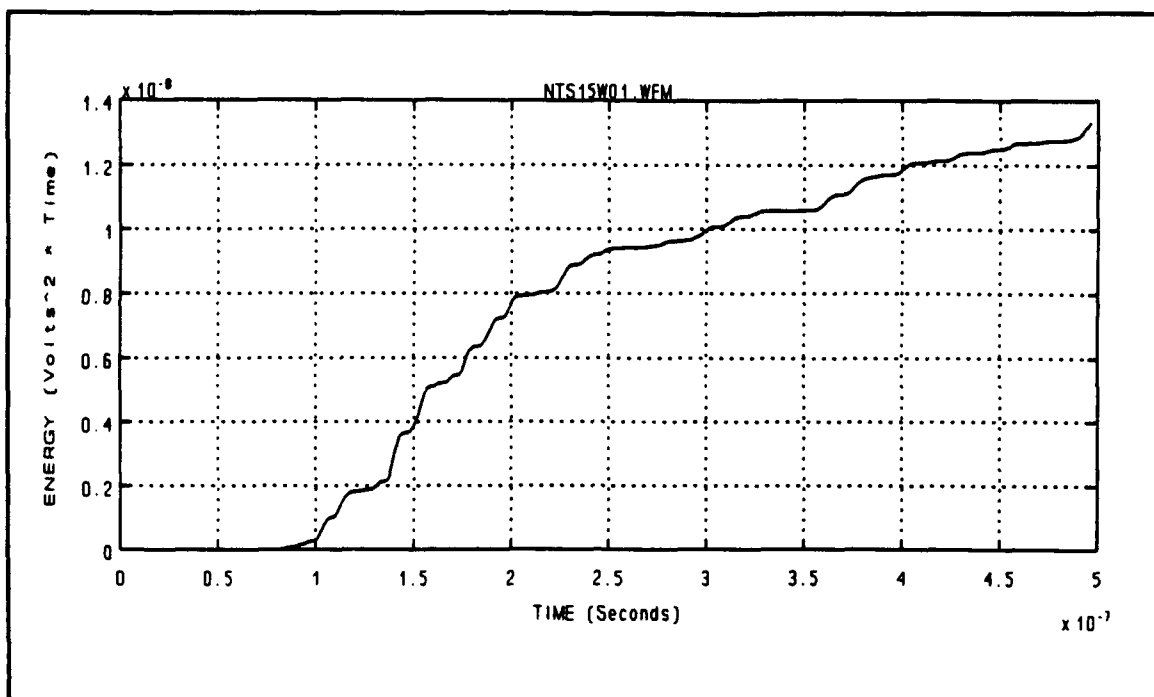


Figure 84 Waveform NTS15W01.WFM [Paired with NTS15V01.WFM]
Horizontal Component \ Elevation Angle = 45 degrees
Energy versus Time Graph - LLNL Log Periodic Antenna

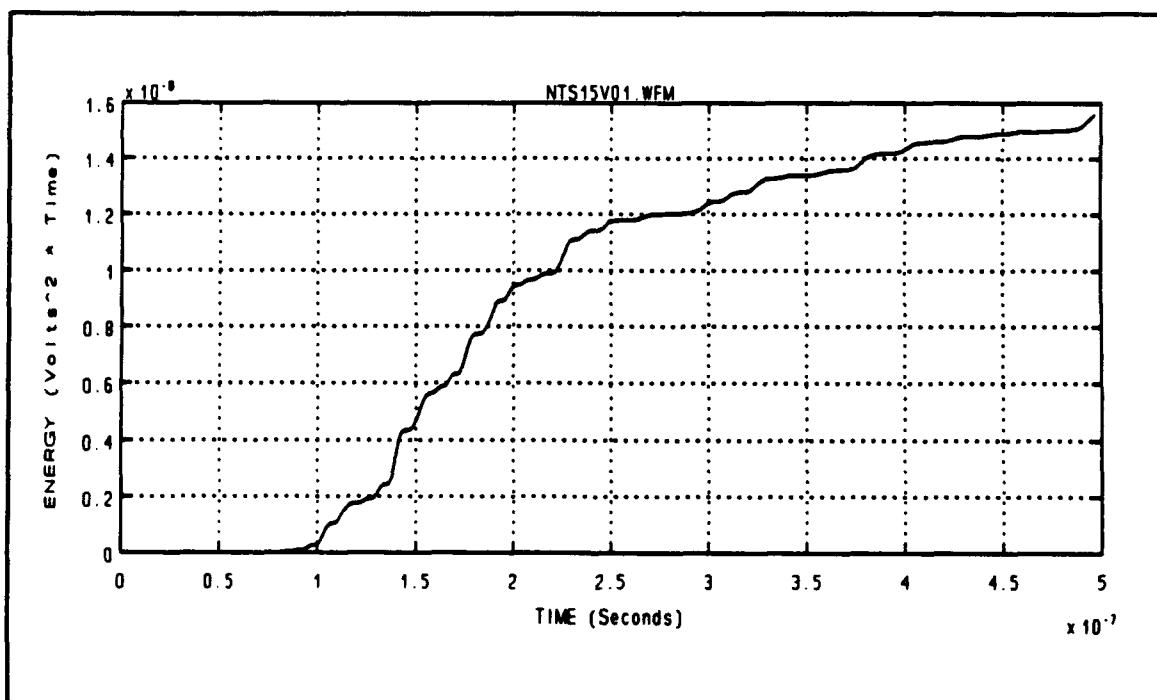


Figure 85 Waveform NTS15V01.WFM [Paired with NTS15W01.WFM]
Vertical Component \ Elevation Angle = 45 degrees
Energy versus Time Graph - LLNL Log Periodic Antenna

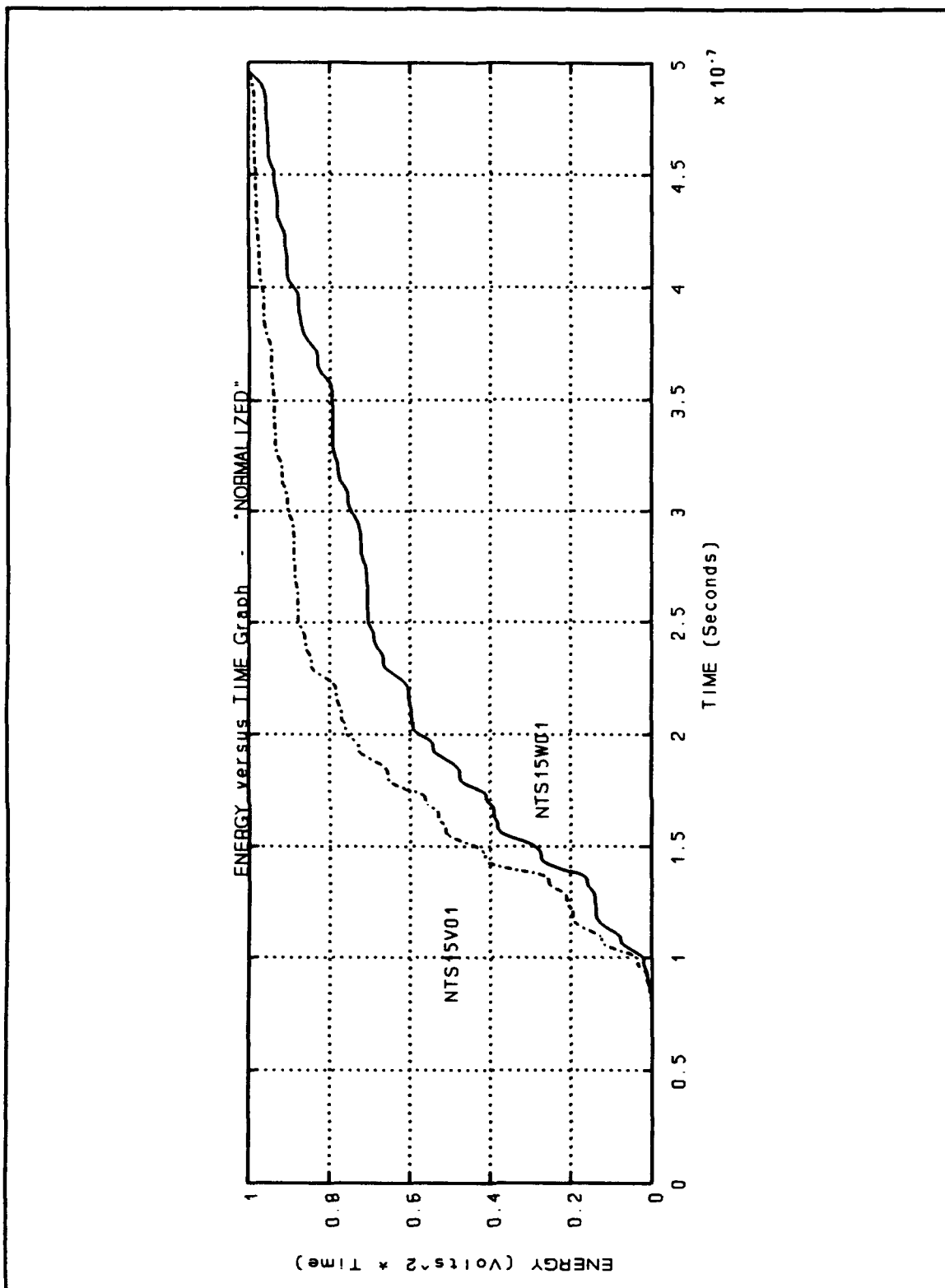


Figure 86 Energy versus Time Graph - "NORMALIZED"
Waveforms NTS15V01.WFM and NTS15W01.WFM

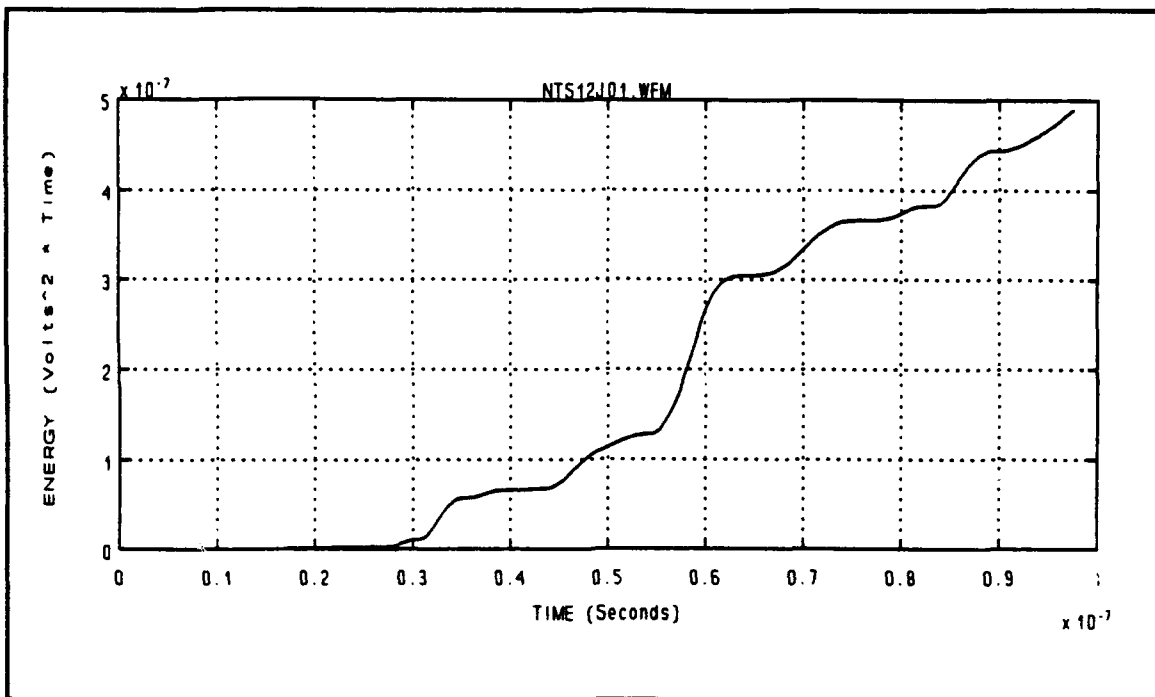


Figure 87 Waveform NTS12J01.WFM [Paired with NTS12K01.WFM]
Horizontal Component \ Elevation Angle = 45 degrees
Energy versus Time Graph - Big TEM Horn Antenna

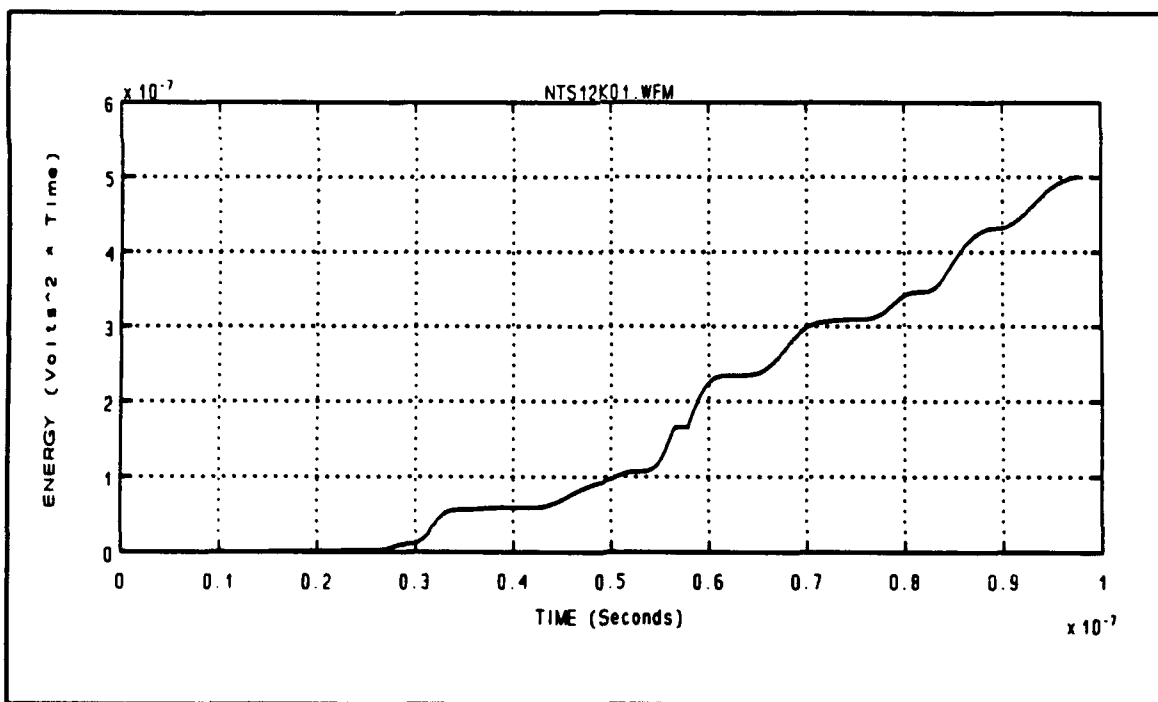


Figure 88 Waveform NTS12K01.WFM [Paired with NTS12J01.WFM]
Vertical Component \ Elevation Angle = 45 degrees
Energy versus Time Graph - Big TEM Horn Antenna

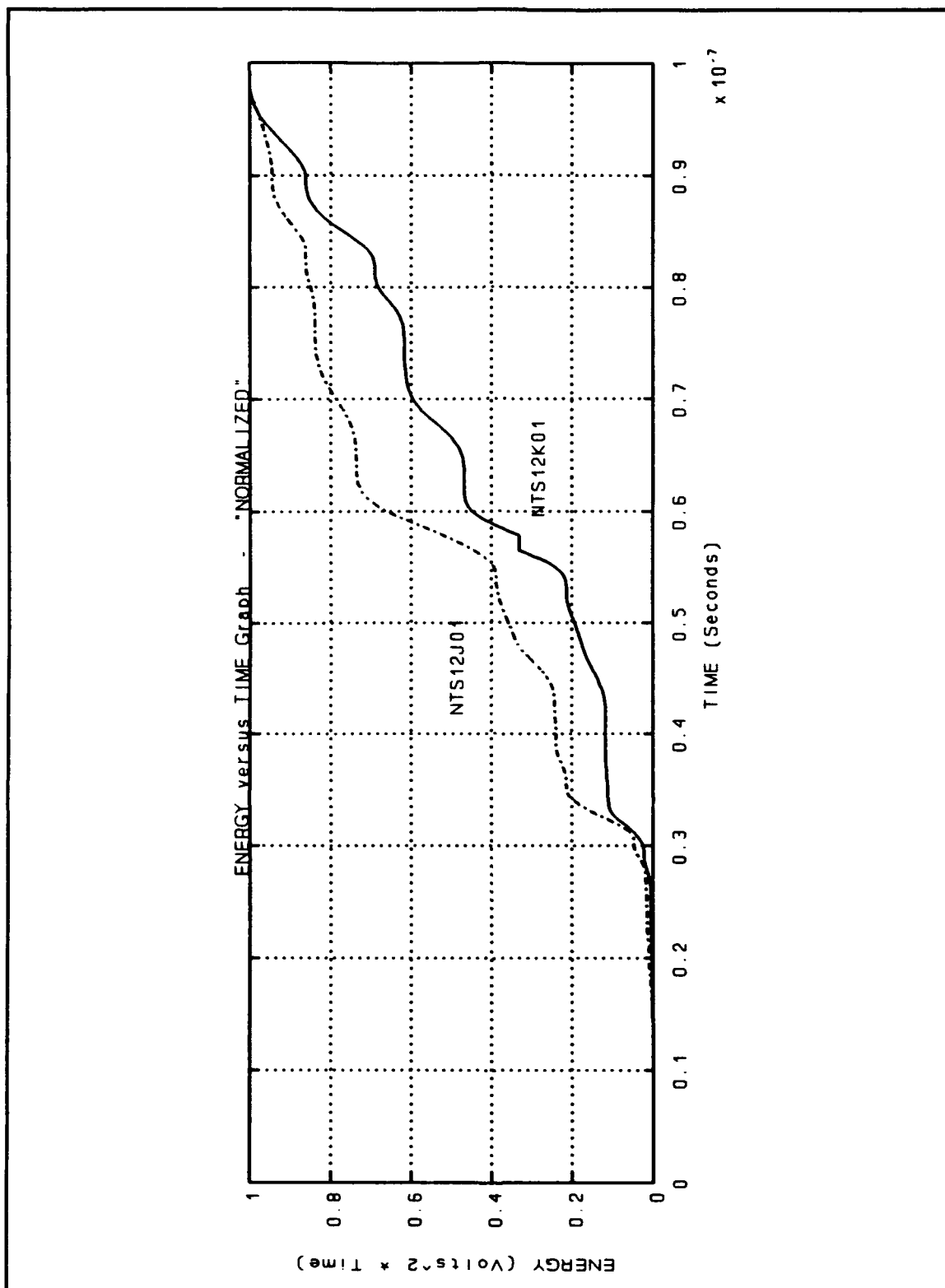


Figure 89 Energy versus Time Graph - "NORMALIZED"
Waveforms NTS12J01.WFM and NTS12K01.WFM

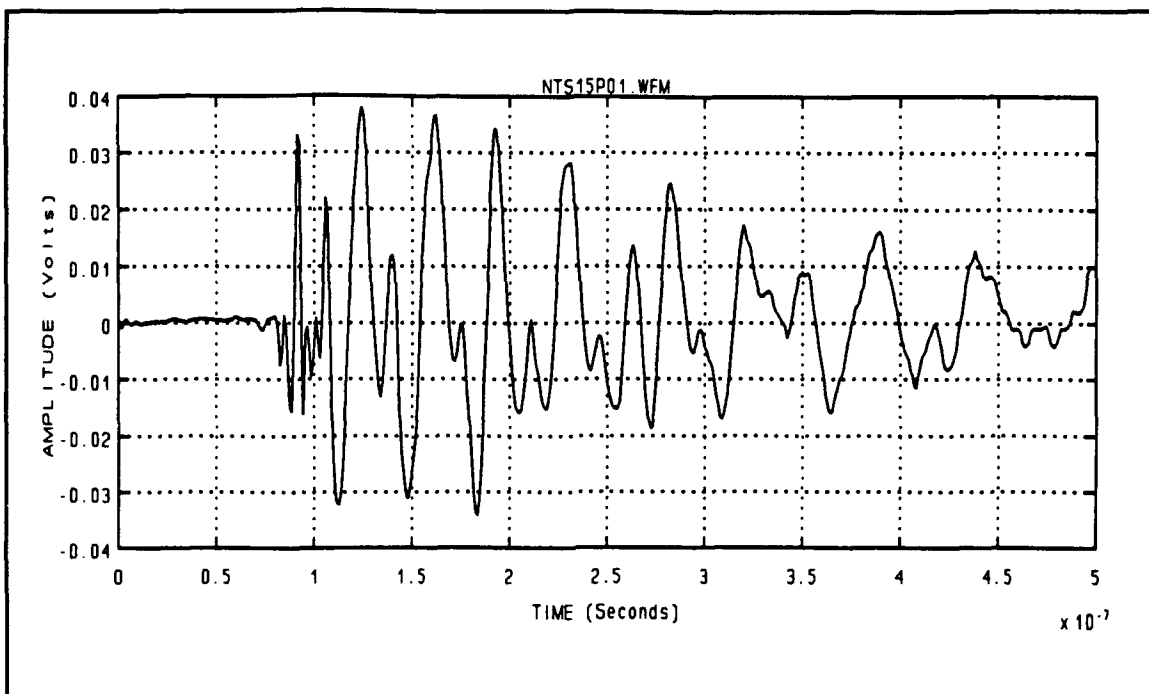


Figure 90 Waveform NTS15P01.WFM [Paired with NTS15N01.WFM]
LLNL Log Periodic Antenna - Horizontal Component

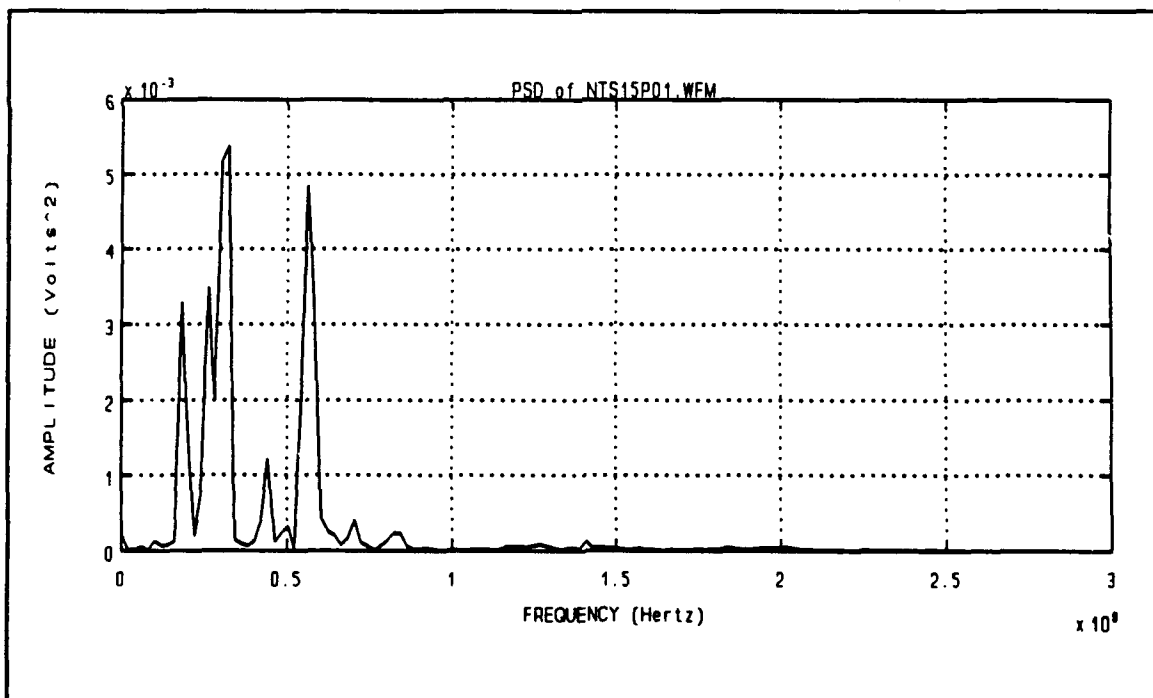


Figure 91 Waveform NTS15P01.WFM [Paired with NTS15N01.WFM]
Power Spectral Density Graph - Horizontal Component

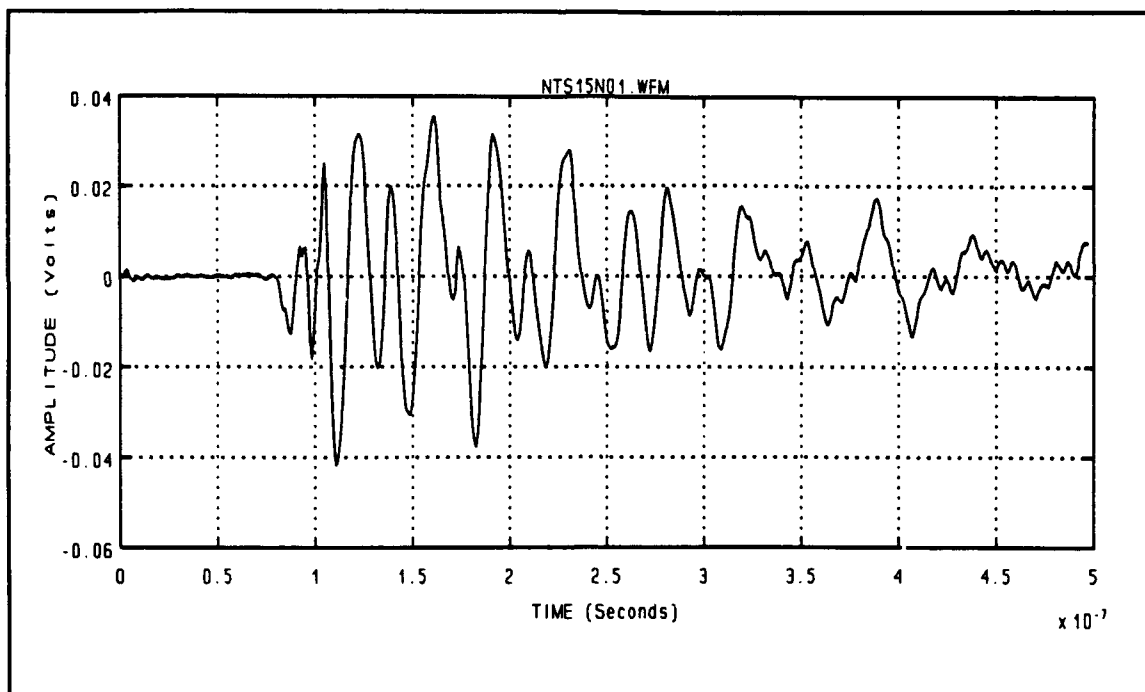


Figure 92 Waveform NTS15N01.WFM [Paired with NTS15P01.WFM]
LLNL Log Periodic Antenna - Vertical Component

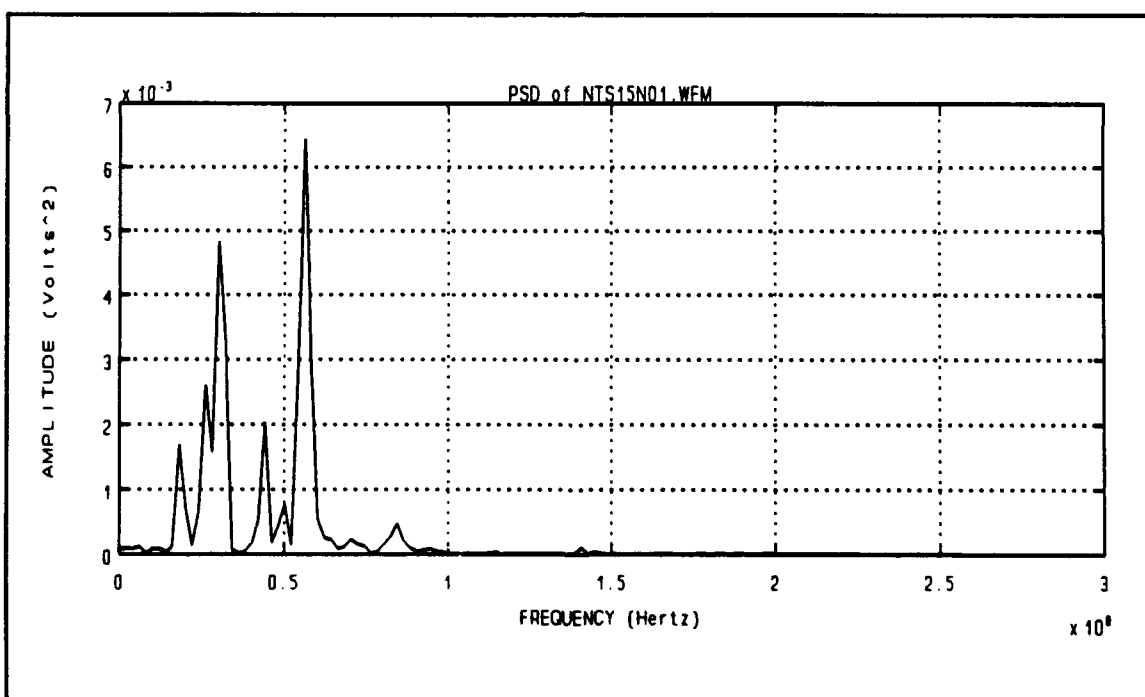


Figure 93 Waveform NTS15N01.WFM [Paired with NTS15P01.WFM]
Power Spectral Density Graph - Vertical Component

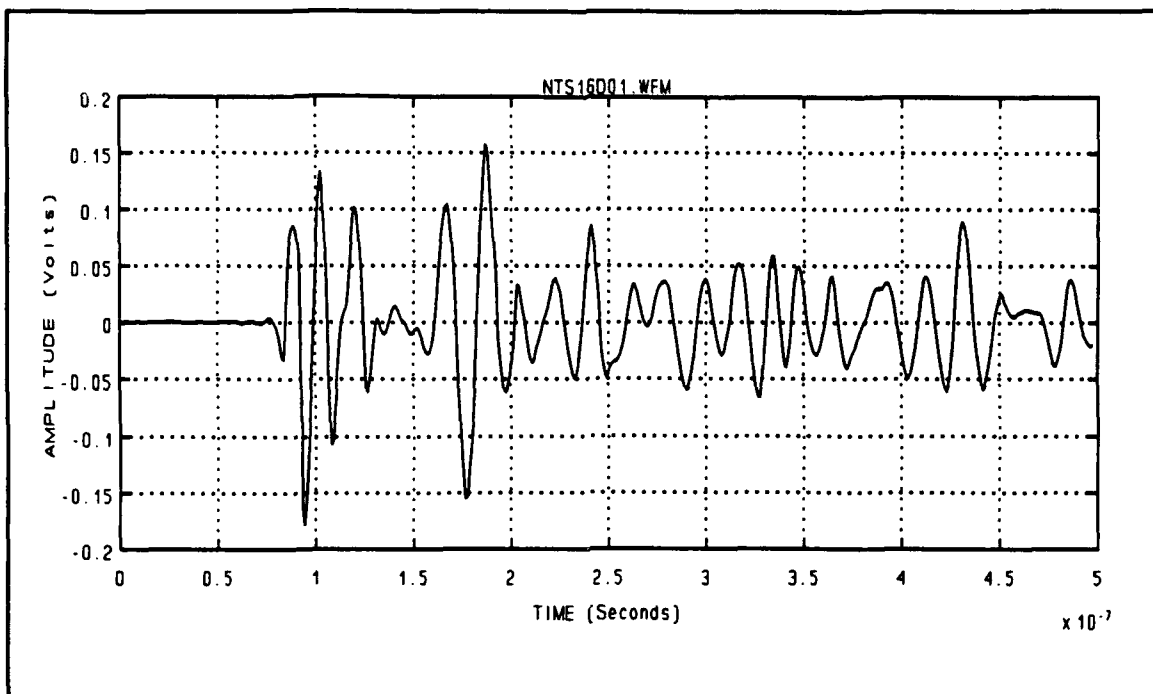


Figure 94 Waveform NTS16D01.WFM [Paired with NTS16C01.WFM]
Big TEM Horn Antenna - Horizontal Component

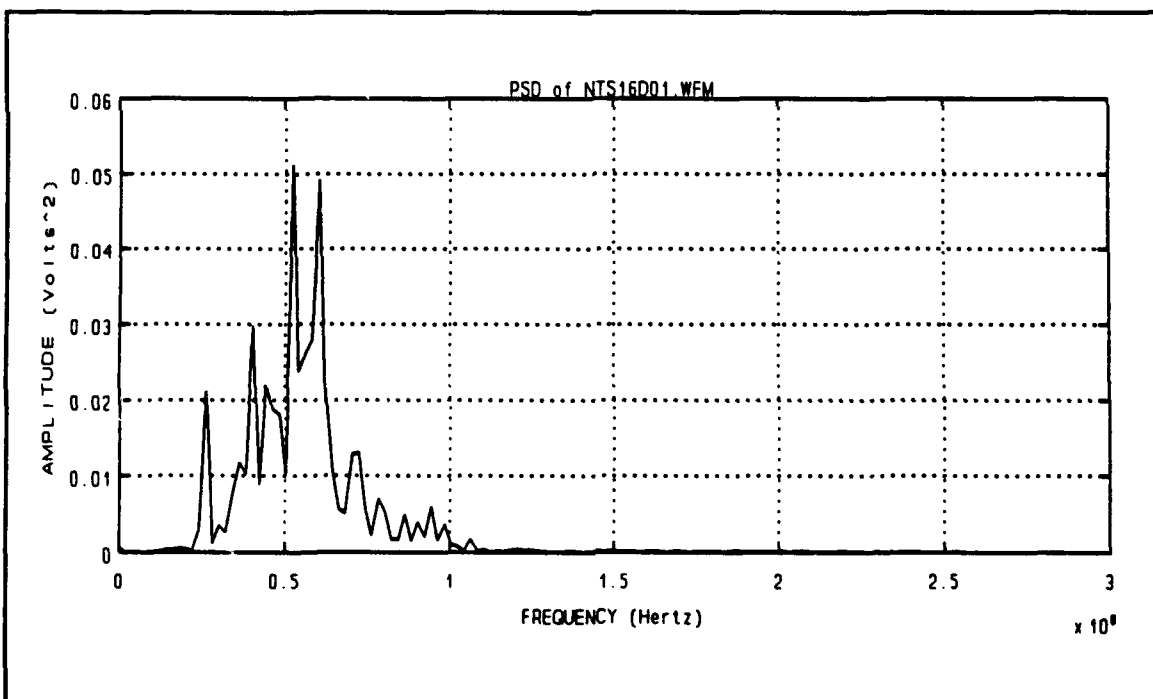


Figure 95 Waveform NTS16D01.WFM [Paired with NTS16C01.WFM]
Power Spectral Density Graph - Horizontal Component

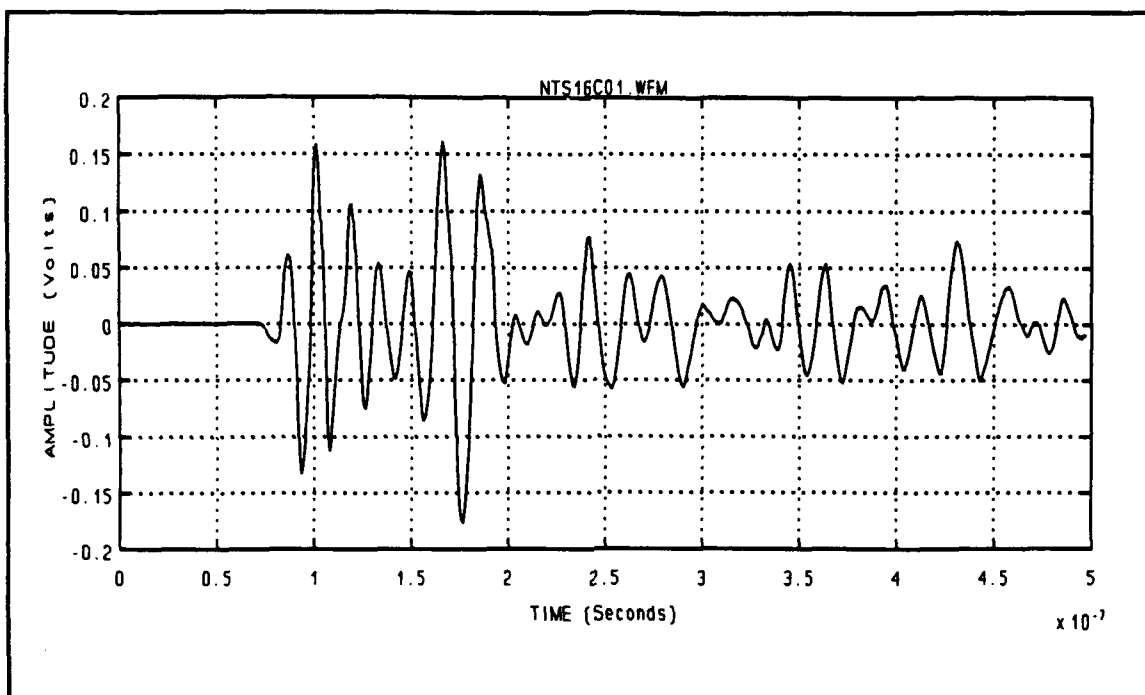


Figure 96 Waveform NTS16C01.WFM [Paired with NTS16D01.WFM]
Big TEM Horn Antenna - Vertical Component

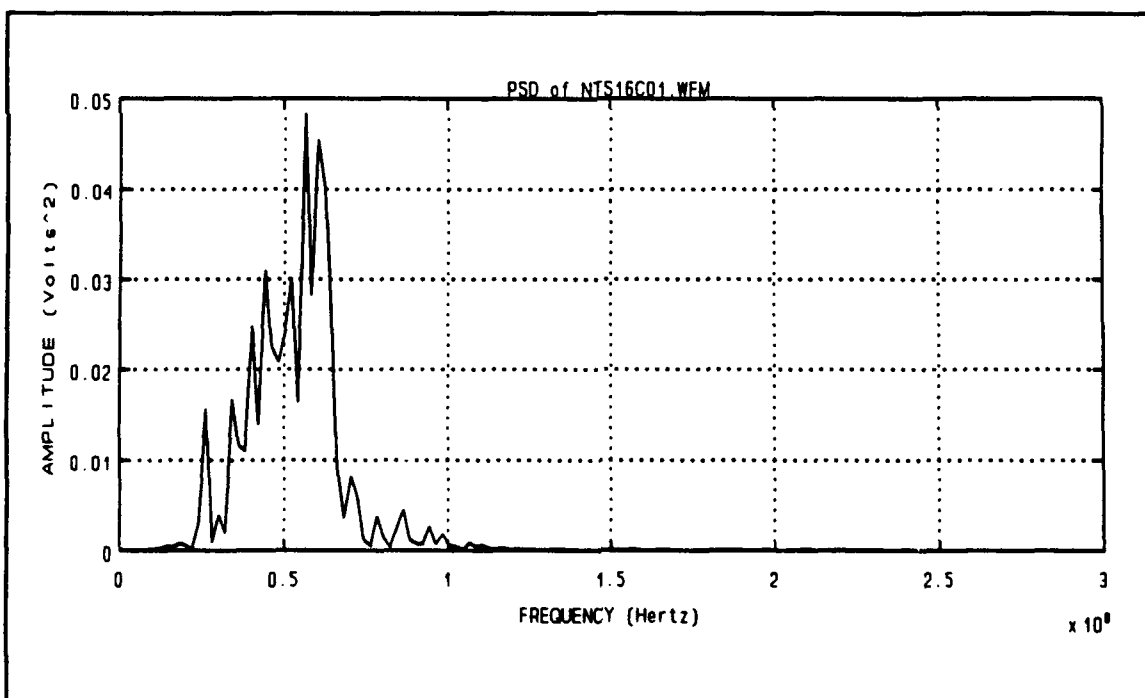


Figure 97 Waveform NTS16C01.WFM [Paired with NTS16D01.WFM]
Power Spectral Density Graph - Vertical Component

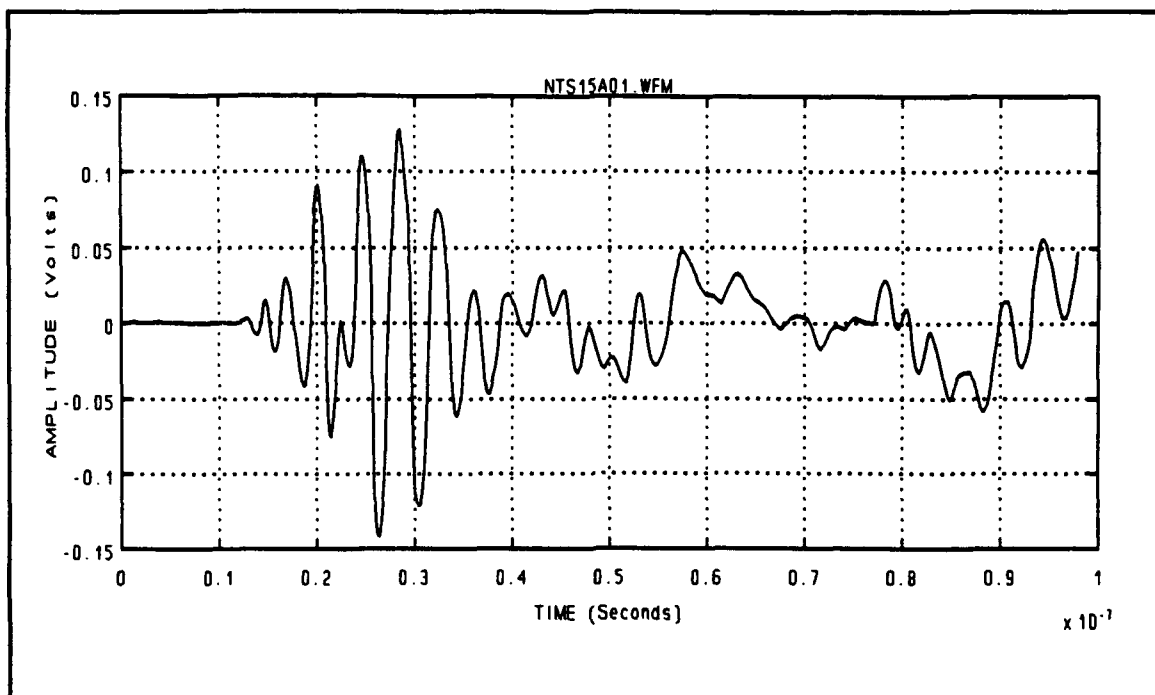


Figure 98 Waveform NTS15A01.WFM [Paired with NTS15D01.WFM]
LLNL Log Periodic Antenna - Horizontal Component

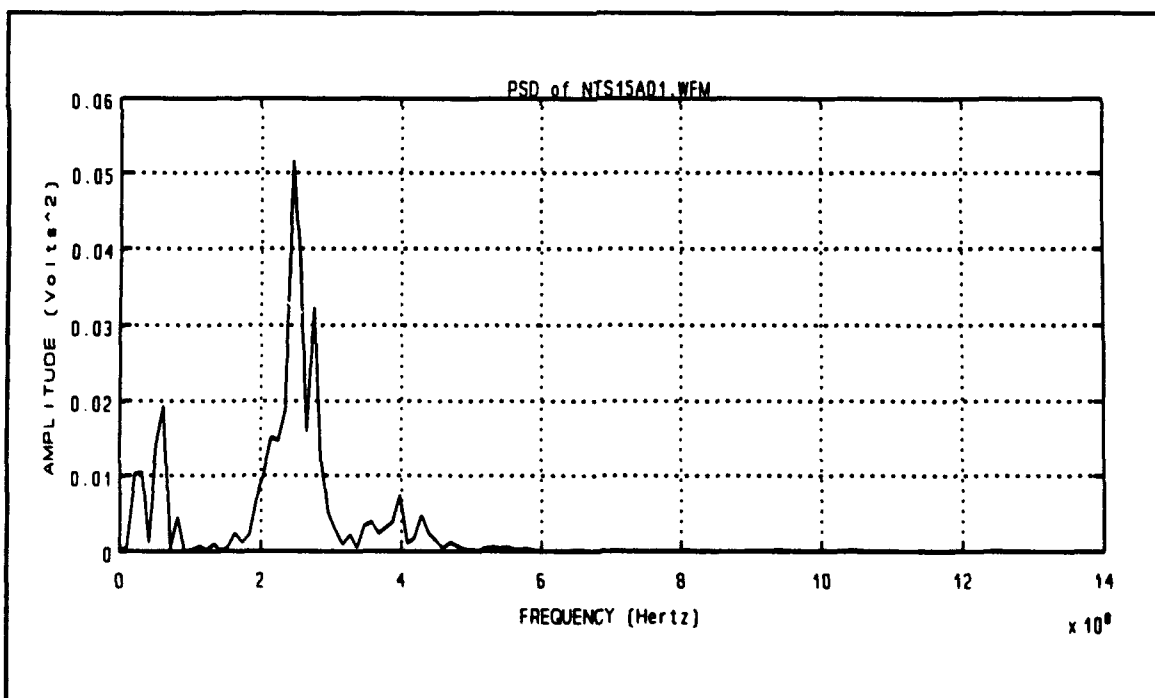


Figure 99 Waveform NTS15A01.WFM [Paired with NTS15D01.WFM]
Power Spectral Density Graph - Horizontal Component

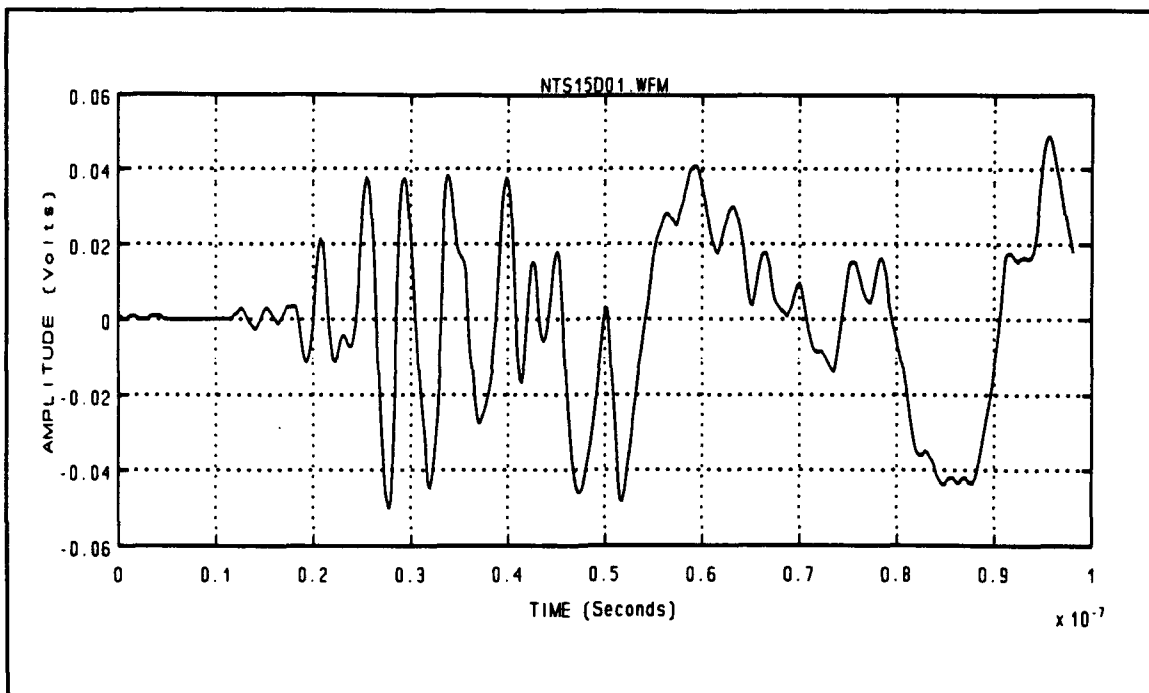


Figure 100 Waveform NTS15D01.WFM [Paired with NTS15A01.WFM]
LLNL Log Periodic Antenna - Vertical Component

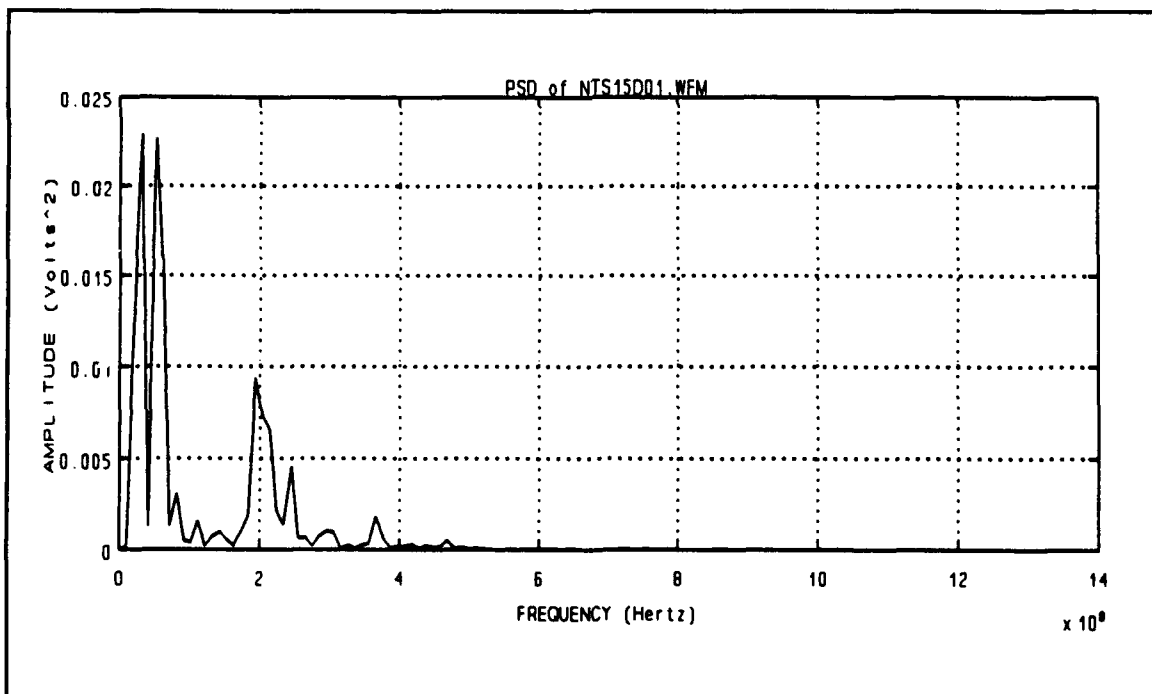


Figure 101 Waveform NTS15D01.WFM [Paired with NTS15A01.WFM]
Power Spectral Density Graph - Vertical Component

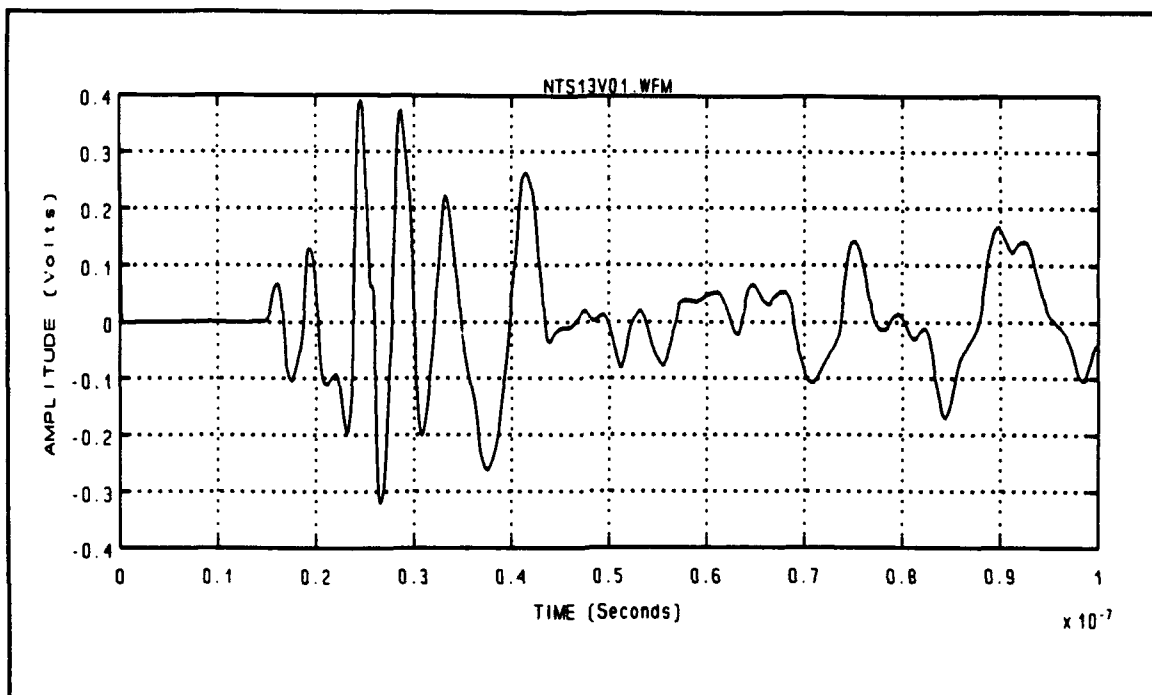


Figure 102 Waveform NTS13V01.WFM [Paired with NTS13W01.WFM]
Big Tem Horn Antenna - Horizontal Component

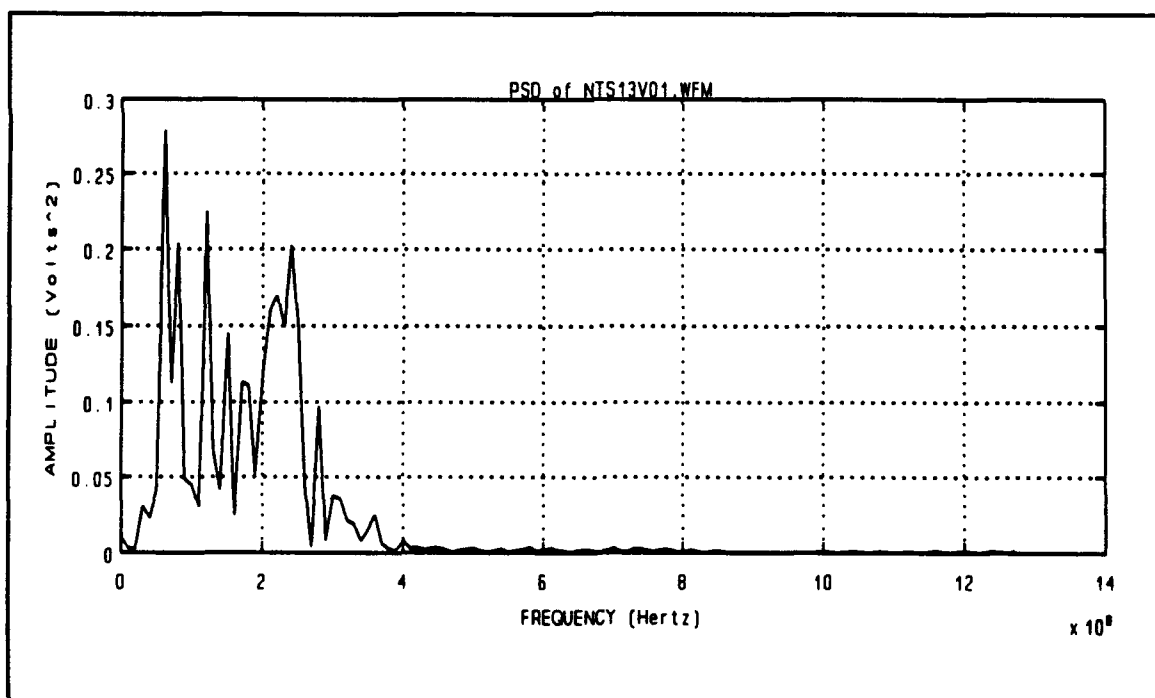


Figure 103 Waveform NTS13V01.WFM [Paired with NTS13W01.WFM]
Power Spectral Density Graph - Horizontal Component

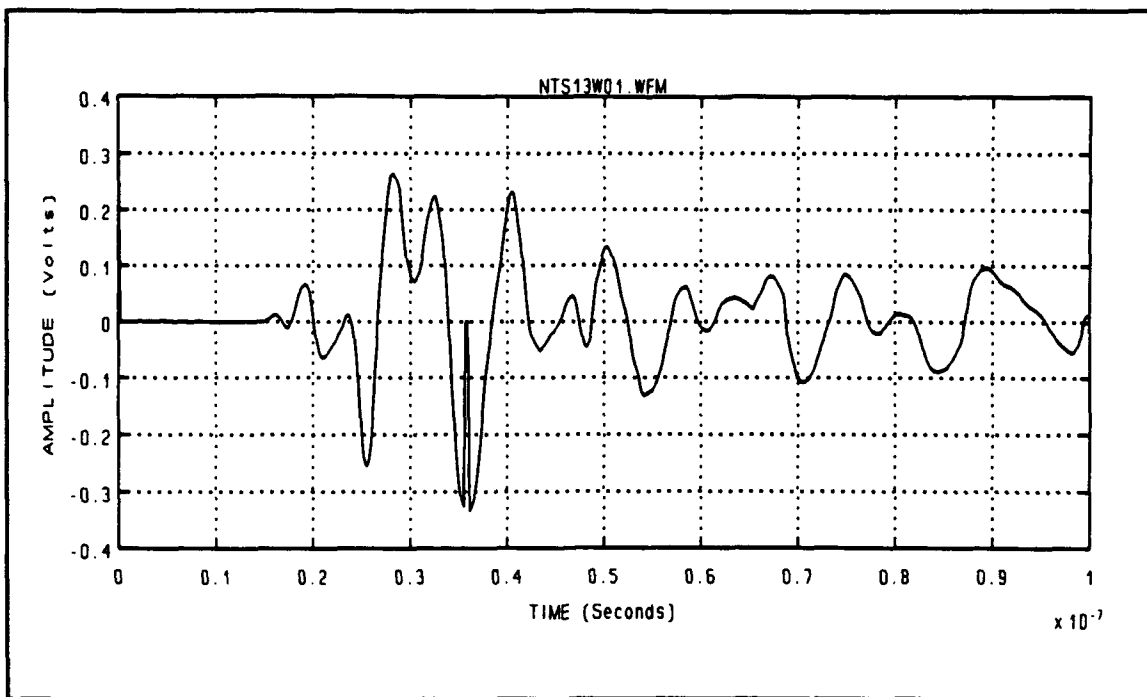


Figure 104 Waveform NTS13W01.WFM [Paired with NTS13V01.WFM]
Big TEM Horn Antenna - Vertical Component

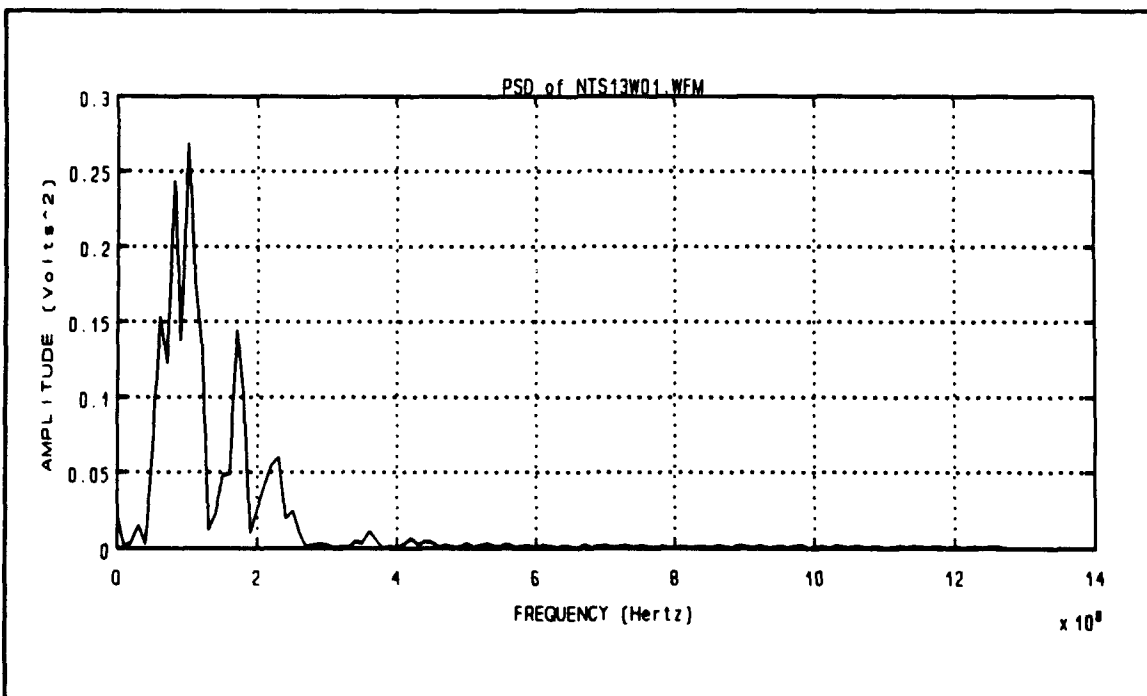


Figure 105 Waveform NTS13W01.WFM [Paired with NTS13V01.WFM]
Power Spectral Density Graph - Vertical Component

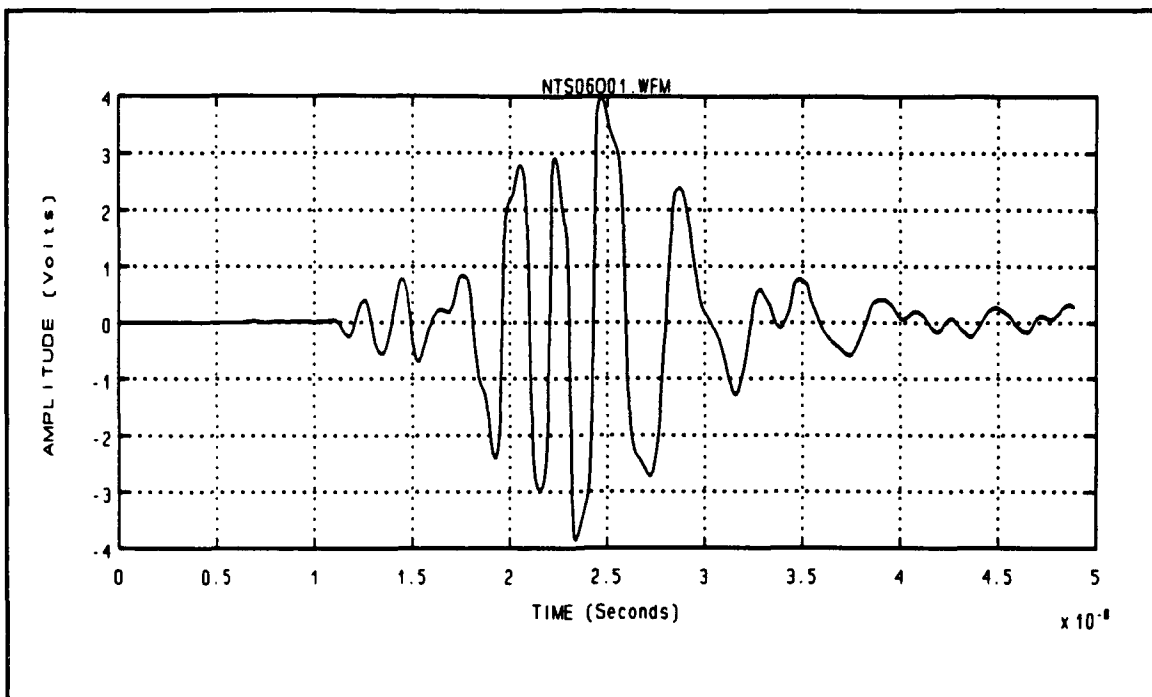


Figure 106 Waveform NTS06001.WFM - Directory 5-1-90
LLNL Log Periodic Antenna

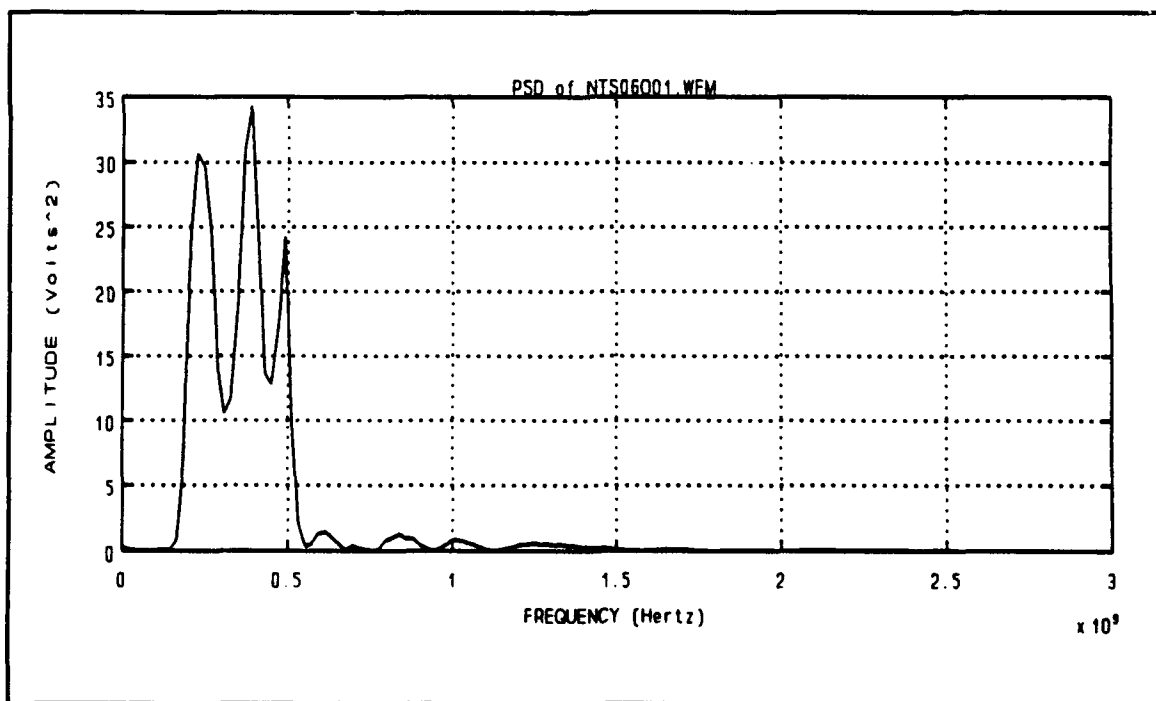


Figure 107 Waveform NTS06001.WFM - Directory 5-1-90
Power Spectral Density Graph

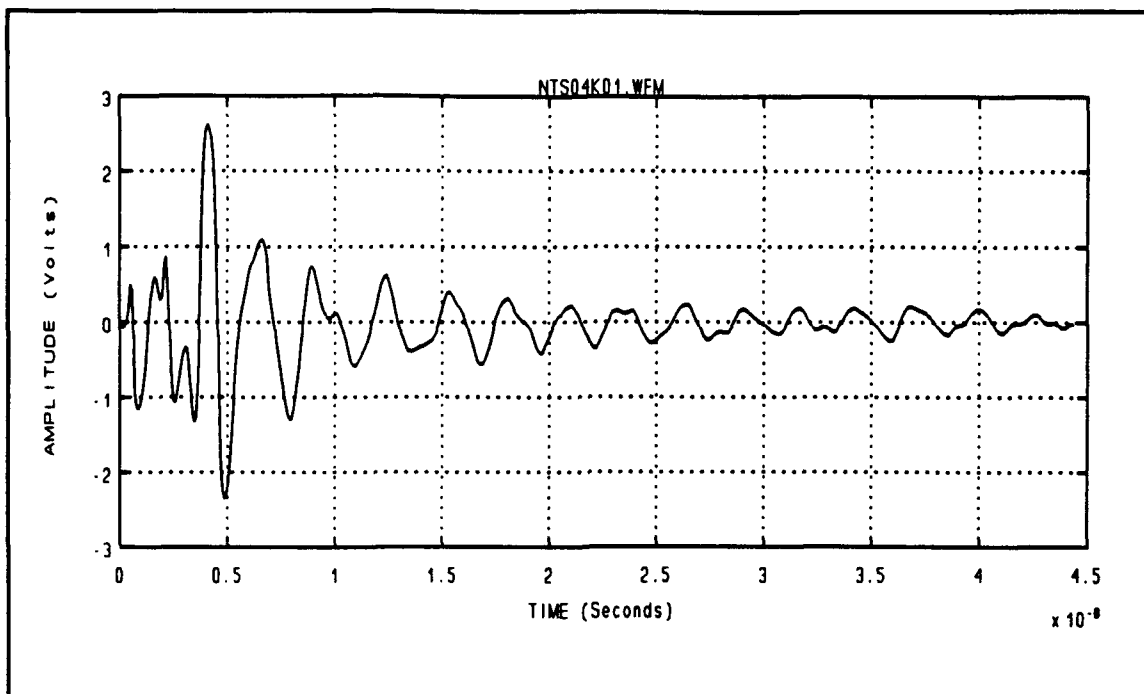


Figure 108 Waveform NTS04K01.WFM - Directory 5-1-90
Big TEM Horn Antenna

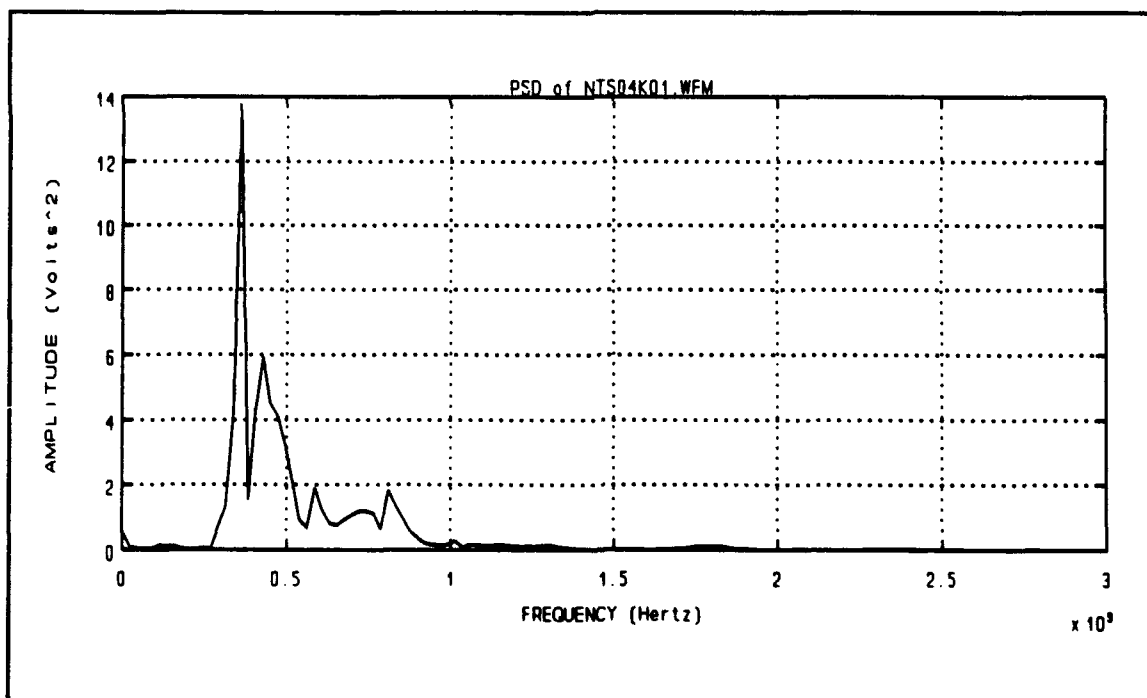


Figure 109 Waveform NTS04K01.WFM - Directory 5-1-90
Power Spectral Density Graph

*** Amplitude decreases as move off center**

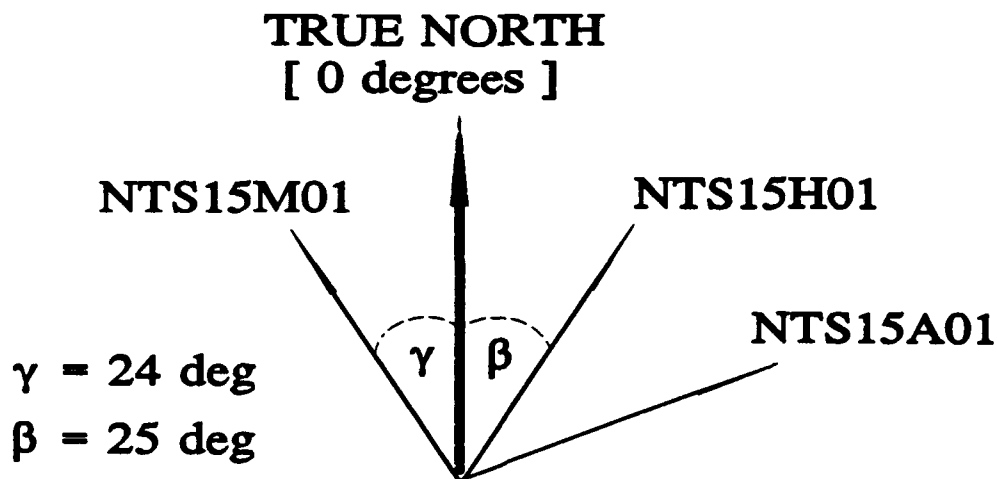


Figure 110 Project Evergreen - LLNL modified LP Antenna
Signal Strength as a Function of Azimuthal Direction

*** Amplitude decreases as move off center**

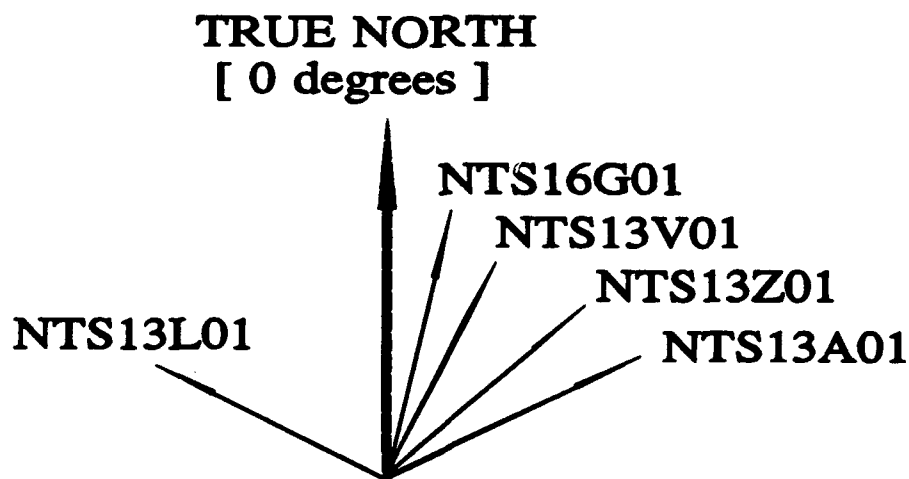


Figure 111 Project Evergreen - Big TEM Horn Antenna
Signal Strength as a Function of Azimuthal Direction

B. ELECTROMAGNETIC CONSIDERATIONS

Dispersive effects experienced by the signal pulse due to the conductive properties of the atmosphere were also considered. Electromagnetic theory states that the phase velocity of an electromagnetic wave propagating through the atmosphere will be a function of the refractive index. The resulting equation shows that different frequencies will experience different phase velocities:

$$V_p = \frac{c}{n} = \left[\sqrt{\left(\frac{2}{\mu\epsilon} \right)} \right] * \left[\sqrt{\left(1 + \left(\frac{g}{\epsilon\omega} \right)^2 \right) + 1} \right]^{-1/2} \quad (6)a$$

where:

- V_p = phase velocity of electromagnetic wave
- μ = permeability of the medium
- ϵ = permittivity of the medium
- g = conductivity of the medium
- ω = angular frequency of electromagnetic wave
- c = speed of light
- $n = \mu\epsilon$ = refractive index

Equation (6)a is equivalent to:

$$V_p = \left[\sqrt{\left(\frac{2}{\mu_r \mu_o \epsilon_r \epsilon_o} \right)} \right] * \left[\sqrt{\left(1 + \frac{g}{\epsilon_r \epsilon_o 2\pi f} \right)^2 + 1} \right]^{-1/2} \quad (6)b$$

where:

- μ_r = relative permeability constant
- μ_o = permeability of free space
- ϵ_r = relative permittivity constant
- ϵ_o = permittivity of free space
- f = frequency of electromagnetic wave such that $\omega = 2\pi f$

Assuming that the earth's atmosphere behaves for all practical purposes as a vacuum, I used the following values for ϵ , μ [Ref. 6] and g [Ref. 7]:

$$\epsilon = \epsilon_r \epsilon_0 = 1 * 8.854 \times 10^{-12} \text{ C}^2/\text{N}\cdot\text{m}^2$$

$$\mu = \mu_r \mu_0 = 1 * 4\pi \times 10^{-7} \text{ N}\cdot\text{s}^2/\text{C}^2$$

where C = coulombs, s = seconds and N = newtons.

$$g \approx 2 \times 10^{-17} \text{ S/m} \quad \text{height above ground} = 0 \text{ meters}$$

$$g \approx 5 \times 10^{-16} \text{ S/m} \quad \text{height above ground} = 10 \text{ kilometers}$$

$$g \approx 2 \times 10^{-15} \text{ S/m} \quad \text{height above ground} = 20 \text{ kilometers}$$

where S = siemens and m = meters.

Electromagnetic theory states that for a conducting medium, the electric and magnetic fields will not be orthogonal for circular or elliptical polarization. Given the extremely low values of conductivity, g , I treated the atmosphere as a non-conducting medium. This simplified the analysis in that I was able to treat the electric and magnetic fields as orthogonal. In doing so, when analyzing the vertical and horizontal component of the electric field of the transmitted signal, non-orthogonal (i.e. 90 degrees) phase relationships between the electric and magnetic fields did not have to be considered, simplifying the analysis. It is important to point out that the atmosphere is a conducting medium (albeit extremely small), and as a result there will be non-orthogonal phase relationships between the electric and magnetic fields. This non-orthogonal phase relationship between the electric and magnetic fields could account for

some of the dispersive effects noted in both the horizontally and vertically received component of the signal.

Inputting a range of values for the frequency, f , from 0 MHz to 2 GHz, the resulting phase velocity v_p remained constant to three significant digits (i.e. $v_p = 2.998 \text{ m/s}^2$). Based on these results, I concluded that any dispersion experienced by the transmitted pulse due to the atmosphere was negligible and imperceptible for the purposes of this analysis. Consequently, the dispersive effects induced in the transmitted pulse due to different phase velocities are a function of the hardware parameters (i.e transmitter characteristics, antenna transfer function, etc.). Additionally, multipath effects, reflection and refraction of the transmitted pulse will most likely also contribute to dispersive effects at the receiving end due to constructive and destructive interference.

C. RECOMMENDATIONS

The following recommendations are suggested:

1. Bookkeeping and accurate records of what actually took place is essential for future experiments. Lack of accurate note taking, properly annotating changing parameters and variables and lack of data hindered and complicated the analysis of this data. The importance of accurate records becomes even more critical when the individual analyzing the data did not participate in the actual experiment.
2. Hardware bandwidths large enough to adequately accommodate the signals of interest are critical for successful data gathering. On future experiments

involving the study of electromagnetic radiation, the experimenter needs to ensure that the equipment used (i.e antenna, receiver, oscilloscope, etc.) is suitable for the signals of interest.

3. The use of narrow band equipment should not be used because an extremely narrow pulse will just give the impulse response of the receiver. Consequently, not much information would be known about the signal except that it is a very narrow, time limited pulse (i.e. wideband in the frequency domain).
4. Further study should be conducted to better understand the effects of extremely short time duration signals on electronic equipment (i.e. antennas, receivers, transmitters, etc.). Atmospheric effects that may be unique to such signals should also be studied.

APPENDIX A. MATLAB PROGRAM - POWER SPECTRAL DENSITY GRAPH

```
% This program will calculate and provide a graphic output of
% the power spectral density (PSD) graph of a signal
% Graphic output will be provided on a log-log plot and a
% semi-log plot. The semi-log plot is used to provide finer
% detail at the lower power levels
% The signal of interest was obtained during the NTS
% experiment

% MATLAB is a mathematics software program developed by
% The MathWorks, Inc. A copy of the program is available
% in the Electrical Engineering computer lab located on
% the 4th floor of Spanagel Hall

m = input('Enter meta file name = ', 's');
eval(['!del ', m, '.met']);

disp('ENTER WAVEFORM DATA FILE without .DAT Extension');
c = input('> ', 's');
eval(['load ', c, '.dat']); % ASCII DATA FILE OF
                           % DIGITIZED WAVEFORM

eval(['C = ', c, ';' ]); % LOADING DATA FILE INTO
                          % COLUMN VECTOR C

C = C'; % TRANSPOSE ASCII DATA
        % COLUMN VECTOR C

disp('Enter SAMPLING FREQUENCY');
Fs = input('> ');

disp('Enter NUMBER of ASCII DATA POINTS');
N = input('> ');

w = fft(C); % FAST FOURIER TRANSFORM
            % OF SIGNAL DATA POINTS

Pyy = (1/N) .* (w .* conj(w)); % POWER SPECTRUM OF
                               % DIGITIZED WAVEFORM

f = (Fs*(0:N-1)./N); % FULL FREQUENCY RANGE
f1 = (Fs*(0:(N/2 - 1))./N); % 1/2 FREQUENCY RANGE
f2 = (Fs*(0:(N/4 - 1))./N); % 1/4 FREQUENCY RANGE
f3 = (Fs./N)*(0:N/8 - 1); % 1/8 FREQUENCY RANGE
```

```

subplot(211), plot(f,Pyy), title(['PSD of ', c]),
    xlabel('FREQUENCY (Hertz)'), ylabel('AMPLITUDE (Volts^2)'),
    grid, pause;
subplot(212), plot(f1,Pyy(1:256)), title(['PSD of ', c]),
    xlabel('FREQUENCY (Hertz)'), ylabel('AMPLITUDE (Volts^2)'),
    grid, pause;
eval(['meta ',m]);
clg;

subplot(211), plot(f2,Pyy(1:128)), title(['PSD of ',c]),
    xlabel('FREQUENCY (Hertz)'), ylabel('AMPLITUDE (Volts^2)'),
    grid, pause;
subplot(212), plot(f3,Pyy(1:64)), title(['PSD of ',c]),
    xlabel('FREQUENCY (Hertz)'), ylabel('AMPLITUDE (Volts^2)'),
    grid, pause;
eval(['meta ',m]);
clg;

subplot(211), semilogy(f,Pyy), title(['PSD of ', c]),
    xlabel('FREQUENCY (Hertz)'), ylabel('AMPLITUDE (Volts^2)'),
    grid, pause;
subplot(212), semilogy(f1,Pyy(1:256)), title(['PSD of ', c]),
    xlabel('FREQUENCY (Hertz)'), ylabel('AMPLITUDE (Volts^2)'),
    grid, pause;
eval(['meta ',m]);
clg;

subplot(211), semilogy(f2,Pyy(1:128)), title(['PSD of ', c]),
    xlabel('FREQUENCY (Hertz)'), ylabel('AMPLITUDE (Volts^2)'),
    grid, pause;
subplot(212), semilogy(f3,Pyy(1:64)), title(['PSD of ', c]),
    xlabel('FREQUENCY (Hertz)'), ylabel('AMPLITUDE (Volts^2)'),
    grid, pause;
eval(['meta ',m]);
clg;

```

APPENDIX B. MATLAB PROGRAM - AMPLITUDE vs. TIME WAVEFORM

```
% This program will provide a graphic output of the amplitude
% versus time waveform using the sampled data points
% The signal of interest was obtained during the NTS
% experiment

m = input('Enter meta file name =      ','s');
eval(['!del ',m,'.met']);

disp('ENTER WAVEFORM DATA FILE in Capital Letters without
.DAT Extension');
c = input('> ','s');
eval(['load ',c,'.dat']);           % ASCII DATA FILE OF
                                   % DIGITIZED WAVEFORM

eval(['C = ',c, ';' ]);           % LOADING DATA FILE INTO
                                   % COLUMN VECTOR C

C = C';                           % TRANSPOSE ASCII DATA
                                   % COLUMN VECTOR

disp('Enter NUMBER of ASCII DATA POINTS');
N = input('> ');

disp('Enter SAMPLING TIME INTERVAL');
T = input('> ');

n = 0:N-1;                        % NUMBER OF DATA POINTS

t = n*T;                          % TIME INTERVAL BETWEEN
                                   % SAMPLED DATA POINTS

subplot(211), plot(t,C), title([c,'.WFM']),
    xlabel('TIME (Seconds)'), ylabel('AMPLITUDE (Volts)'), grid;
eval(['meta ',m]);
```

APPENDIX C. MATLAB PROGRAM - POWER vs. TIME WAVEFORM

```
% This program will provide a graphic output of the
% power versus time waveform
% The signal of interest was obtained during the NTS
% experiment

m = input('Enter meta file name = ', 's');
eval(['!del ', m, '.met']);

disp('ENTER WAVEFORM DATA FILE in Capital Letters without
.DAT Extension');
c = input('> ', 's');
eval(['load ', c, '.dat']); % ASCII DATA FILE OF
                           % DIGITIZED WAVEFORM

eval(['C = ', c, ';' ]); % LOADING DATA FILE INTO
                           % COLUMN VECTOR C

C = C'; % TRANSPOSE ASCII DATA
        % COLUMN VECTOR C

disp('Enter NUMBER of ASCII DATA POINTS');
N = input('> ');

disp('Enter SAMPLING TIME INTERVAL');
T = input('> ');

n = 0:N-1; % NUMBER OF DATA POINTS

t = n*T; % TIME INTERVAL BETWEEN
          % SAMPLED DATA POINTS

B = C.^2; % SQUARING THE ELEMENTS IN ROW VECTOR C

subplot(211), plot(t,B), title([c, '.WFM']),
    xlabel('TIME (Seconds)'), ylabel('POWER (Volts^2)'), grid;
eval(['meta ', m]);
```

APPENDIX D. MATLAB PROGRAM - ENERGY vs. TIME WAVEFORM

```
% This program will provide a graphic output of the
%           energy versus time waveform
% The signal of interest was obtained during the NTS
%           experiment

m = input('Enter meta file name =      ','s');
eval(['!del ',m,'.met']);

disp('ENTER WAVEFORM DATA FILE in Capital Letters without
      .DAT Extension');
c = input('> ','s');
eval(['load ',c,'.dat']);           % ASCII DATA FILE OF
                                   % DIGITIZED WAVEFORM

eval(['C = ',c, ';' ]);           % LOADING DATA FILE INTO
                                   % COLUMN VECTOR C

C = C';                           % TRANSPOSE ASCII DATA
                                   % COLUMN VECTOR C

disp('Enter NUMBER of ASCII DATA POINTS');
N = input('> ');

disp('Enter SAMPLING TIME INTERVAL');
T = input('> ');

n = 0:N-1;                        % NUMBER OF DATA POINTS

t = n*T;                          % TIME INTERVAL BETWEEN
                                   % SAMPLED DATA POINTS

B = C.^2;                         % SQUARING THE ELEMENTS IN ROW VECTOR C

E = zeros(1,N);                  % DEFINE SIZE OF VECTOR
D = 0;                           % INITIALIZING VARIABLE
Z = 0;                           % INITIALIZING VARIABLE

for a=1:1:N;
    Z = B(a) * t(a);              % ELEMENT BY ELEMENT MULTIPLICATION
    D = D + Z;                    % CUMULATIVE SUM OF (POWER * TIME)
    E(a) = D;
end;
```



```
subplot(211), plot(t,E), title([c, '.WFM']),  
  xlabel('TIME (Seconds)'), ylabel('ENERGY (Volts^2 * Time)'),  
  grid;  
eval(['meta ',m]);
```

APPENDIX E. MATLAB PROGRAM - ENERGY vs. TIME (NORMALIZED)

```
% This program will provide a graphic output of the
% energy versus time curve
% This program will normalize the energy versus time curve
% and graph both curves for the horizontal and vertical
% polarization on the same plot
% The signal of interest was obtained during the NTS
% experiment

m = input('Enter meta file name =      ','s');
eval(['!del ',m,'.met']);

% *****

disp('ENTER WAVEFORM DATA FILE in Capital Letters without
.DAT Extension');
c = input('> ','s');
eval(['load ',c,'.dat']);           % ASCII DATA FILE OF
                                   % DIGITIZED WAVEFORM

eval(['C = ',c,';']);              % LOADING DATA FILE INTO
                                   % COLUMN VECTOR C

C = C';                           % TRANSPOSE ASCII DATA
                                   % COLUMN VECTOR C

disp('Enter SAMPLING TIME INTERVAL');
T = input('> ');

%
% *****

disp('ENTER WAVEFORM DATA FILE in Capital Letters without
.DAT Extension');
d = input('> ','s');
eval(['load ',d,'.dat']);           % ASCII DATA FILE OF
                                   % DIGITIZED WAVEFORM

eval(['D = ',d,';']);              % LOADING DATA FILE INTO
                                   % COLUMN VECTOR D

D = D';                           % TRANSPOSE ASCII DATA
                                   % COLUMN VECTOR D

disp('Enter SAMPLING TIME INTERVAL');
TT = input('> ');
```

```

% *****

disp('Enter NUMBER OF ASCII DATA POINTS');
N = input('> ');

%*****

n = 0:N-1;                % NUMBER OF DATA POINTS

t = n*T;                  % TIME INTERVAL BETWEEN
                        % SAMPLED DATA POINTS

B = C.^2;                 % SQUARING THE ELEMENTS IN
                        % ROW VECTOR C

X = zeros(1,N);           % DEFINING SIZE OF VECTOR
Y = 0;                   % INITIALIZING VARIABLE
Z = 0;                   % INITIALIZING VARIABLE

for a=1:1:N;
    Z = B(a) * t(a);      % ELEMENT BY ELEMENT MULTIPLICATION
    Y = Y + Z;            % CUMULATIVE SUM OF (POWER * TIME)
    X(a) = Y;
end;

M = max(X), pause;
XM = X./M;

%*****

n = 0:N-1;                % NUMBER OF DATA POINTS

tt = n*TT;               % TIME INTERVAL BETWEEN
                        % SAMPLED DATA POINTS

BB = D.^2;               % SQUARING THE ELEMENTS IN
                        % ROW VECTOR D

XX = zeros(1,N);         % DEFINING SIZE OF VECTOR
YY = 0;                 % INITIALIZING VARIABLE
ZZ = 0;                 % INITIALIZING VARIABLE

for aa=1:1:N;
    ZZ = BB(aa) * tt(a); % ELEMENT BY ELEMENT MULTIPLICATION
    YY = YY + ZZ;        % CUMULATIVE SUM OF (POWER * TIME)
    XX(aa) = YY;
end;

MM = max(XX), pause;
XXMM = XX./MM;

```

```

% *****
subplot(211), plot(t,XM,'b',tt,XXMM,'-.g'),
    title('ENERGY versus TIME Graph - "NORMALIZED"'),
    xlabel('TIME (Seconds)'),
    ylabel('ENERGY (Volts^2 * Time)'), grid;
eval(['meta ',m]);

```

APPENDIX F. MATLAB PROGRAM - PHASE VELOCITY

```
% This program will calculate the phase velocity of an
% electromagnetic (E-M) wave for a range of frequencies.
% The parameters for wave frequency (f), permittivity (e),
% permeability (u) and conductivity (g) are inputted from the
% keyboard. Specifying these parameters tailors the equation
% for the particular medium under consideration.

m = input('Enter meta file name = ', 's');
eval(['!del ', m, '.met']);

disp('Enter Lower Limit WAVE FREQUENCY ( in Hertz ) EXCLUDE
0');
LL = input('> ');

disp('Enter Upper Limit WAVE FREQUENCY ( in Hertz )');
UL = input('> ');

disp('Enter PERMITTIVITY Constant');
e = input('> ');

disp('Enter PERMEABILITY Constant');
u = input('> ');

disp('Enter CONDUCTIVITY Constant');
g = input('> ');

X = UL;
XX = LL;
Z = X - XX;
Vp = zeros(1,Z);           % DEFINE SIZE OF ROW VECTOR

Y=1;                       % INITIALIZE COUNTER

for f=LL:1:UL;
    V = sqrt(2/(u*e)) * 1/(sqrt(sqrt(1+(g/(e*2*pi*f))^2) + 1));
    Vp(1,Y) = V;
    Y = Y + 1;
end;

f = LL:1:UL;

plot(f,Vp,'+b'), title('ATMOSPHERIC PHASE VELOCITY of
E-M WAVE '), xlabel('FREQUENCY (Hertz)'),
ylabel('PHASE VELOCITY (m/s)'), grid;
eval(['meta ', m]);
```

LIST OF REFERENCES

1. Eugene P. Binnal, EVERGREEN: Project Introduction and Request for Site Use at NTS, (Livermore, CA: Lawrence Livermore National Laboratory, 9 February, 1990), p.7.
2. Gerry Burke, "Technical Note 2-1-90," Preliminary Analysis of a Modified Log-Periodic Antenna for Pulse Transmission, (Livermore, CA: Lawrence Livermore National Laboratory, 30 April, 1990).
3. Robert A. Lawton and Arthur R. Ondrejka, Antennas and the Associated Time Domain Range for the Measurement of Impulsive Fields, (Boulder, CO: National Bureau of Standards, November 1978), pp. 13-15, 19-21, 48-49.
4. Eugene P. Binnall, "EVERGREEN Review Meeting," EVERGREEN SITE, (Livermore, CA: Lawrence Livermore National Laboratory, 28 August, 1990).
5. Robert D. Strum and Donald E. Kirk, Discrete Systems and Digital Signal Processing (New York: Addison-Wesley Publishing Company, April 1989), pp. 389 -392.
6. John R. Reitz and Frederick J. Milford and Robert W. Christy, Foundations of Electromagnetic Theory (London: Addison-Wesley Publishing Company, 1980), p. 26 and p. 161.
7. United States Air Force, Handbook of Geophysics and the Space Environment (Air Force Geophysics Laboratory, 1985), p. 20-2.

BIBLIOGRAPHY

1. Anton, Howard and Rorres, Chris, Elementary Linear Algebra with Applications, John Wiley and Sons, New York, 1987.
2. Binnall, Eugene P., EVERGREEN: Project Introduction and Request for Site Use at NTS, Lawrence Livermore National Laboratory, Lawrence, California, 9 February, 1990.
3. Binnall, Eugene P., "EVERGREEN Review Meeting", EVERGREEN Site, Lawrence Livermore National Laboratory, Lawrence, California, 28 August, 1990.
4. Burke, Gerry J., "Technical Note 2-1-90", Preliminary Analysis of a Modified Log-Periodic Antenna for Pulse Transmission, Lawrence Livermore National Laboratory, Lawrence, California, 30 April, 1990.
5. Burke, Gerry J., Evaluation of Modified Log-Periodic Antennas for Transmission of Wide-Band Pulses, Briefing presented at the 7th Annual Review of Progress in Applied Computational Electromagnetics, Naval Postgraduate School, Monterey, California, 18-22 March, 1991.
6. Cornish, W. D., Microwave Frequency Dividers: Devices and Applications, IEE Proceedings, Volume 129, Part F, Number 3, June 1982.
7. Dreyer, Kenneth A., Ground Wave Propagation of a Video Pulse Source, Lawrence Livermore National Laboratory, Applied Technology Program, Livermore, California, 30 April, 1990.
8. Gnanalingham, Class Notes, PH 3352 Electromagnetic Waves and PH 4353 Topics in Advanced Electricity and Magnetism, Naval Postgraduate School, Monterey, California, January 1991 - June 1991.
9. Iverson, A. Evan, Ultra Wideband Radar, Research and Development Considerations, Mechanical and Engineering Division, Los Alamos National Laboratory, New Mexico, June 1989.
10. Kildal, P. S., Gaussian Beam Model for Aperture-Controlled and Flareangle-Controlled Corrugated Horn Antennas, IEE Proceedings, Volume 135, Part H, Number 4, August 1988.

11. Kildal, P. S., Technical Memorandum, Bandwidth of a Square Hard Horn, IEE Proceedings, Volume 135, Part H, Number 4, August 1988.
12. Kisenwether, Liz, UWB Radar and Related Technologies, HRB Systems, State College, Pennsylvania, June 1991.
13. Kisenwether, Liz, Impulse Radar: Review and Analysis, HRB Systems, State College, Pennsylvania, December, 1987.
14. Lawton, Robert A. and Ondrejka, Arthur R., Antennas and the Associated Time Domain Range for the Measurement of Impulsive Fields, National Bureau of Standards, Boulder, Colorado, November, 1978.
15. Parkes, D. M. and Smith, P. D., Practical Method of Predicting Transient Fields and Monopole Current Waveforms, IEE Proceedings, Volume 135, Part H, Number 4, August 1988.
16. Moule, G. L., SAW Compressive Receivers for Radar Intercept, IEE Proceedings, Volume 129, Part F, Number 3, June 1982.
17. Reitz, John R. and Milford, Frederick J., Foundations of Electromagnetic Theory, Addison-Wesley Publishing Company, London, 1980.
18. Skolnik, Merrill I., An Introduction to Impulse Radar, Radar Division, Naval Research Laboratory, Washington, D.C., November, 1990.
19. Strum, Robert D. and Kirk, Donald E., First Principles of Discrete Systems and Digital Signal Processing, Addison-Wesley Publishing Company, New York, April 1989.
20. Temes, C. L., Impulse Arrays, Radar Division, Naval Research Laboratory, Washington, D.C., May 1991.
21. United States Air Force, Handbook of Geophysics and the Space Environment, Air Force Geophysics Laboratory, 1985.

INITIAL DISTRIBUTION LIST

- | | | | |
|----|------------------------------------------------------------------------------------------------------------------------------------------------------------------|---|---|
| 1. | Defense Technical Information Center
Cameron Station
Alexandria, Virginia 22304-6145 | 2 | |
| 2. | Library, Code 52
Naval Postgraduate School
Monterey, California 93943-5002 | 2 | |
| 3. | Naval Postgraduate School
Attn: Professor Xavier Maruyama, Code PH/MX
Department of Physics
Monterey, California 93943-5000 | 5 | 1 |
| 4. | Naval Postgraduate School
Attn: Professor Stephen Jauregui, Code 62Ja
Department of Electrical and Computer Engineering
Monterey, California 93943-5000 | 1 | |
| 5. | Naval Postgraduate School
Attn: Professor S. Gnanalingham, Code PH/GN
Department of Physics
Monterey, California 93943-5000 | 1 | |
| 6. | Naval Postgraduate School
Attn: Professor John Neighbours, Code PH/NG
Department of Physics
Monterey, California 93943-5000 | 1 | |
| 7. | Antonio Gala
7340 South West 9th Street
Miami, Florida 33144 | 1 | |
| 8. | Dr. Edna Didwell
Lawrence Livermore National Laboratory / L-389
P.O. Box 808
Livermore, California 94550 | 1 | |
| 9. | Elizabeth C. Kisenwether
HRB Systems, Inc.
P.O. Box 60
Science Park
State College, Pennsylvania 16804-0060 | 1 | 1 |